City Research Online

City, University of London Institutional Repository

This is the accepted version of the paper.

This version of the publication may differ from the final published version.

DETERIORATION AND SPALLING OF HIGH STRENGTH

CONCRETE AT ELEVATED TEMPERATURES

Chellathurai Thiruchelvam

Thesis submitted for the Degree of Doctor of Philosophy

SCHOOL OF ENGINEERING & MATHEMATICAL SCIENCES

CITY UNIVERSITY

LONDON

2003

Summary

The objective of this research was to examine the *deterioration and explosive spalling of high strength concrete at elevated temperatures*. The following three types of concrete beam specimens were considered; using three different types of aggregates. These concrete specimens were:

     a). Plain concrete beams

     b). Reinforced concrete beams and

     c). Fibre concrete beams.

The three aggregate types used were:

     a). Limestone

     b). Lightweight aggregate (LWA) and

     c). Limestone partly replaced by LWA (modified normal concrete).

A fractional factorial method of experimentation was adopted to investigate six factors at three levels each. The factors were *curing before heating, rate of heating, loading level, water cement ratio, type of aggregate and polypropylene fibre content.* Three main series of tests were carried out on 27 plain concrete beams, 27 reinforced concrete beams and 27 fibre reinforced concrete beams.

The high temperature work was carried out in a purpose built rig capable of applying loads to beams in flexure within the furnace and at the same time measuring the loads, deflections and expansions of the specimens.

All the beams tested deteriorated after heating to 700 °C. None of the plain concrete beams and reinforced concrete beams were immune from explosive spalling given certain combination of factors. The beams that deteriorated early during heating were unlikely to spall explosively. Although the fibre concrete beams deteriorated at high temperatures, none of them failed violently.

A change in the factor level sometimes influenced the deterioration, linearly in the plain concrete specimens and non-linearly for the reinforced concrete specimens. In some cases a change in the level of a factor influenced the behaviour of the reinforced concrete specimens but not the plain concrete specimens. At times a change of factor created a maximum deterioration in the reinforced concrete specimens but had minimal effect on the plain concrete specimens.

Acknowledgement

Contents

CHAPTER 1

Introduction

CHAPTER 2

Structural properties of concrete at high temperatures

2.1 Effect of high temperature on concrete: compressive strength,

CHAPTER 5

The fractional factorial method

CHAPTER 6

Experimental programme

CHAPTER 7

The experimental results and fractional factorial analysis

CHAPTER 8

Analysis of test results

Figures

Tables

CHAPTER 1

Introduction

1.1 General remarks

The work presented in this thesis reports the research carried out at the City University, London, under the title of " Deterioration and spalling of high strength concrete at elevated temperatures using Fisher's fractional factorial method".

The aim of this project was to investigate the deterioration and spalling of different types of concrete during fire using the factorial method.

Previous experience indicated that explosive spalling was not a deterministic phenomenon and hence a probabilistic method of experimentation was adopted using the fractional factorial approach.

There are several *suspected* factors influencing the behaviour of concrete at high temperatures. In this project six important factors considered as influencing the behaviour of concrete at high temperatures were investigated, each factor being tested at three different levels; thus allowing to study the non-linear effects. The six factors were:

        a. Curing of concrete prior to testing

        b. Rate of heating

        c. Loading prior to heating

        d. Water cement ratio

        e. Type of aggregate

        f. Polypropylene fibre

Chapter 5 considers in details the selection of factors for this project.

In this project, parallel test series of normal and reinforced concrete beams were tested under similar conditions. Previous experiments suggest that polypropylene fibre can be used in concrete to reduce spalling when concrete is exposed to fire. In order to assess the effectiveness of polypropylene fibre, it was chosen as a factor in another series of tests, where all the concrete beams were maintained at 100% R.H. This high humidity curing on fibre concrete is a more severe condition than other forms of curing for high temperature performance.

During the initial testing of the first series of plain concrete beams, a specimen with water cement ratio of 0.5 and cured at 65% relative humidity exploded. Because of this, it was decided to change the R.H. of the higher level of the curing factor from a nominal 100% to 65% and to maintain the lowest level at 0%, for the first series of plain concrete. There were some anomalies in these initial results. Therefore these tests were repeated at a nominal curing R.H. of 100% (85%), 65% and 45%, and apart from curing, all the other factors were maintained similar to the first series of plain concrete.

The fibre concrete beams were all tested with the concrete cured at 100% RH prior to testing. Cold tests were also carried out on control cubes at 28 days and at

the time of testing, together with the capillary rise test to assess the surface permeability of the concrete.

This thesis describes the experimental method, the data obtained, the processed results and their analysis by the fractional factorial method.

1.2 Objectives of this study

The main objective of the experimental programe was to examine the influence of six main factors on the spalling and deterioration of high strength concrete during fire, using the fractional factorial method. The experimental furnace tests were carried out on **81 specimens** consisting of three sets of 27 tests on plain, fibre and reinforced concrete beams of the same overall dimensions. Nine beams were strength tested for each set to establish their 'room temperature' ultimate strength. The design of the experimental programe was based on the fractional factorial method of analysis. All the factors have been investigated at three levels. As said earlier, three levels have been selected so that the non-linear variations in individual and interacting factors can be determined.

A description of these factors and levels are given in Table 6.2 and Table 6.3 in Chapter 6. The use of three sets of 27 tests constitute a $\frac{1}{9}^{th}$ fractional factorial set of experiments and statistical analyses allows to determine the significance of the individual and interaction factors as well as their non-linear variations.

1.3 Classification of test series.

Series 1.   Plain concrete beams

Series 2.   Fibre concrete beams

Series 3.   Reinforced concrete beams.

The high temperature tests have been carried out in a purpose built testing rig on 81 (27x3) concrete beams with similar overall dimensions and a further test series consisting of 27 plain concrete beams, as explained earlier. Nine additional control beams were cast for each test series and these were then tested to failure in the cold state. An additional beam with embedded thermocouples was tested to obtain the thermal response data for the three different rates of heating.

1.4 Subject background

The use of high strength concrete as a structural material is increasingly growing in the UK and worldwide. Its usefulness in allowing designers to minimise the sizes of structural elements and to support high load weight along with its increased usage has increased the probability that they will be exposed to high temperatures and fire. Findings in 1984 by Hertz [1.01], in 1993 by Castillo and Durani [1.02], in 1993 by Sanjayan and Stocks [1.03], in 1991 by Jumpannen and Diederichs [1.04] and in 1994 Tachibana [1.05] suggest that high strength concrete is more susceptible to spalling than normal concrete. During exposure to fire, the

effect of heat and mass transfer in concrete becomes very important. Where there is a steep temperature gradient, a build-up of water pressure develops which might cause concrete spalling. Spalling is a phenomenon in which forces are created within the body of concrete when exposed to a heating regime, which can cause the surface to erupt in a number of ways.

A number of types of spalling have been identified:

a). Aggregate spalling, which is the breaking up of aggregate on or near the surface up to a depth of 10mm;

b). Corner spalling, which is the breaking off of the corner or arrises of concrete elements;

c). Surface spalling, which is dislodging of the concrete surface and can remove as much as 50mm from the surface;

d). Explosive spalling, which is the violent disintegration of sometimes whole elements of heated concrete.

The structural implications of spalling can vary due to the type of spalling induced and the application for which the concrete is being used. All types of spalling though will reduce the fire resistance of the concrete element.

An international survey of laboratories for fire safety testing of structural concrete members carried out by Conseil International du Batiment (C.I.B.) in 1970 confirmed that there is "no real understanding of the fundamental mechanisms of spalling nor of the effect of individual parameters in determining

the susceptibility of concrete to spalling". There is therefore a real need to establish the importance of factors involved in spalling so that the design of concrete members can incorporate risk minimisation of the occurrence of spalling.

As a full quantitative and qualitative study into the factors affecting spalling has not been carried out, their analysis cannot be built into numerical modelling for thermal analysis of fire resistance. Therefore, current models of fire resistance are likely to produce incorrect and possibly dangerous predictions.

Considerable work has been carried out over the past two decades on the phenomenon of spalling of normal strength concrete at high temperatures, which have highlighted the effect of various factors on the susceptibility of concrete to spalling. These factors are summarised in Table 1.1 below [1.11].

Table 1.1 [1.11]
Factors that influence concrete spalling at high temperatures.

Factor	Nature	Effect on susceptibility to spalling (by reference)
Compressive Strength	Increase	More susceptible 1.20,1.14,1.03,1.04
Age	Older	More susceptible 1.10 Less susceptible 1.13,1.021,1.20,1.06
Moisture Content	Increased	More susceptible 1.18,1.13,1.06,1.09,1.19

Aggregate size	Increased	More susceptible 1.18,1.20,1.08
Water / Cement ratio	Higher	More susceptible 1.20,1.10
Rate of heating	Higher	More susceptible 1.21,1.18,1.20,1.10
Nature of heating	Two sided	More susceptible 1.20,1.06
Applied load	Imposition	More susceptible 1.18,1.20,1.06,1.09,1.12, 1.02
Restraint	Imposition	More susceptible 1.20
Element thickness	Increased	Less susceptible 1.17,1.20,1.06,1.07,1.09, 1.02
Curing	Water curing	More susceptible 1.21,1.20
Cracking	Presence	Less susceptible 1.20,1.10,1.03

There are a number of theories as to the mechanism of explosive spalling (the worst of the spalling types) but it is convenient to group them under two broad headings: spalling due to thermal stresses; spalling due to pore pressure.

In 1965 Saito [1.32] carried out a research on thermal stresses and describes spalling as a compression failure at the heated face. He stated that spalling

occurred when the surface stresses created by a non-uniform temperature distribution across the concrete section surpass the compressive strength of the concrete. This theory does suggest though that thicker sections are more susceptible to spalling, which, as later research has shown, this is not the case [1.20, 1.06, 1.09].

In 1972 Dougill [1.26] suggested that explosive spalling in a fire was due to the presence of a strain-softening region in the stress-strain curve where the curve has a negative slope in this region. Both of these theories, though, neglect to explain the importance of the moisture content in spalling.

Concerning research into spalling due to high pore pressures, a number of theories have been developed. All follow the basic principle that on heating, the free-water within the body of concrete creates pressures, which can cause stresses large enough to dislodge lumps of the concrete surface.

In 1965 Shorter and Harmathy [1.24] proposed the theory of 'moisture clog spalling'. When heat starts to penetrate into the concrete section, desorption of moisture occurs in a thin layer adjoining the surface exposed to the fire. A large proportion of the released vapours migrates towards the colder regions and becomes reabsorbed in the pores of an adjoining layer. With the dry layer increasing, a saturated layer known as the moisture clog builds up at a distance from the exposed surface. This then creates a boundary between the dry and saturated regions. The process of the dry region undergoing further desorption

creates a steep temperature gradient across it. This creates a heat flow and super-desorption. The moisture has now no passage towards the colder regions and therefore vapours try to leave through the dry layer, which is expanding and restricting its movement. When the permeability is high, it allows the moisture to move under this increasing pressure difference, the moisture clog will move towards the colder regions thus allowing the pressure to ease off. When the permeability of the concrete is low, however, the pressure at the boundary between saturated and dry where the dry region is growing will ultimately exceed the tensile strength of the concrete. When this happens, the dry layer of the concrete may dislodge.

Another pore pressure theory has been proposed by Meyer-Ottens in 1972 [1 09], which suggests that the bursting stresses are a result of the drag forces generated by water vapour escaping from the moisture clog to the heated surface.

In general, spalling in high strength concrete is caused by the combination of the same factors that causes spalling in normal strength concrete. The risk of spalling though is higher in high strength concrete due to many factors, some of which are listed below:

> 1). The low permeability of high strength concrete retains the moisture inside the concrete, resulting in a high moisture content being present for prolonged periods.

2). Although high strength concrete tends to have a low free water/cement ratio, the high cement content used to obtain these high strengths mean that there can be as much water per unit volume as normal strength concrete.

3). The low porosity of high strength concrete creates higher pore pressure.

4). High strength concrete tends to be subjected to higher compressive stresses.

5). High strength concrete is more brittle than normal strength concrete.

It is the author's opinion that the mechanism of explosive spalling can be explained by the combination of two phenomena which may in some way interact:

1) The development of a high pore pressure during the process of moisture clog,

2) Brittle fracture of the concrete, which releases the high strain energy developed and stored within the specimen.

From this research it is evident that moisture clog plays an important role in the mechanism of spalling. This can be confirmed by the condition of the furnace and the surroundings immediately after explosive spalling. When the specimens exploded (always at a furnace temperature of between 300 °C and 500 °C) the

resultant dust and particles that are blown out brings with them droplets of water. After an explosion, the furnace has small pools of water within and around it. This concentration of water cannot come from anywhere but the hardened concrete as it breaks, with the moisture collecting in layers as described in the moisture clog theory. Furthermore, all the specimens that exploded in the research matured in the curing region above 65% RH, resulting in a high concentration of moisture within the specimens.

In the experiment all the beams that exploded did so violently throwing debris as far as six metres across the room. The pore pressure can only serve to trigger a crack but there will not be enough force to drive the explosion as mentioned. There must be some other phenomena present which caused the concrete to break up so violently. This must come therefore from some other source of energy in the form of strain energy. This means that the phenomena of spalling may be analysed using fracture mechanics. There is scant literature on the fracture mechanics of concrete at high temperatures, thus the analysis in this project will concentrate on the view that concrete acts chaotically.

1.5 Previous work on deterioration and spalling of high strength concrete at elevated temperatures.

There has been much work carried out on the behaviour of high strength concrete in the last 50 years and, as can be seen from Table 1.1, much work has also been

carried out on spalling of normal strength concrete. However, only a small

number of studies have been carried out on the deterioration and spalling of high

strength concrete at elevated temperatures.

1.5.1 Chemical analysis of high strength concrete at high temperature.

In 1989 Diederichs *et al* [1.30] produced thermographs of high strength normal

density (ND) concrete and their cement paste. This is illustrated in Figure 1.1 on

the next page.
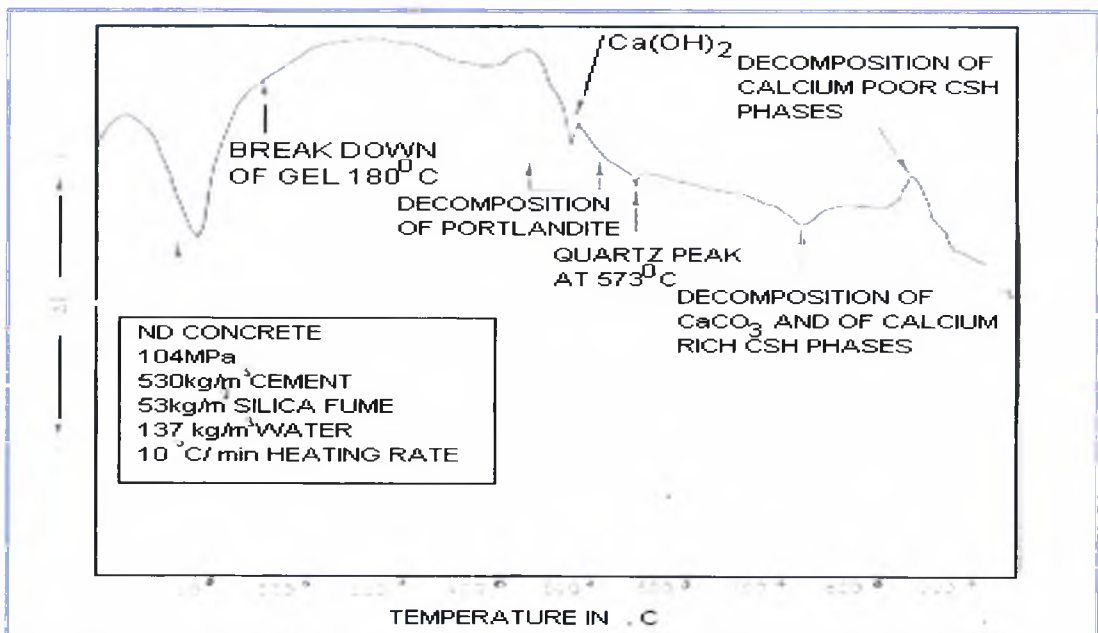
Figure 1.1. Sketch of a thermograph of ND concrete with compressive cylinder strength of 104Mpa

The above graph illustrates that decomposition of portlandite happens at about 450 °C and also marks out chemical events, which can help to explain the general disintegration of high strength concrete during the heating process.

In 1965 Jensen *et al* [1.31] have investigated the responses of high strength lightweight concrete. Figure 1.2 illustrates the strength loss of lightweight and normal weight high strength concrete.
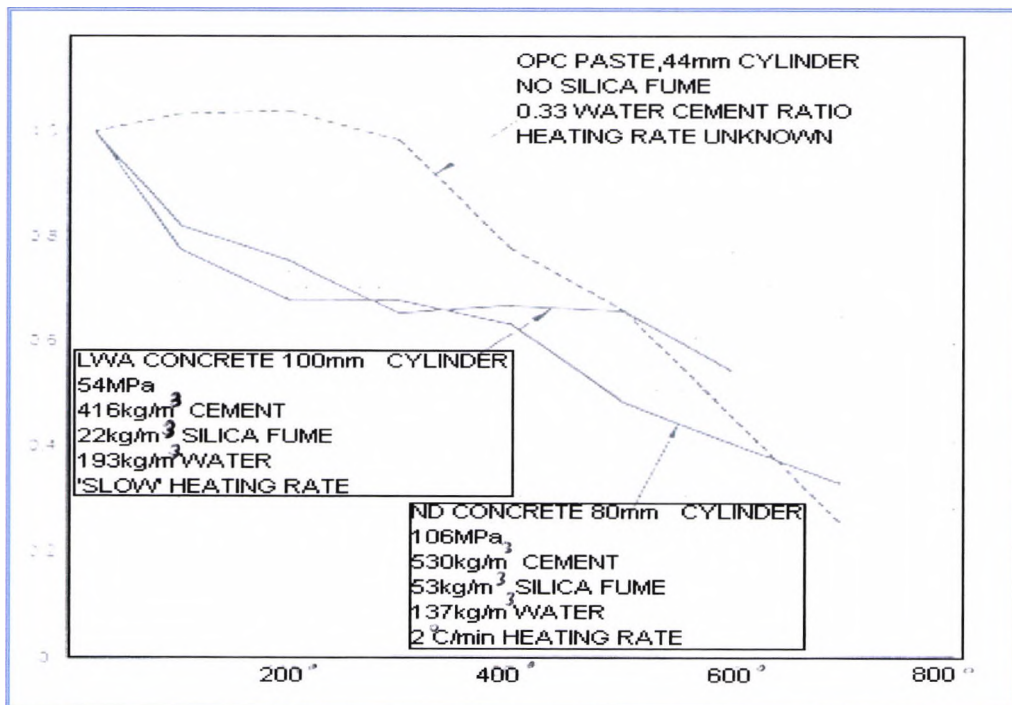
Figure 1.2.Response of high strength lightweight and high strength normal weight concrete to fire

1.6 Effect of loading on the deterioration of high strength concrete.

In 1990 tests carried out by Castillo and Durrani [1.02] showed that about one-third of their high strength, preloaded specimens failed explosively during the heating

period at 320 $^{\circ}$C to 360 $^{\circ}$C. They argue that preloading in compression prevents cracks from forming which will prevent the loss of strength expected during heating, but that by inhibiting the formation of cracks, the concrete will stop the release of water vapour and increase its propensity to spall. It is also worth noting that none of the preloaded specimens were able to sustain the load past 700 $^{\circ}$C. Referring back to Figure 1.2 it can be seen that there is no chemical event between 320 $^{\circ}$C and 360 $^{\circ}$C where most of the Castillo and Durrani specimens failed although in 1989 Diederichs et al [1.30] reported that the decomposition of Ca (OH)$_2$ may begin at 350 $^{\circ}$C for normal strength concretes.

In1989 Diederichs *et al* [1.30] conducted a study of the effect of different levels of loading on three different types of high strength concrete. These are illustrated in Table 1.2 below.

Table 1.2.
Fracture temperatures for loaded high strength ND concrete ($^{\circ}$ C)

Mix with	Strength at test MPa	Preloaded stress level as a % of the room temperature ultimate capacity				
		70%	60%	50%	40%	30%
Silica fume	106		110	420	560	-
Fly ash	91		120	-	-	-
No supplementary cementing material	85	110	360	-	-	-

This shows how preloading can have an effect on the durability of high strength concrete at high temperatures. Considering that 50% stress levels are typical for structural service conditions these findings have wide implications for the construction industry and may necessitate the need for project specific fire tests.

1.7 Effect of heating rate on high strength concrete.

In 1984 Hertz [1.1] tested high strength cylinders at temperatures up to 650 °C with a heating rate of 1 °C/minute. He concluded that explosive spalling could happen even at a slow heating rate. One third of his test specimens spalled explosively.

In 1987 Jensen et al [1.33] carried out tests to show that hydrocarbon fires, which cause the fastest heating rate, can cause serious spalling to high strength concrete very quickly.

1.8 Comparison of tendency to spall between high strength and normal strength concretes.

In 1994 Jumppanen and Diederichs [1.04] carried out several tests to investigate the mechanical high temperature properties and spalling behaviour of high strength concrete. They concluded that fire behaviour of concrete is strongly dependent on the microstructure and binder content. By testing ultra-high strength concrete (approximately 200 MPa) against high strength concrete (100 MPa) and normal strength concrete (33 MPa) they found that the ultra-high strength concrete

"cannot be used at high temperatures (even when reasonably protected) due to their strong tendency to spalling even with very low heating rates".

In 1993 Sanjayan and Stocks [1.03] carried out a test on two full sizes concrete T-beams, one with high strength (105MPa) and the other with normal strength (27MPa).

Explosive spalling was observed in the high strength specimen while none occurred in the normal strength specimens. The spalling was restricted though to a region with 75mm cover to the reinforcement. This suggests that the safe maximum limit for cover in high strength concrete lies between 25 mm and 75mm. It was also found that for concrete under high compressive stresses, the safe limit for cover is expected to be less than this. They concluded that care should be taken when using high strength concrete for pre-stressed members and slender members subjected to high compressive stresses.

1.9 Effect of aggregate type on the tendency to spall

In 1994 Tachibana et al [1.05] reported surface spalling during fire tests on high strength concrete (88 MPa). Tests were carried out on realistically sized walls (1200 mm x 1200 mm x 150 mm), which were heated at a rate of approximately 35 °C/minute. Two types of aggregates were used: crushed hard sandstone & crushed quartz schist. Surface spalling was observed over 100% of the surface of the slab containing crushed quartz schist and over only 40% of the slab containing crushed hard sandstone.

1.10 Effect of curing type on the tendency to spall

In 1987 Jensen *et al* [1.33] carried out tests on cubes, cylinders and $1m^2$ x 100 mm thick slabs (all 69 MPa) and reported that moist cured units were much more damaged than dry cured units, In this project curing did not have much effect on explosive spalling.

1.11 Measures to prevent spalling

There are two types of prevention available. The first is "rule of thumb" prevention, which is by looking at what unfavourable conditions should be avoided. Some of the unfavourable conditions illustrated in Table 1.1 can be avoided during the design stage. For example, by not water curing or by decreasing the maximum aggregate size for the mix, the susceptibility of the concrete to spall can be lowered.

The second is by the introduction of additional materials, which will act to offset spalling. In 1984 Hertz [1.01] proposed the addition of steel fibres so that the tensile strength of the concrete could be increased. On testing this theory though, he found that the addition of steel fibres increased the concrete's tendency to spall.

In 1995 Schneider and Diederichs [1.04] proposed the addition of short polypropylene fibres. Tests using cylinders of 100 mm diameter with and without the addition of fibres were carried out. They found that "most of the concrete

specimens without fibre showed deep spalling and rupture after the tests. While the fibre concrete specimens, on the other hand, showed partial or non-spalling behaviour". They also concluded that spalling was worse in low water/cement ratio (0.25) concretes without fibres. With fibres there was only minor spalling. With water/cement ratio of 0.55, no spalling occurred with or without fibres.

1.12 Concluding remarks

It is widely known that high strength concrete is more brittle than normal strength concrete and its performance at high temperatures may be drastically reduced. There is therefore a real need to understand the behaviour of high strength concrete at elevated temperatures in order to help designers of concrete structures to take precaution to ensure durability during its service life. Spalling in particular must be defined along with its contributing factors if design of high strength concrete is to be both safe and economical.

The objectives of this study are:

1) To identify / confirm the importance of factors which contribute to high strength concretes tendency to spall.

2) To identify any interactions between factors.

3) To test the preventative capabilities of polypropylene fibres to spalling.

4) To give recommendations as to the findings of our study.

In order to achieve the objectives the main study will be experimental which will include looking at the deterioration of high strength concrete due to the effect of different material and environmental factors and examining ways of eliminating concrete spalling. The experimental side of the work will investigate factors which can be controlled, as their adjustment would enable the risk of concrete spalling to be minimised. The factors to be controlled are as follows and each will be tested at three levels 0, 1 and 2 respectively as illustrated below:

1) The rate of heating (Low, Medium and High).

2) Aggregate type (Lightweight, Modified density and Normal weight).

3) Curing conditions (Dry, Air cured and Wet)

4) Loading levels (For plain concrete 0%, 10% and 20%; for reinforced concrete 20%, 40% and 60%)

5) Free water / cement ratio (0.25, 0.35 and 0.5)

6) Polypropylene fibres (1, 2 and 3 kg/m^3)

These factors will be used on mixes of plain concrete, plain concrete with polypropylene fibres and reinforced concrete. The conclusion and recommendations given in the final Chapter should eliminate / minimise the threat of explosive spalling and minimise the deterioration of high strength concrete structures during fire.

CHAPTER 2

Properties of Concrete at High Temperatures: A summary of previous work

In this Chapter a summary of previous research carried out on the properties of concrete at high temperature is given. Section 2.1 covers work where the main properties under consideration are the effect of elevated temperature on compressive strength, coefficient of linear expansion, modulus of elasticity and creep/shrinkage. For each of these aspects a number of research programmes are summarised.

Section 2.2 deals with further work covering a wide range of specialised aspects where in same cases only a single paper is involved.

2.1 Effect of high temperature on concrete: compressive strength, coefficient of expansion, modulus of elasticity, creep/shrinkage

An overview of previous research on the main effect of high temperature is given in Table 2.1. Section 2.1.1 to 2.1.5 and Tables 2.2 to 2.5 considers in turn compressive strength, coefficient of expansion, modulus of elasticity and creep/shrinkage.

Table 2.1

Previous research on concrete properties at elevated temperature														
Ref. No	Name	Date	Test				Variables						Heating	
			fc	α	E	Creep / shrinkage	Cement Type	Agg	W/C	Spec. type	Curing	Cycling	Range	H.soaking
2.01	Woolson	1905	√	-	√	-	-	-	-	√	-	-	√	-
2.02	Norton	1913	√	√	-	-	-	-	-	√	-	√	-	-
2.03	Lea	1920	√	√	-	-	-	-	-	-	-	-	√	-
2.04	Grun & Beckman	1930	√	-	-	-	√	√	-	-	-	-	√	-
2.05	Willis & De Reus	1939	-	√	√	-	√	√	-	-	-	-	√	-
2.06	Giles	1939	√	-	-	-	√	-	-	-	-	-	√	√
2.07	Walker & Bloem	1952	√	√	-	-	-	-	-	-	-	√	-	-
2.08	Mitchell	1953	-	√	-	-	-	-	-	-	-	-	√	-
2.09	Harada	1953	-	√	-	-	√	-	-	-	-	-	√	-
2.10	Murashev	1956	√	-	-	-	√	-	-	-	-	-	√	-
2.11	Malhotra	1956	√	-	-	-	-	√	-	-	-	-	√	-
2.12	Seaman & Washa	1959	√	-	√	-	-	-	-	-	-	-	√	-
2.13	Philleo	1958	-	√	√	√	-	√	-	-	-	-	√	-
2.14	Dougill	1960	√	-	-	-	-	-	-	-	-	-	√	-
2.15	Zolders	1960	√	-	-	-		√	-	-	-	-	√	-
2.16	Hannant	1962	-	-	-	√	-	-	-	-	-	-	√	-
2.17	Hatano	1964	√	-	-	-	-	-	-	-	-	-	√	-
2.18	Campbell	1965	√	-	√	-	-	-	-	-	-	√	-	-
2.19	Cruz	1966	-	-	√	-	-	-	-	-	-	-	√	-
2.20	Harmathy & Berndt	1966	-	-	√	-	-	√	-	-	-	-	√	-
2.21	Furumura	1966	√	-	√	-	-	-	-	-	-	-	√	-
2.22	Campbell	1967	√	-	√	√	-	√	√	-	-	√	-	-
2.23	Harada	1970	√	√	-	-	-	√	-	-	-	-	√	-
2.24	Takeda	1970	√	-	√	-	√	-	-	-	√	-	√	-
2.25	Nasser & Marzouk	1974	√	-	-	-	√	-	-	-	-	√	-	-
2.26	Grainger	1979	√	-	-	-	√	-	-	-	-	-	√	-
2.27	Diederichs	1989	√	-	-	-	√	-	-	-	-	-	√	-
2.28	Sullivan	1992	√	-	-	-	√	-	-	-	-	-	√	-
2.29	Khoury	1993	√	-	-	-	√	-	-	-	-	-	√	-
2.30	Hammer	1995	√	-	-	-	√	-	-	-	-	-	√	-
2.31	Ghosh	1998	√	-	√	-	√	-	-	-	-	-	√	-
2.32	Khoury	1999	√	-	-	-	-	-	-	-	-	-	√	-
2.33	Wang	2000	√	-	-	-	√	-	-	-	√	-	√	-
2.34	Wu	2002	√	-	√	-	-	-	-	-	-	√	-	-

F_c ---- Compressive strength

α ---- Coefficient of expansion

E ---- Modulus of elasticity

2.1.1 Compressive strength

In this section Table 2.2 gives an overview of previous research on the effect of

high temperature on compressive strength.

Table 2.2

				Compressive strength (f_c)	
Ref	Name	Date	Tem. range	Experiment Details	Results
2.01	Woolson	1905	250 – 1250 ºC	f_c of prism and cubes	f_c of prism < f_c of cubes
2.02	Norton	1913	20 – 800 ºC	f_c of 200mm cubes and 150mm cubes	f_c of heated specimens were affected by the specimens size f_c of large cubes < f_c of small cubes
2.03	Lea	1920	430 – 20 ºC	100mm cubes tested at hot and cooling from 430 ºC	Specimens tested hot 12% stronger than tested after cooling
2.04	Grun & Beckman	1930	20 – 1200 ºC	Effect of types of cement and aggregate on f_c, specimens heated to 1200 ºC	Pozzolana cement performed better than Portland cement. Blast furnace slag performed better than limestone or gravel aggregate
2.06	Giles	1939	Max 500 ºC	f_c of high alumina cements concrete with different heat soaking time. Sudden water cooling from 500 ºC	f_c not affected by heat soaking time. f_c reduced due to sudden water cooling
2.07	Walker, Bloem and Muller	1952	5 – 60 ºC	Effect of thermal cycling on f_c with different rate of heating	Fast rate of heating lowers f_c more than slow rate of heating
2.10	Murashev	1956	Max 1100 ºC	f_c of heat resistant concrete made from aluminous cement and sodium silicate cement	f_c of Aluminous cement concrete reduced more than the sodium silicate cement
2.11	Malhotra	1956	20 – 700 ºC	Effect of w/c on f_c at high temperature w/c varied between 0.4 to 0.65	w/c in the range 0.4 to 0.65 did not have significance effect on f_c
2.12	Seaman ans Washa	1959	5 – 232 ºC	Investigated the effect of temperature on f_c	f_c increased below 20 ºC, decreased by 10% with increasing temperature Recovered at around 200 ºC to its room temperature level
2.14	Dougill	1960	Max 800 ºC	Investigated the effect of temperature on f_c	f_c reduces by 10% due to different thermal movement of aggregate and the cement matrix
2.15	Zolders	1960	20 – 600 ºC	Effect of temperature on f_c concrete made from different aggregate, Deterioration analysed after cooling	All the concrete deteriorated rapidly and f_c reduces by 10%, Sandstone concrete performed better than limestone, gravel aggregate concrete. Deteriorated during cooling
2.17	Hatano	1964	40 – 60 ºC	Effect of 40 – 60 ºC temperature range on f_c	f_c of concrete reduced by 5% as temperature increases.
2.18	Campbell	1965	0 – 300 ºC	Investigated the effect of thermal cycling on HSC f_c	f_c reduced at the first cycle by 15% and by five cycles 36% and by ten cycles 40%
2.21	Furumura	1966	20 – 700 ºC	Investigated for changes in f_c when heat changing	f_c changes by 5% up to 400 ºC and it changes by 20% between 400 – 700 ºC
2.22	Campbell	1967	20 – 300 ºC	Investigated the effect of temperature, temperature cycles on f_c	f_c reduces with increasing temperature, Most damage takes places during the first cycle; almost 50% by the fifth cycle
2.23	Harada	1970	20 – 800 ºC	f_c is investigated for different aggregate concretes at high temperature	Aggregate influence the f_c, f_c reduces by 25% at maximum temperature
2.24	Takeda	1970	40 – 80 ºC	Effect of curing temperature on f_c	f_c reduces by 10% when the specimens cured at 80 ºC
2.25	Nasser & Marzouk	1974	21 – 232 ºC	f_c of concrete with 25% lignite fly ash by weight	f_c increased by 5% between 121-149 ºC and reduced by 27% when temperature reaches 232 ºC
2.26	Grainger	1979	100 – 500 ºC	Performance of slag cement , 0,50,70,90% slag cement by weight of OPC	All slag cement increased in strength between 100-250 ºC, beyond 250 ºC starts to decreases
2.27	Diederichs	1989	Max 900 ºC	Investigating the f_c of granulated furnace slag (GGBS), pulverized fly ash (PFA), condensed silica fume (CSF) concrete mixes, specimens tested after cooling	f_c of GGBS>PFA>CSF
2.28	Sullivan	1992	50 – 600 ºC	Hot f_c were calculated for FA concrete and OPC concrete	Depression is large at 100 ºC, FA concrete's f_c recovered about 90% at 200 ºC, OPC concrete's f_c recovered almost 100%, then they lost 50 and 70% at 600 ºC
2.29	Khoury	1993	Max 600 ºC	Hot f_c were determined for 30% PFA concrete, OPC concrete and slag concrete. f_c is measured at every 100 ºC	Slag concrete gave the best results and f_c of slag concrete were 102% and 80% of initial cold strength at 400 ºC and 600 ºC
2.30	Hammer	1995	Max 600 ºC	f_c is tested for five specimens with 0-5% silica fume , all tested after cooling.	No silica fume concrete f_c < silica fume concrete f_c
2.31	Ghosh	1998	Max 232 ºC	f_c is tested for concrete with silica fume concrete and high calcium lignite fly ash concrete	f_c of PFA concrete mix < f_c of high calcium lignite fly ash concrete. f_c reduced by almost 40% in both concrete
2.32	Khoury	1999	105 – 600 ºC	Tested for high temperature effect on f_c of HPC and UHPC.	UHPC retrain its f_c even at 600 ºC but HPC lost 45% of it's original strength at 600 ºC
2.33	Wang	2000	20 – 700 ºC	Studied the effect of PFA in concrete	All PFA specimens showed better performance up to 650 ºC , an increase in strength was observed at 250 ºC
2.34	Wu	2002	20 – 900 ºC	Effect of single heat cycling on f_c of confined and unconfined HSC	f_c gradually decreases from 21 ºC to 232 ºC

2.1.1.1 Comments on compressive strength

High temperature reduces the compressive strength of concrete by 5 to 50% due to differential thermal movement of the aggregates and the cement matrix, thus causing cracks and drop in strength [2.12, 2.14, 2.15, 2.17, 2.18, 2.21, 2.22, 2.23, 2.24, 2.34].

Compressive strength of prisms is lower than cubes because it is now widely known for a large height to width ratio the state of stress is uni-axial where as platens friction on a cube causes some form of tri-axial compression, and hence the lower strength for the prisms [2.01].

In general when the specimens are tested hot they are normally stronger than those tested after cooling. This is due to further cracking of the specimens during cooling [2.03]. Duration of the heat soaking period had a deleterious effect on the compressive strength of concrete [2.03].

Normally during cooling progressive deterioration occurs, indicated by extensive cracking during cooling. This is due to formation of $Ca(OH)_2$ as the CaO formed at about 400 °C reacts with the moisture present in the atmosphere. This results in volume expansion and hence more cracking of concrete and compressive strength reduction after cooling [2.15]. If the specimens were subject to sudden cooling in water, this also affects the compressive strength adversely due to additional stresses induced by thermal shock [2.06].

Generally an increase in the proportion of finer particles in the mix improves the compressive strength at the hot stage. This is due to more uniform inter-particle temperature distribution [2.04, 2.10, 2.26, 2.27, 2.28, 2.29, 2.30, 2.31, 2.33].

In general fast rate of temperature change over a given range was more detrimental to concrete than a slow rate, which indicates that the deterioration was primarily due to temperature gradient within the concrete mass rather than due to differential volume change among the constituents themselves [2.07].

Heat cycling caused progressive deterioration of the mechanical properties of concrete with most damages takes place during first cycle [2.22].

The increase in strength by 152%, for the concrete containing fly ash was observed in the temperature range of 121 – 149 °C and reduces when temperature reaches 232 °C, the increase in strength is due to the formation of tobermorite (a product of lime and PFA at high pressure and temperature) [2.25].

Ultra high performance concrete (UHPC) normally maintained its strength better at high temperature than high performance concrete and this may be due to the smaller aggregate size used in UHPC [2.32].

2.1.2 Coefficient of expansion

In this section Table 2.3 considers an overview of previous research on

coefficient of thermal expansion.

Table 2.3					
Thermal coefficient of expansion (α)					
Ref	Name	Date	Tem. range	Experiment Details	Results
2.02	Norton	1913	20 – 800 °C	Tested reinforced concrete beams up to 800 °C	Difference between α of steel and concrete produces more cracks
2.05	Willies	1939	5 – 60 °C	Comparing the α of different aggregates	α of quartzite and sandstone ranging between 11-13 x 10^{-6} / °C α of limestone ranging between 4-7 x 10^{-6} / °C α of granite basalt and dolomite ranging between these two values
2.07	Walker, Bloem and Muller	1952	5 – 60 °C	Effect of temperature on HSE with different aggregate (α) and with different rate of heating	Concrete with high α more liable to damage. Fast rate of heating damages more than slow rate
2.08	Mitchell	1953	-12 12 °C	Investigating the α with fineness of cement	α increases with cement fineness
2.09	Harada	1953	Max 700 °C	Specimens with different aggregate heated to 700 °C to study α values and damage assessment	Damage increases with increasing α value of aggregate. Pumice concrete < cinder concrete < andesite concrete < sandstone concrete
2.13	Phelleo	1958	20 – 815 °C	Calculated α for gravel concrete for above and below 250 °C	α for gravel concrete was 7.5x 10^{-6}/°C below 250 °C, and 22.5 x 10^{-6}/°C above 250 °C
2.23	Harada	1970	20 – 800 °C	α is investigated for different aggregate concretes	α of pumice aggregate concrete < α of limestone aggregate concrete < α of sandstone concrete

2.1.2.1 Comments on coefficient of thermal expansion

Concrete with a higher coefficient of thermal expansion is more liable to damage

than concrete with a low coefficient of thermal expansion. Concrete containing

quartz aggregates suffer more damage than concrete with limestone aggregates

(2.05, 2.09)

Due to the different thermal expansion of concrete and steel, reinforced concrete

generally produce more cracks than plain concrete [2.02].

The coefficient of thermal expansion of concrete depends on the aggregate type as well as on the volume fraction of the coarse aggregate and concrete with higher coefficient of thermal expansion is more liable to damage than concrete with a low coefficient of thermal of expansion. ie. Concrete containing quartz aggregate suffered more damage than concrete with trap rock aggregate [2 07]. Coefficient of thermal expansion of neat cement specimens is independent of its age but increases with its fineness. Specimens with fine cement normally shows an increase in initial expansion with temperature up to about 120 °C above which the expansion decreased as the rate of moisture loss increased becoming nil at around 200 °C [2 08].

2.1.3 Modulus of elasticity

In this section Table 2.4 considers an overview of previous research on the effect of high temperature on modulus of elasticity.

Table 2.4

				Modulus of elasticity (E)	
Ref	Name	Date	Tem. range	Experiment Details	Results
2.12	Seaman and Washa	1959	5 – 232 °C	Effect of temperature on E	E increased below 20 °C decreased with increasing temperature.
2.13	Philleo	1958	Max 800 °C	Effect of increasing temperature on E	E reduces with increasing temperature The greater the moisture lost greater the lost in E value
2.18	Campbell	1965	0 – 300 °C	Investigated the effect w/c on E at high temperature	Concrete with lower w/c ratio retain great deal of modules value at high temperature
2.19	Cruz	1966	20- 515 °C	Effect of high temperature on E	E dropped shapely with increasing temperature
2.20	Harmathy & Berndt	1966	20- 750 °C	Effect of increasing temperature on E Specimens are cylinders and tested under hot condition	Test results indicated that up to 200 °C E virtually unaffected, Above 250 °C E decreased sharply with increasing temperature
2.22	Campbell	1967	20 – 300 °C	Investigating the effect of temperature cycles and w/c on E	E reduces with increasing heat cycling Lower w/c concrete considerably retain its E values at high temperatures
2.24	Takeda	1970	40 – 80 °C	Effect of curing temperature on E of concrete with gravel aggregate and Portland cement Specimens are cured at room temperature and 60 °C constant temperature	E reduces when the specimens cured above 20 °C
2.31	Ghosh	1998	Max 232 °C	E is tested for concrete with silica fume and high calcium lignite fly ash concrete	PFA concrete lost more E value than high calcium lignite fly ash concrete after heating. In general E decreases with increasing temperature
2.34	Wu	2002	20 – 900 °C	Effect of single heat cycling on E of confined and unconfined HSC. Specimens were moisture and air cured	E gradually decreases with increasing temperature Dropped sharply between 200 °C to 600 °C. More gradually within the temperatures of 100 - 200 °C and 600 – 900 °C Moisture cured specimens suffer more than air cured specimens

2.1.3.1 Comments on modulus of elasticity

The modulus of elasticity decreases with rise in temperature [2.12, 2.13, 2.18, 2.19, 2.24, 2.34] Concrete with a lower water-cement ratio retains a greater percentage of the room temperature modulus value [2.22].

The moist cured specimens normally suffer greater reduction in modulus of elasticity than air cured ones. The greater the moisture loss, the greater is the reduction in the modulus value, indicating that the loss of moisture removes an incompressible phase from the concrete [2.34].

2.1.4 Creep/shrinkage

In this section Table 2.5 considers an overview of some of the previous research

on the effect of high temperature on creep/shrinkage.

Table 2.5					
				Creep/ Shrinkage	
Ref	Name	Date	Tem. range	Experiment Details	Results
2.13	Phelleo	1958	Max 1100 °C	Investigated the effect of high temperature on creep and shrinkage on concrete with admixtures	Increases with increasing temperatures Stabilised beyond 550 °C
2.16	Hannant	1962	600 °C	Effect of high temperature on creep and shrinkages	Creep and shrinkage increases with increasing temperatures Stabilises beyond 600 °C
2.22	Campbell	1967	20 – 300 °C	Investigating the effect of temperature cycles on creep / shrinkage Specimens were made from different aggregates	Increasing with increasing number of heat cycling Micro-cracks more in limestone than shale concrete

2.1.4.1 Comments on creep/ shrinkage

In general high temperature increases creep and shrinkage [2.16]. Shrinkage

stabilises as the moisture loss also stabilises [2.13]. A finely ground admixture can

be used concrete to reduce the shrinkage in the cement paste. By adding these

admixtures the difference between the thermal expansion of aggregate and matrix

is kept to a minimum thus shrinkage is minimize [2.13].

Considering the heat cycles generally, shrinkage of concrete increases with

increasing number of heat cycles, this will attributes to progressive micro-

cracking which is most prominent in the case of limestone concrete and least with

expanded shale concrete [2.22].

2.2 Previous research on other aspects of the properties of concrete at high temperatures

Table 2.6 considers an overview of other aspects of behaviour of concrete at high temperature.

Table 2.6					
				Different high temperature tests	
Ref	Name	Date	Tem. range	Experiment type	Results
2..35	Davis	1967	Elevated temperature	Bond strength analysis of reinforced concrete beams	Dimensional changes in concrete during heating leaves high loss in bond strength between concrete and reinforcement.
2.36	Crook and Murray	1970	620 °C	Heat soaking analysis	Heat soaking will reduce the strength. Soaking in water will increase the strength by sealing many pores due to re- hydration of the cement
2.37	Sullivan	1970	Elevated temperature	Deterioration of reinforced and plain concrete	Deterioration of reinforced concrete less than plain concrete due to restraining effect imposed by the steel on the cracked concrete sections.
2.38	Nishizawa	1972	20 - 90 °C thermal cycling	Creep of Sealed concrete specimens	During thermal cycling of loaded specimens creep of concrete is governed by highest temperature rather than by thermal cycling
2.39	Khoury	1986	Max 600 °C	Strain of concrete during first heating to a max temperature	Thermal strains induced by first – time heating of concrete under load can be determined in terms of free thermal strain of unloaded concrete and the load induced thermal strain.
2.40	Fu	1999	200°C	Effect of admixture on concrete paste using latex, methylcellulose, silica fume and short carbon fibres	Combined use of silica fume and methylcellulose gave lower thermal conductivity than the use of silica fume alone. Thermal diffusivity decreases with increasing latex content. Methylcellulose increases specific heat more than latex
2.41	Baker	2000	Max 600 °C	Performance of reinforced and Pre-Stressed concrete beam exposed to elevated temperature	Moment capacity of simply supported beam tested under point load reduces with temperature. At 600 °C the capacity was still 75% of the room temperature values.
2.42	Binsheng	2002	Max 600 °C	Effect of heating temperature, exposure time and curing on the fracture toughness	The quick evaporation of the capillary water do not affect fracture toughness (FT) Evaporation of gel reduces FT. FT increases with increasing temperature Longer curing led to a higher FT

2.2.1 Comments for research listed in Table 2.2

Dimensional changes of concrete during heating apparently destroy the bond between the concrete and the plain reinforcement and cause a high loss in the bond strength. Ultimate bond strength is little affected when using deformed steel bars [2.35].

Heat soaking reduces the strength but part of it can be regained by soaking in water [2.36].

Generally reinforced concrete deteriorates less than the plain concrete due to restrained produced by the reinforcing bars [2.37].

During thermal cycling of loaded specimens the creep of concrete was governed by the highest temperature rather than by the history of thermal cycling [2.38].

Fracture toughness represents the resistance of concrete to cracking and fracture. A higher heating temperature of over 200 °C generally reduces FT [2.42]. Moment capacity of simply supported reinforced concrete beam under point load reduces with increasing temperature [2.42].

2.3 Concluding Remarks

The preceding review of the existing literatures shows that the properties of concrete affected by high temperature as influenced, among other factors, by the differential thermal expansion between the constituents, temperature cross-fall (one face to the other face) across the specimen and the loss of chemically combined water from the cement hydrates.

Concrete incorporating limestone aggregates performs poorly primarily due to its larger coefficient of thermal expansion and abrupt volume changes at critical temperatures.

The temperature cross-fall is influenced by the heating rate. A fast rate of heating is accompanied by a sharper temperature gradient, causing greater loss in concrete strength and modulus of elasticity. This is primarily due to the loss of chemically combined water, which weakens the matrix.

The other important parameters influencing the concrete properties at high temperatures are the conditioning procedure, the test condition and the test environment. Conditioning is the curing process which the specimen undergoes over a period of time before testing. Many researchers have shown that the manner of testing also has important bearing on the concrete properties. For example, the hot strength of concrete is generally higher than its strength after it has been cooled. This is usually attributed to additional stresses resulting from rapid cooling. The higher strength of specimens heated under stressed condition is considered to be due to the process of crack arresting.

Tests on sealed and unsealed specimens shows that the presence of free moisture in a specimen during heating can have a further damaging effect on its properties. When the tests on concrete properties are carried out under steady state temperature attained after prolonged heating, it is probable that most of the free

moisture is lost in the process. So it may not be appropriate to use results from such tests in the analysis of structures exposed to transient heating as under fire conditions, where considerable amount of free moisture, especially in the case of relatively younger and thicker sections, may still be present.

CHAPTER 3

Behaviour of structural concrete elements exposed to high temperatures

3.1 Introduction

Concrete, at the beginning of its widespread application as a construction material, was considered to have an indefinite fire resistance. However the considerable damage suffered by reinforced concrete structures in fires has changed this view, resulting in the investigation of the effect of high temperatures on concrete both on the material level and at structural level. Standard furnace tests were devised to be carried out on individual structural elements in accordance with certain specified procedures including heating rate, moisture conditioning and state of loading, with a view to assessing on a comparative basis, the behaviour of such elements exposed to a transient heating rate considered to be severe enough to represent certain fire conditions. A general review of such tests is presented in this Chapter.

3.2 Previous research on the behaviour of structural concrete elements exposed to elevated temperatures

In 1920 Hull [3 01] published the results of some standard furnace tests on reinforced concrete columns carried out in Pittsburgh laboratories, USA. The variable included two types of aggregates i.e. gravel and limestone, and two kinds

of lateral reinforcements. The columns, either circular or square in cross - section with 40 mm clear cover, were axially loaded with design load and heated according to a standard temperature - time curve. The columns made from limestone concrete performed better than similar ones made from gravel concrete. With the latter, the concrete cover showed a marked tendency to disintegrate and spall early in the heating period causing the steel temperatures to rise rapidly. This trend was most prominent with spirally reinforced circular columns. The round columns with ties spaced at 305 mm suffered much less from such spalling of the concrete cover. Square columns also had extensive spalling. Limestone aggregate columns did not show such spalling. The poor results of the gravel concrete were attributed to excessive thermal expansion of gravel aggregates, particularly at high temperatures.

Later tests on concrete columns made from blast furnace slag and trap rock aggregates also did not show any spalling of the concrete cover, and thus confirmed that the behaviour of concrete columns were largely influenced by the aggregate type. However, the blast furnace slag concrete showed surface blisters due to miniature surface explosions.

Younger specimens (4 months old) unlike the older ones (6 to 9 months old) showed steam and water issuing from the surfaces during heating. Hull suggested the use of expanded metal mesh for gravel concrete columns to prevent the spalling of the concrete cover during fire.

In 1943 Menzal [3.03] followed up his previous works [3.02] on fire resistance and strength of walls of concrete masonry units by test on 1625 mm by 1830 mm reinforced concrete slabs with variable thickness (150 to 200mm). The specimens were loaded in a vertical position to simulate solid wall section and carried an imposed stress of 2.8 to 3.5 N/mm^2 on the longer edge. Two thermal cycles limiting the average temperature rise on the unexposed surface to 121 °C were applied and then loaded to failure at room temperature. The other variables included aggregate type i.e. gravel with either siliceous or calcareous sand, fine and crushed haydite, and maximum aggregate size of 10 mm and 20 mm.

The fire endurance period of the slabs increased greatly with increase in slab thickness. For each type of aggregate, the fire endurance period was doubled when the thickness was increased by 35 to 40%. The slabs made from haydite concrete gave a 10 to 40% longer fire endurance period compared to slabs of equal weight but made from siliceous or calcareous gravel aggregate concrete. This was attributed to what Hull termed 'tenaciously held moisture' with the thicker haydite slabs.

He suggested that the fire endurance period of reinforced concrete slabs could be related to the time taken to attain critical temperature, taken to be 538 °C in the reinforcement nearest to the exposed surface. Accordingly, he established the thickness of concrete cover necessary for a given fire endurance period for the particular types of concrete used by him.

In 1951 Ashton [3 04] presented the results of standard furnace test on pre-stressed concrete floors carried out at Borehamwood fire research station. The floor specimen (3050 mm x 3650 mm x 150 mm), made from a number of precast pre-stressed concrete units, was naturally air-dried before testing. The results indicated that with thin pre-stressed sections, concrete could suffer spalling at high temperatures. The steel temperature was between 300 °C and 400 °C before collapse occurred.

Ashton suggested that at the initial stage, the specimens deflected under temperature gradient. But with rise in temperature, the pre-stress was gradually lost which led to increased deflection. The deflections were similar to those unrestrained reinforced concrete specimens tested under similar conditions but were much higher than those for restrained reinforced concrete beams.

He reported that use of larger diameter pre-stressing wires increased the tendency of the concrete cover to spall off early in the test. As expected the application of plaster to the exposed surface increased the fire endurance period appreciably.

In 1959 Robertson and Ryan [3 05] suggested on the basis of tests on fifty specimens, that the structural failure of floors and beams could be satisfactorily defined as the point at which either the central deflection reached $L^2 / 800\,h$ or the rate of central deflection reached $L^2 / 150h$ where L and h denote the span and the effective depth respectively.

In 1961 Ashton and Bate [3.06] carried out tests to investigate the fire resistance of post-tensioned pre-stressed concrete beams made from rapid hardening Portland cement and Thames Valley aggregates. The other variables included specimen size and shape, location of pre-stressing tendon. Their findings suggested that the mode of failure was influenced by the specimen size. For bigger specimens (4/5 scale), secondary mild steel reinforcement was needed to ensure that the concrete cover did not spall off thereby exposing the reinforcement to direct flame resulting in premature failure of the specimens. For even bigger specimens (6/5 scale), web reinforcement was necessary to prevent shear failure. They also observed an increase in fire resistance for the beams of 1/4 [th] and 3/8 [th] scale models by 58 and 26% respectively, whereas a decrease of 16 % occurred with the ½ scale models.

A 25 mm thick vermiculite concrete lining applied to the beam soffits increased the fire resistance by more than two hours. However, for beams of 4/5 and 3/8 scale, such treatment led to explosive spalling of the concrete. They suggested that this was due to insufficient drying of the interior of the larger specimens due to the vermiculite lining.

These findings led them to conclude that the standard furnace tests must always be carried out on full-scale models as required by the codes. However, it is probable that the main reason for the discrepancy in the test results was the fact that only the specimens were scaled linearly without any due consideration to other factors such as heating rate, as suggested by Issen [3.20] later on.

In 1961 Harmathy [3.07] developed a numerical method capable of solving one dimensional transient heat flow problems which can be applied to calculate the temperature history of building elements during fire exposure. In cases where structural failure is not anticipated, such calculations can yield the fire endurance periods.

In 1962 Selvaggio and Carlson [3.08] described the results of an exploratory study of the effect of varying intensities of restraint of the thermal expansion of precast pre-stressed concrete double-tee floor elements during the course of a standard furnace test. The main variable involved was the amount of linear expansion along the axis of the span allowed before further expansion was stopped.

The results indicated that a large amount of longitudinal thermal expansion in restrained flexural members could be accommodated with very satisfactory structural performance in the standard furnace test. The large thermal thrusts developed in some of the tests indicated that full restraint in an actual building fire is not likely to occur, since the forces were greater than most abutting or restraining constructions found in buildings can accommodate without significant deformation. The property of plastic flow of concrete at high temperature apparently can play an important part during fire exposure to relieve high stresses. Their results also indicated that artificial drying could result in appreciably lower thermal endurance period by lowering the moisture level

In 1964 Selvaggio and Carlson [3 09] tested 16 pre-tensioned pre-stressed concrete I beams measuring 6100 mm span. The variables were aggregate type, i.e gravel, siliceous, limestone and three types of commercially available expanded shale aggregates. Two degrees of load intensity, calculated from $U = (1.2 D + 2.4 L)$ or $1.8 (D + L)$ where U denotes the ultimate load, D and L denote the dead load and the live load respectively, were used.

They observed that the structural fire endurance period was dependent on both loading intensity and aggregate type. Beams with lightweight aggregate had an average of 155 minutes fire endurance, up to 33% more than the beams made from normal weight concrete when the live load was calculated from the first consideration. With the second type of load intensity, the improvement in the fire endurance period was up to 40% more for the lightweight aggregate concrete specimens. However, this loading intensity led to more rapid increase in mid-span deflection and failure occurred at a lower average strand temperature.

In 1965 Ashton [3 10] reported the results of a series of test carried out at Borehamwood Fire Research Station, UK, on simply supported and restrained pre-stressed concrete beams. He noted that for the specimens with a span of 3050 mm, the fire resistance was not appreciably affected by the longitudinal restraint to thermal expansion. This observation was in contradiction to that made by Salvaggio and Carlsun [3 09]. However, he indicated that the mode of failure itself was influenced by the end restraint. Such end restraint also resulted in

considerable reduction, by more than two-thirds, in the central deflection of the specimen. However, structural failure of the end restraint beams was sudden, without much prior warning. Ashton [3.10] pointed out that any inferences from such tests on end restraint beams would be inconclusive in the absence of a quantitative evaluation of the degree of restraint imposed and the forces involved.

In 1966 Pearse and Stanzak [3.11] showed that the structural fire resistance of simply supported, composite floor construction was higher than that of a simply supported non-composite floor. They also observed that the improvement in the fire endurance was proportional to the degree of composite action involved, which also influenced the magnitude of the restraint forces developed.

In 1966 Selvaggio and Carlson [3.12] showed that in actual fire conditions, complete restraint is never realized due to the deformation of the restraining construction. The maximum degree of restraint to floors or roofs in building fires occurs in the situation where an interior bay of a multibay construction becomes highly heated by an isolated and confined fire. The surrounding much larger and cooler construction restricts the thermal expansion of the floor or roof construction of the bay.

They suggested that when test conditions simulating maximum actual restraint are sought with fixed type restraining frames, the factors involving the elastic

deformation of the restraining construction, drying shrinkage of the specimen and cracking of the restraining construction should be considered.

In 1966 Harmathy [3.13] extended Dorn's creep theory into a form applicable to the calculation of deformations of structural elements at high temperatures and stresses. He presented both rigorous and simplified techniques the calculation of deflections of joists and beams during standard furnace tests, using the extended form of Dorn's creep theory [3.47].

In 1966 Bletzacker [3.14] studied the effect of varying level of end restraint on the fire endurance of 12 beams and slab constructions. Some of these were composite construction whereas others had what he termed a pseudo - composite action. He observed that the end restraint increased the fire endurance by up to 25% compared to unrestrained specimens. The increase, in endurance time for an optimal level of restraint was nearly 50%. The optimum was defined by him when the magnitude of restraint generated was sufficient to produce simultaneously the negative bending moment hinges near the beam ends and positive bending moment hinge at the mid-span.

For unrestrained assemblies, the degree of composite action involved did not materially affect the fire endurance period. He noted that the temperature rise in the steel section did not give any proper indication of impending structural failure and questioned the validity of such critical limits. However, he concluded that in

cases where it was not possible to apply superimposed loads on the structural members, such temperature rise criteria could serve a useful purpose in evaluating the structural fire endurance period.

In 1966 Dougill [3.15] used a theoretical approach to show that the fire endurance of reinforced concrete columns is appreciably reduced if thermal expansion is restrained, as usually happens to the columns in a multi-storey building when fire breaks out in a lower storey. The amount by which the fire endurance is affected depends on the degree of restraint employed which under practical condition depends on the number of storeys situated above the affected one. Accordingly, he questioned the current practice where reinforced concrete columns are tested without any degree of restraint whatsoever. He also questioned the general practice in standard furnace tests where the continuity effect is ignored not with standing the ability of reinforced concrete structural members to achieve a redistribution of forces and bending moments within a continuous structure.

In 1966 Issen [3.16] developed similitude relationships for thermo-elastic and thermo-inelastic behaviour, heat transfer and mass transfer, which may be useful in deriving full scale test results from model furnace tests. He showed that the most difficult physical restriction imposed by the similitude requirements was that of thermal scaling. For similitude of thermal scaling, the time intervals in a model test must be proportional to the square of the scale factor. His pilot tests on

models larger than prototype showed the general validity of the similitude relations derived.

In 1967 Gustaferro and Selvaggio [3.17] tested eleven pre-tensioned, pre-stressed concrete slabs supported on rocker-roller arrangements over a 3650 mm span and loaded to various fractions (40 and 60%) of their calculated ultimate load by five equispaced hydraulic rams. The other variables included aggregate types i.e. gravel and lightweight aggregates, and the cover thickness i.e. 25 mm and 75 mm.

In general they noticed that the fire endurance of the lightweight aggregate concrete specimens was better than the gravel aggregate concrete ones. They suggested that the ultimate moment capacity of simply supported, pre-stressed concrete slab or beam sections could be estimated within reasonable limits by using concrete and steel strengths at the temperatures attained by these.

Their test data from 915 mm x 915 mm slab specimens with varying thickness and made from 10 mm maximum size carbonate, siliceous or expanded shale aggregates, showed that, at a given distance from the exposed surface, the internal concrete temperature was practically independent of the slab thickness in the 100 mm to 250 mm range for any type of aggregate used.

In 1968 Abrams and Gustaperro [3.18] studied the effect of slab thickness ranging from 25 mm to 190 mm, aggregate types i.e. siliceous carbonate and expanded

shale, as well as moisture conditioning method via natural and kiln drying, on the fire endurance of concrete slabs. They observed that the temperature rise on the unexposed surface could be divided into four distinct stages: a no rise period, followed by an initial rise period, which ended in a constant temperature plateau succeeded by a fairly uniform rate of temperature rise. The duration of the temperature plateau period varied with aggregate type and slab thickness. They inferred that it was essentially dependent on the amount of moisture present in the specimen at the time of test.

The expanded shale concrete slab had the highest fire endurance period followed by those made with concrete containing carbonate and siliceous aggregates respectively. For the 100 mm thick slabs, the fire endurance periods were 2.33, 1.45 and 1.33 hours respectively.

By comparing the results of their tests on 915 mm square slabs with those of full scale specimens (4250 mm x 5500 mm) having the same thickness and made from similar concrete, they noticed that in general small scale tests gave somewhat less conservative results.

Their test results indicated that the moisture-conditioning method used could appreciably affect the fire endurance of otherwise similar specimens. The kiln-dried specimens gave poorer performance. They also suggested empirical expressions to determine the fire endurance of specimen with standard moisture content, from test results of specimen with non - standard moisture content.

In 1968 Saito [3.19] presented the results of his theoretical analysis of the effect of end restraint on both reinforced and pre-stressed concrete flexural members, 100 mm thick and exposed to a standard heating rate on one side. The theoretical temperature distribution assumed by him allowed for moisture migration and its evaporation. In the analysis, tensile cracking of concrete was also taken into account. The variables studied included different degrees of restraint for axial thrust and/or moment and heating from either the tension or the compression side. His analysis indicated that for unrestrained flexural members heated on the tension side, yielding failure similar to that of an under-reinforced beam occurred, whereas, for similar members heated from the compression side, compression failure of concrete similar to that in the case of over-reinforced beams occurred. The analysis also indicated that, with end restraint, the behaviour of flexural members exposed to high temperature was affected by the initial strain in the reinforcement, and hence a difference in the behaviour between the reinforced and pre-stressed concrete members existed. However, in the case of end restraint, the influence of initial strain in reinforcement was overshadowed by that due to end restraint.

In the case of axial restraint only, the restraining force increased with rise in temperature till the specimen yielded and, if the specimen did not collapse, it decreased thereafter according to the diminishing effective sectional area of the member. His results indicated that for axial restraint, the concrete in the exposed surface of a flexural member heated on the tension side was subjected to

compressive strain. This strain might reach a critical limit to cause the concrete to suffer compressive failure in the form of explosive spalling. However, if the compressive strain did not exceed the critical limit, then a marked improvement in the fire endurance would result due to a reduction of the working stresses in the reinforcement. For restrained flexural members, heating on the compression side could not only result in the lowering of the critical compressive strain value but also would cause an increase in the concrete strain on the compression side resulting in compression failure.

In 1970 Isson, Gustaferro and Carlson [3.20] investigated the fire resistance characteristics of a large number of reinforced and pre-stressed concrete flexural members, which included beam-slab construction, double T-beams and I-beams, tested under varying degree of restraint to thermal expansion, ranging from 1.0 mm to 35 mm in 5500 mm length. Both gravel aggregate and lightweight aggregate concrete were used.

They reported that, within a reasonable degree of tolerance, the thermal thrust was directly proportional to the heated perimeter i.e. the portion of the perimeter of the cross-section of the specimen at right angle to the direction of the thrust, which was actually exposed to heat. The thermal thrust was also proportional to the initial modulus of elasticity of concrete when all other parameters such as maximum allowable expansion, aggregate type and initial stress distribution were

unaltered. They suggested the following expression to calculate the thermal thrust.

$$T_f = T_o \cdot (S_p/S_o) \cdot (E_{cp}/E_{co}) \quad \text{...} \quad (3.2)$$

where,

T_f = estimated maximum thermal thrust for new test specimen for a given allowable thermal expansion,

T_o = maximum thermal thrust obtained from specimens with similar concrete and having same allowable thermal expansion,

E_{cf} = modulus of elasticity of concrete in new test specimen at 28 days,

E_{co} = modulus of elasticity of reference concrete type at 28 days,

S_f = heated perimeter of new test specimen,

S_o = heated perimeter of reference concrete type.

T_o, E_{co} and S_o could be obtained from charts and data supplied by them for the particular types of concrete.

In 1973 Abrams, Gustaferro and Salse [3 21] tested eight 4275 mm x 5500 mm reinforced concrete pan-joist floors made from carbonate, siliceous and expanded shale aggregates. The other variables included slab thickness i.e. 64 mm and 133 mm and the amount of permissible thermal expansion ranging from 7.5 mm to 28.0 mm in the 5500 mm length.

The results indicated that, early in the test, the resulting longitudinal thermal thrust acted near the bottom of the joists, but gradually its line of action rose as

the test progressed. However, the line of action of the lateral thrust was generally near the bottom of the slab throughout the tests. They verified the method of Issen, *et al* [3.20] and showed that the thermal thrusts could be estimated to within 15% of the measured value, which varied between 3.5×10^6 N and 0.5×10^6 N. They also developed interaction diagrams to explain the structural integrity of the specimens in terms of thermal thrust.

The fire endurance of all the specimens was determined by the temperature rise on the unexposed surface when the steel temperature ranged between 700 °C and 980 °C.

They found that good correlation existed between the unexposed surface temperature of the full-scale specimens and 915 mm x 915 mm slabs of similar thickness and concrete.

In 1974 Gustaferro, Abrams and Salse [3.22] tested thirteen pre-stressed and reinforced concrete beams, simply supported on roller bearings with 12.2 m span and loaded to around 50% of their calculated ultimate load capacities at room temperature. The variables included aggregate type (i.e. gravel and lightweight aggregates), steel type and pre-stressing type (i.e. pre-tensioning and post-tensioning). Apart from confirming better performance by lightweight aggregate concrete specimens, they showed that for reinforced concrete beams, the grade of steel, and for pre-stressed concrete beams, bonded or unbonded tendons, did not materially affect the fire endurance. However, they reported that reinforcing mesh

within the concrete cover had no significant effect on the performance of the specimens. The specimens without such supplementary reinforcement spalled less, a finding, which directly contradicted those of Malhotra [3.23].

They also presented a method for calculating the ultimate load capacities and deflections of pre-stressed and reinforced concrete beams during standard furnace tests, in which the thermal and creep strains of concrete and steel were used.

3.3 Previous research on explosive spalling of concrete

This section deals with work covering explosive spalling of concrete at high temperature.

In 1955 Meyer-Ottens [3.24] tested a series of 27 reinforced concrete slabs to investigate the spalling of concrete. The variables included four different mixes, slab dimensions, exposure condition and amount of reinforcement. The simply supported slabs with no superimposed load were heated either from one side only or from both sides. In general, the heating rate employed was that recommended by the German standards, but for some of the specimens, a faster rate was used.

In all the tests, some spalling of the aggregates occurred in which materials of up to 80 mm diameter and 5 mm deep were removed from the surfaces, The greater tendency of the specimens which had isolated blocks (70 mm x 70 mm x 20 mm)

of Limonite (hydrated iron oxide, $2Fe_2O_3 \cdot 3H_2O$) cast into them, might have been due to:

a) The increased free water content during test as limonite is decomposed to form hematite (Fe_2O_3) with the liberation of water, and,

b) Volumetric expansion in the solid phase of this reaction.

A faster rate of heating (1125 °C reached in 15 minutes) caused more extensive spalling where materials to a depth of 5 to 10 mm from regions 100 to 250 mm across were lost from the surfaces. Such a type of failure was termed by Meyer-Ottens as surface spalling. Although surface spalling occurred during the period of visible water vaporisation, the presence of limonite blocks, which increased the free water content during test, in the slabs did not materially affect the behaviour of the slabs.

The more heavily reinforced slabs, heated in accordance with the German standard rate, experienced extensive surface spalling whereby the reinforcement was exposed. Two slabs with the thinnest section (only 50 mm thick) which were heated from both sides suffered destructive spalling. One of these had reinforcing mesh in the mid-plane and the other contained reinforcing mesh at each face with a few limonite blocks in between.

He attributed the cause of the violent failures to the internal stresses due to thermal gradient and the stresses in the aggregates, as well as to the vapour pressure within the concrete mass. He also suggested that the stresses due to

restraining forces and stresses from applied load might also contribute towards such a type of failure.

His observation that the surface spalling occurred during a period of visible water vapourisation and the assertion that presence of limonite blocks (which increased the free water content during test) in the slabs did not cause greater surface spalling than the slabs which did not contain limonite blocks, seem to be contradictory. It may be interesting to observe that the general classification for spalling adopted by Meyer - Ottens [3.24] was similar to those suggested earlier by Dougill [3.25]

Dougill in 1964 [3.25], also in 1969 [3.26] and in 1971 [3.27] suggested that any attempt to attribute spalling of concrete solely to pore pressure as proposed by Shorter and Harmathy [3.28], and Harmathy [3.29] for their moisture clog phenomenon, or solely to thermal stresses as Saito [3.33] in 1965, must be a simplification, since both of these produce stresses in concrete, which together with any other stresses induced by applied load, will determine the behaviour of structural elements. Therefore, he suggested that it may be misleading to classify spalling according to the mechanism supposed to be involved, as Shorter and Harmathy [3.28] had done, and he put forward an alternative classification for spalling as described below.

a. General or destructive spalling-: This is violent in nature and occurs at an early stage of heating. This form of spalling causes extensive damages or complete destruction of a structural member.

b. Local spalling-: This is initiated by the behaviour within a small region of the structure, even though some of the exacerbating influences may affect the structures as whole. It has been further subdivided into:

1. Surface spalling-: This include pitting, blistering and local removal of surface material sometimes in a violent manner,

2. Aggregate splitting-: Failure of aggregate near the surface, often accompanied by surface spalling.

3. Corner separation-: Removal of external corners from beams and columns, occasionally in violent manners.

c. Sloughing off -: This is a gradual progressive form of break down, as reported by Ashton and Bate [3.06] in 1961, involving partial separation of layers of surface material from the member that may continue slowly through the later stages of heating.

d. Shorter and Harmathy and Harmathy's moisture clog phenomenon to explain surface spalling where surface material is dislodged violently, as described in Chapter 4.

Dougill also proposed [3.26] an explanation for spalling of concrete near the surface; he suggested that before heating, the slab may already contain some

shrinkage cracks oriented at right angles to the exposed surface. At the start of heating, drying of the surface may cause additional shrinkage, so causing the cracks to open further before they are closed by thermal expansion. On further heating, the stresses near the exposed surface increase rapidly to a peak value and are then reduced with the increasing thermal strain. When these stresses reach a value of about half the peak stress (Newman's [3.30] discontinuity level), progressive micro-cracking will occur to form planar cracks within the material, parallel to the heated surface. Under increasing thermal strain, the material outside those cracks may become unstable thereby causing spalling at the exposed surface.

Dougill used a simplified analysis based on Timoshenko [3.31] to propose a mechanism of minor surface spalling, which involves exfoliation of the thin mortar layer covering the large aggregate particles nearest to the heated surface, which can occur under actual fire conditions.

In 1965 Odeen [3.32] developed a computer programme capable of calculating temperature profile across a concrete section exposed to high temperature. This calculation took into account such factors as the various temperature dependent thermal properties and the initial moisture content of the concrete section.

In 1965 Saito [3.33] suggested that explosive spalling of pre-stressed concrete exposed to high temperature was a compressive failure in nature, caused entirely

by the thermal stresses induced by the non-linear temperature distribution across its section. He completely rejected the notion that the steam pressure of the heated water within the concrete voids caused such failure as suggested by others, [3.24, 3.34]. He presented a series of expressions derived entirely from elastic considerations, to give the critical stress condition at which such failure can occur. His analysis indicated that for a pre-stressed or reinforced concrete section subjected to standard furnace test, a stress profile develops which consists of compressive stresses acting both on the heated and an the unexposed faces with tensile stresses acting on the central part. In the case of a simply supported reinforced concrete member, the tensile strain at the interior reaches the ultimate strain early, causing the inside of the specimen to crack, Thereby the tensile and subsequently the compressive stresses are relieved. However with pre-stressed concrete members, the internal tensile strain may not reach the ultimate tensile strain due to the large compressive strain induced by the pre-stressing. On the other hand the compressive strains become larger by the addition of this pre-stressing strain to that resulting from the thermal stresses. Finally a situation may arise when the compressive strain reaches the critical limit to cause failure of the specimen. This, he suggested, was the mode of explosive spalling of pre-stressed concrete exposed to high temperature.

Saito further indicated that the explosive spalling of pre-stressed concrete was not necessarily influenced by the specimen thickness. However, he suggested that for thinner sections, the compressive failure on the surface might induce total failure

of the specimen as a whole, thereby giving the impression that, for thinner sections, the failure was more destructive.

He suggested that presence of excess moisture in the specimen assisted in the explosive spalling in an indirect way by causing steeper temperature gradient across the specimen and hence increased compressive stresses during vapourisation when the internal temperature remained constant at around 100 °C for sufficient time.

He suggested that explosive spalling of pre-stressed concrete members could be avoided by adding fireproof covering to its surface thereby minimising the temperature gradient across the section.

In 1969 Malhotra [3.23] reported the results of a comprehensive series of tests carried out at the Fire Research Station, Borehamwood. on simply supported reinforced, pre-stressed and concrete encased steel beams with rectangular sections, all of which were designed to have a four - hour fire endurance period. Some of these specimens with 7300 mm span were provided with an overhang at either end to produce negative bending moments at the supports during testing. The other variables included aggregate type (i.e. gravel and lightweight aggregates), and steel type (i.e. mild steel, cold worked steel and hot rolled alloy steel). The concrete cover for the reinforced concrete specimens varied from 25 mm to 63 mm, and the cross-section of some of the pre-stressed concrete beams were altered to I-section with a slab section cast on top.

The test results indicated that, with gravel aggregate concrete, spalling occurring within the first half hour of the test leading to premature failure, For concrete cover greater than 40 mm, supplementary reinforcement in the form of wire fabric mesh or stirrups at 150 mm spacing was needed to prevent it from spalling, and thus an increase in the fire endurance resulted. None of the lightweight aggregate concrete beams showed any sign of spalling and as such did not require any supplementary reinforcement.

The tests clearly demonstrated that the thermal insulation property of lightweight aggregate concrete was better than the gravel aggregate concrete. The difference in the performance of the types of steel was nominal and remained within 10% of each other.

The continuity effect of the beams with overhang did not affect the performance of the specimens materially.

The results indicated that existing data on the fire resistance of pre-stressed concrete beams of rectangular section were adequate to enable one to design from current recommendations for a specific fire endurance time. This was not the case with pre-stressed concrete beams with I-section which required supplementary reinforcement in the web to prevent premature failure. He suggested that the cover for the reinforcement of the I-section beams should be increased to take into account the increased heat transfer brought about by such a cross-section.

In 1976 Dougill [3.35] reported the results of an experimental and theoretical investigation into the spalling of concrete. Tests were carried out on a concrete

wall unit consisting of eight separate panels, 100 mm thick by 2450 mm high by 305 mm wide containing only nominal reinforcement close to the unheated surface. The panels had a rhomboidal cross-section to minimise flame passage and radiation loss through the joints. The concrete consisted of 12 mm down Thames Valley gravel aggregates and ordinary Portland cement. The aggregate-cement ratio and the water-cement ratio for the eight panels were varied between 3.0 to 6.0 and between 0.45 to 0.85 respectively.

Dougill observed steam issuing from the hot face after 12 minutes of exposure to standard furnace test heating rate. From about the 15th minute of heating, the unheated side curved visibly with the exposed side showing some splitting and blowholes. Free water appeared on the unexposed surface after 25 minutes of heating and continued to be driven off for some time. The internal temperature readings showed steps at above 100 °C indicating vapourisation of moisture from the "interface" of varying saturation between a dry zone near the exposed surface and an inner wet zone. The depth of the interface was estimate to be 19 mm from the hot face where moisture had evaporated at 150 °C at about the 15th minute of heating.

The close similarity of the temperature readings of all the panel units made with different concrete mixes led him to conclude that the thermal properties of concrete were only nominally affected by the mix proportions. Dougill also showed experimentally that larger sized aggregates were more liable to splitting failure than smaller sized aggregates.

For analytical purposes, Dougill developed computer programs capable of calculating internal temperature distributions for the panel units during heating. The analysis considered an initial, parabolic moisture distribution within the specimen and assumed moisture to evaporate from the interface between the dry zone near the exposed surface and an interior wet zone as the interface receded from the exposed surface but he ignored the small amount of moisture lost from the cement hydrates at the dry zone. The results showed good agreement with the experimentally determined internal temperature at various locations.

The calculated temperature distributions were used to determine the stresses in the heated wall panels by a step-by-step analysis. He considered cracking and crack closure as well as the behaviour of concrete under compression notably that beyond the peak stresses and also during unloading. He neglected creep since explosive spalling occurred during the first half hour of a standard furnace test. His computational analysis indicated a number of different modes of progressive structural deterioration of concrete under fire conditions and also suggested the circumstances when sudden failure could occur as a result of instability of the entire panel.

Hertz in 1984 [3.36] performed an investigation on high strength (60 - 200 MPa) concrete cylinders (200 x 100 mm) to study the behaviour of high strength concrete under high temperatures. Hertz exposed the specimens to the relatively slow heating rate of 1 °C/min up to a maximum temperature of 650 °C. The

moisture content of the concrete varied between 1.2 to 3% (by weight). Explosive spalling took place in 33% of the tested cylinders. It was concluded that high strength concrete might explode at slow rates of heating.

In 1985, Williamson and Rashed [3 37] heated concrete cubes of strengths ranging from 41 to 121 MPa containing different amounts of silica fume. The specimens were exposed to constant temperatures 20 °C, 320 °C, 520 °C, and 700 °C. No spalling was recorded in either the normal or high strength concrete specimens. An important conclusion of the study was that the loss of compressive strength at elevated temperatures was greater for high strength concrete containing silica fume than for concrete without silica fume.

In 1988 Shirley *et al* [3 38] performed tests on high strength 900 x 900 x 100 mm concrete slabs. The slabs were made using four high strength concretes (69 - 117 MPa) and one normal strength concrete (55 MPa). No Spalling was observed in any slab and the study concluded that the fire resistance of normal and high strength concrete was not significantly different.

In 1990 a study by Castillo [3 39] demonstrated that the imposition of axial loads on high strength concrete increases its susceptibility to spalling. During experimental research on normal strength (31 - 63 MPa) and high strength (89 MPa) concrete cylinders, violent explosive spalling were recorded only in high

strength concrete specimens loaded to 40% of their cold compressive strength. Unloaded specimens of both concrete types did not spall but showed a reduction in strength of 30%.

In 1992 Hertz [3.40] prepared a series of specimens with granite aggregate and silica fume contents of 0, 5, 10, and 15% of cement by weight, and moisture content in equilibrium with air conditions. None of these specimens exploded when heated at rates of 1 °C and 5 °C per minute to 600 °C. He concluded that concretes densified by means of silica fume at high moisture contents are more likely to explode and suggested an upper limit of 10% by weight of cement on silica fume to avoid spalling. In 1993 these conclusions were also verified by Sanjayan and Stocks [3.40] after conducting a fire test on monolithic beam-slab (T-beam) specimen containing 8% silica fume.

In 1993 Stocks [3.41] exposed two realistically sized T-beams to fire according to time-temperature curve AS 1530.4. One beam was fabricated from normal strength concrete (27 MPa) and the other from high strength concrete (105 MPa). The high strength concrete T-beam explosively spalled after eighteen minutes at 128 °C (concrete temperature) while the normal strength concrete remained stable.

They concluded that:

- High strength concrete is more prone to explosive spalling than normal strength concrete.

- The presence of cracks reduces the possibility of explosive spalling.

- Large concrete covers increase the possibility of concrete exploding.

In 1993 Furumura *et al.* [3.42] tested normal (29 - 45 MPa) and high strength (66 MPa) concrete 50 x 100 mm cylinders under constant temperatures ranging from 100 °C to 700 °C. The temperatures were raised at the rate of 1 °C/min. The cylinders were axially loaded as the authors intended to obtain the stress-strain curve of concrete at high temperatures. The samples were tested at different ages and the oldest was 1.5 years old. They did not observe spalling in any of the specimens tested.

In 1994 Tachibana *et al* [3.43] reported surface spalling during fire tests on high strength concrete (88 MPa) Two realistically sized walls (1200 x 1200 x 150 mm) were heated at a rate of approximately 35 °C/min. Two types of coarse aggregates were used: crushed hard sandstone and crushed quartz schist. Surface spalling was observed over 100% of the surface of the slab containing crushed quartz schist and over only 40% of the slab containing crushed hard sandstone.

In 1996 to 1999 Marcel Cheyrezy [3.44] and his team carried out research on high performance concrete at high temperature. Their main objective was "To understand the response of High Performance Concretes (HPC) and Ultra High

Performance Concrete (UHPC) under high temperatures, thus making it possible to design structures specifically for accidental loads, or use in high temperature environments".

Their project investigated a number of different concretes, with compressive strengths in a range from 60 MPa to 200 MPa. Each of these concretes was meticulously characterized and specimens were then exposed to fire in a carefully controlled test.

Six different types of concretes were tested in their project, designed to cover a wide range, from a type of HPC which can be routinely made and is used more and more, to a type of concrete termed UHPC. Both of the UHPC's tested, one known as Reactive Powder Concrete (RPC) and the other known as Compact Reinforced Composite (CRC) are extremely dense with micro silica/cement contents of 20 - 25% and water/binder ratios of 0.12 - 0.16. The HPC's are described by strength class, and as two different types of C60 concrete have been included, the one with micro silica. The capillary porosity in C60 varies from one part of the paste to another corresponding to a difference in w/c ratio of 0.15. Capillary porosity is high in the transition zone between aggregate and paste, particularly around the largest aggregates.

Their fire testing was carried out in two stages. In the first stage a number of short columns were tested with and without load, primarily to test spalling behaviour. Some of the columns were prepared with two chamfered edges, and two edges without chamfers, and it was quickly evident, that thermal stresses

would cause the corners to spall. A few of the small columns (cross sections of 200 x 200 mm and 280 x 280 mm) showed considerable surface spalling, especially under load. The stronger of the concretes - C90, CRC and RPC - showed the most severe degree of spalling.

The project also included a number of fire tests on larger specimens, large columns, beams, and a container for nuclear waste storage and tunnel section. The tests showed that larger section sizes would reduce the risk of spalling. From the experimental results they claimed that for spalling, it is not so easy to arrive at a clear conclusion. Whether or not spalling will occur depends on a number of parameters, such as section size, stress/strength ratio, heating rate, permeability and moisture content. A number of these parameters are linked, for instance, reducing the moisture content by drying will also affect properties such as strength and permeability, which makes it difficult to prepare a simplified model. Furthermore, spalling appears to present stochastic behaviour, in part due to concrete being an inhomogeneous material - at least on the level of importance for pore pressure and transport.

In 1998 Felicetti and Gambarova [3.45] prepared concretes with 6.7% and 9.7% silica fume, flint aggregates and Type V Portland cement. They found that the addition of silica fume highly densifies the pore structure of concrete, which results in explosive spalling due to the build-up of pore pressure by water vapours. Since the evaporation of physically absorbed water starts at 80 °C,

which induces thermal cracks, such concretes show poorer performance as compared to pure OPC concretes at elevated temperatures.

In 2001 Chi-sun Poon [3.46] and his team carried out tests to find the strength and durability performance of normal and high strength pozzolanic concretes incorporating silica fame, fly ash and blast furnace slag at elevated temperatures up to 800 °C. The strength properties were determined using an unstressed residual compressive strength test, while durability was investigated by the rapid chloride diffusion test, mercury intrusion porosimetry (MIP) and crack pattern observations. The mix proportions of 9 high strength and 5 normal strength concrete mixes were prepared and different percentage pozzolanas were introduced as cement replacement material for different strength mixes. At an age of 60 days, with the rate of heating 2.5 °C per minute, the specimens were heated in an electric furnace up to 200, 400, 600 and 800 °C and then allowed to cool naturally to room temperature.

From the experiment results they concluded that pozzolanic concretes containing fly ash and blast furnace slag give the best performance particularly at temperatures below 600 °C as compared to the pure cement concretes. Explosive spalling occurred in most high strength concretes containing silica fume. A distributed network of fine cracks was observed in all fly ash and blast furnace slag concretes but no spalling or splitting occurred. The high strength pozzolanic concretes showed a severe loss in permeability-related durability than the

compressive strength loss. Thirty percent replacement of cement by fly ash in high strength concrete (HSC) and 40% replacement of cement by blast furnace slag in normal strength concrete (NSC) was found to be optimal to retain maximum strength and durability after high temperatures.

Previous researches given in this chapter are a few of the important researches carried out on the behaviour of structural concrete elements exposed to elevated temperatures.

CHAPTER 4

Effect of moisture in concrete exposed to elevated temperatures.

4.1 General consideration

Like other passageway porous materials, the properties of concrete are liable to be influenced by water subject to the state in which it occurs. The states in which water can occur in concrete are classified on the basis of its degree of attraction to the solid phase. Powers and Brownyard [4 01] used this principle to classify the water present in concrete as evaporable and non-evaporable water depending on whether it could be removed under specific conditions of pressure and temperature. Evaporable water is usually present in the capillary and gel pores of the concrete mass and the non-evaporable water occurs as the water of hydration of the cement hydrates.

4.2 Classification of water present in concrete.

Luikov [4 02] suggested that the degree of attraction or the form of bond between the moisture and a moist capillary porous material such as concrete could be classified on the basis of the bond energy expressed in terms of the heat of evaporation. He classified the evaporable water described by Power and Brownyard [4 01] into two parts according to the following principle:

a. Adsorptionally bound water, which is represented by a mono-molecular layer on the internal and external surfaces of a capillary porous material,

b. Capillary bound water contained in the capillaries, except for the very thin layer of water, which is adsorptionally bound to the walls of the capillaries,

Nielsen [4 03] classified Luikov's [4 02] capillary bound water into two categories:

a. Water, which is capillarily fixed to the cement gel,

b. Water, which is contained in comparatively large voids in the concrete without being chemically or physically fixed to the solid constituents,

He referred to the last category of water as free water.

Ishai [4 04] sub-divided the evaporable water into five separate states:

a. Capillary water,

b. Gel pore water,

c. Water adsorbed on crystal surfaces,

d. Water adsorbed and confined between adjacent crystal surfaces

e. Zeolitic intra - crystalline water.

From the above subdivisions the water present in high strength concrete can be conveniently divided into four major states:

a. Chemically bound water or water of hydration,

b. Adsorptionally bound water mainly present in the gel pores of the hardened cement paste,

c. Capillarily fixed water present in comparatively small capillaries,

d. Free water present in the larger capillaries.

At any given time, the water present in concrete tends towards a condition of equilibrium between the above four states. This condition of equilibrium depends, among other factors, on the specific properties of the cement, the mix proportions and on the environmental condition. So long as the hydration of the cement paste continues, the condition of equilibrium changes as the water passes gradually from states (c) and (d) into the states (a) and (b).

The formation of the water of hydration in the cement paste is not reversible under normal thermal conditions (i.e. at 23 °C) and under water vapour pressures higher than 6×10^{-4} mm of mercury, according to Powers and Brownyard's [4.01] definition of non-evaporable water. However, the water in states (b), (c) and (d) generally tends to be in equilibrium with the water in the surroundings of the concrete. The free water contained in the larger capillaries evaporates if the water vapour pressure in the surrounding drops below the saturation pressure. On the other hand, if the vapour pressure of the surroundings is above the saturation pressure of the air within the concrete, it will absorb moisture from the surroundings by an amount depending on the volume of the larger pores. The

amount of adsorptively and capillarily fixed water also varies with the water vapour pressure in the surroundings of the concrete [4 01].

Generally speaking, when concrete is exposed to fire, the order in which the evaporable water is lost bears some relationship to the pore size in which it occurs [4 05] with the water from the largest pores being lost first, followed by water from the next sized pores and so on. However this process not a discrete one as may appear here, in fact it is a continuous process in the sense that, when water is being lost from the large pores, moisture movement in the next sized pores may already be in progress. This is particularly so under higher temperature and lower vapour pressures. A reversed order is followed during curing, when concrete absorbs moisture from the surroundings, i.e. the smaller sized pores become saturated first and the largest sized pores are saturated last of all.

4.3 Effect of moisture on concrete properties at room temperature

Strength, modulus of elasticity and the rheological properties of concrete are directly dependent on the amount of chemically bound water present in the concrete, which assists in the hydration of cement paste and thus leads to strength development. The adsorptionally and capillarily bound water, generally speaking, result in a reversible reduction of the concrete strength. For example, Gilkey [4 06] showed that concrete specimens gently air-dried before testing exhibit ultimate compressive strengths 20 to 30% higher than those obtained from saturated

specimens. Lea [407] also pointed that if matured and dried concrete is subsequently wetted in water there is a drop in compressive strength of 20 to 40 %, this is due to the following reasons:

a) A general weakening of the cement gel due to the adsorbed water

b) A reduction of the surface forces (van der Waals) between gel particles in the presence of adsorbed moisture, or, in other words, removal of adsorbed water causes an increase in van der Waals forces thereby producing a stronger, more rigid structure.

Mills [408] suggested that the strength of cement gel is due to a combination of inter-locking gel particles plus van der Waals forces between gel particles.

The thermal properties, density, permeability and the ability to absorb electro-magnetic radiation are dependent only on the total amount of water present rather than on their individual states [403] The fire resistance of concrete primarily depends on the amount of water which can evaporates at the temperature in question.

It should be noted that a property such as the frost resistance of concrete, though directly dependent on the percentage of freezable water (which roughly corresponds to the free water content), might also depend indirectly on other types of water present. For example, the ultimate strength and rheological properties of concrete, which are dependent on the gel pore water, would dictate the stresses and strains in concrete under frost action.

Various research workers have carried out tests to study the properties of concrete as influenced by moisture content at elevated temperatures. These will be briefly discussed in the next section.

4.4 Effect of moisture on concrete properties at elevated temperatures.

Sealed and unsealed specimens have been tested to investigate the effect of moisture on compressive strength, flexural strength and modulus of elasticity of concrete at elevated temperatures. In a such series of tests, Hannant [4 10] observed that sealed concrete specimens which were heated to 1500 °C and then cooled to room temperature, retained only 65% of the reference strength as opposed to 85% for the unsealed specimens tested under similar conditions. His specimens consisted of 150mm diameter by 300mm long cylinders, some with a 50mm diameter concentric hole. These were made from ordinary Portland cement and limestone aggregates, and were cured for two months under water at 20 °C and for a further period of two months either under water or in laboratory air. Some of the specimens were covered with copper foil wrappings to prevent any chance in the moisture content of specimens during testing. The specimens, which were heated up to 150 °C at a rate of 15 °C per hour to avoid thermal shock were loaded tri-axially compression to failure, after they had been cooled to room temperature. He observed that the strength of all cylinders tested at 100 °C could be related to the moisture loss, the drier specimens showing greater strength. He

also established that the residual strength was dependent on the moisture content of the specimen at the time of test as well as on the test temperature.

Lanyard, *et al* [4.11] also tested scaled and unsealed cylinders (100 mm diameter by 200 mm long) as well as beam specimens (255 mm by 150 mm by 62.5 mm) made from ordinary Portland cement and gravel or limestone aggregates. The specimens, after curing in a fog room for 28 to 200 days, were heated to 260 °C, with some tested hot and some tested after being cooled to room temperature. They observed that with the unsealed specimens:

    a) The compressive strength either increased or slightly decreased.

    b) The flexural strength increased slightly at 80 °C, but showed moderate to slight decreases at 120 °C and 260 °C,

    c) The modulus of elasticity showed slight decrease at all temperatures.

They also observed that the evaporable water was nearly completely lost at 120 °C. Further, an increase in the chemically combined water occurred at 80 °C, and a loss of 10, 20 and 40% of this water took place at 120 °C, 190 °C and 260 °C respectively. They attributed the apparent increase in the compressive strength for unsealed specimens slowly heated up to 260 °C to the removal of the free moisture, since this leads to drier concrete. The drop in the flexural strength after 80 °C was attributed to the loss of the chemically combined water, which offset the beneficial effect of the removal of the evaporable water. The reduction in the

modulus of elasticity under all heating conditions was due to the loss of an incompressible phase, i.e. the evaporable water in the concrete system.

In general, their test results indicated a further deterioration when the specimens were tested after being cooled to room temperature. Though they did not give any explanation for this, it is probable that this was due to reabsorption of moisture by the specimens during cooling.

They suggested that test conditions capable of producing a large thermal gradient or of influencing the moisture content in a given concrete, or both, at the time of testing can override the effects produced by the removal of evaporable water under unsealed condition. They also proposed that parameters such as aggregate type, water – cement ratio, age etc which do not affect the thermal gradient or the moisture content condition will not have a significant influence on the structural properties of concrete. Though this observation itself may be correct, the parameters mentioned by them such as aggregate type can have a considerable effect on the properties of concrete at high temperatures.

In case of the sealed concrete specimens, they observed that:

a) The compressive strength decreased continuously with increased temperature and retained only about 50% of that at room temperature,

b) The modulus of elasticity was severely reduced at all temperatures, particularly at 260 °C where it was only about 30% of that at room temperature.

Lanyard, *et al* also noticed that for the sealed concrete specimens, a change in the hydrated cement phase took place after heating to 190 °C and 260 °C. An X- ray analysis showed the presence of new and more highly crystalline phases which had poorer cementing qualities than the original highly cementitious calcium silicate hydrates. Further, the steam pressure developed in the pore structure of the cement paste and concrete acted as a potential crack driving force. However, they claimed that the vapour pressure of the adsorbed water associated with the cement phase was not the same as that of bulk water at the same temperature, consequently changes in the surrounding water vapour pressure would be expected to modify the behaviour of the adsorbed water with unknown consequences. Local variations in temperature in the specimen could also result in steam pressures inside existing cracks, thereby producing stress intensity sufficient to propagate the same.

They suggested that since exposure time at different temperature determines the amount of evaporable water content, it must be taken into consideration while using results from tests on unsealed specimens. In fact, this parameter can assume great significance under transient heating conditions. They further pointed out that with sealed concrete specimens, the possibilities of hydro-thermal reactions should be considered as well.

4.5 Effect of moisture on the fire resistance of concrete

The presence of moisture may have either a beneficial or a detrimental effect depending upon the amount of moisture present, various properties of the material and the geometry of the element. The effect is taken to be beneficial if the presence of moisture in the structural element increases the fire endurance period. This is caused by the absorption of heat associated with the evaporation of moisture, which slows down the rise of temperature in a structural element during a standard furnace test.

Various research workers have correlated the improvement in the fire endurance in terms of the percentage moisture content of the element. In a theoretical study, Harmathy [4.12, 4.13] showed that for a given material and geometry of construction, the fractional gain in fire endurance in relation to the fire endurance under oven dry condition, $(T_\phi - T_d)/T_d$, is proportional to the volumetric moisture content, ϕ. Thus he concluded [4.14] that the percentage increase in fire endurance in relation to the % moisture content (by volume) is given by:

$$\Psi = (T_\phi - T_d)/T_d * \phi \dots\dots\dots\dots\dots\dots\dots\dots\dots\dots\dots\dots(4.1)$$

It is dependent on the properties of the material and its geometry of construction only. He termed this dimensionless group, Ψ as figure of merit of moisture. He carried out a series of tests as well as theoretical calculations to establish how Ψ

is affected by these parameters [4 14], and showed that Ψ could be directly correlated with T_d, since T_d itself is a function of the properties of the material and the geometry of construction, in the form:

$$\Psi = b/1 + 0.25 \ T_d \ \dots\dots\dots\dots\dots\dots\dots\dots\dots\dots\dots\dots\dots\dots\dots(4.2)$$

Where b is a function of the permeability with the following suggested values:

b= 5.5 for brick, dense concrete and gun applied concrete,

b= 8   for lightweight concrete,

b=10   for cellular concrete.

These values of b were derived experimentally and show that Ψ increases with increased permeability of the material, Harmathy's theoretical analysis on the assumption of zero permeability in the direction of heat flow yielded a value of 4.3 for b.

He combined expressions (4.1) and (4.2) to obtain:

$$T_d^2 + T_d (4 + 4b.\phi - T_\phi) - 4T_\phi = 0 \dots\dots\dots\dots\dots\dots\dots\dots\dots\dots\dots\dots\dots(4.3)$$

which can be readily solved to obtain T_d in terms of fire endurance, T_ϕ at any moisture content, ϕ, and may be used subsequently to find the fire endurance at

any other moisture content. A homogram was derived from the above expression for convenience of solution.

Harmathy [4.14] reported on the basis of his theoretical analysis that fire endurance was not only dependent on the total moisture content but also on the moisture distribution within the body in the form of the movement of the moisture distribution about the surface exposed to heating. With natural conditioning, the moisture distribution of standard furnace test specimens is symmetrical and thus moisture movement is same for both faces, and so the fire endurance period in this case is independent of the moisture distribution itself, and depends on the average moisture content only.

Abrams and Gustaferro [4.15] carried out tests on 915 mm x 915 mm slabs of different thicknesses and aggregate types and moisture contents. Apart from confirming that expanded shale aggregate concrete performs best in a standard furnace test followed by limestone aggregate and siliceous aggregate, they also observed that the fire endurance of the specimens depended on the moisture content of the specimens. They put forward an empirical expression to correlate the fire endurance at the time of test, R_n, to the fire endurance, R_s, at specified moisture content:

$$R_s = ((K.A + (75-H)/5)/100) R_n \dots\dots\dots\dots\dots(4.4)$$

where K and A are constants depending upon the conditioning atmosphere and the concrete type respectively, and H is the relative humidity at the mid depth of the specimen. However, apart from the moisture content, the method of drying employed can also have an important bearing on fire endurance. This fact is significant when an artificial drying method is employed to reduce the conditioning time.

Abrams and Orals [4 16] reported their findings in this regard from a series of tests on 915 mm x 915 mm x 150 mm gravel aggregate concrete slabs, conditioned under both natural drying and artificial methods at different ambient relative humidities. Some specimens were dried by heating to 93 °C others were dried by infrared heat radiation.

A comparison was then made of naturally air-dried slabs with slabs subjected to different drying procedures, in terms of the time required to reach the desired concrete humidities and the humidity gradient through the concrete sections. They expressed the fire endurance of artificially conditioned specimens in terms of the results obtained from companion slabs, which were air dried at 23 °C and 35% relative humidity.

Their results indicated that the ambient relative humidity under which the slabs were naturally air-dried had little effect upon their fire endurance when the slabs had the same relative humidity at mid-depth. However, the fire endurance of the specimens were longer for a higher mid-depth relative humidity. This, they

argued, was due to the variation in the evaporable water made available to the specimens because of the difference in the test relative humidity at mid-depth, which influenced the rate and the degree of hydration as well as the amount of moisture lost during conditioning and hence controlled the amount of evaporable water present.

Abrams and Orals reported a steeper relative humidity gradient across the specimen depth with artificial drying, which indicates that the amount of evaporable water within the concrete had been reduced substantially below that retained by the naturally conditioned specimen. Hence considerably more evaporable water had been removed by artificial drying which resulted in more than 10% drop in the fire endurance period.

Artificially dried specimens were also tested after they had been rehumidified under controlled conditions to produce a uniform relative humidity of 50% and 75 % across the specimen depth. The relative humidity gradient thus obtained, between the mid depth and the outer 20 mm. was similar to those obtain for the companion slabs naturally air dried at 35 % relative humidity and 23 °C. However, the fire endurance periods of these rehumidified slabs were only nominally better than those for the oven dried specimens. This indicated that partial rehumidification of concrete following artificial drying does not simulate the moisture conditioning from natural air-drying. This was presumably due to the sorption characteristics of concrete, which indicates that the moisture lost during the first drying phase cannot be completely replaced except at very low

relative vapour pressures. This means that for the same relative humidity, concrete has a lower moisture content at the end of the adsorption process than during the desorption phase.

The sorption isotherms for neat cement paste obtained by Power and Brownyard [4 01], and by Jesser [4 17] showed a loss of evaporable water due to sorption hysteresis for hardened cement paste at 75 % relative humidity, depending upon the mix ratio and the maturity of the specimens. This observation enabled Abrams and Orals [4 16] to conclude that artificially dried concrete specimens which were later rehumidified contained less evaporable water because of this hysteresis effect, and hence resulted in a reduction in the fire endurance period as compared to naturally dried specimens.

In the preceding sections the beneficial effects of moisture content in a structural element during a standard furnace test were discussed. Where the element contains either an excess of moisture or has a dense pore structure so that the evaporable water when turned into steam cannot leave the interior of the specimen, presence of moisture can have a detrimental effect. If the rate at which the evaporable water turns into steam exceeds the rate at which it can escape, the entrapped steam can increase stresses within the pore structure of the concrete. These stresses in association with stresses due to thermal gradient and/or restraint to expansion reach the critical limits causing the specimen to fail violently by explosive spalling. Spalling of concrete adversely affects the fire endurance period of structural elements by causing either structural collapse or by allowing

unhindered propagation of flame through the damaged sections. Various authors have tried to explain explosive spalling in terms of compressive failure induced entirely by the thermal stress [4 18] or considered it to be primarily due to induced pore pressure [4 19]. Harmathy [4 14] classified such failures into thermal spalling and moisture clog spalling, depending upon whether it was primarily induced by thermal stresses resulting from temperature gradient and/or restraint, or induced by pore pressure due to restricted movement of fluid within the concrete mass. He observed that the latter was more violent in nature than the former type of failure and, together with Shorter [4 20], proposed the following explanation for the moisture clog spalling for a concrete specimen heated from one side:

"When heat begins to penetrate into a concrete slab, desorption of moisture starts in a thin layer adjoining the surface exposed to fire. A major portion of the released vapour leaves towards the colder regions and becomes readsorbed in the pores of some neighbouring layer. As the thickness of the dry layer gradually increases, a fully saturated layer termed moisture clog, builds up at some distance from the exposed surface, A little later, a sharply defined front forms between the dry and the saturated Layers as shown in Figure 4.1. Further desorption will obviously take place from this frontal area indicated by C-D line. In the meantime the temperature of the exposed surface keeps rising and a very steep temperature gradient develops across the dry layer resulting in high heat flow and intensified desorption at the C-D plane. Having little passage toward the colder regions, vapour has to leave through the dry layer, gradually expanding meeting

increasing resistance along the flow path. With further steepening of the temperature gradient there will be a rapid pressure build -up at the C -D plane. This build- up will soon level off if the moisture does not meet a high resistance in the colder region i.e. at the E-F plane and the moisture clog is able to move away from the exposed face. If on the other hand, the permeability of the material is low the pressure at the plane C-D continues to grow and will eventually exceed the ultimate tensile strength of the material. When this condition is reached, a layer of a thickness approximately equal to that of the dry layer separates from the material."
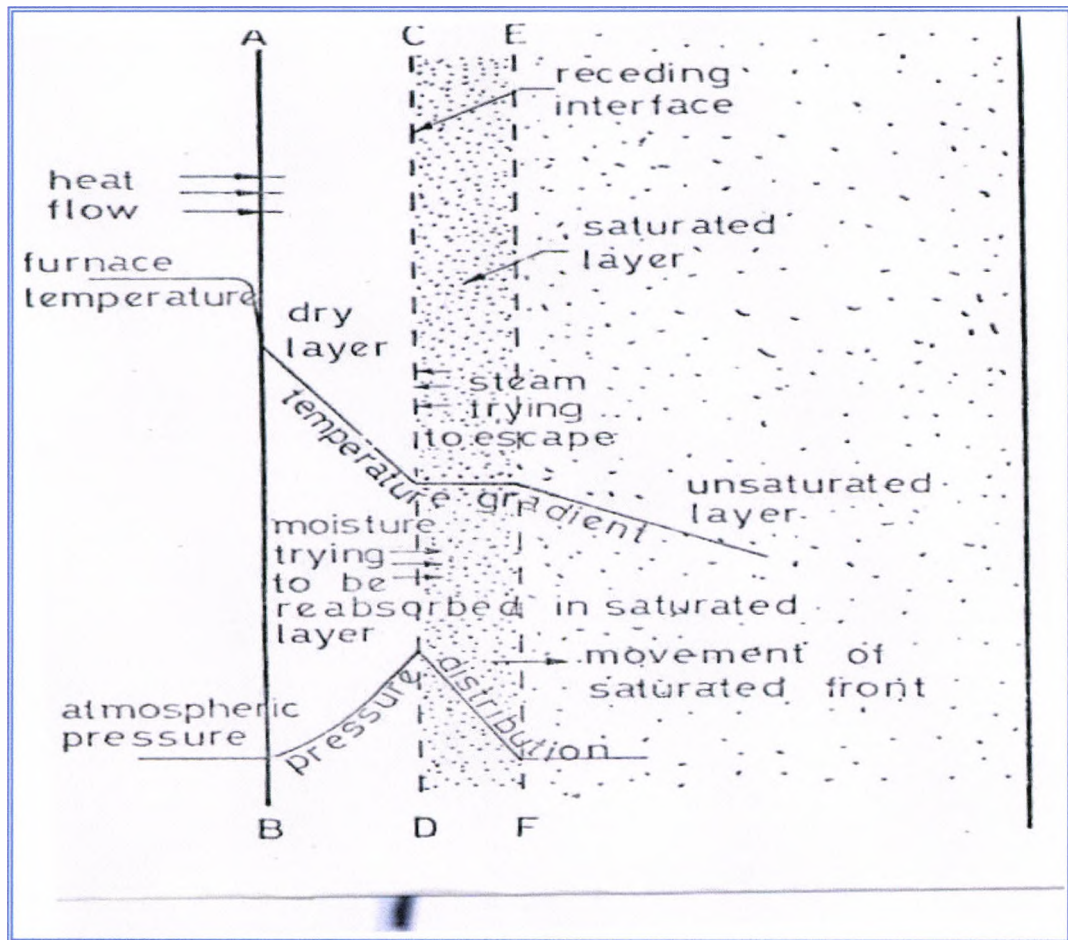
Figure 4.1 Formation of moisture clog when heated from one side [Ref.4.14]

They also proposed on the basis of certain simplified models mathematical expressions connecting the moisture content, permeability, porosity, temperature, thermal conductivity and vapour pressure, to represent the critical conditions at which spalling of concrete occur. Their analysis, as Dougill [4.21] pointed out later, did not consider the passage of the vapour through the dry region to the atmosphere, which can have significant bearing on the pressure build-up. He suggested that a more direct estimate of the pore pressure can be obtained from

temperatures measured at various depths from the heated surface since the period of vaporisation appears as a step in a temperature - time plot, and thus the temperature at which the vaporisation occurs and hence the pore pressure can be determined.

Dougill [4.21] used Shorter and Harmathy's [4.20] and Harmathy's [4.14] concept of moisture clog phenomena to explain surface spalling in terms of pore pressure and stresses due to induced thermal strains. He assumed that after the thermal stresses in a dry layer next to the heated surface reached the peak stress under bi-axial compression, they would follow the descending branch of the stress-strain curve. The tensile stresses caused by the pore pressure when superimposed, would produce an effective tri-axial state of stress i.e. compression-compression-tension. He suggested that the effect of the tensile principal stress would be to reduce the possible peak values of the compressive stresses and also to steepen the descending branch of the stress-strain curve, which would result in extensive cracking, approximately parallel to the heated face. However, he argued that these would be limited to the local region of the heated surface because of the limited depth of the dry layer. This process of cracking could produce a situation where the material between the heated surface and a crack would be regarded as a potential spall. Failure would occur once the stresses due to pore pressure overcome the shear resistance at the edges of the potential spall. Though a slip occurs at a peak value of shear stress, it can continue under much reduced level of shear stress once the critical peak has been reached. Thus if the potential spall

were to be pushed out by stress (due to constant pore pressure) required to overcome the peak shear stress, an unstable situation would develop. Only a part of the work done by forces pushing the potential spall out, would be required to propagate the slip, the most of the remainder would appear as the kinetic energy of the moving spall, and the failure would be explosive in nature,

However, during the expulsion of the potential spall, any reduction in the pore pressure due to release of steam or otherwise, may terminate the process prematurely. But the reduction in the peripheral area of the potential spall and also the reduction in the normal stress acting on the peripheral area would encourage the spalling to continue. Thus the explosive nature of the spalling would depend on which of these opposing effects predominate. If the drop in pore pressure during slip is significant, movement of the spall may be intermittent with the pore pressure being repeatedly built-up to induce successive increments of slip. Alternatively, with little drop in pore pressure or considerable reduction of the normal stress, explosive spalling would occur when peak shear stress is reached.

It should be remembered that the moisture clog phenomenon deals with the situation where the specimen is heated from one side only, as in the case of a standard furnace test on a beam-roof construction. However, in cases where the specimen is heated from all sides as in case of a column in a standard furnace test, or with beam-roof construction in an actual fire condition where two consecutive storeys are on fire, the situation may become still worse since the

moisture cannot find any escape passage and is thus forced to form a moisture clog core within the specimen surrounded by a hot, dry outer core as shown in Figure 4.2. Under such situation, the pressure build - up cannot level off as is possible in the case of a specimen heated from one side only. Dougill [4.21] indicated that for heating from both side the situation becomes extremely critical for thinner sections and explosive spalling is almost certain to occur. This was demonstrated by Meyer-Utten's [4.22] tests where all the specimens heated from bath sides suffered explosive spalling but none of the specimens heated from one side only showed explosive spalling.
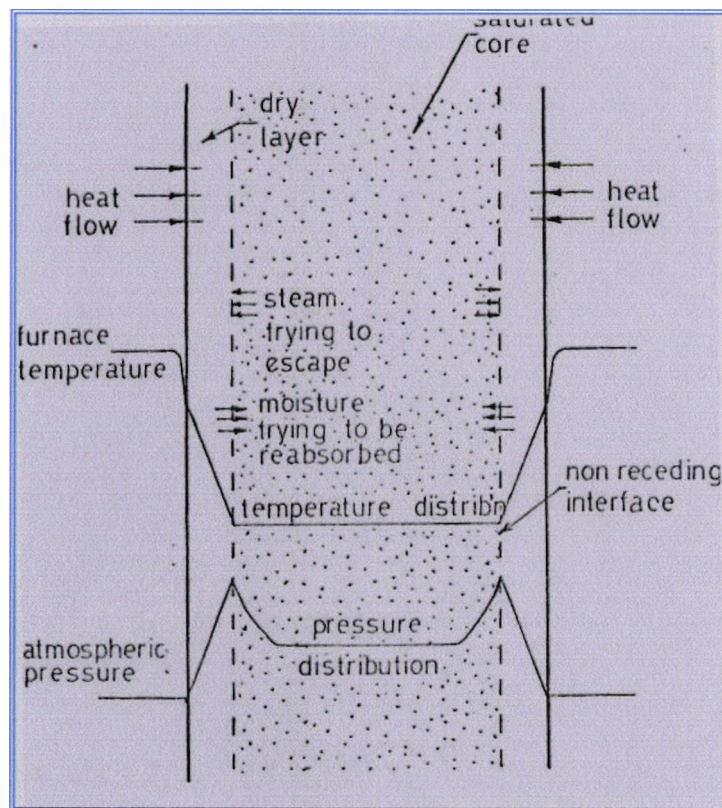
Figure 4.2 Formation of moisture clog when heated from all sides (Ref.4.21)

Dougill [4.21] further indicated that for thicker slabs heated from both sides, the longer time needed for the central saturated core to develop delays the pore pressure build-up until the outer dry zone becomes of appreciable thickness. Because of this, greater pore pressure would be required to cause spalling in thick slabs than in thin ones.

4.6 Diffusion convection model by Harada

Since moisture has significant effect on concrete exposed to fire the thermal responses of concrete to fire have been well studied by many authors with respect to moisture. There are many computer programs to predict the temperature of concrete. In some of the programs not only heat, but transfer of moisture and gas in the pore, are considered in connection with the evaporation on water. [4.23, 4.24]. However, the thermal decomposition of crystalline water is neglected in most of the model.

In 1989 Harada and Terai.[4.26] produced a model of heat and mass transfer, considering the desorption of physically adsorbed water and the decomposition of crystalline water, called the "Diffusion Model". However, in this model their calculated vapour content was considerably higher than the measured value, which was due to neglecting the convection of the gas in the pore. Currently Harada has developed a model including the convection of the gas in the pores this is called the "Diffusion- Convection Model" [4.25]. The convection of mixed gas in the pore is taken into account in addition to the "Diffusion Model".

In his program, concrete is treated as a porous material as shown in Figure 4.3. Its skeleton is made of aggregate and cements paste. Cement paste contains the crystalline water. In the pore, liquid water is physically adsorbed. In the gas phase of the pore, water vapour, which is mixed with air, is in equilibrium with the physically adsorbed water. The physically adsorbed water, water vapour and air, can move through the pore, while the crystalline water cannot move.
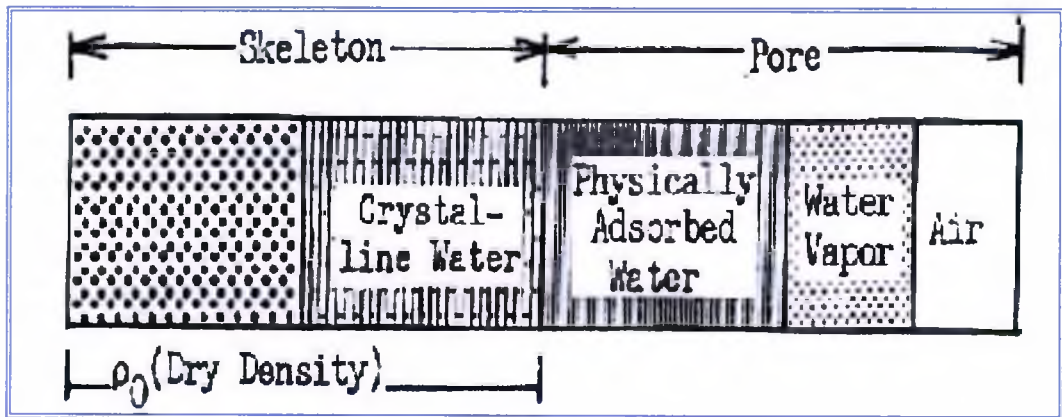
Figure 4.3 Model of concrete for Harada's program.

The governing equations for the above model are,

Heat:

$$\rho c \frac{\partial \theta}{\partial t} = \nabla(\lambda \nabla \theta) - L(R_{sorp} + Rd_{cmp}) \dots\dots\dots\dots\dots\dots\dots\dots\dots\dots\dots\dots\dots 4.5$$

Mixed Gas (Water vapour and Air):

$$\frac{\partial(\varepsilon \rho_g)}{\partial t} + \nabla(\rho_g u) = R_{sorp} + d_{cmp} \dots\dots\dots\dots\dots\dots\dots\dots\dots\dots\dots\dots\dots\dots 4.6$$

Water vapour:

$$\frac{\partial(\varepsilon\rho_v)}{\partial t} + \nabla(\rho_v u) = \nabla(D_v \nabla \rho_v) + R_{sorp} + d_{cmp} \dots\dots\dots\dots\dots\dots\dots\dots\dots\dots\dots\dots\dots\dots\dots\dots 4.7$$

Physically Adsorbed Water:

$$\rho_O \frac{\partial w}{\partial t} = \nabla(\rho_o D_w \nabla_w) - R_{sorp} \dots\dots\dots\dots\dots\dots\dots\dots\dots\dots\dots\dots\dots\dots 4.8$$

Crystalline water:

$$\rho_O \frac{\partial \omega_c}{\partial t} = - R_{dcmp} \dots\dots\dots\dots\dots\dots\dots\dots\dots\dots\dots\dots\dots\dots\dots\dots 4.9$$

In the above equations, symbol u denotes the volume flow rate of gas in the pore per unit cross sectional area assuming that the flow in the pore is laminar. It can be expressed by Darcy's equation.

$$U = - K_D \nabla P_g$$

The rate of desorption of physically adsorbed water is assumed to be proportional to the displacement from the equilibrium point, therefore expressed by the Langumuir equation.

$$R_{sorp} = \gamma (w - w_{eq})$$

On the other hand the rate of thermal decomposition of the crystalline water is expressed by

$$R_{dcmp} = \gamma (1 - P_v / P_e) (W_c - W_{Ct}).$$

A visit to Kyoto University in Japan, provided an opportunity for familiarise with the Diffusion- Convection Model program in order to use it in this project.

The total pressure distribution, vapour pressure distribution and water content distribution for a normal concrete when exposed to fire is obtained using Harada's program are given in Appendices A.4. This shows that the pressure within the high strength concrete just before the explosion is in the region of 1.1x105 MPa. Harada's program is capable of producing the results of temperature, total pressure, vapour pressure, and water content for the beams laterally or axially loaded.

Programs developed at Aston University, UK, by Purkiss and Tenchev and Li [4.27], [4.28] are capable of producing the similar results for an axially loaded column and also of calculating the stresses when it is exposed to fire. Therefore, combining these two programs and developing a user-friendly program would be the next step forward.

A fully coupled non- linear formulation is designed by Khoury and his team [4.29] to predict the behaviour and potential for spalling. In their model concrete is considered as a multiphase material consisting of a solid phase, two gas phases and three water phases. A finite element program called HITECOSP (High temperature concrete spalling) has been written. This software is claimed to predict in a fully integrated fashion the thermal, hydral and structural responce of concrete structures when exposed to fire. Using their model they determine the ultimate tensile strength at cracking. The author claimed that HITECOSP will be developed to predict explosive spalling. It is the author's opinion that if

HITECOSP program measures ultimate tensile strength it may be able to predict spalling but it is unlikely that it will predict explosive spalling.

4.7 Concluding remarks

The preceding discussion of the effect of moisture on the behaviour of concrete at high temperatures indicates that:

i) The moisture content influences the properties of concrete both at room temperature and at elevated temperatures. However, the extent and manner in which the various properties are affected by moisture content. depends on the states in which it occurs. These states can be classified in terms of the bonding energy existing between moisture and the solid phase.

ii) The presence of capillary water and adsorptively bound water is detrimental for concrete strength and other rheological properties.

Since the temperature level and the heat soaking time govern the amount of evaporable water, any comparison between two steady state test results must take the duration of soaking time in account. For transient condition, this would be of still greater significance.

iii) The presence of moisture in a structural unit may have a beneficial effect on a standard furnace test result in that the rise of temperature on the

unexposed surface may be hindered by its absorption of heat of evaporation. However, the presence of excess moisture or a faster rate of heating may cause the specimen to fail violently if the escape of steam is retarded in a critical manner. Although the exact mechanism of such failure is not fully understood, the important part played by moisture content is demonstrated by the fact that such failure usually occurs during visible evaporation of moisture from the specimens. However, there may be a number of other factors contributing to such failures.

CHAPTER 5

The fractional factorial method

5.1 Background to the fractional factorial analysis

Sir John Fisher first used this method of analysis in the early 30's and Yates in 1936 and Taguchi further developed it in 1947. Fractional factorial analysis is a branch of statistical theory concerned with the resolution of a set of descriptive variables in terms of a small number of categories or factors. This resolution is achieved by the analysis of inter-correlations of the variables. A successful solution will generate factors, which convey all of the essential information of the original set of variables. It is therefore the main aim of the analysis to attain an economic description of the data used.

The analysis in no way attempts to uncover all of the relevant factors in a field of study. Although this would be desirable, it is not likely that the analysis would be based upon a set of variables which measures all aspects, completely and accurately.

As the theoretical possibility of complete and accurate description is unlikely or impossible to implement, it can be approached practically in a limited field of investigation where a relatively small number of variables is considered exhaustive.

However, the factorial analysis does give a simple interpretation of a given body of information and therefore gives a fundamental description of the particular set of variables analysed.

5.2 Selection of Factors for our experiment.

It is known that a number of factors influence the spalling and deterioration of high strength concrete upon heating. These factors are:

- Compressive strength - as the strength increases, the permeability will decrease thus the concrete tends to become more susceptible to spalling.

- Age - as the concrete ages, it become more susceptible to spalling and deterioration.

- Moisture content - an increase in the moisture content tends to make the concrete more susceptible to spalling.

- Aggregate size - as the size of the aggregate is increased the concrete tends to become more susceptible to spalling.

- Water/cement ratio - as this is increased, the concrete tends to become more susceptible to spalling.

- Rate of heating - as the rate of heating is increased; the concrete tends to become more susceptible to spalling.

- Applied load - the larger the proportion of applied load to ultimate load, the more susceptible the concrete tends to become to spall.

- Nature of heating - as the numbers of heated sides to the specimen are increased, the concrete has a higher tendency to spall.

- Restraint - the more restrained a specimen is (number of restraints), the higher the tendency of the concrete to spall.

- Element thickness - as the element thickness is increased, the concrete becomes more susceptible to spalling.

- Curing - water curing tends to make the concrete more susceptible to spalling than curing at lower moisture levels.

- Cracking - the presence of cracks tends to make the concrete less susceptible to spalling.

- Polypropylene fibres - the presence of these fibres tends to lower the tendency of the concrete to spall.

- Aggregate type - as each aggregate type has a different coefficient of thermal expansion they all react differently to heating. Also certain aggregate types, such as crushed quartz schist are known to increase the tendency of concrete to spall.

The above are the fourteen salient factors which have been shown to influence the propensity of concrete to spall. When a large number of factors are known to influence simultaneously in a set of experiments, a factorial method of analysis gives the most reliable results accurate to a specific confidence level [5.02].

As described in Chapter 6 section 6.1.2, the 1/9 [th] fractional factorial method, which studies five variables at three levels, was used. The reason for selecting three levels is that using the three sets of 27 tests, each set representing a full fractional analysis, will allow the determination of non-linear variations in factors and interactions.

The five factors chosen for each of the three separate fractional factorial series are given in Tables 6.2 for the plain and reinforced concretes and Table 6.3 for fibre reinforced concretes.

The factors used for the experiments had to be easily controlled and practical to test. Therefore the factors chosen for the plain and reinforced concrete series are: curing type, heating rate, aggregate type, loading level and water/cement ratio.

The factors chosen for fibre reinforced concrete are: fibre concentration, heating rate, loading level, water/cement ratio and aggregate type.

The types of coarse aggregates used were limestone for normal concrete, 45% Lytag replacement (by volume) of limestone for the modified normal concrete and Lytag for lightweight concrete. The aggregate size was kept constant at 6-10 mm sieved for the carbonaceous limestone and 4-12 mm sieved for the Lytag lightweight aggregates.

Age is not used as a factor as all specimens were tested at 3 months or later.

The nature of heating is kept constant with three sides, along the length of the top and sides of the furnace, heater.

The concrete specimens are not restrained at their ends; however, restraint is produced by the thermal gradient within the beam during the heating process.

The element thickness is kept constant at 50 mm in line with the optimum needed for the purpose built furnace.

Strength is not used as a factor as it is difficult and impractical to ensure consistent strength to the accuracy needed for this analysis. Instead, water/cement ratio is used as a factor which is easier to control. However, the strength is recorded for the specimens and this data can then be analysed against the results to determine its significance.

The moisture content is an important factor that affects the concrete differently with different factor level. In order to analyse the moisture content the factors determine the moisture content were chosen as experimental factors. Water/cement ratio, curing type, and the moisture loss during each test is recorded for the moisture content analysis.

The loading is used as a factor as this has influence on beam deflections. The beams are loaded at three levels: 0%, 10% and 20% of the ultimate load in flexure. These loads were chosen, just enough to influence the deflection without causing serious damage to the specimens.

Different rates of heating are known to influence the spalling and deterioration in different manner, therefore the rate of heating is used as a factor at three levels to

study the significance of the rate of heating. The rates of heating used in the experiments are high rate (15.5 °C/minute), medium rate (10 °C/minute) and low rate (4 °C/minute).

The curing is tested as a factor as three different represented as relative humidities: 100% (85%); 65%; 45%. Here 100% humidity was impractical to achieve, because, by the time beam prepared for the experiment since it removed from the moisture cured environment it tends to lose some of its initial humidity, therefore 85% humidity is taken as the average instead of 100% humidity.

The Polypropylene fibres are used as a factor in place of curing in the fibre-reinforced series. They are used tested at three dosages: 1 kg/m³, 2kg/m³ and 3kg/m³.

5.3 Design of experiments using the fractional factorial method

The most thorough method of studying a number of factors, which interact during testing, is by applying a complete factorial design to the experiments. However for five factors tested at three different levels, the number of mixes that would need to be carried out to obtain the complete factorial is 3^5 or 243 for each series and 729 in total. This number of mixes would be uneconomical, in time and effort and may be impractical, especially when trying to find the effects of a large number of factors.

As the fractional factorial experiment is only a fraction of the full factorial, in this case a ninth of 243 tests (or 27), this will inevitably give an incomplete set of information on all the factors and all the interactions factors. However the significance of the five factors at three different levels together with three interactions factors can be established.

If the factors are A, B, C, D and E, the 1 / 9 [th] fractional factorial method chosen for the experiment ensures that all individual factors and interaction factors AB, BC and AC can be determined with confidence. Interactions of D and E are confounded and cannot be determined. Hence the factors, which are known by experience or intuition to influence the results more strongly have been, selected as the first three factors, i.e. A, B and C.

It should be noted that A, B and C form a complete factorial and D and E exhibit a balanced pattern which ensures that A, B and C at a given level are given similar treatment when combined with levels of D and E.

The six factors selected for investigation have been grouped into two sets of five factors each. The first set contains factors 1 to 5 in Table 6.2. In the second set factor 1 (Curing) is kept constant and the set of 27 specimens were kept at a nominal 100% saturation, which is expected to give the most critical condition for explosion. Factor 6 (polypropylene fibre) is introduced in place of factor 1 in the second series of tests. Table 6.2 and Table 6.3 show the factors and their respective levels (0, 1, 2) for each experiment.

The first step in the analysis is to examine how a change in level in each factor (or the deviance of each factor) compared with the overall average. The next stage in the analysis of variance is to check whether the effect of a change in factor is a true change or whether it is due to the error in the experiment

The mechanics of how this is done is now explained. The overall average sum of squares is subtracted from the average sum of variance at each level of each factor. This gives the average effect of change of level of each individual factor and is equivalent to the deviance of individual factors. The deviance is therefore a measure of the effect that each factor level has on the overall average.

The deviances of the individual and interacting factors divided by their respective degrees of freedom (df), say V_f divided by the selected error factor, which is also divided by it's df, say E_f. When V_f divided by E_f give values, which can be compared with tabulated standard statistical Tables in our case Fisher's Tables (Table 5.7). These Tables determine the percentage significance that a change in factor level has and indicates whether it is a true effect rather than being the effect of the experimental error. The error factor is selected from one of the interacting factors and this is explained in the paragraph below.

The df of each factor is 3 - 1 = 2 and the df of the complete 27 experiments is 27 - 1 = 26. If all the individual and interacting factors from A to DE are examined, the df of the error, calculated from 26 - df of all the sources would be 0 and analyses would not be possible. DE therefore chosen as the error with a degree of freedom of 4 (6 - 2). The analysis can now proceed with DE as the error factor. The reason for choosing this source as the error factor is that the factors towards the end of the factorial Table are more prone to be aliased or confounded.

The advantage of the fractional factorial method other than the ones mentioned earlier is that the same 27 experiments can be used over and over again for different properties such, as the flexural stiffness, the coefficient of thermal expansion, permeability etc. Section 5.4 shows the details involved in calculating the significance factors using expansion as the criterion.

5.4 Finding the significance factor

This section gives an example of how the significance factors affecting spalling or deterioration using Fisher's fractional factorial methods of analysis is calculated.

5.4.1 Fisher's factorial table with experimental results (Table 5.1)

For a simple case consider the expansion of each beam selected at the same average concrete temperature. These overall expansion values are given in Table 5.1, column 7.

The last column in Table 5.1 gives the strain values per unit temperature by dividing the values of overall expansion by the length of the beam and the average concrete temperature. These strain values include strains due to shrinkage or non-reversible expansions due to deterioration.

Table 5.1

ANALYSIS OF VARIANCE (ANOVA) USING EXPANSION

Factors	Cure	Heat	Load	W/C	Aggregate	Expansion.	Strain
Test No.	A	B	C	D	E	(mm)	$(10^{6}/^{\circ}C)$
1	65% RH	L	00	O.25	LWA	3.6	6.5
2	"	L	10	0.5	M	7.1	14 5
3	"	L	20	0.35	N	10.7	21.3
4	"	M	00	0.5	N	7.9	15.7
5	"	M	10	0.35	LWA	5.9	10.6
6	"	M	20	0.25	M	6.6	12.6
7	"	H	00	0.35	M	7.0	14.4
8	"	H	10	O.25	N	1.8	8.7
9	"	H	20	0.5	LWA	3.9	7.9
10	45% RH	L	00	0.35	M	7.0	12.6
11	"	L	10	O.25	N	8.6	17.0
12	"	L	20	0.5	LWA	4.4	7.9
13	"	M	00	O.25	LWA	4.7	8.4
14	"	M	10	0.5	M	6.0	12.0
15	"	M	20	0.35	N	10.5	21.6
16	"	H	00	0.5	N	0.3	1.3
17	"	H	10	0.35	LWA	4.9	10.0
18	"	H	20	0.25	M	7.2	14.2
19	0% RH	L	00	0.5	N	7.2	14.2
20	"	L	10	0.35	LWA	5.7	10.2
21	"	L	20	0.25	M	7.8	15.0
22	"	M	00	0.35	M	7.1	14.1
23	"	M	10	O.25	N	8.8	18.1
24	"	M	20	0.5	L	4.9	8.9
25	"	H	00	O.25	LWA	4.3	8.8
26	"	H	10	0.5	M	6.8	13.5
27	"	H	20	0.35	N	3.4	16.7

5.4.2 Calculation for main effects of individual factors (Table 5.2)

In Table 5.2, SUM (X_0) for the factor A is equal to the sum of the strain values in the last column of Table 5.1, when the level of factor A is 0 in column two of Table 5.1. Similarly for factor B the sum of the strain values in the last column of Table 5.1, when the level of factor B is 0 in column three of Table 5.1.

SUM (X_1) for the factor A is equal to the sum of the strain values in the last column, when the level of factor A is 1 in column two of Table 5.1. Similarly for factor B the sum of the strain values in the last column, when the level of factor B is 1 in column three of Table 5.1.

SUM (X_2) for the factor A is equal to the sum of the strain values in the last column of Table 5.1, when the level of factor A is 2 in column two of Table 5.1. Similarly for factor B the sum of the strain values in the last column, when the level of factor B is 2 in column three of Table 5.1.

Similarly SUM (X_0), SUM (X_1) and SUM (X_2) can be calculated for factor C, D and E. Hence the main effect of individual factor S (Tot), which is equal to SUM (X_0)+ SUM (X_1)+ SUM (X_2), can be calculated.

Table 5.2
Main Effects of individual factors

	A	B	C	D	E
SUM (X_0)	112.2	119.3	96.0	109.3	79.2
SUM (X_1)	105.0	121.9	114.5	131.5	122.9
SUM (X_2)	119.4	95.4	126.1	95.8	134.5
S(Tot)	336.6	336.6	336.6	336.6	336.6

5.4.3 Calculation for interaction factor effect (Table 5.3)

In Table 5.3, (X_0Y_0) means the sum of the interaction factor for factor X, Y when there levels are 0, 0 in the same experiment.

(X_0Y_0) for the factor A and B is equal to the sum of the strain values in the last column of Table 5.1, when the factor A level is 0 in column two and the factor B level is 0 in column three of Table 5.1 In other words, the sum of the strain values in the last column of Table 5.1 when the factor A level is 0 and the factor B is level 0 in the same experiment.

(X_0Y_1) for the factor A and B is equal to the sum of the strain values in the last column of Table 5.1, when the factor A level is 0 in the second column and the factor B level is 1 in the third column of Table 5.1. In other words, the sum of the strain values in the last column of Table 5.1 when the factor A level is 0 and the factor B level is 1 in the same experiment.

(X_0Y_2) for the factor A and B is equal to the sum of the strain values in the last column, when the factor A level is 0 in the second column and the factor B level is 2 in the third column of Table 5.1. In other words, the sum of the strain values in the last column of Table 5.1 when the factor A level 0 and the factor B level is 2 in the same experiment.

Similarly other interaction factors can be calculated.

In Table 5.3, Tot S(XY) is the sum of each 2 level interaction in each column. This is numerically equal to S(Tot) in Table 5.2. As S(Tot) is equivalent to the sum of all the effect of individual factor.

Table 5.3

Interaction effect Table

COMBIN.	AB	AC	BC	DE	CD	CE
X_0Y_0 (00)	42.3	36.6	33.3	23.8	23.8	23.8
X_0Y_1 (01)	38.9	33.8	41.7	41.8	41.1	41.1
X_0Y_2 (02)	31.0	41.8	44.2	43.8	31.2	31.2
X_1Y_0 (10)	37.5	22.3	38.2	30.8	43.8	30.8
X_1Y_1 (11)	42.0	39.0	40.7	41.1	30.8	39.9
X_1Y_2 (12)	25.5	43.7	43.1	59.6	39.9	43.8
X_2Y_0 (20)	39.4	37.1	24.5	24.7	41.8	24.7
X_2Y_1 (21)	41.1	41.8	32.1	39.9	59.6	41.8
X_2Y_2 (22)	39.0	40.5	38.8	31.2	24.7	59.6
Tot S(XY)	336.6	336.6	336.6	336.6	336.6	336.6

5.4.4 Calculation for deviance of individual factor (Table 5.4)

Table 5.4 gives the average sum of squares of the individual factors, $SSX_0X_1X_2/9$, which is equal to $\{(SUMX_0)^2+(SUMX_1)^2+(SUMX_2)^2\}/9$ and the average sum of squares of total, $SST/27$, which is equal to $(STot/27)^2$. Both are obtained from Table 5.2.

The difference of these two values gives the average effect of each individual factor from A to E on the overall average as each changes from one level to the other. These values are equivalent to the deviance of individual factor, shown as Sa...to. .Se in Table 5.4 and Table 5.6

Table 5.4

Sum of squares for individual factors

	A	B	C	D	E
$SSX_0X_1X_2/9$	4207.9	4243.5	4247.4	4268.5	4384.8
SSTot/27	4196.3	4196.3	4196.3	4196.3	4196.3
Sa -to-Se Deviances	12	47	51	72	188

5.4.5 Calculation for deviance of interaction factor (Table 5.5)

In Table 5.5, SSXY is the sum of squares of all the two level interactions from Table 5.3 and SSXY/3 gives the average sum of squares of the interaction factors. SST/27 is $(STot/27)^2$ as before. Thus S(axb) is equal to SSXY/3 - SST/27

The average effect of the interacting factors on the overall average is Sab or deviance of interaction factor is equal to

Sab = Saxb - Sa - Sb

Where Saxb is from Table 5.5, Sa and Sb from Table 5.4

This value is shown as Sab... in column 3 of Table 5.6 to include interactions of AB, AC, BC and DE.

The degree of freedom df of Sab is 4 as the two factor interactions have each a df of $6 - 2 = 4$ shown in Table 5.6.

Table 5.5

Sum of squares for interacting factors

	AB	AC	BC	DE	CD	CE
SSXY	12839.1	12922.0	12909.4	13590.9	13590.9	13590.9
Saxb	83.4	111.0	106.8	334.0	334.0	334.0
Sab	24.6	48.4	94.5	73.3	210.8	94.5

5.4.6 Analysis of variance (Table 5.6)

Table 5.6 calculates the variance of each individual and interaction factor from the sum of squares already calculated and the degrees of freedom (df) of the factors. From this the variance of the error factor is estimated. If all the factors are assumed to have an effect, the error factor would be 0 as in column 3 and it would not be possible to test for significance. Column 4 assumes that interaction DE cannot be discriminated from the other factors and is the error factor with df = 4 ie 27 - 1 - 5(2) - 3(4). Column 5 estimates the Fisher factor F for all the factors with the estimated error. F is then compared with values in statistical Tables, reproduced as Table 5.7 below, which gives the significance of the effect of a change in level for each experimental factor at a given percentage.

It will be observed, that in column 5 factor E the aggregates has the largest numerical value i.e. 5.14. This figure is higher than 4.32 in Table 5.7 below indicating 90 % significance, for a df of 4 for the error (2nd column) and 2 for the factor (2nd row). To improve the discrimination of the results, the numerical value of the sum of squares of the error factor has to be decreased and its Df increased. This decreases the denominator in F(a) in Table 5.6 and increases its value making it more sensitive as a check for significance. One way of achieving this is to scan down the variances column (column 4 in Table 5.6) and select the smaller values of the factors and interacting factors. These are unlikely to have an effect on the overall average as the smaller the variance of a factor, the lower

is the influence of the factor with a change in level. Thus Error (2) has been chosen as the sum of A (curing) and interaction factor AB

This increases the values of F (a) (see column 5 and 6 in Table 5.6 for the increase of F (a)) with the result that the significance of a change in level of factor E increases and the remaining factors also become significant to better than 90%. In the analysis 99% is considered extremely significant, 95% very significant and indicates a real effect in a change in factor level and 90% can be considered as just significant.

Table 5.6

Analysis of variance

		From Table 5.4		F(a)=	F(a)=	Significance
Source	df	Sa...Se	V	V(a)/V(Er1)	V(a)/V(Er2)	%
A (Curing)*	2	11.61	5.81	0.32	Chosen for error	-
B (Heating)	2	47.18	23.59	1.29	3.91	90
C (Load)	2	51.02	25.51	1.39	4.23	>90
D (W/C)	2	72.18	36.09	1.97	5.99	>95
E (Aggregate.)	2	188.48	94.24	5.14	15.63	>99
		From Table 5.5 Sab...				
AB*	4	24.57	6.14	0.34	Chosen for error	
AC	4	48.36	12.09	0.66	2.00	-
BC	4	8.61	17.78	0.12	2.95	-
DE=(e)+	4	73.29	18.32	Chosen for error	3.04	-
Error	0	0				
(Error) 1+	4	73.29	18.32			
(Error) 2*	6	36.18	6.03			

5.4.6.1 Details of analysis of variance (Table 5.6)

Column 1 shows the source or the factors to be investigated

Column 2 gives the degree of freedom df of each source. It should be observed that the df of the complete 27 experiments is 27 - 1 = 26. If therefore all the sources from A to DE are taken for the analysis, the df of the error, calculated from (26 - df) of all the sources, would be 0, as indicated in the last row but two. The calculation procedure includes division by the df of the error, which would defy analysis. Therefore the next row in the Table assumes DE as the error shown as (Error) 1. The reasons for initially choosing this source, as the error factor is that, with the principal fraction of the factorial experiment selected, the factors towards the end of the Table are more prone to be aliased (or confused with other interactions).

The 3rd column gives the effect of individual Sa…and interacting factor Sab… on the overall average as derived from Tables 5.4 & 5.5.

Dividing the values of the 3rd column by the number of degrees of freedom (df) of each source gives the variance V shown in the 4th column. The higher the variance, the greater is the influence of a change in the level of a factor on the overall average.

The result of this division for Error (1) gives the Fisher factor F(a) in the 5th column. A copy of the appropriate page from a Table of statistical data [5.2] is

shown in Table 5.7 below. The calculated values in this column for the df's of the factors and the error selected have to be higher than those in the Fisher Table for the percentage of significance quoted in the Table to apply to the present results.

Comparing the figures in the 5th column of Table 5.6 for factor E (5.13) with the value (4.32 for 90% significance) in the Fisher Table 5.7 for the df's of the sources and the error selected, gives 90% significance for factor E, with the remainder giving inconclusive evidence of significance.

By inspection the variance V for curing is small, indicating that a change in the level in curing has little or no influence on the overall average and should be close to 0. Also, interaction AB has a low value of V. Therefore these values arising from curing and its interaction with heating can be replaced as the error. This is what has been done in the last row with the result that the df of (Error) 2 has increased and the variance of the error decreased. Since the variance of the error is the divisor in the calculation of F(a), the values in the last but one column increase, thus increasing the sensitivity of the analyses.

The significance in the last column expresses the percentage probability of the effect on a change in level of a source or a factor on the overall average. Traditionally 95% is considered as significant and 99% as highly significant.

Another way of looking at the sequence of the analysis is that the variances are calculated to assess the influence of a change in level of each factor on the

average. The next stage (of calculating $F(a)$) compares this latter influence with that of the error. If the influences are of the same order as the error, then the variation is probably due to the error of the experiment rather than a real effect and the factor is said to be not significant.

The Fisher distributions with the values of significance have been produced below from reference [5.2]

5.5 Concluding remarks

In this Chapter only one series of tests has been analysed using expansion as a criterion for the fractional factorial analysis. The remaining series are analysed in Chapter 7 using several criteria. The results from fractional factorial analyses discussed in Chapter 8.

Table 5.7 [(5.02)]

Fisher Table for finding significance factor.

PROBABILITY POINTS OF THE VARIANCE RATIO (F-DISTRIBUTION)

Probability point	ϕ_2	ϕ_1 (corresponding to greater mean square)																			ϕ_2
		1	2	3	4	5	6	7	8	9	10	12	15	20	24	30	40	60	120	∞	
0·1	1	39·9	49·5	53·6	55·8	57·2	58·2	58·9	59·4	59·9	60·2	60·7	61·2	61·7	62·0	62·3	62·5	62·8	63·1	63·3	1
0·05		161	199	216	225	230	234	237	239	241	242	244	246	248	249	250	251	252	253	254	
0·01		4052	4999	5403	5625	5764	5859	5928	5982	6022	6056	6106	6157	6209	6235	6261	6287	6313	6339	6366	
0·1	2	8·53	9·00	9·16	9·24	9·29	9·33	9·35	9·37	9·38	9·39	9·41	9·42	9·44	9·45	9·46	9·47	9·47	9·48	9·49	2
0·05		18·5	19·0	19·2	19·2	19·3	19·3	19·4	19·4	19·4	19·4	19·4	19·4	19·4	19·5	19·5	19·5	19·5	19·5	19·5	
0·01		98·5	99·0	99·2	99·2	99·3	99·3	99·4	99·4	99·4	99·4	99·4	99·4	99·4	99·5	99·5	99·5	99·5	99·5	99·5	
0·1	3	5·54	5·46	5·39	5·34	5·31	5·28	5·27	5·25	5·24	5·23	5·22	5·20	5·18	5·18	5·17	5·16	5·15	5·14	5·13	3
0·05		10·1	9·55	9·28	9·12	9·01	8·94	8·89	8·85	8·81	8·79	8·74	8·70	8·66	8·64	8·62	8·59	8·57	8·55	8·53	
0·01		34·1	30·8	29·5	28·7	28·2	27·9	27·7	27·5	27·3	27·2	27·1	26·9	26·7	26·6	26·5	26·4	26·3	26·2	26·1	
0·1	4	4·54	4·32	4·19	4·11	4·05	4·01	3·98	3·95	3·94	3·92	3·90	3·87	3·84	3·83	3·82	3·80	3·79	3·78	3·76	4
0·05		7·71	6·94	6·59	6·39	6·26	6·16	6·09	6·04	6·00	5·96	5·91	5·86	5·80	5·77	5·75	5·72	5·69	5·66	5·63	
0·01		21·2	18·0	16·7	16·0	15·5	15·2	15·0	14·8	14·7	14·5	14·4	14·2	14·0	13·9	13·8	13·7	13·7	13·6	13·5	
0·1	5	4·06	3·78	3·62	3·52	3·45	3·40	3·37	3·34	3·32	3·30	3·27	3·24	3·21	3·19	3·17	3·16	3·14	3·12	3·10	5
0·05		6·61	5·79	5·41	5·19	5·05	4·95	4·88	4·82	4·77	4·74	4·68	4·62	4·56	4·53	4·50	4·46	4·43	4·40	4·36	
0·01		16·3	13·3	12·1	11·4	11·0	10·7	10·5	10·3	10·2	10·1	9·89	9·72	9·55	9·47	9·38	9·29	9·20	9·11	9·02	
0·1	6	3·78	3·46	3·29	3·18	3·11	3·05	3·01	2·98	2·96	2·94	2·90	2·87	2·84	2·82	2·80	2·78	2·76	2·74	2·72	6
0·05		5·99	5·14	4·76	4·53	4·39	4·28	4·21	4·15	4·10	4·06	4·00	3·94	3·87	3·84	3·81	3·77	3·74	3·70	3·67	
0·01		13·7	10·9	9·78	9·15	8·75	8·47	8·26	8·10	7·98	7·87	7·72	7·56	7·40	7·31	7·23	7·14	7·06	6·97	6·88	
0·1	7	3·59	3·26	3·07	2·96	2·88	2·83	2·78	2·75	2·72	2·70	2·67	2·63	2·59	2·58	2·56	2·54	2·51	2·49	2·47	7
0·05		5·59	4·74	4·35	4·12	3·97	3·87	3·79	3·73	3·68	3·64	3·57	3·51	3·44	3·41	3·38	3·34	3·30	3·27	3·23	
0·01		12·2	9·55	8·45	7·85	7·46	7·19	6·99	6·84	6·72	6·62	6·47	6·31	6·16	6·07	5·99	5·91	5·82	5·74	5·65	
0·1	8	3·46	3·11	2·92	2·81	2·73	2·67	2·62	2·59	2·56	2·54	2·50	2·46	2·42	2·40	2·38	2·36	2·34	2·32	2·29	8
0·05		5·32	4·46	4·07	3·84	3·69	3·58	3·50	3·44	3·39	3·35	3·28	3·22	3·15	3·12	3·08	3·04	3·01	2·97	2·93	
0·01		11·3	8·65	7·59	7·01	6·63	6·37	6·18	6·03	5·91	5·81	5·67	5·52	5·36	5·28	5·20	5·12	5·03	4·95	4·86	
0·1	9	3·36	3·01	2·81	2·69	2·61	2·55	2·51	2·47	2·44	2·42	2·38	2·34	2·30	2·28	2·25	2·23	2·21	2·18	2·16	9
0·05		5·12	4·26	3·86	3·63	3·48	3·37	3·29	3·23	3·18	3·14	3·07	3·01	2·94	2·90	2·86	2·83	2·79	2·75	2·71	
0·01		10·6	8·02	6·99	6·42	6·06	5·80	5·61	5·47	5·35	5·26	5·11	4·96	4·81	4·73	4·65	4·57	4·48	4·40	4·31	

CHAPTER 6

Experimental programme

6.1 Objective

The objective of the experimental programme was to examine the influence of six main factors, namely curing of concrete prior to testing, heating rate, loading prior to heating, water/cement ratio, types of aggregates and different polypropylene fibre content, on spalling and deterioration of high strength concrete during fire. The use of polypropylene fibres was shown in previous testing to alleviate explosive spalling. The coarse aggregates for the samples were limestone for normal concrete, 45% Lytag replacement of limestone for the modified normal concrete and Lytag for lightweight concrete.

The high temperature tests were carried out in a purpose built testing rig on (27x3) plain, fibre and reinforced concrete beams. Nine additional control beams were cast for each test series and these were tested to failure in the cold state. Three additional beams with embedded thermocouples were tested to obtain thermal response data for the three different rates of heating and the three different types of aggregates.

The design of the experimental programe has been based on the fractional factorial method of analysis. All the factors were investigated at three levels. A description of these factors and levels is given are Table 6.1. Three levels were

selected so that the non-linear variations in individual and interacting factors could be determined.

Table 6.1
Factors and Levels

Factor for concrete /RC	Level	Description
A. Curing	0	Nominally 100% RH (65%)+
	1	Nominally 65% RH (45%)+
	2	Nominally 45% RH (0%)+
B. Heating Rate (A)*	0	Low
	1	Medium
	2	High
C. Loading (B)*	0	0% of Load capacity at 20 °C
	1	10% of Load capacity at 20 °C
	2	20% of Load capacity at 20 °C
D. Water/cement Ratio (C)*	0	0.25
	1	0.35
	2	0.50
E. Aggregate (D)*	0	Light Weight (Lytag, L)
	1	Modified (Mixed N & L, 45% Lytag replacement of Limestone by volume)

Table 6.1 continues

Factor for concrete /RC	Level	Description
	2	Normal Weight (Limestone, N)
Fibre Content E*	0 F1*	1 kg/m^3 of polypropylene (Fibrin) fibres
	1 F2*	2 kg/m^3 fibres
	2 F3*	3 kg/m^3 fibres

6.1.1 Reasons for choice of the fractional factorial method

Fractional factorial experimentation is a well-established method based on statistical analysis which was explained with an example on Chapter 5. A defined fraction of the full factorial has been selected to assess the influence of each of the factors and the important interacting factors on the overall average effect. One of the advantages of this experimental method is the enormous amount of saving in time and cost compared to performing the full factorial experiments which would require $3^5 = 243$ tests for five factors at three levels. Although three factor and higher interactions are aliased for a 1/9 fraction used in these tests, and cannot be determined, some of the 2 factor interactions and all the single factor effects can be safely assessed. The assessment of the interaction of factors is a useful advantage. Unlike the classical, one-factor-at-a-time testing, which assumes certainties in testing conditions, factorial experimentation allows the error inherent in any test due to instrumentation, material uncertainties, or even human errors to be estimated. The resulting variations due to a change in

level of any factor investigated can then be compared with the error factor to assess the significance of the change.

The six factors, as described in Table.6.1, are grouped into two sets of five factors each. The first set contains the first five factors (see also Table 6.2). In the second set, factor A (curing) is kept at a constant nominal 100% RH (85%) as this is expected to give the most critical condition for explosive spalling, and sixth factor (polypropylene fibre) is introduced (see also Table 6.3). Since one ninth of the full factorial experiment has been designed for each set, only 27 tests for each series are required. With the additional 27 tests for the reinforced concrete beams, a total of 81 furnace tests and 27 further plain concrete tests shown in Table 6.4 were carried out.

The principal fraction of the 1/9 fractional factorial experiment for the plain and reinforced concrete test series with the test beam number in the left hand column and the levels of each factor in the other columns are shown in Table 6.3. The principal fraction for the fibre concrete is shown in Table 6.4. These fractions ensure that all individual factors and interaction factors AB, BC and AC can be determined with sufficient confidence. Interactions of D and E may be aliased and cannot be determined with the same confidence. Hence the factors which are known by experience or intuition to influence the results more strongly are selected as A, B and C.

It should be observed that A, B and C form a complete factorial and D and E exhibit a balanced pattern. This ensures that A, B and C at a given level are given

similar treatment when combined with levels of D and E. Similarly C, D and E

form a complete factorial and, in their turn, are given similar treatment when

combined with A and B. This balanced treatment ensures that none of the factors

have any biased effect on the overall average.

Table 6 .2
The principal 1/9 fractional factorial Table for plain and reinforced concrete beams

Test/Beam No.	Factor Levels				
	A(Curing)	B (Heat)	C (Load)	D (W/C)	E (Aggregate)
1	0	0	0	0	0
2	0	0	1	2	1
3	0	0	2	1	2
4	0	1	0	2	2
5	0	1	1	1	0
6	0	1	2	0	1
7	0	2	0	1	1
8	0	2	1	0	2
9	0	2	2	2	0
10	1	0	0	1	1
11	1	0	1	0	2
12	1	0	2	2	0
13	1	1	0	0	0
14	1	1	1	2	1
15	1	1	2	1	2
16	1	2	0	2	2
17	1	2	1	1	0
18	1	2	2	0	1

Table 6.2 continues

Test/Beam No.	Factor Levels				
	A(Curing)	B (Heat)	C (Load)	D (W/C)	E (Aggregate)
19	2	0	0	2	2
20	2	0	1	1	0
21	2	0	2	0	1
22	2	1	0	1	1
23	2	1	1	0	2
24	2	1	2	2	0
25	2	2	0	0	0
26	2	2	1	2	1
27	2	2	2	1	2

Table 6. 3
The principal 1/9 fractional factorial Table for the fibre concrete beams

Test/Beam No.	Factor Levels				
	A (Heat)	B (Load)	C (W/C)	D (Aggregate)	E (fibres)
1	0	0	0	0	0
2	0	0	1	2	1
3	0	0	2	1	2
4	0	1	0	2	2
5	0	1	1	1	0
6	0	1	2	0	1
7	0	2	0	1	1

Table 6. 3 continues

Test/Beam No.	Factor Levels				
	A (Heat)	B (Load)	C (W/C)	D (Aggregate)	E (fibres)
8	0	2	1	0	2
9	0	2	2	2	0
10	1	0	0	1	1
11	1	0	1	0	2
12	1	0	2	2	0
13	1	1	0	0	0
14	1	1	1	2	1
15	1	1	2	1	2
16	1	2	0	2	2
17	1	2	1	1	0
18	1	2	2	0	1
19	2	0	0	2	2
20	2	0	1	1	0
21	2	0	2	0	1
22	2	1	0	1	1
23	2	1	1	0	2
24	2	1	2	2	0
25	2	2	0	0	0
26	2	2	1	2	1
27	2	2	2	1	2

Table 6.4
Schedule of Specimens

Specimen No.	Specimen Code Plain, Reinforced concrete	Specimen No.	Specimen Code Fibre concrete
1	L/0.25/00/HL/C1	1F	L/0.25/00/HL/F1

Table 6.4 continues

Specimen No.	Specimen Code Plain, Reinforced concrete	Specimen No.	Specimen Code Fibre concrete
2	M/0.50/10/HL/C1	2F	N/0.35/00/HL/F2
3	N/0.35/20/HL/C1	3F	M/0.50/00/HL/F3
4	N/0.50/00/HM/C1	4F	N/0.25/10/HL/F3
5	L/0.35/10/HM/C1	5F	M/0.35/10/HL/F1
6	M/0.25/20/HM/C1	6F	L/0.50/10/HL/F2
7	M/0.35/00/HH/C1	7F	M/0.25/20/HL/F2
8	N/0.25/10/HH/C1	8F	L/0.35/20/HL/F3
9	L/0.50/20/HH/C1	9F	N/0.50/20/HL/F1
10	M/0.35/00/HL/C2	10F	M/0.25/00/HM/F2
11	N/0.25/10/HL/C2	11F	L/0.35/00/HMF3
12	L/0.50/20/HL/C2	12F	N/0.50/00/HM/F1
13	L/0.25/00/HM/C2	13F	L/0.25/10/HM/F1
14	M/0.50/10/HM/C2	14F	N/0.35/10/HM/F2
15	N/0.35/20/HM/C2	15F	M/0.50/10/HM/F3
16	N/0.50/00/HH/C2	16F	N/0.25/20/HM/F3
17	L/0.35/10/HH/C2	17F	M/0.35/20/HMF1
18	M/0.25/20/HH/C2	18F	L/0.50/20/HM/F2
19	N/0.50/00/HL/C3	19F	N/0.25/00/HHF3
20	L/0.35/10/HL/C3	20F	M/0.35/00/HH/F1
21	M/0.25/20/HL/C3	21F	L/0.50/00/HH/F2
22	M/0.35/00/HM/C3	22F	M/0.25/10/HH/F2
23	N/0.25/10/HM/C3	23F	L/0.35/10/HH/F3
24	L/0.50/20/HM/C3	24F	N/0.50/10/HH/F1
25	L/0.25/00/HH/C3	25F	L/0.25/20/HH/F1
26	M/0.50/10/HH/C3	26F	N/0.35/20/HH/F2
27	N/0.35/20/HH/C3	27F	M/0.50/20/HH/F3

NOTATION USED IN Table 6.4:

L.........................Lightweight aggregate concrete (Lytag) – level 0

M.........................Modified normal weight concrete – level 1

N.........................Normal weight concrete – level 2

0.25, 0.35, 0.50........ Water/Cement Ratio – levels 0, 1, 2 respectively

00, 10, 20..............Percentage of applied load to Load capacity of beam at

$\qquad$ 20°C – levels 0, 1, 2 respectively

HL.......................Low rate of heating – level 0

HM.......................Medium rate of heating – level 1

HH.......................High rate of heating – level 2

C1+......................Moist curing 85% to 100% RH - level 0

C2.......................Curing room at 65% RH – level 1

C3.......................Air curing ambient temp 45% RH – level 2

F1.......................1 kg polypropylene fibre per m^3 of concrete - level 0

F2.......................2 kg polypropylene fibre per m^3 of concrete – level 1

F3.......................3 kg polypropylene fibre per m^3 of concrete – level 2

+Note that for the initial plain concrete set of beams, the curing was nominally at 65%, 45% and 0% RH respectively.

+The load capacity for the reinforced concrete was taken at the yield strength of the beams.

6.2 Furnace details

The purpose built electrical furnace is capable of heating, loading beams in bending simultaneously while temperatures, deflections and expansion or dilation of the beams are being monitored. Figure 6.1. shows a schematic diagram of the experimental set up. The 850 mm long beam is placed on a roller C, and a rocker support D, 680 mm apart within the furnace enclosure. The load is applied at two points approximately 227 mm apart, equidistant from each other and the supports. The deflections are measured at mid point, third points and adjacent to the supports and axial deformation is measured by the sum of dilations at either end. The displacement transducers P are supported outside the furnace and are in contact with silica rods of 10 mm diameter passing through apertures within the end walls and floor of the furnace. The other ends are ground to 2mm diameter making point contact with the beam specimen inside the furnace.

Three sets of electrical elements T, one above and two at either side of the beam specimen, apply heat to the furnace. Varying the power supplied to the elements controls the heating rate. The power ratings have been fixed for the tests at 90%, 60% and 30% to impart high, medium and low rates of heating. See Figure 6.2, 6.3 and 6.4 for time -temperature graph of high, medium and low rates of heating. Here measurement of temperature is temperature of thermal couples that placed in the furnace; this temperature is not the actual furnace temperature. The furnace can be set to a specified maximum required temperature, and in the tests

described, has been set to 700 °C. However if the beam fails before reaching 700 °C, the furnace is turned off. Once the set temperature is reached the furnace maintains the temperature within a tolerance of + or - 1.5 % or less. The distribution of heat in the furnace is not uniform and creates a higher temperature at the centre than at the ends of the furnace, which is reflected in the beam specimens imposing a certain amount of internal lateral restraint during heating.

The system of applying load remotely from the furnace and concurrently taking load and displacement readings is also shown in Figure 6.1 and a description of the loading and unloading sequence follows.

The loading on the beam is applied by means of a saddle supported on a rocker B and a roller A 227mm apart placed centrally above and in contact with the top of the beam within the furnace. The saddle contains two apertures in line with the centre of the rocker and two apertures in line with the centre of the roller to allow four threaded rods or hangers J to hang astride the beam specimen and the loading system below. The loading system comprises a motorised screw jack Q, R, F fixed below the furnace and a load cell G attached to the piston below via a ball race. The bottom end of the load cell is attached to a cross beam H also via another ball race to allow free rotation of the load cell. The crossbeam sits astride two steel beams I each with a pair of apertures at 227 mm centres allowing the bottom threaded end of the hangers through. Four nuts below the steel beams, threaded into the four hangers, support the steel beams, which in their turn support the load cell. When the electrical motor is turned on, the piston pushes

down on the load cell against the remainder of the loading system below the furnace and applies tension to the hangers between the concrete beam in the furnace and the steel beams below, thus loading the concrete beam. When the motor is switched to reverse, the tension in the hangers is reduced thus lowering the applied load. The hangers and all the steel within the furnace is temperature resistant titanium steel. The screw jack is used for loading the control beams to failure to establish their flexural strength and also for applying the required load to the reinforced concrete prior to heating the beams. During heating, the applied load on the reinforced concrete beams alters as the beam deforms with temperature change and no attempt was made to keep this load constant. For the plain and fibre concrete beams the value of the loads applied is very small and dead weights were suspended to the hangers for the tests, which required loads to be applied during heating.

An Orion data logger connected to an IBM PC was used to log automatically the data and store them in a file on the hard disk of the computer for subsequent processing. The rig is a unique facility, as detailed beam deformations can be determined. If strain gauges are embedded within the beam, strains can also be established. Unfortunately temperature resistant strain gauges were not allowed for in the research budget and strains are therefore not available. Previous experience with electrical strain gauges (ERS) embedded in concrete gave unsatisfactory results. With recent developments, high temperature ERS have greatly improved (temperature resistance up to 300 ^{0}C) and trials carried out in

some of beams show promise. The set up has permitted the behaviour of plain, reinforced and fibre concrete simply supported beams to be investigated under different transient temperature conditions. Since the testing has shown that internal restraints to beams influence explosive spalling, further development of the rig should allow external restraints to be included as a factor in future factorial based testing.

LONG SECTION ON CENTRE LINE

CROSS - SECTION Y - Y

PLAN X - X
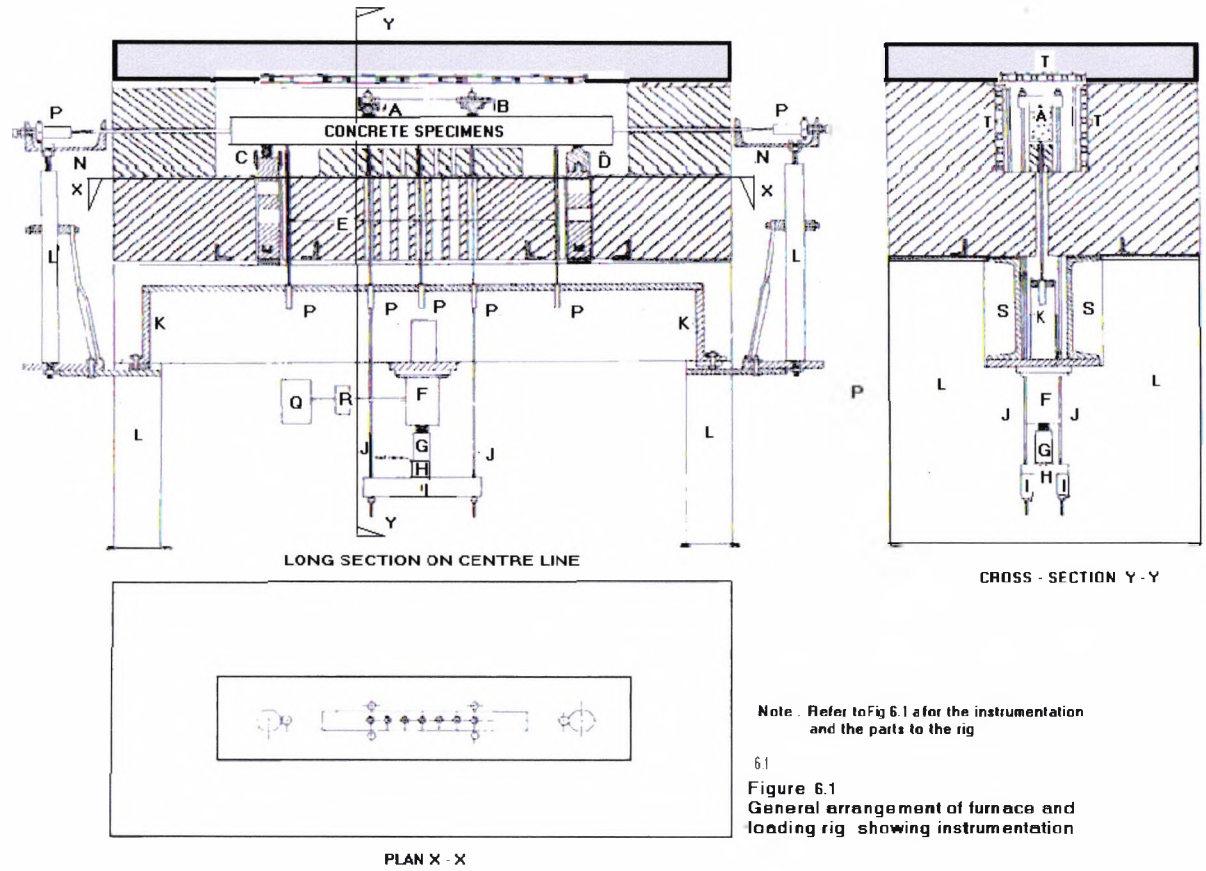
Note : Refer toFig 6.1 a for the instrumentation
and the parts to the rig

6.1

Figure 6.1
General arrangement of furnace and
loading rig showing instrumentation

Figure 6.1.a Instrumentation and parts to the rig.

KEY	DESCRIPTION	PURPOSE
A	Roller	Part of loading saddle
B	Rocker	"
C	Roller	Supporting concrete specimens
D	Rocker	"
E	Aperture	Monitoring
F	Screw jack	Load application
G	Load cell	Load measurement
H	Cross beam	Load transmission
I	Beam	"
J	Hangers	"
K	Deflection bridge	Holding vertical transducers
L	Column	Supporting horizontal transducer channels
M	"	Supporting concrete beams on roller C and rocker D
N	Channel	Supporting horizontal transducers
P	Transducers	Horizontal and vertical movement measurement
Q	Electric motor	Load application
R	Reduction box	"
S	Channel	Supporting furnace and loading rig
T	Heating elements	
U	Column (wall)	Supporting Channels S

Figure 6.2b

SYSTEM OF APPLYING LOAD-MEASURING HORIZONTAL & VERTICAL MOVEMENT FOR BEAM SPECIMEN IN FURNACE
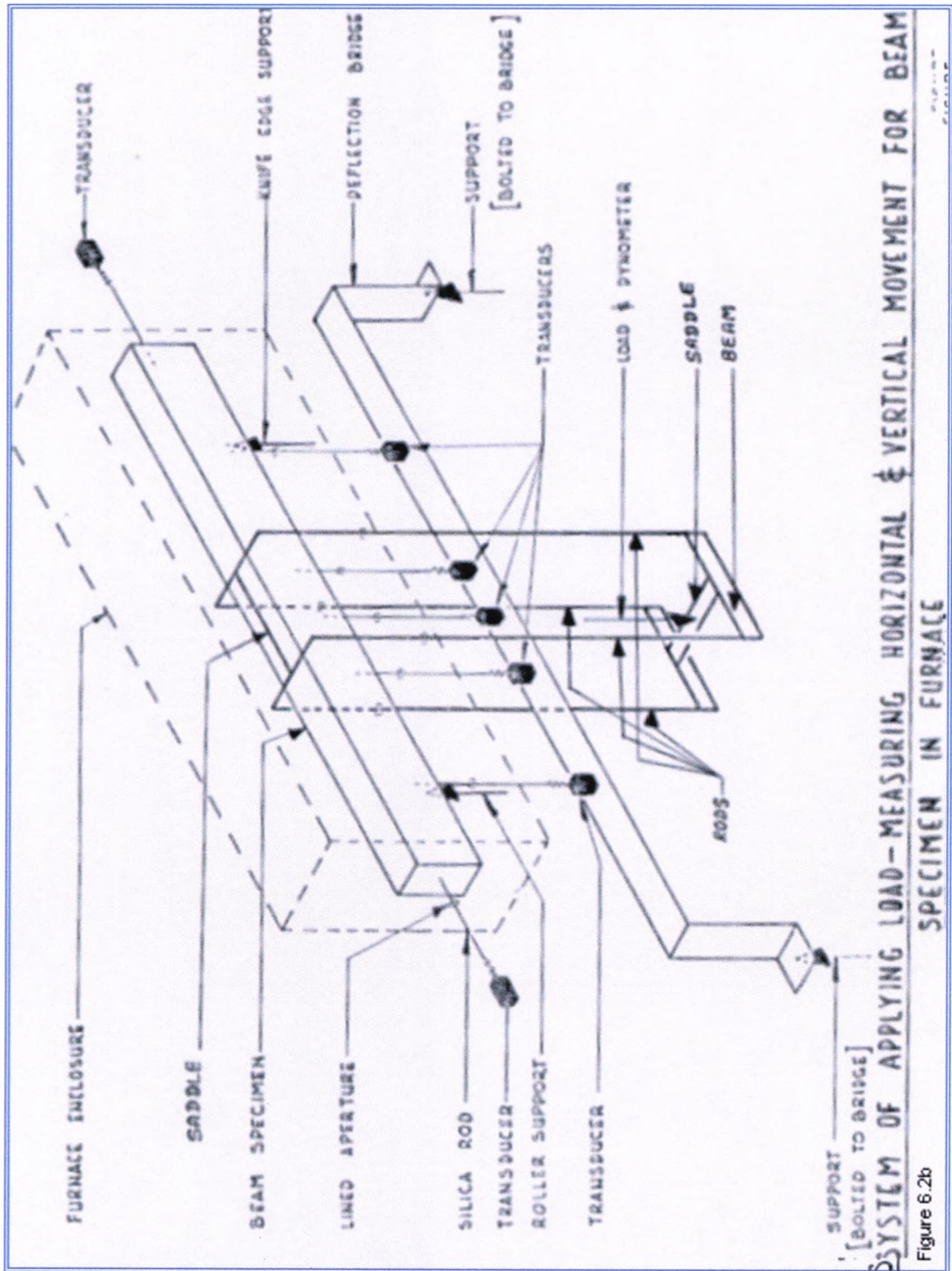
Ref [6.1].

Time temperature curve for the furnace is given below in Fig 6.2, 6.3, and 6.4.
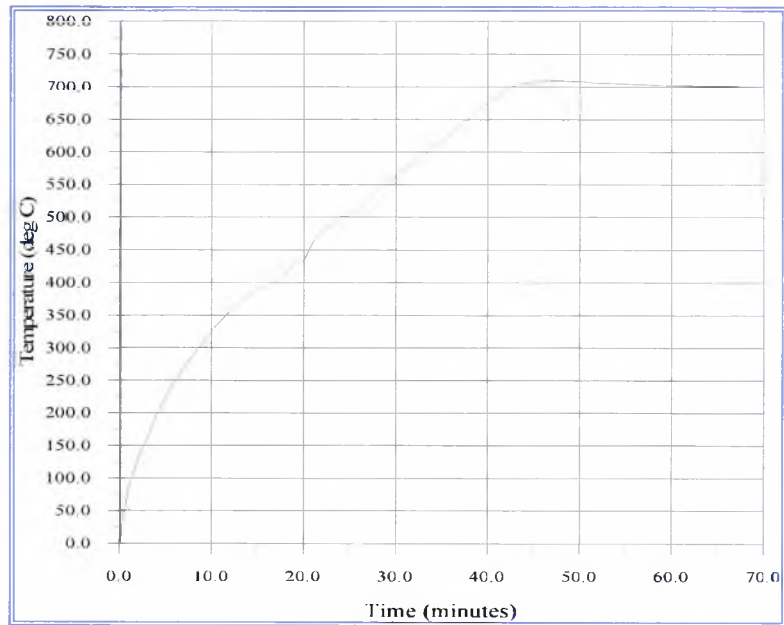
Figure 6.2 Time - Temperature Curve for High Rate of Heating
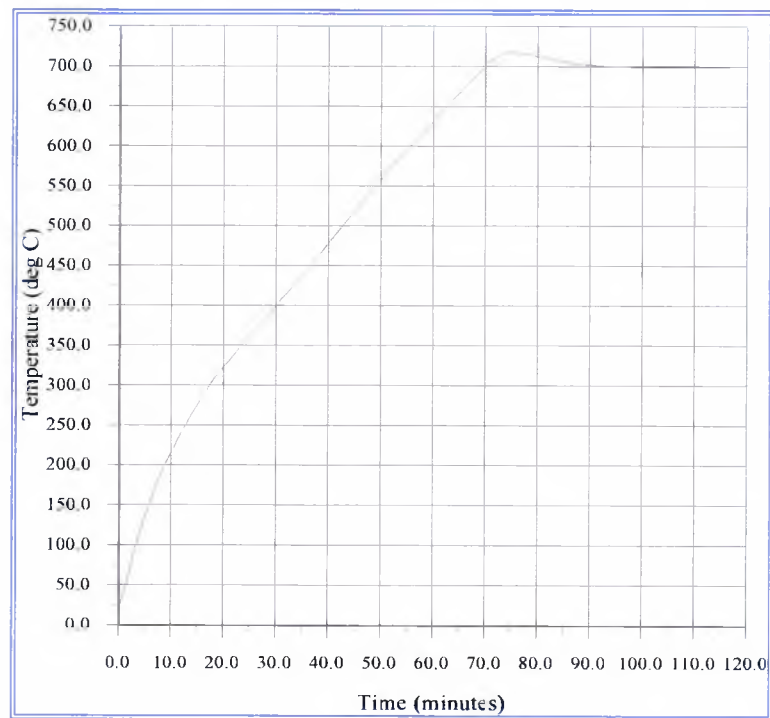
Figure 6.3 Time - Temperature Curve for Medium Rate of Heating
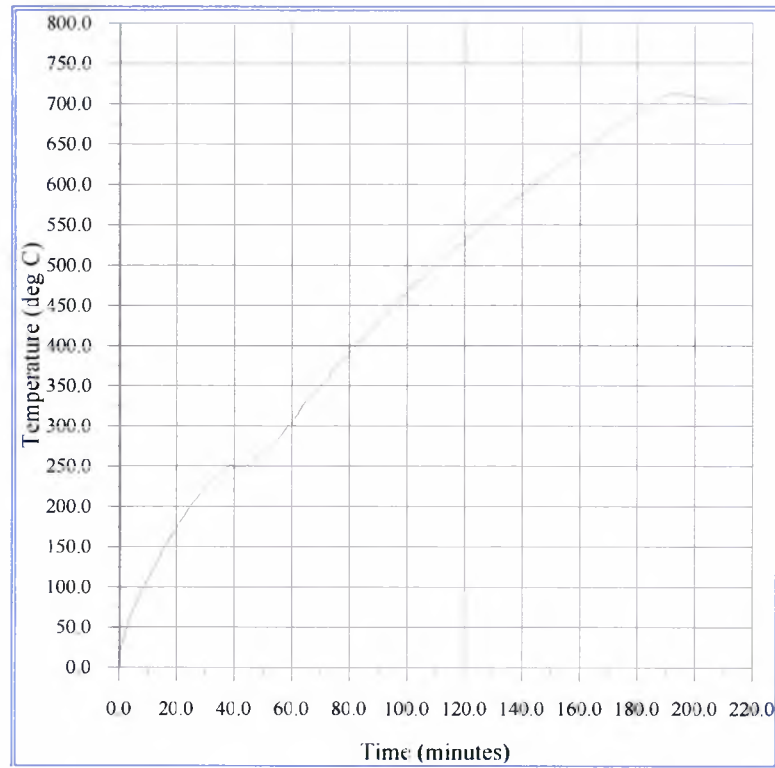
Figure 6.4 Time - Temperature Curve for Low Rate of Heating

6.3 Specimens details

The plain concrete and fibre reinforced concrete specimens for temperature testing were beams each having the dimensions of 850 mm in length and 50 x 75mm in cross section. The reinforced concrete specimens had a cross section of 60 x 85mm to allow sufficient cover to the reinforcing stirrups. The same moulds were used for the plain concrete beams, which were cured in the similar manner as the reinforced concrete beams.

The specimens were cast in steel moulds four beams at a time for each mix. One of the beams was used to find the ultimate load capacity of the beams at room temperature at the time of testing, in conjunction with control cubes and other

samples. Fifteen cubes and four small cylindrical discs were cast for testing room temperature permeability and strength properties at time of testing for each mix.

6.4 Concrete mixes

The limestone concrete mix data was selected from the mixes used by the Building Research Establishment, who were carrying out parallel tests in compression, on concrete varying in strength from 40 to 100 N/mm^2. The modified normal concrete was based on a practical mix used offshore by Mobil Oil on the Hibernia Platform. A number of trial mixes were carried out to determine the mix proportions of the lightweight and modified concrete trying as much as possible to match the strength of the limestone mixes at BRE. It was not possible to match the higher strength and have practical workable mixes for these latter concrete types, even though superplasticisers had to be used and so water/cement ratio was chosen as one of the factors instead of strength. Final mix proportions being used for plain, reinforced and fibre reinforced concrete beams are given in Tables 6.5 to 6.7.

Table 6.5

Mix Proportions of Normal Weight Concrete in kg/m^3

	Mix Code No.		
	N0.50	N0.35	N0.25
Cement	360.00	366.37	489.55
Micro Silica	-	-	-
Limestone	1355.00	1099.22	1174.83
Lytag	-	-	-
Sand	501.00	806.03	636.05
Superplasticiser	1.25	7.0	15.15
Water	193.59	146.53	137.85
28 day strength N/mm^2	49.70	77.14	98.92

Table 6.6

Mix Proportions of Modified Normal Weight Concrete in kg/m^3

	Mix Code No.		
	M0.50	M0.35	M0.25
Cement	360.00	366.37	431.82
Micro Silica	-	-	95.96
Limestone	745.25	604.57	662.13
Lytag	383.44	311.16	340.78
Sand	501.00	806.03	619.38
Superplasticiser	3.0	6.75	10.88
Water	187.82	138.85	147.19
28 day strength N/mm^2	46.82	65.34	68.14

Table 6.7
Mix Proportions of Light weight Concrete in kg/m^3

	Mix Code No.		
	L0.50	L0.35	L0.25
Cement	550.00	504.00	504.00
Micro Silica	-	25.00	50.00
Limestone	-	-	-
Lytag	600.63	582.75	582.75
Sand	620.00	771.75	771.75
Superplasticiser	-	4.38	10.38
Water	281.63	193.38	146.75
28 day strength N/mm^2	36.8	56.1	65.1

The materials used in the mixes are shown below

Cement:-   OPC, Class 42.5 (Blue Circle). Density 3110 kg/m^3.

Fine aggregates:-   Thames Valley, Zone 2. Particle density* (sat. & surface dry –SSD) 2550 kg/m^3. Water absorption in saturated and surface dry state 1.82%.

Coarse aggregates – Limestone:-   Crushed carboniferous limestone, screened 6-10mm. Particle density* on saturated and surface dry state 2720 kg/m^3. Water absorption in the SSD state relative to dry mass 0.33%.

Coarse aggregates *– Light weight* *(Lytag):-*	4-12mm. Bulk density 825 kg/m3. Absorption in SSD state relative to dry is 12-14%. Particle density in a SSD state is 1711 kg/m^3. Moisture content variable but averages 5.23% as packaged.
Microsilica:-	Densified microsilica 93 supplied by Carbon Enterprise Ltd.
Superplasticiser:-	For mixes with microsilica Cormix SP6, SP1 LP

*BS812:Pt2:1995

6.5 Casting and curing procedure

The concrete was caste and compacted in steel moulds on a vibrating table. For the reinforced concrete beams, the steel cage had horizontal steel plates, each with a threaded hole, welded to the bottom reinforcing bars. The steel plates and cage were then firmly bolted on to the steel mould to ensure 5mm cover to the stirrups without the necessity of placing spacers along the length of the beam with different properties to the parent concrete. When the concrete hardened, the bolts were removed and the resulting cavities at the ends were filled with a mortar of the same proportions and consistency as that of the parent concrete. The moulds filled with concrete were covered with polythene sheets allowing the concrete to harden for 24 hours before de-moulding. After de-moulding all the specimens were placed in water at 20 °C. The standard control cubes were kept

in water for a further 27 days before testing. The remainder of the concrete was cured in water for 7 additional days before transferring the samples to their specified curing regime until required for testing. For the nominal 100% RH, the samples were covered with burlap, which was maintained wet. The measured RH prior to testing was in excess of 85%. Some samples were stored in the curing room, which was maintained at 65% RH and 20 $^{\circ}$C, while others were stored in the laboratory at 45% RH and 20 $^{\circ}$C. For the initial plain concrete series the beams were oven-dried for the low curing rate.

An additional beam had instrumentation installed within the moulds before casting. The beam had 32 thermocouples placed at the central and support cross-sections and along the length of the beam as shown in Figure 6.5. In addition to the 15 thermocouples embedded in the limestone concrete beam (w/c 0.5), 17 thermocouples were also placed on the surface surrounding the beam within the furnace during the test. These beams established the concrete temperature regimes at the three furnace rates of heating.
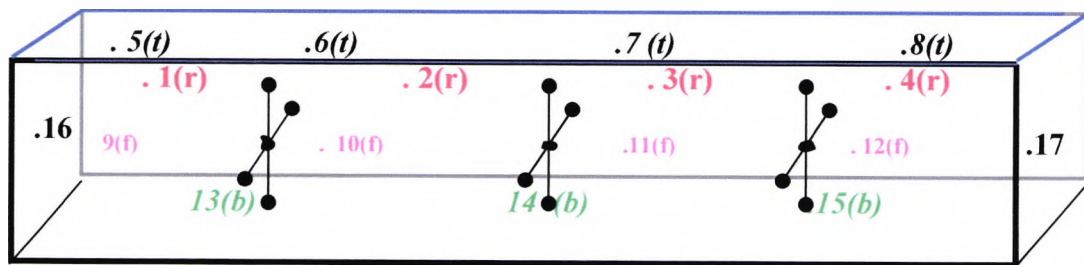
Figure 6.5 Sketch of thermocouple positioning within beam (15) and on beam (17)

6.6 High temperature testing procedures

The following procedures have been observed for all the heat tests.

- Weigh the specimens

- Place the specimen in the steel mesh and in the furnace

- Place the loading equipment in place, if required.

- Close the furnace lid

- Set the maximum temperature to 700 °C

- Set the safety cut off temperature to 800 °C

- Set the power according to the required heating rate

- Start the data logger and apply the load, if required.

- Start the furnace

- Maintain the furnace temperature at 700 °C for 30 minutes

- Switch the furnace off

- Continue to log the data for every 10 minutes during the cooling period with the lid slightly open

During the heating period the data was define at one-minute intervals. During the cooling off period the data was define at ten-minute intervals. When the specimen exploded or failed prematurely, the test was stopped immediately.

In all the experiments beams were placed in the steel mesh before it placed was in the furnace in order to minimise the damage to the furnace due to explosive

spalling if there is an explosive spalling takes place. Figure 6.6 shows the damage to the mesh due to explosion.

Figure 6.6 shows the damage to the mesh due to explosion

6.7 Design of isotherm graphs

The temperature distributions were calculated using data logged information on thirty-two thermocouples placed at 15 points inside and 17 on the surface of the beam (see Figure 6.5). These points were used to form the isotherm graphs shown in Appendix 1.5. These graphs were plotted using the SURFER package on Golden Software. Their two dimensional co-ordinates were used as input and the changing temperatures at these points were then used to create the graphs as shown in Appendix 1.5. It is clear from the isotherm graphs that the high heating rate causes the largest variation in temperature along the length and when the centre section of the beam first reaches 700 $^{\circ}$C the outside sections have only

reached a maximum of 420 $^{\circ}$C. This is important, as when the beam spalls explosively, the end pieces have been the only parts left intact after the test.

This Chapter presented the experimental procedure and the results of all the experiments are given in the next Chapter.

CHAPTER 7

The experimental results and the fractional factorial analysis

This Chapter contains observations of 108 high temperature beam tests, typical fractional factorial calculations of significance factors for the deterioration and explosive spalling, properties of concrete tested to high temperatures, capillary rise test results and typical plots of temperatures against deformations of beams tested to high temperatures. Analyses of these results are included in Chapter 8.

7.1 General observations of 108 high temperature beam tests

Table 7.1 gives a description of the state after testing. of the plain concrete beams subjected to a curing relative humidity (RH) of 65, 45 and 0% respectively. For fractional factorial testing the selection of beams for testing is random and the second column of Table 7.1 showing test numbers is from Table 6.4.

Beam 16 in the first series is exploded; in order to study if the beam 16 will explode again the whole first series of experiments have to be repeated, because factorial analyses calculates the overall average. repeating one experiment alone may not produce the true results.

Tables 7.1 & 7.2 have been rearranged from Table 6.4 to give testing in order of the type of concrete i.e. limestone concrete, modified normal concrete and lightweight aggregate (Lytag) concrete.

Table 7.1

Observations for plain concrete (tested after curing at 65, 45 & 0% RH)

Test Reference	Test No.	Rate of heating	Curing	Remarks
Limestone concrete				
N/0.5/HH/0/C2	16	H	Air	**_Explosive spalling_** after 26 minutes – Furnace temperature approx.480 °C (Av. Conc. Temp 260 °C)
N/0.25/HH/I0/C1	8	H	Moist	Severe cracking at top middle loading zone. Cracks at all surface. Permanent 5.5mm deflection at centre
N/0.35/HH/20/C3	27	H	Dry	Minor cracking but beam broke during cooling.
N/0.5/HM/0/C1	4	M	Moist	Cracking only at the top surface of beam
N/0.25/HM/10/3	23	M	Dry	Severe cracking at the top
N/0.35/HM/20/2	15	M	Air	Minor cracking – beam broken during cooling
N/0.5/HL/0/C1	19	L	Dry	Cracking only on the bottom surface of beam
N/0.25/HL/10/C2	11	L	Air	Small cracks at top 5 mm deep over middle 100mm
N/0.35/HL/20/C3	3*	L	Moist	Minor cracking
Modified concrete				
M/0.35/HH/0/C1	7	H	Moist	Severe cracking mainly on top surface
M/0.5/HH/10/C3	26	H	Dry	Minor cracking
M/0.25/HH/20/2	18	H	Air	Minor cracking – failed during cooling
M/0.35/HM/0/C3	22	M	Dry	Minor cracking
M/0.5/HM/10/C2	14	M	Air	Minor cracking
M/0.25/HM/20/1	6	M	Moist	Minor cracking – failed during cooling
M/0.35/HL/0/C2	10	L	Air	Minor cracking
M/0.5/HL/10/C1	2	L	Moist	Minor cracking
M/0.25/HL/20/C3	21	L	Dry	Minor cracking – failed during cooling
Lightweight aggregate concrete				
L/0.25/HH/0/C3	25	H	Dry	Minor cracking –top surface

Table 7.1 continues

L/0.35/HH/10/C2	17	H	Air	Minor cracking
L/0.5/HH/20/C1	9	H	Moist	Severe cracking
L/0.25/HM/0/C2	13	M	Air	No visible cracking
L/0.35/HM/10/C1	5	M	Moist	No visible cracking
L/0.5/HM/20/C3	24	M	Dry	Minor cracking
L/0.25/HL/0/C1	1	L	Moist	No visible cracking
L/0.35/HL/10/C3	20	L	Dry	No visible cracking
L/0.5/HL/20/C2	12	L	Air	Minor cracking
*Beam 16 spalled explosively.				

Table 7.2 shows a summary of the observations for the plain and reinforced concrete beams subjected to a regime of curing of RH of 85, 65 and 45% respectively. The fibre concrete beams, cured at a nominal 100% RH, are also shown for comparison. Again the Table has been laid out to show the types of aggregate concrete together to facilitate comparison of the beam condition of the beams tested.

Notation used in Tables 7.2 and 7.3

*Beams were loaded to 20% of cold strength prior to heating

+Beams were loaded to 10% of cold strength prior to heating

Glossary: FOC = Failed on cooling; FOH = Failed on heating; CAS = Cracks along sides; SC = Severe cracking at top and bottom; MC = Minor cracking at top and bottom.

(BS) = Beam sags at end of test; (BH) = Beam hogs at end of test.

Table 7.2

Observations for beams tested after curing at 85, 65 & 45% RH (the beams that failed violently are shown in bold italic red print)

Test No.	Rate of heating	Plain Concrete (RH of beams C1 = 85%, C2 = 65% & C3 = 45 %)	Reinforced Concrete	Fibre Concrete (RH = 85%)
Limestone concrete				
16	H	*Explosion C2, W/C = 0.5*	*Explosion C2, W/C = 0.5*	Failed on cooling (FOC)
8+	H	*Explosion C1, W/C = 0.25*	*Explosion C1, W/C = 0.25*	FOC
27*	H	Failed on cooling (FOC)	*Explosion C3, W/C = 0.35*	FOC
4	M	Cracks at sides (CAS)	CAS Beam hogs (BH)	Severe cracking (SC)
23+	M	FOC	CAS (BH)	FOC
15*	M	FOC	*Explosion C2, W/C = 0.35*	SC
19	L	CAS	CAS (BH)	Minor cracking (MC)
11+	L	FOC	CAS	MC
3*	L	FOC	CAS	MC
Modified concrete				
7	H	*Explosion C1, W/C = 0.35*	*Explosion C1, W/C = 0.35*	FOC
26+	H	FOC	CAS	FOC
18*	H	FOC	CAS Beam sags (BS)	FOH
22	M	*Explosion C3, W/C =0.35*	CAS (BS)	FOC
14+	M	FOC	CAS (BH)	SC
6*	M	FOC	CAS (BS)	SC
10	L	CAS	CAS (BH)	MC
2+	L	FOC	CAS (BS)	MC
21*	L	FOC	CAS (BS)	MC
Lightweight aggregate concrete				
25	H	*Explosion C3, W/C = 0.25*	CAS (BH)	
17+	H	FOC	*Explosion C2, W/C = 0.35*	(FOH)
9*	H	FOH	*Explosion C1, W/C = 0.5*	FOC
13	M	CAS	CAS (BH)	FOC
5+	M	FOC	CAS (BS)	SC
24*	M	FOC	CAS (BS)	SC
1	L	CAS	CAS (BH)	MC
20+	L	FOC	CAS (BS)	MC
12*	L	FOC	CAS (BS)	MC

Table 7.3 shows Table 7.2 rearranged for the plain and reinforced concrete beams, in the order of rate of heating since this was observed to be the most predominant factor in causing violent failure in subsequent analysis.

Table 7.3.

Observations for plain and RC beams rearranged in heating rate order (the beams that failed violently are shown in bold italic red print)

Test No.	Plain Concrete (Wo-Wt) kg	Remarks	Reinforced Concrete (Wo-Wt) kg	Remarks
Low heating rate				
1	-	CAS	-	CAS, BH
2+	-	FOC	-	CAS, BS
3*	-	FOC	-	CAS
10	-	CAS	-	CAS, BH
11+	-	FOC	-	CAS
12*	-	FOC	-	CAS, BS
19	-	CAS	-	CAS, BH
20+	-	FOC	-	CAS, BS
21*	-	FOC	-	CAS, BS
Medium heating rate				
4	-	CAS	-	CAS, BH
5+	-	FOC	-	CAS, BS
6*	-	FOC	-	CAS, BS
13	-	CAS	-	CAS, BH
14+	-	FOC	-	CAS, BH
15*	-	FOC	*5.82*	*Explosion C2, W/C = 0.35*
22	*5.51*	*Explosion C3, W/C = 0.35*	-	CAS, BS
23+	-	FOC	-	CAS, BH
24*	-	FOC	-	CAS, BS

Table 7.3 Continues

Test No.	Plain Concrete (Wo-Wt) kg	Remarks	Reinforced Concrete (Wo-Wt) kg	Remarks
High heating rate				
7	*7.64*	*Explosion C1, W/C = 0.35*	*6.37*	*Explosion C1, W/C = 0.35*
8+	*8.14*	*Explosion C1, W/C = 0.25*	*6.12*	*Explosion C1, W/C = 0.25*
9*	-	FOH	*3.49*	*Explosion C1, W/C = 0.5*
16	*7.36*	*Explosion C2, W/C = 0.5*	*5.20*	*Explosion C2, W/C = 0.5*
17+	-	FOC	*4.14*	*Explosion C2, W/C = 0.35*
18*	-	FOC	-	CAS, BS
25	*6.4*	*Explosion C3, W/C = 0.25*	-	CAS, BH
26+	-	FOC	-	CAS
27*	-	FOC	*4.53*	*Explosion C3, W/C = 0.35*

! Wo–Wt = Weight before test less weight after test

Note: C1 was curing at 85%, C2 at 65% & C3 at 45% RH.

Table 7.4 shows the highest expansions for the three series of tests after heating to 700 °C at different rates of heating and maintained at this temperature for a period of 30 minutes. For the beams that exploded, the expansions were taken just before failure and the expansions are shown in italic bold red print in the Table. The mean expansion at the three rates of heating for the three types

concrete types are also given as is the overall mean expansion for each of the three types of concrete beams in bold print. Those beams that exploded were not included in the averaging.

Table 7.4

Highest expansions in mm for all beams tested (Values in bold italic taken prior to explosive spalling)

Test No.	Rate of heating	Plain Concrete (RH of beams C1 = 85%, C2 = 65% & C3 = 45 %)	Reinforced Concrete	Fibre Concrete (RH = 85%)
Limestone concrete				
16	H	*1.59*	*2.12*	9.32
8+	H	*1.49*	*2.38*	7.43
27*	H	9.62	*1.78*	9.30
Mean		**9.62**	-	**8.68**
4	M	9.75	8.69	9.16
23+	M	10.10	8.23	10.68
15*	M	9.29	*2.57*	7.81
Mean		**9.71**	**8.46**	**9.31**
19	L	9.87	8.25	9.35
11+	L	9.2	5.84	8.45
3*	L	8.39	8.95	7.37
Mean		**9.15**	**7.68**	**8.39**
O/A Mean		**9.46**	**7.99**	**8.76**
Modified concrete				
7	H	*1.37*	*1.96*	7.44
26+	H	10.31	7.7	9.76
18*	H	9.30	8.27	6.68
Mean		**9.81**	**7.99**	**7.96**
22	M	*2.03*	7.52	11.12
14+	M	7.81	7.91	10.10
6*	M	10.22	7.06	4.95
Mean		**9.02**	**7.50**	**8.72**
10	L	9.62	7.85	10.01

Table 7.4 continues

Test No.	Rate of heating	Plain Concrete (RH of beams C1 = 85%, C2 = 65% & C3 = 45 %)	Reinforced Concrete	Fibre Concrete (RH = 85%)
2+	L	9.16	8.28	9.87
21*	L	7.36	8.83	5.93
Mean		**8.71**	**8.32**	**8.60**
O/A Mean		**9.11**	**7.93**	**8.42**
Lightweight aggregate concrete				
25	H	*1.99*	7.95	9.62
17+	H	9.64	*1.67*	10.22
9*	H	6.99	*1.79*	8.63
Mean		**8.32**	**7.95**	**9.49**
13	M	6.80	6.48	9.66
5+	M	9.16	7.64	9.46
24*	M	5.59	7.86	8.68
Mean		**7.18**	**7.32**	**9.27**
1	L	5.56	8.55	9.44
20+	L	4.85	8.59	9.98
12*	L	7.40	7.83	8.32
Mean		**5.94**	**8.32**	**9.20**
O/A Mean		**7.00**	**7.84**	**9.32**

Notation used in Table 7.4

*Beams were loaded to 20% of cold strength prior to heating

+Beams were loaded to 10% of cold strength prior to heating

7.2 Properties of concrete

The control cube strength of the normal, modified normal and the lightweight

aggregate concrete used in the tests and the compressive and flexural strength at

day of testing are shown in Tables 7.5 for plain and reinforced concrete and in

Table 7.6 for fibre reinforced concrete.

Tested specimens are concrete cubes (100 x 100 x 100 mm) and beams (850 x 50

x 75 mm).

Table 7.5

Properties of concrete for plain and reinforced concrete

	PLAIN CONCRETE			REINFORCED CONCRETE			
TEST NO	Compressive strength N/mm^2		Flexural strength N/mm^2	Fail. load kN	Compressive strength N/mm^2		Yield load kN	Fail. load kN
	28 Days	Test day	Test day	Test day	28 Days	Test day	Test day	Test day
1	64.1	67.3	4.61	2.28	63.7	66.7	8.8	28.1
2	43.4	46.9	4.52	2.21	45.6	46.7	8.8	27.5
3	70.3	76.7	5.90	2.94	71.2	74.4	11.7	29.7
4	56.4	63.5	5.59	2.79	58.4	61.2	9.4	28.3
5	54.2	58.3	3.12	1.53	55.3	56.6	7.9	25.8
6	81.4	84.1	4.77	2.88	80.4	83.4	13.3	28.7
7	75.3	77.6	5.10	2.5	77.3	79.2	9.8	28.1
8	92.1	95.2	6.31	3.16	90.3	92.8	15.7	30.6
9	40.4	43.4	2.53	1.23	39.2	41.3	5.4	21.9
10	75.3	78.2	5.10	2.5	77.3	78.2	9.8	28.1
11	92.1	93.4	6.31	3.16	90.3	91.3	15.7	30.6
12	40.4	41.6	2.53	1.23	39.2	39.8	5.4	21.9
13	64.1	66.4	4.61	2.28	63.7	64.4	8.8	28.1
14	43.4	45.5	4.52	2.21	45.6	47.5	8.8	27.5
15	70.3	73.3	5.90	2.94	71.2	73.4	11.7	29.7
16	56.4	58.4	5.59	2.79	58.4	60.2	9.4	28.3
17	54.2	55.3	3.12	1.53	55.3	58.2	7.9	25.8
18	81.4	83.5	5.90	2.88	80.2	83.4	13.3	28.7
19	56.4	58.4	5.59	2.79	58.4	60.8	9.4	28.3
20	54.2	55.2	3.21	1.53	55.3	59.8	7.9	25.8
21	81.4	83.6	5.90	2.88	80.2	83.3	13.3	28.7
22	75.3	77.1	5.10	2.5	77.3	79.2	9.8	28.1
23	92.1	95.2	6.31	3.16	90.3	91.2	15.7	30.6
24	40.4	45.5	2.53	1.23	39.2	42.4	5.4	21.9
25	64.1	68.3	4.61	2.28	63.7	65.3	8.8	28.1
26	43.4	44.5	4.52	2.21	45.6	48.2	8.8	27.5
27	70.3	72.3	5.90	2.94	71.2	73.6	11.7	29.7
AVE	64.2	67.0	4.80	2.39	64.6	66.8	10.1	27.6
STDEV	16.3	16.3	1.2	0.6	15.8	15.8	2.9	2.4

Table 7.6

Properties of fibre concrete at ambient temperature

TEST NO	Compressive strength N/mm^2		Flexural strength	Fail. Load Kn
	28 Days	Test day	Test day	Test day
1	58.3	61.7	5.21	2.07
2	92.4	101.3	7.04	2.82
3	44.3	49.3	4.51	1.79
4	96.4	114.3	8.36	3.36
5	71.9	70.2	6.56	2.63
6	41.4	46.7	4.86	1.94
7	72.1	74.3	6.45	2.78
8	51.4	52.4	4.57	1.82
9	72.7	93.6	6.70	2.67
10	72.1	76.9	6.45	2.78
11	51.4	48.7	4.57	1.82
12	72.7	86.5	6.70	2.67
13	58.3	59.1	5.21	2.07
14	92.4	99.4	7.04	2.82
15	44.3	53.1	4.51	1.79
16	96.4	103.9	8.36	3.36
17	71.9	74.1	6.56	2.63
18	41.4	44.8	4.86	1.94
19	96.4	111.6	8.36	3.36
20	71.9	69.8	6.56	2.63
21	41.4	41.4	4.86	1.94
22	72.1	71.7	6.45	2.78
23	51.4	50.9	4.57	1.82
24	72.7	91.4	6.70	2.67
25	58.3	64.3	5.21	2.07
26	92.4	96.8	7.04	2.82
27	44.3	49.7	4.51	1.79
AVE	66.8	72.5	6.03	2.43
STDEV	18.5	22	1.24	0.52

7.3 Capillary rise test

Table 7.7 shows the capillary rise test results with the square root of time for concrete used for the plain and reinforced concrete beams. Air cured specimens were placed in 5 mm water and measured mass absorbed in an hour intervals. Since fibre concrete is 100% moisture cured this test will not give efficient results for fibre reinforced specimens. In Chapter 8 these results are used for comparison with significance of W/C ratio from fractional factorial analysis.

Table 7.7

Capillary rise test results

Mass absorbed (g) against time (min)

TIME (Min)	60	120	180	240	300	360	1320	1380	1440	1500
SQRT.TIME	7.75	10.95	13.42	15.49	17.32	18.97	36.33	37.15	37.95	38.73
N0.25(A)	0.46	0.92	1.42	1.73	2.22	2.73	6.16	6.23	6.24	6.31
N0.35(A)	0.49	0.89	1.27	1.56	2.04	2.54	6.03	6.29	6.32	6.32
N0.50(A)	0.83	1.31	1.84	2.21	2.73	3.14	8.63	8.81	8.84	8.85

SQRT.TIME	7.75	10.95	13.42	15.49	17.32	18.97	36.33	37.15	37.95	38.73
M0.25(A)	5.83	6.67	7.30	7.42	8.06	8.84	13.39	13.61	13.94	14.13
M0.35(A)	5.74	6.63	7.16	7.33	8.21	8.96	13.81	13.84	13.92	14.23
M0.5(A)	12.42	13.91	16.23	17.78	19.06	20.77	26.64	26.86	26.93	27.11

SQRT.TIME	7.75	10.95	13.42	15.49	17.32	18.97	36.33	37.15	37.95	38.73
L0.25(A)	4.70	5.50	7.00	8.03	8.80	9.91	16.50	16.64	16.70	16.71
L0.35(A)	11.98	13.50	15.58	17.04	18.02	19.40	29.54	29.70	30.23	30.28
L0.50(A)	20.76	23.9	25.7	27.31	28.69	30.88	42.74	44.04	44.79	44.84

Figure 7.1 in the next page shows the capillary rise test results plotted against the square root of time for concrete used for the plain and reinforced concrete beams.
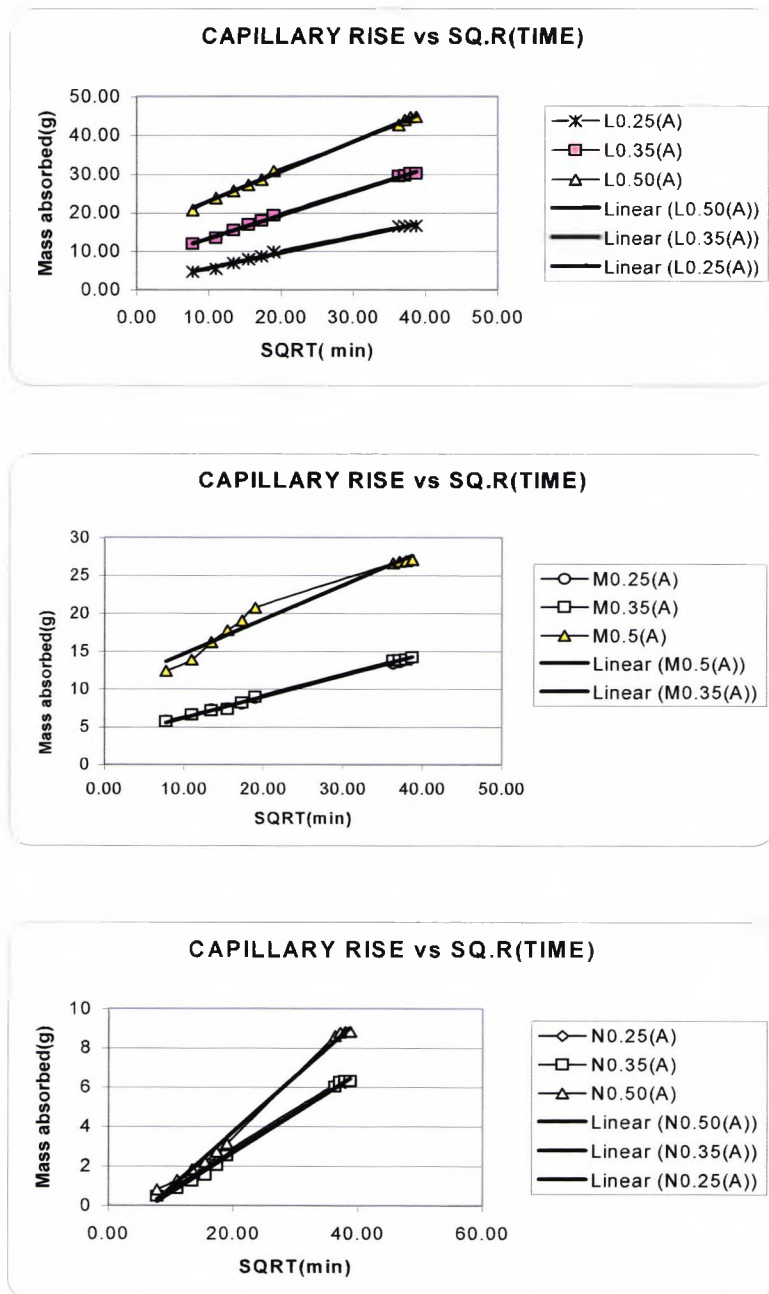
Figure 7.1 Capillary rise of limestone (N), modified normal (M) and LWA (L) concrete.

7.4 Fractional factorial analyses.

This section contains analysis of deterioration and spalling of concrete using the fractional factorial method. Only typical five fractional factorial analyses are presented in this section. There are more fractional factorial analyses for deterioration and spalling using different criterions are presented in Appendix A. Results of significance factor from analysis of variance (ANOVA) Tables are discussed in Chapter 8.

7.4.1 Analysis of explosive spalling of plain concrete

The criterion for assessing the factors influencing explosive spalling of plain concrete was based on the weight of intact concrete remaining after failure, which will give weight lost due to explosion. Although only 5 of the 27 plain concrete beams exploded, it is possible to obtain meaningful averages for the analyses of the experiments using fractional factorial analyses.

Tables 7.8a to 7.8f shows a fractional factorial analysis for the plain concrete series of tests using weight lost due to explosion, where the beams were cured at 85%, 65% & 45% RH prior to heating. For this analysis the calculation details are given in full details.

Table 7.8b gives the sum of all the interaction factors XnYn (where n = 0,1,2). For factors A and B, XnYn is equal to the sum of all the combinations of A and B from Table 7.8a, and so on for the other factors combinations.

The main effects of each factor at each level are shown in Table 7.8c. In this Table the processed results in the last column of Table 7.8a are summed over their level. So SUM (Xi) for factor A is the sum of the first nine values in the last column of Table 7.8a as these are all at level 0.

Since there are only three values of interacting factor combination at the same level, the totals of the interaction effects in Table 7.8b are same as the total of main effect result of Table 7.8c.

Similarly SUM (Xj) for factor A is the sum of the second nine values in the last column of Table 7.8a as these are all at level 1, etc.

Table 7.8d gives the mean sum of squares for individual factors in the first row shown as SSXiXjXk/9. These values, less the sum of squares of the total 27 test results {SS (Tot)/27 in Table 7.8d} give the effect of the main factor, Sa. Sa is used to estimate the variance of each main factor.

Finally, Table 7.8e gives the mean sum of the squares for the interacting factors shown as SSXiYk/3 in the first row. These values, less the sum of squares of the total 27 test results {SS(Tot)/27 in Table 7.8d} gives Saxb.

S(axb) is equal to SSXY/3 − SST/27

The average effect of the interacting factors on the overall average Sab is equal to Sab = Saxb (Table 7.8e)-Sa (Table 7.8d)-Sb (Table 7.8d). This value is shown as Sab... in column 3 of Table 7.8f to include interactions of AB, AC, BC and DE.

The values for the effect of each individual and interacting factor are shown in the third column of Table 7.8f showing the analyses of variance. These sums of

squares together with those of the error factor divided by the degrees of freedom (df) of each individual and interacting factor give the variances V shown in the 4th column of Table7.8f. These variances divided by the error factor give the Fisher (F) factors, which are used for checking the significance of the effect of a change in level for each factor. This procedure is further explained in the Chapter 5 and a standard Fisher Table from reference 5.2 has been added.

Although there is a great deal of statistical and arithmetical work in deriving the Tables, the procedure is programmed in Microsoft Excel so that any other selected result can be very easily analysed.

Table 7.8a
Fractional factorial analyses for plain concrete
(Exploded beams only)

FACTORS	CURING	HEATING	LOAD	W/C	AGGREG	Weight.loss
Test No.	A	B	C	D	E	kg
1	C1	L	0	0.25	LIGHT	0.00
2	C1	L	10	0.50	MOD	0.00
3	C1	L	20	0.35	NORMAL	0.00
4	C1	M	0	0.50	NORMAL	0.00
5	C1	M	10	0.35	LIGHT	0.00
6	C1	M	20	0.25	MOD	0.00
7	C1	H	0	0.35	MOD	7.64
8	C1	H	10	0.25	NORMAL	8.14
9	C1	H	20	0.50	LIGHT	0.90
10	C2	L	0	0.35	MOD	0.00
11	C2	L	10	0.25	NORMAL	0.00
12	C2	L	20	0.50	LIGHT	0.90
13	C2	M	0	0.25	LIGHT	0.00
14	C2	M	10	0.50	MOD	0.00
15	C2	M	20	0.35	NORMAL	0.00
16	C2	H	0	0.50	NORMAL	7.36
17	C2	H	10	0.35	LIGHT	0.90
18	C2	H	20	0.25	MOD	0.00
19	C3	L	0	0.50	NORMAL	0.90

Table 7.8a continues

FACTORS	CURING	HEATING	LOAD	W/C	AGGREG	Weight.loss
Test No.	A	B	C	D	E	kg
20	C3	L	10	0.35	LIGHT	0.00
21	C3	L	20	0.25	MOD	0.00
22	C3	M	0	0.35	MOD	5.51
23	C3	M	10	0.25	NORMAL	0.00
24	C3	M	20	0.50	LIGHT	0.00
25	C3	H	0	0.25	LIGHT	6.40
26	C3	H	10	0.50	MOD	0.00
27	C3	H	20	0.35	NORMAL	0.00

Table 7.8b
Interaction table

COMBINATION	AB	AC	BC	DE	CD	CE
XiYi 00	0.00	7.64	0.00	6.40	6.40	6.40
XiYj 01	0.00	8.14	0.00	0.00	13.15	13.15
XiYk 02	15.78	0.00	0.00	8.14	7.36	7.36
10	0.00	7.36	5.51	0.00	8.14	0.00
11	0.00	0.00	0.00	13.15	0.00	0.00
12	7.36	0.00	0.00	0.00	0.00	8.14
20	0.00	11.91	21.40	0.00	0.00	0.00
21	5.51	0.00	8.14	0.00	0.00	0.00
22	6.40	0.00	0.00	7.36	0.00	0.00
TOT (SUMXiYk)	35.05	35.05	35.05	35.05	35.05	35.05

Table 7.8c
Main effect

	CURING	HEATING	LOAD	W/C	AGGREG
	A	B	C	D	E
SUM1 (Xi)	15.78	0.00	26.91	14.54	6.40
SUM2 (Xj)	7.36	5.51	8.14	13.15	13.15
SUM3 (Xk)	11.91	29.54	0.00	7.36	15.50
Tot (SXijk)	35.05	35.05	35.05	35.05	35.05

Table 7.8d
Sum of squares from main effect

SSXiXjXk/9	49.447	100.330	87.823	48.723	50.459
SSTot/27	45.500	45.500	45.500	45.500	45.500
SSXiXjXk/9 -SSTot/27=Effect of factor X on O/A average					
Sa	3.947252	54.8301	42.3229	3.22254	4.959074

Table 7.8e
Sum of squares from interaction effect

	AB	AC	BC	DE	CD
SSXiYk	374.50	320.65	554.58	334.31	334.31
SSXiYk/3 -SSTot/27	79.33	61.38	139.36	65.94	65.94
Sab	20.56	15.11	42.21	57.76	

Table 7.8f
Analyses of variance

Source	df	Sa --- Sab	V	F(a)= V(a)/V(Er1)	Significance %	F(a)= V(a)/V(Er3)
A (Curing)	2	3.95	1.97	0.14		0.30
B (Heating)	2	54.83	27.42	1.90	>95	4.22
C (Loading)	2	42.32	21.16	1.47	90	3.26
D (W/c)	2	3.22	1.61	0.11		0.25
E (Aggregate)	2	4.96	2.48	0.17		0.38
AB	4	20.56	5.14	0.36		
AC	4	15.11	3.78	0.26		
BC	4	42.21	10.55	0.73		
DE	4	57.76	14.44			2.22
(Error)1	4	57.76	14.44			
(Error)2	12	77.87	6.49			

7.4.2 Analysis of deterioration for plain concrete

Tables 7.9a to 7.9f shows a fractional factorial analysis of deterioration for the plain concrete series of tests. The criterion for assessing the factors influencing deterioration in the experiment where explosive spalling did not take place, was based on the maximum dilation of all the beams in the fractional factorial experiment with fictitious extrapolated expansion values given to the beams that exploded for the plain concrete.

Table 7.9a
Fractional factorial analyses for plain concrete
(Using fictitious high expansions for beams that exploded)

FACTORS	CURING	HEATING	LOAD	W/C	AGGREG	Expansion
Test No.	A	B	C	D	E	mm
1	C1	L	0	0.25	LIGHT	5.60
2	C1	L	10	0.50	MOD	9.20
3	C1	L	20	0.35	NORMAL	8.40
4	C1	M	0	0.50	NORMAL	9.60
5	C1	M	10	0.35	LIGHT	9.20
6	C1	M	20	0.25	MOD	10.20
7	C1	H	0	0.35	MOD	30.00
8	C1	H	10	0.25	NORMAL	25.00
9	C1	H	20	0.50	LIGHT	6.90
10	C2	L	0	0.35	MOD	9.60
11	C2	L	10	0.25	NORMAL	9.20
12	C2	L	20	0.50	LIGHT	7.30
13	C2	M	0	0.25	LIGHT	6.80
14	C2	M	10	0.50	MOD	7.80
15	C2	M	20	0.35	NORMAL	9.20
16	C2	H	0	0.50	NORMAL	30.00
17	C2	H	10	0.35	LIGHT	9.60
18	C2	H	20	0.25	MOD	9.30
19	C3	L	0	0.50	NORMAL	9.80
20	C3	L	10	0.35	LIGHT	4.80
21	C3	L	20	0.25	MOD	7.30

Table 7.9a continues

FACTORS	CURING	HEATING	LOAD	W/C	AGGREG	Expansion
22	C3	M	0	0.35	MOD	15.00
23	C3	M	10	0.25	NORMAL	10.10
24	C3	M	20	0.50	LIGHT	5.50
25	C3	H	0	0.25	LIGHT	20.00
26	C3	H	10	0.50	MOD	10.80
27	C3	H	20	0.35	NORMAL	9.60

Table 7.9b
Interaction table

COMBINAT	AB	AC	BC	DE	CD	CE
XiYi 00	23.20	45.20	25.00	32.40	32.40	32.40
XiYj 01	29.00	43.40	23.20	26.80	54.60	54.60
XiYk 02	61.90	25.50	23.00	44.30	49.40	49.40
10	26.10	46.40	31.40	23.60	44.30	23.60
11	23.80	26.60	27.10	54.60	23.60	27.80
12	48.90	25.80	24.90	27.20	27.80	44.30
20	21.90	44.80	80.00	19.70	26.80	19.70
21	30.60	25.70	45.40	27.80	27.20	26.80
22	40.40	22.40	25.80	49.40	19.70	27.20
TOT (SUMXiYk)	305.80	305.80	305.80	305.80	305.80	305.80

Table 7.9c
Main effect

	CURING	HEATING	LOAD	W/C	AGGREG
	A	B	C	D	E
SUM1 (Xi)	114.10	71.20	136.40	103.50	75.70
SUM2 (Xj)	98.80	83.40	95.70	105.40	109.20
SUM3 (Xk)	92.90	151.20	73.70	96.90	120.90
Tot (SXijk)	305.80	305.80	305.80	305.80	305.80

Table 7.9d
Sum of squares from main effect

SSXiXjXk/9	3490.073	3876.271	3688.349	3467.891	3585.771
SSTot/27	3463.468	3463.468	3463.468	3463.468	3463.468
SSXiXjXk/9-SSTot/27=Effect of factor X on O/A average					
Sa..Se	26.60519	412.803	224.8807	4.422963	122.303

Table 7.9e
Sum of squares from interaction effect

	AB	AC	BC	DE	CD	CE
SSXiYi	11897.84	11272.3	13159.42	11609.74	11609.74	11609.74
SSXiYk/3-SST/27	502.48	293.97	923.01	406.45	406.45	406.45
Saxb=Sab-Sa-Sb	63.07	42.48	285.32	279.72		

Table 7.9f
Analyses of variance

Source	df	Sa --- Sab	V	F(a)= V(a)/V(Er1)	F(a)= V(a)/V(Er3)	Significanc %
A (Curing)	2	26.61	13.30	0.19	0.41	
B (Heating)	2	412.80	206.40	2.95	6.34	>>95
C (Loading)	2	224.88	112.44	1.61	3.45	95
D (W/c)	2	4.42	2.21	0.03	0.07	
E (Aggregate)	2	122.30	61.15	0.87	1.88	
AB	4	63.07	15.77	0.23		
AC	4	42.48	10.62	0.15		
BC	4	285.32	71.33	1.02		
DE	4	279.72	69.93		2.15	
Error	0	0				
(Error)1	4	279.72	69.93			
(Error)2	16	670.59	41.91			
(Error)3	12	390.87	32.57			

7.4.3 Analysis of deterioration for reinforced concrete

Tables 7.10a to 7.10f shows a fractional factorial analysis of deterioration of the reinforced concrete series of tests. The criterion for assessing the factors influencing deterioration in the reinforced concrete fractional factorial experiment, where explosive spalling did not take place, was based on the maximum dilation of all the beams in the experiment. For the beams that exploded actual expansion values were taken prior to explosion.

Table 7.10a
Fractional factorial analyses for reinforced concrete
(Using   expansions prior to explosion)

FACTORS	CURING	HEATING	LOAD	W/C	AGGREG	exp
Test No.	A	B	C	D	E	mm
1	C1	L	0	0.25	LIGHT	8.55
2	C1	L	10	0.50	MOD	8.27
3	C1	L	20	0.35	NORMAL	8.95
4	C1	M	0	0.50	NORMAL	8.60
5	C1	M	10	0.35	LIGHT	7.60
6	C1	M	20	0.25	MOD	7.00
7	C1	H	0	0.35	MOD	1.90
8	C1	H	10	0.25	NORMAL	2.30
9	C1	H	20	0.50	LIGHT	1.70
10	C2	L	0	0.35	MOD	9.80
11	C2	L	10	0.25	NORMAL	5.80
12	C2	L	20	0.50	LIGHT	7.80
13	C2	M	0	0.25	LIGHT	6.40
14	C2	M	10	0.50	MOD	7.90
15	C2	M	20	0.35	NORMAL	2.50
16	C2	H	0	0.50	NORMAL	2.10
17	C2	H	10	0.35	LIGHT	1.60
18	C2	H	20	0.25	MOD	8.20
19	C3	L	0	0.50	NORMAL	8.20
20	C3	L	10	0.35	LIGHT	8.50
21	C3	L	20	0.25	MOD	8.80
22	C3	M	0	0.35	MOD	7.50
23	C3	M	10	0.25	NORMAL	8.20
24	C3	M	20	0.50	LIGHT	7.80
25	C3	H	0	0.25	LIGHT	7.90
26	C3	H	10	0.50	MOD	7.70
27	C3	H	20	0.35	NORMAL	1.70

Table7.10b
Interaction table

COMBINATION	AB	AC	BC	DE	CD	CE
XiYi 00	25.77	19.05	26.55	22.85	22.85	22.85
XiYj 01	23.20	18.17	22.57	24.00	19.20	19.20
XiYk 02	5.90	17.65	25.55	16.30	18.90	18.90
10	23.40	18.30	22.50	17.70	16.30	17.70
11	16.80	15.30	23.70	19.20	17.70	23.87
12	11.90	18.50	17.30	13.15	23.87	16.30

Table7.10b continues

COMBIN ATION	AB	AC	BC	DE	CD	CE
20	25.50	23.60	11.90	17.30	24.00	17.30
21	23.50	24.40	11.60	23.87	13.15	24.00
22	17.30	18.30	11.60	18.90	17.30	13.15
TOT (SUMXiYk)	173.27	173.27	173.27	173.27	173.27	173.27

Table 7.10c
Main effect

	CURING	HEATIN	LOAD	W/C	AGGREG
	A	B	C	D	E
SUM1 (Xi)	54.87	74.67	60.95	63.15	57.85
SUM2 (Xj)	52.10	63.50	57.87	50.05	67.07
SUM3 (Xk)	66.30	35.10	54.45	60.07	48.35
Tot (SXijk)	173.27	173.27	173.27	173.27	173.27

Table 7.10d
Sum of squares from main effect

SSXiXjXk/9	1124.53	1204.4	1114.2	1122.37	1131.41
SSTot/27	1111.944	1111.94	1111.94	1111.944	1111.944
SSXiXjXk/9-SSTot/27=Effect of factor X on O/A average					
Sa..Se	12.59103	92.4857	2.34936	10.42581	19.47025

Table 7.10e
Sum of squares from interaction effect

	AB	AC	BC	DE	CD
SSXiYi	3710.34	3403.0	3645.0	3444.94	3444.94
SSXiYk/3-SST/27	124.84	22.39	103.08	36.37	36.37
Saxb=Sab-Sa-Sb	19.76	7.45	8.24	6.47	

Table7.10f
Analyses of variance

Source	df	Sa --- Sab	V	F(a)= V(a)/V(Er1)	Significanc %	F(a)= V(a)/V(Er2)
A (Curing)	2	12.59	6.30	3.89	>90	2.40
B (Heating)	2	92.49	46.24	28.57	>>99	17.65
C (Loading)	2	2.35	1.17	0.73		0.45
D (W/c)	2	10.43	5.21	3.22	>95	1.99
E (Aggregate)	2	19.47	9.74	6.02	>>95	3.71
AB	4	19.76	4.94	3.05	>90	
AC	4	7.45	1.86	1.15		ERRORS
BC	4	8.24	2.06	1.27		
DE	4	6.47	1.62			
Error	0	0				
(Error)1	4	6.47	1.62			
(Error)2	16	41.93	2.62			
(Error)3	12	35.46	2.95			

7.4.4 Analysis of explosive spalling for reinforced concrete

Tables 7.11a to 7.11f shows a fractional factorial analysis of the reinforced concrete series of tests using weight lost due to explosion. The criterion for assessing the factors influencing explosive spalling of reinforced concrete was based on the weight of intact concrete remaining after failure, which will give weight lost due to explosion.

Table 7.11a
Fractional factorial analyses for reinforced concrete
(Explosion only)

FACTORS	CURING	HEATING	LOAD	W/C	AGGREG	Weight.loss
Test No.	A	B	C	D	E	kg
1	C1	L	0	0.25	LIGHT	0.00
2	C1	L	10	0.50	MOD	0.00
3	C1	L	20	0.35	NORMAL	0.00
4	C1	M	0	0.50	NORMAL	0.00

Table 7.11a continues

FACTORS	CURING	HEATING	LOAD	W/C	AGGREG	Weight.loss
5	C1	M	10	0.35	LIGHT	0.00
6	C1	M	20	0.25	MOD	0.00
7	C1	H	0	0.35	MOD	6.37
8	C1	H	10	0.25	NORMAL	6.12
9	C1	H	20	0.50	LIGHT	3.49
10	C2	L	0	0.35	MOD	0.00
11	C2	L	10	0.25	NORMAL	0.00
12	C2	L	20	0.50	LIGHT	0.00
13	C2	M	0	0.25	LIGHT	0.00
14	C2	M	10	0.50	MOD	0.00
15	C2	M	20	0.35	NORMAL	5.82
16	C2	H	0	0.50	NORMAL	5.20
17	C2	H	10	0.35	LIGHT	4.14
18	C2	H	20	0.25	MOD	0.00
19	C3	L	0	0.50	NORMAL	0.00
20	C3	L	10	0.35	LIGHT	0.00
21	C3	L	20	0.25	MOD	0.00
22	C3	M	0	0.35	MOD	0.00
23	C3	M	10	0.25	NORMAL	0.00
24	C3	M	20	0.50	LIGHT	0.00
25	C3	H	0	0.25	LIGHT	0.00
26	C3	H	10	0.50	MOD	0.00
27	C3	H	20	0.35	NORMAL	4.53

Table 7.11b
Interaction table

COMBINA	AB	AC	BC	DE	CD	CE
XiYi 00	0.00	6.37	0.00	0.00	0.00	0.00
XiYj 01	0.00	6.12	0.00	0.00	6.37	6.37
XiYk 02	15.98	3.49	0.00	6.12	5.20	5.20
10	0.00	5.20	0.00	4.14	6.12	4.14
11	5.82	4.14	0.00	6.37	4.14	0.00
12	9.34	5.82	5.82	10.35	0.00	6.12
20	0.00	0.00	11.57	3.49	0.00	3.49
21	0.00	0.00	10.26	0.00	10.35	0.00
22	4.53	4.53	8.02	5.20	3.49	10.35
TOT (SUMXiYk)	35.67	35.67	35.67	35.67	35.67	35.67

Table 7.11c
Main effect

	CURING	HEATING	LOAD	W/C	AGGREG
	A	B	C	D	E
SUM1 (Xi)	15.98	0.00	11.57	6.12	7.63
SUM2 (Xj)	15.16	5.82	10.26	20.86	6.37
SUM3(Xk)	4.53	29.85	13.84	8.69	21.67
Tot (SXijk)	35.67	35.67	35.67	35.67	35.67

Table 7.11d
Sum of squares from main effect

SSXiXjXk/9	56.166	102.761	47.841	60.893	63.147
SSTot/27	47.113	47.113	47.113	47.113	47.113
SSXiXjXk/9-SSTot/27=Effect of factor X on O/A average					
Sa..Se	9.052543	55.64746	0.727357	13.77993	16.03339

Table 7.11e
Sum of squares from main effect

	AB	AC	BC	DE	CD	CE
SSXiYi	396.85	188.75	337.28	241.49	241.49	241.49
SSXiYk/3-SST/27	85.17	15.80	65.31	33.38	33.38	33.38
Saxb=Sab-Sa-Sb	20.47	6.02	8.94	3.57		

Table7.11f
Analyses of variance

				F(a)=	Significanc	F(a)=
Source	df	Sa --- Sab	V	V(a)/V(Er1)	%	V(a)/V(Er2)
A (Curing)	2	9.05	4.53	5.07	>90	1.86
B (Heating)	2	55.65	27.82	31.19	>>99	11.42
C (Loading)	2	0.73	0.36	0.41		0.15
D (W/c)	2	13.78	6.89	7.72	>95	2.83
E (Aggregate)	2	16.03	8.02	8.99	>>95	3.29
AB	4	20.47	5.12	5.74	>90	
AC	4	6.02	1.51	1.69		ERRORS
BC	4	8.94	2.23	2.50		
DE	4	3.57	0.89			

Table7.11f continues

Source	df	Sa --- Sab	V	F(a)= V(a)/V(Er1)	Significanc %	F(a)= V(a)/V(Er2)
Error	0	0				
(Error)1	4	3.57	0.89			
(Error)2	16	39.00	2.44			
(Error)3	12	35.43	2.95			

7.4.5 Analysis of deterioration for polypropylene fibre concrete

Tables 7.12a –7.12f below shows fractional factorial analysis of deterioration of polypropylene fibre concrete using maximum deflection as a criterion to obtain the significance factor of deterioration of fibre concrete.

Table 7.12a
Fractional factorial analysis using residual deflection before failure

FACTORS Test No.	HEATING A	LOAD B	W/C C	AGGT D	FIBRE E	Deflection (mm)
1	L	0	0.25	LIGHT	F1	3.98
2	L	0	0.35	NORMAL	F2	0.79
3	L	0	0.50	MOD	F3	1.11
4	L	10	0.25	NORMAL	F3	2.37
5	L	10	0.35	MOD	F1	4.53
6	L	10	0.50	LIGHT	F2	5.65
7	L	20	0.25	MOD	F2	18.17
8	L	20	0.35	LIGHT	F3	19.55
9	L	20	0.50	NORMAL	F1	20.07
10	M	0	0.25	MOD	F2	1.82
11	M	0	0.35	LIGHT	F3	1.96
12	M	0	0.50	NORMAL	F1	0.90
13	M	10	0.25	LIGHT	F1	8.85
14	M	10	0.35	NORMAL	F2	2.72
15	M	10	0.50	MOD	F3	3.71
16	M	20	0.25	NORMAL	F3	5.39
17	M	20	0.35	MOD	F1	6.76

Table 7.12a continues

FACTORS	HEATING	LOAD	W/C	AGGT	FIBRE	Deflection
Test No.	A	B	C	D	E	(mm)
18	M	20	0.50	LIGHT	F2	19.24
19	H	0	0.25	NORMAL	F3	1.77
20	H	0	0.35	MOD	F1	2.31
21	H	0	0.50	LIGHT	F2	2.47
22	H	10	0.25	MOD	F2	10.87
23	H	10	0.35	LIGHT	F3	16.14
24	H	10	0.50	NORMAL	F1	2.35
25	H	20	0.25	LIGHT	F1	23.64
26	H	20	0.35	NORMAL	F2	5.40
27	H	20	0.50	MOD	F3	9.37

Table 7.12b
Interaction table

COMBINAT	AB	AC	BC	DE	CD
XiYi 00	5.88	24.52	7.57	36.47	36.47
XiYj 01	12.55	24.86	5.06	27.36	30.86
XiYk 02	57.78	26.83	4.48	37.65	9.53
10	4.68	16.06	22.09	13.59	37.65
11	15.28	11.44	23.38	30.86	13.59
12	31.39	23.85	11.71	14.19	8.90
20	6.55	36.29	47.20	23.31	27.36
21	29.36	23.84	31.70	8.90	14.19
22	38.40	14.18	48.67	9.53	23.31
TOT (SUMXiYk)	201.87	201.87	201.87	201.87	201.87

Table 7.12c
Main effect

	A	B	C	D	E
SUM1 (Xi)	76.21	17.11	76.87	101.48	73.37
SUM2 (Xj)	51.35	57.18	60.14	58.65	67.12
SUM3 (Xk)	74.31	127.58	64.86	41.74	61.37
Tot (SXijk)	201.87	201.87	201.87	201.87	201.87

Table7.12d
Sum of squares from main effect

SSXiXjXk/9	1551.80	2204.26	1525.78	1719.95	1517.25
SSTot/27	1509.25	1509.25	1509.25	1509.25	1509.25
SSXiXjXk/9-SSTot/27=Effect of factor X on O/A average					
Sa..Se	42.55	695.01	16.53	210.70	8.00

Table7.12e
Sum of squares from interaction effect

	AB	AC	BC	DE	CD
SSXiYi	7151.1	4983.0	6876.8	5548.0	5548.0
SSXiYk/3-SST/27	874.5	151.7	783.0	340.1	340.1
Saxb=Sab-Sa-Sb	136.9	92.7	71.5	121.4	

Table 7.12f
Analyses of variance

Source	df	Sa --- Sab	V	F(a)= V(a)/V(Er1)		F(a)= V(a)/V(Er3)
A (Heat)	2	42.55	21.28	0.70		0.85
B (Load)	2	695.01	347.50	11.45	>>99	13.85
C (W/C)	2	16.53	8.26	0.27		0.33
D (Aggr)	2	210.70	105.35	3.47	>>90	4.20
E (Fibre)	2	8.00	4.00	0.13		0.16
AB	4	136.90	34.22	1.13		
AC	4	92.66	23.16	0.76		
BC	4	71.48	17.87	0.59		
DE	4	121.40	30.35			1.21
Error	0	0				
(Error)1	4	121.40	30.35			
(Error)2	16	422.43	26.40			
(Errror)3	12	301.04	25.09			

7.5 Deflection of exploded beams

Table 7.16 gives deflections of the exploded beams prior to explosion for comparison with beams those are not exploded. Deflections prior to explosion are discussed in details in Chapter 8.

Exploded beams are:

Plain concrete series: L/0.25/00/HH/C3 ----- Test No. 25

                                  N/0.25/10/HH/C1 ------- Test No. 8

                                  M/0.35/00/HH/C1 ------ Test No. 7

                                  M/0.35/00/HM/C3 ------ Test No. 22

                                  N/0.5/00/HH/C2 --------- Test No. 16

Reinforced concrete series: L/0.35/10/HH/C2 ------- Test No. 17

                                  L/0.5/20/HH/C1 --------- Test No.9

                                  M/0.35/00/HH/C1 ------- Test No.7

                                  N/0.25/10/ HH//C1 ------ Test No.8

                                  N/0.35/20/HH/C3 -------- Test No. 27

                                  N/0.35/20/HM/C2 -------- Test No.15

                                  N/0.5/00/HH/C2 ---------- Test No.16

Table 7.13
Deflections of exploded beams (mm) at RH 85, 65, 45%

Beam	L.25/0/H	L.35/10/H	L.5/20/H	M.35/0/H	M.35/0/H	M.35/0/M	N.25/10/H	N.25/10/H	N.35/20/H	N.35/20/M	N.5/0/H	N.5/0/H
TIME (min)	25	17 (R)	9 (R)	7	7(R)	22	8	8 (R)	27 (R)	15 (R)	16 (R)	16
0.00	0.00	0.00	0.00	0.00	0.00	0.00	0.000	0.00	0.00	0.00	0.00	0.00
1.00	0.01	0.00	0.01	0.01	0.00	0.00	0.000	0.00	0.00	0.00	0.00	0.00
2.00	0.01	0.01	0.03	0.01	0.00	0.05	0.009	-0.01	0.01	0.00	0.00	0.00
3.00	0.03	0.02	0.06	0.03	0.01	0.04	0.030	-0.01	0.01	0.00	0.02	0.01
4.00	0.04	0.05	0.10	0.03	0.03	0.04	0.062	-0.01	0.03	0.02	0.07	0.02
5.00	0.05	0.09	0.14	0.05	0.05	0.05	0.107	-0.01	0.06	0.05	0.12	0.04
6.00	0.08	0.14	0.18	0.08	0.08	0.07	0.165	-0.01	0.11	0.07	0.19	0.07
7.00	0.12	0.20	0.23	0.12	0.13	0.09	0.227	-0.01	0.17	0.11	0.26	0.10
8.00	0.17	0.26	0.28	0.17	0.17	0.12	0.299	-0.01	0.24	0.14	0.34	0.14
9.00	0.21	0.33	0.34	0.21	0.22	0.15	0.373	0.00	0.31	0.18	0.45	0.18
10.00	0.25	0.40	0.40	0.25	0.28	0.19	0.458	0.01	0.40	0.23	0.51	0.22
11.00	0.31	0.47	0.46	0.30	0.35	0.22	0.544	0.02	0.49	0.27	0.61	0.28
12.00	0.35	0.54	0.53	0.35	0.42	0.26	0.640	0.04	0.59	0.32	0.70	0.33

Table 7.13 continues

Beam	L.25/0/H	L.35/10/H	L.5/20/H	M.35/0/H	M.35/0/H	M.35/0/M	N.25/10/H	N.25/10/H	N.35/20/H	N.35/20/M	N.5/0/H	N.5/0/H
TIME (min)	25	17 (R)	9 (R)	7	7(R)	22	8	8 (R)	27 (R)	15 (R)	16 (R)	16
13.00	0.40	0.61	0.59	0.40	0.49	0.29	0.746	0.07	0.69	0.37	0.80	0.40
14.00	0.44	0.67	0.65	0.44	0.56	0.33	0.850	0.11	0.79	0.43	0.92	0.46
15.00	0.49	0.73	0.72	0.49	0.64	0.38	0.958	0.15	0.89	0.48	1.04	0.53
16.00	0.53	0.80	0.78	0.53	0.72	0.42	1.068	0.20	0.99	0.54	1.07	0.60
17.00	0.58	0.86	0.84	0.58	0.81	0.47	1.176	0.25	1.10	0.61	1.19	0.67
18.00	0.62	0.92	0.91	0.62	0.89	0.51	1.284	0.30	1.21	0.67	1.20	0.75
19.00	0.67	0.98	0.97	0.67	0.98	0.56	1.388	0.35	1.31	0.74	1.31	0.82
20.00	0.71	1.04	1.03	0.71	1.07	0.61	1.486	0.41	1.43	0.80	1.42	0.90
21.00	0.76	1.10	1.09	0.75	1.17	0.66	1.487	0.47	1.54	0.87	1.51	0.98
22.00	0.80	1.16	1.15	0.79	1.28	0.71	1.489	0.53	1.66	0.93	1.62	1.05
23.00	0.84	1.22	1.21	0.82	1.38	0.76	1.502	0.59	1.78	1.00	1.73	1.13
24.00	0.89	1.27	1.27	0.89	1.49	0.82	1.505	0.66	1.79	1.07	1.83	1.21
25.00	0.94	1.33	1.33	0.94	1.60	0.87	1.508	0.73	1.79	1.14	1.93	1.28
26.00	0.98	1.40	1.39	0.98	1.72	0.92	1.511	0.80	1.79	1.21	2.03	1.36
27.00	1.03	1.46	1.45	1.02	1.84	0.98	1.514	0.87	1.79	1.27	2.13	1.44
28.00	1.07	1.52	1.51	1.07	1.96	1.03	1.515	0.95	1.80	1.34		1.51
29.00	1.12	1.59	1.58	1.12		1.08	1.519	1.04	1.81	1.41		1.59
30.00	1.16	1.67	1.64	1.16		1.14		1.12	1.81	1.48		
31.00	1.20		1.71	1.20		1.19		1.21		1.56		
32.00	1.25		1.79	1.25		1.24		1.29		1.63		
33.00	1.29			1.29		1.30		1.37		1.70		
34.00	1.34			1.34		1.35		1.45		1.77		
35.00	1.38			1.38		1.41		1.54		1.85		
36.00	1.43			1.43		1.46		1.63		1.93		
37.00	1.48			1.48		1.52		1.72		2.00		
38.00	1.53			1.53		1.58		1.83		2.08		
39.00	1.58			1.58		1.64		1.93		2.16		
40.00	1.63			1.63		1.70		2.03		2.24		
41.00	1.68			1.68		1.76		2.13		2.32		
42.00	1.72			1.72		1.82		2.24		2.41		
43.00	1.77			1.77		1.88		2.38		2.49		
44.00	1.82			1.82		1.95				2.57		
45.00	1.87			1.87		2.00						
46	1.92					2.00						
47	1.96					2.00						
48	1.96					2.00						
49	1.99					2.03						
50						2.03						

7.6 Typical processed results of heating and cooling cycles

In this project each series of experiments has 27 furnace tests, making a total of 81. With the repeated series this becomes 108. It is not practicable to present all the furnace test results in full details in this thesis, thus only three typical processed results of heating and cooling cycles showing furnace temperature, time from start of heating together with lateral displacements and deflections of the beams are presented in Appendix A.6, one each for normal, modified and lightweight concrete.

Plots of temperature against deformations for these three typical processed results are presented here (sections 7.6.1, 7.6.2 and 7.6.3) for each concrete and discussed in the section on thermal cycles in Chapter 8.

The results obtained from the data logger were programmed using FORTRAN 77 in order to obtain the actual value in mm and in a convenient form to analyse these results.

The original format of the experimental results obtained from the data logger and the source code of the programs are given in Appendix. B

Figure.7.2 shows the diagrammatic representation of the silica rods/transducer location in contact with the beam in the furnace.
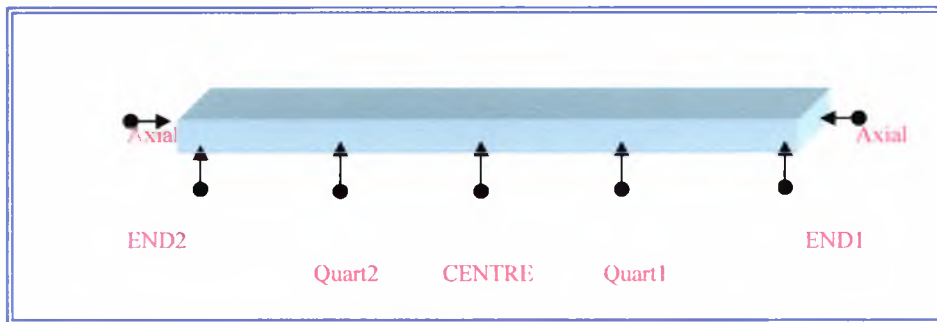
Figure. 7.2 Diagrammatic representation of silica rods/transducer location in contact with beam in furnace.

7.6.1 Plots of deformation against temperature (L0.35/00/HM/F3)

Graphs below plotted from typical processed results of heating and cooling cycles of lightweight concrete presented in Appendix A.6.1.
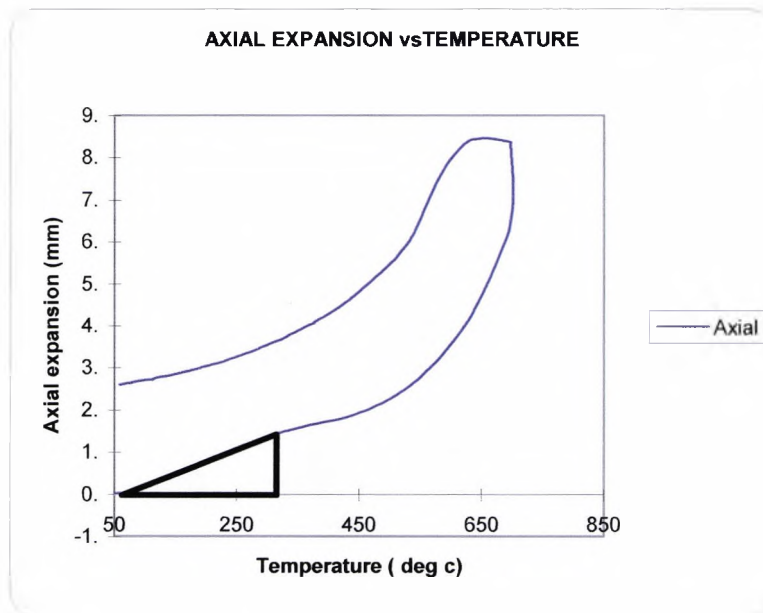
Figure 7.3.1
Relationship between axial expansions vs. Average concrete temperature
Beam (L0.35/00/HM/F3)
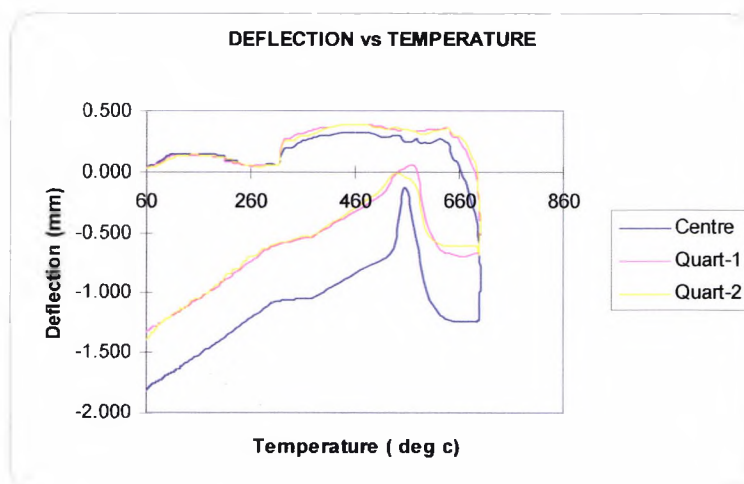
Figure 7.3.2
Centre and quarter point deflections vs. Average concrete temperature
Beam (L0.35/00/HM/F3)

- 174 -

7.6.2 Plots of deformation against temperature (M/0.25/HM/F2)

Graphs below plotted from typical processed results of heating and cooling cycles of modified concrete presented in Appendix A.6.2.
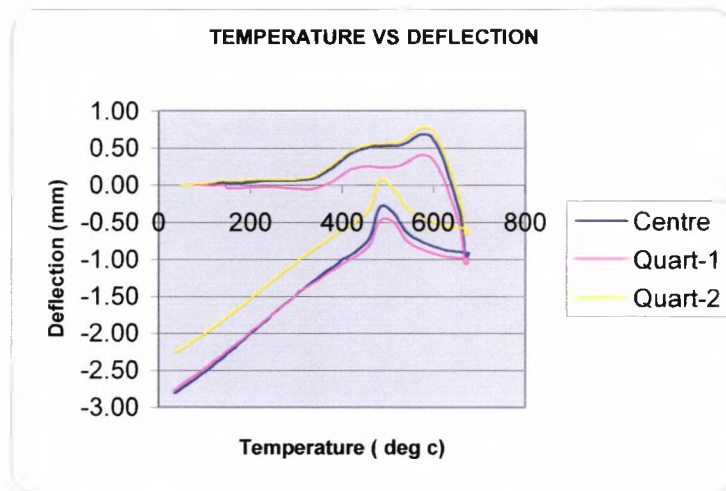
Figure 7.4.1
Center and quarters vs. Average concrete temperature Beam (M/0.25/HM/F2)
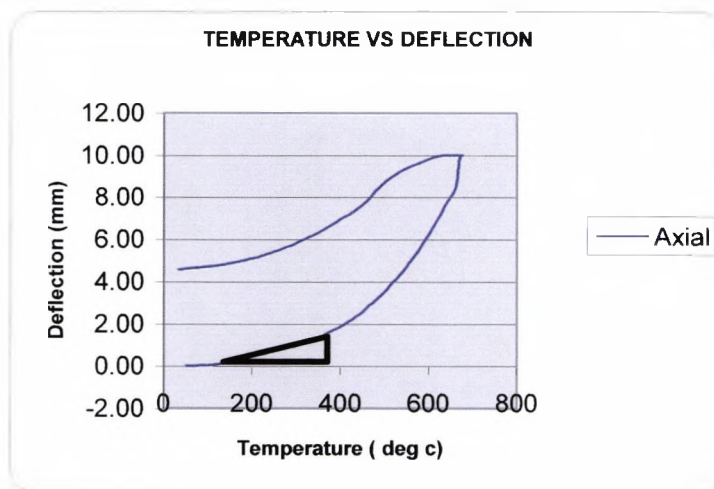
Figure 7.4.2
Relationship between axial expansions vs. Average concrete temperature Beam (M/0.25/HM/F2)

7.6.3 Plots of deformation against temperature (N/0.5/C1/HM)

Graphs below plotted from typical processed results of heating and cooling cycles of normal concrete presented in Appendix A.6.3.
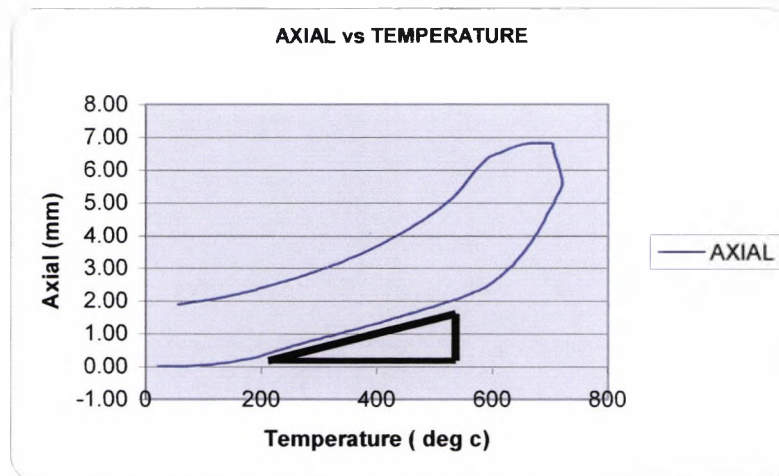
Figure 7.5.1
Relationship between axial expansions vs. average concrete temperature
Beam (N/0.5/C1/HM)
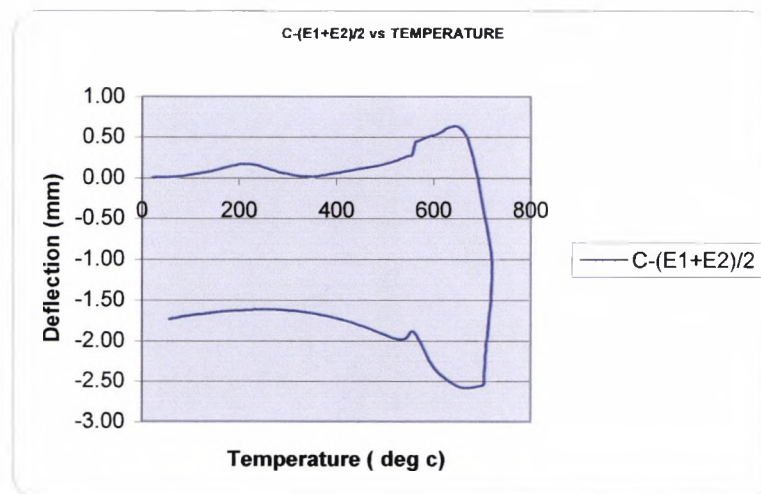
Figure 7.5.2
Centre less average end deflection vs. Average concrete temperature
Beam (N/0.5/C1/HM)

7.7 Concluding remarks

In this chapter typical fractional factorial analysis and typical experimental results are presented. The full results are discussed in detail in Chapter 8.

Appendix A gives   a). Sample fractional factorial analysis using different criteria for spalling and deterioration.

b). Temperature profile at three rate of heating.

c). Contour plots of pressure and moisture distribution results obtained from Harada's moisture model program.

Appendix B gives   a) Samples of the high temperature test results obtained from data logger.

b) All the Fortran programs used to convert this data to actual value.

c) Harada's moisture model program and Matlab programs used to draw the contour plots.

CHAPTER 8

Analysis of test results

8.1 Discussion

This Chapter contains discussion on all of the experimental results and makes recommendations to industry from the findings. It also gives recommendations for future work relating to explosive spalling, spalling and deterioration of high strength concrete.

8.1.1 Thermal cycles

Thermal cycles can be divided into two groups: expansion thermal cycle and deflection thermal cycles.

8.1.1.1 Expansion thermal cycle

The typical expansion thermal cycles shown in Figures 7.3.1, 7.4.2 and 7.5.1 in Chapter 7 embrace three separate parts. During heating the lateral displacements initially increase nearly linearly. These lateral displacements or beam expansions include an element of thermal coefficient of expansion which is equal to the tangent of the initial linear part of the curve as shown in Figure 7.3.1, 7.4.2 and 7.5.1, and an element of shrinkage as the concrete loses its moisture.

At a certain temperature these expansions become non-linear and the expansion rate starts increasing observably. This increase is due to concrete deterioration. The test temperature 700 °C is reached and maintained for 30 minutes to ensure that the all parts of the beam reache equal temperature. During this period further expansion occurs indicating increased deterioration. This increased expansion at peak temperature is more clearly defined at the high rate of heating rather than at the low rate of heating, because the concrete temperature lags much more behind that of the furnace temperature at the high rate.

During cooling a curve similar to heating emerges, but it is displaced in the positive direction by the amount of the accumulated overall crack widths of the beam. This is equivalent to the non-reversible expansion of the beam. These expansions will vary in accordance with the aggregate used in the concrete mixes. Now consider the mean expansion of the plain limestone concrete beams, the modified normal concrete beams and the lightweight concrete beams individually, as illustrated in Table 7.4. The mean expansion of the plain limestone concrete beams was higher than that of the modified normal concrete beams and, in turn the modified normal concrete beams expanded more than the lightweight concrete beams. This is due to the coefficient of thermal expansion of the aggregates, where limestone aggregate has a higher coefficient than the lightweight aggregate.

The non-reversible expansion for the reinforced concrete beams exhibited similar but smaller mean expansions at 700 °C for the limestone and modified concrete,

indicating that the steel reinforcement, even at this high temperature, is restraining cracking.

However the mean dilations of the plain lightweight aggregate (LWA) concrete beams were lower than those of the LWA reinforced concrete and still lower than that of the LWA fibre concrete beams. This indicates that both the steel and particularly the fibres, which have higher thermal coefficients of expansion than the matrix. Thus the mean dilations of the plain lightweight (LWA) concrete beams were lower than those of the LWA reinforced concrete and of the LWA fibre concrete beams.

Furthermore, the difference in concrete matrix thermal coefficient of expansion will introduce incompatibilities in movement between the concrete matrix and the fibres and steel at these elevated temperatures thus resulting in cracking. This was proved when the concrete beams were examined after heat cycling. They all had their extensive residual micro-cracking on the surface of the beam but fibre beams had more than the steel reinforced beams and steel reinforced beams had more than plain concrete beams.

8.1.1.2 Deflection thermal cycles

The deflections thermal cycles are quite different from those for the expansions thermal cycle, see Figures 7.3.2, 7.4.1 and 7.5.2 in Chapter 7. As the furnace temperature is higher at the top and lower at the bottom due to the heating

characteristic of the furnace, the top part of the beam will expand before the bottom part of the beam, this will cause initial hogging of the beams, particularly the unloaded ones.

Furthermore, the high temperature test carried out with strain gauges shows that, initially the top layer of the beam in is compression while it is hogging and the bottom layer is in tension. To discuss this uncommon behaviour, consider the beams as different layers. While the top layer is expanding due to high temperature the second layer will not expand as much as the first because its temperature is lower. This will cause restraint to the first layer by the second layer. Thus the first layer is in compression relative to the lower layers.

With further heating the concrete temperature becomes more uniform and the hogging starts to decrease until the creep deflections due to the applied loading and/or self weight start to predominate and the cracked beam starts to sag.

When the furnace is turned off the lid is slightly opened in order to shorten the cooling period without applying thermal shock to the beam. Heat flows from the upper surface of the beams towards the cooler lower surface and to the outside thus reversing the tendency to hog and the beam continues to sag.

Two phenomena can be detected during the deflection thermal cycling as listed on the next page.

a. It was observed that the hogging during heating seems to reduce at the furnace temperatures of 200 °C to 300 °C and at around 400 °C. These furnace temperatures approximate to an average concrete temperature of 100 °C to 150 °C and 200 °C respectively. These temperatures will cause the evaporable moisture and gel pore water to evaporate, thus the beam resulted in reducing hogging. See Chapter 4 for more details.

b. A dip is observed in the deflections at around 600 °C (550 °C concrete temperature) during heating and again at 550 °C during cooling. These reflect the calcium hydroxide in the cement matrix dehydrating during heating and re-hydrating during cooling, and contribute to additional movements and further deterioration, also explained in Chapter 4.

8.1.2 Explosive spalling for plain and reinforced concrete.

At this stage it is important to distinguish between *spalling and explosive spalling*. Spalling of particle from concrete is the breaking off of parts of the surface due to the tensile strength of the concrete being exceeded. When the structure fails due to *spalling* this is normally a ductile failure. See Figure 8.1.2.a
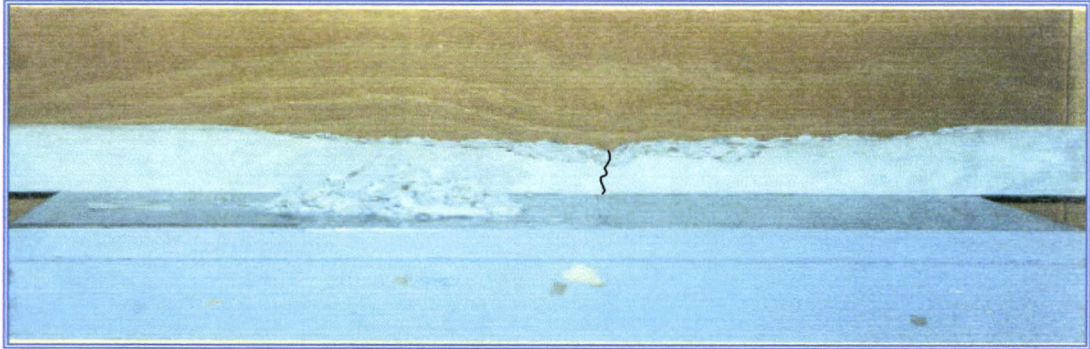
Figure 8.1.2.a Beam after spalling.

Explosive spalling is a violent failure and can occur locally or can completely destroy a beam. This is due to the sudden release of strain energy built in within the concrete due to moisture vapour and other imposed stresses, such as thermal gradients or restraints imposed on the beam. When concrete fails due to explosive spalling it fails in a brittle manner. In this project in most cases explosive spalling leads to complete destructive failure of the beam span. See Figure 8.1.2.b

Figure 8.1.2.b Beam after an explosive spalling.

A specimen that has not failed at 700 °C does not normally fail violently. Explosive spalling normally occurred after 27 to 50 minutes at a furnace

temperature varying from around 400 °C to 600 °C, the explosions being more violent if the beam exploded at the higher temperature. The reason for this is that, at higher temperature the strain energy is much higher than at the lower temperature and the violence is therefore more intense.

It can be observed from Table 7.4 that the expansion prior to explosion was always less than for those which did not explode. This is because the beams were either more intact at this temperature or the expansion was restrained by the internal concrete matrix resulting in an increase in the built-in internal strain energy and leading to violent failure when a small flaw developed in the concrete, releasing this high strain energy.

For the initial series of the plain concrete beam tests cured at the lower relative humidity (i.e. 65%, 45%, 0%), only one beam exploded at 45% RH and the expansions at peak temperature at the same instant of time were taken for analyses. These expansions were converted into strains/ °C by dividing them by the average concrete temperature and length of the beams, as explained in Chapter 7. This series of tests was repeated under different curing conditions, followed by the steel reinforced concrete series of tests. More explosive failures were recorded in the series of tests at higher humidity, than the first series of normal concrete at the lower R.H.

When the beams were cured at a relative humidity of 45% three of the 108 beams tested exploded. However, when the relative humidity was above 65% all

types of concrete except the fibre concrete were susceptible to explosive spalling (10 of the 13 exploded) with the limestone concrete (6 out of 10) being more affected than the other two concrete types (Table 7.2). This clearly indicates without any numerical analyses that curing is an important factor for explosive spalling.

The other predominant factor on explosive spalling was the rate of heating as indicated in Table 7.3. Ten out of 54 beams exploded at a high rate of heating, only 3 from 81 beams exploded at a medium rate of heating but none of the beams exploded at the low rate of heating. When the beam exploded at medium rate of heating the failure was more violent than those which exploded at high rate of heating. This may be due to the exposure time to elevated temperature being longer in the medium rate than the high rate, resulting in higher built- in strain energy.

Figure 8.1.2c, shows two beams: $M0.35C_1$ heated at a medium and $N0.5C_2$ at a high rate of heating.
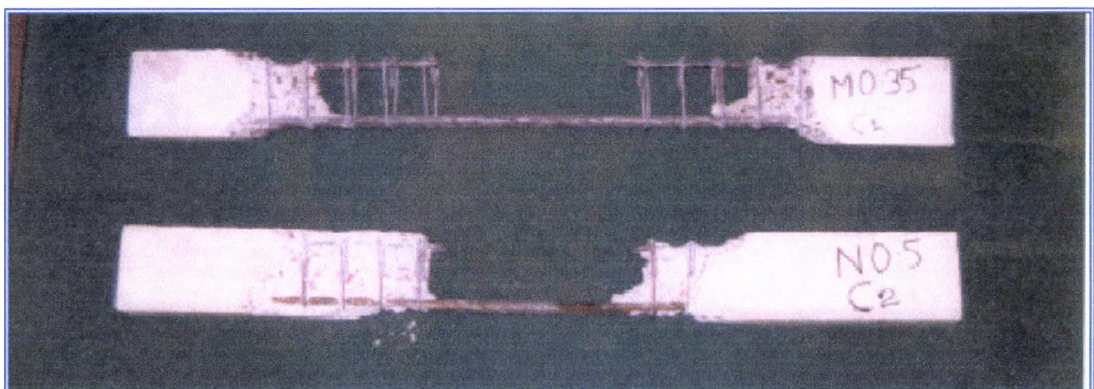
Figure 8.1.2c $M0.35C_1$ had medium rate of heating and $N0.5C_2$ had high rate of heating for explosion.

Table 7.7, in Chapter 7, shows that the surface absorption of the concrete with W/C of 0.25 & 0.35 was not vastly different between the water - cement ratio (W/C) of the beams that exploded was not a major factor in explosive failure.

The other factor that could have an influence on the explosive spalling is loading. The beams initially loaded before heating could have prematurely cracked the concrete thus relieving the high strain energy built-in within the concrete preventing explosive failure.

For plain concrete, only one of the six beams that exploded was loaded. The beam that exploded did so at a higher temperature than the others and was loaded with 10% of the initial failure load. This explosion was very violent as evidenced from the high loss in material (see Table 7.4). This is due to the additional restraint produced by the load, resulting in high built-in strain energy and violent explosive failure. This was evident from the deflection graph that shows the load on the beam to be sufficient to restrain the hogging due to temperature but not enough to produce any cracks by sagging, to relieve the high built-in strain energy.

For reinforced concrete only two of the seven beams that exploded were unloaded. In this case the reinforcing steel prevented initial cracking due to load and could have also added an additional restraint increasing the internal strain energy prior to failure. During casting the steel reinforcing bars had steel plates welded at their ends to hold the bars in location with enough cover (5mm). These

steel plates could have also added an additional restraint along with steel bars resulting in violent explosive failure. See Figure 8.1.2d
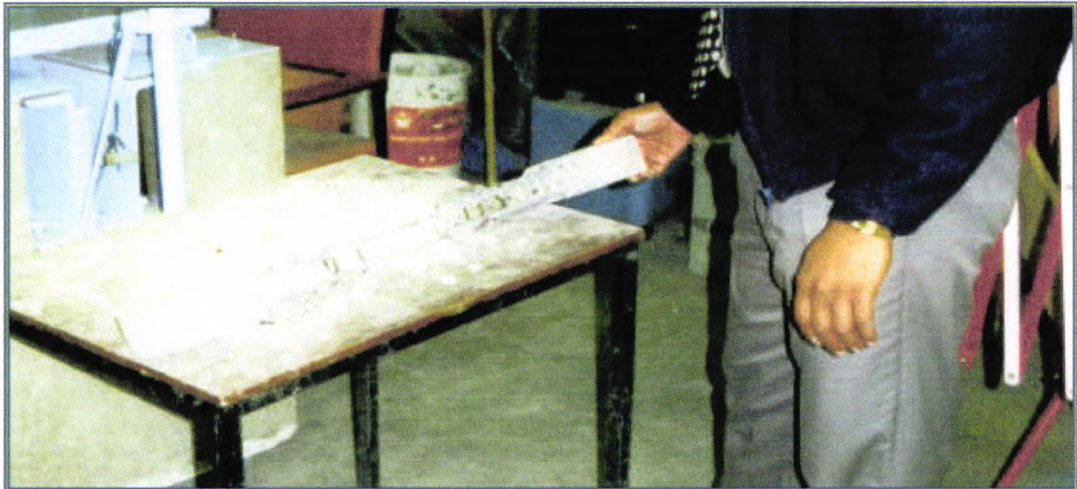
Figure 8.1.2d Typical explosive failures of reinforced concrete beams.

In the fibre concrete series none of the 27 fibre concrete beams failed by spalling or explosive spalling. This is because polypropylene melts at 160 °C and decomposes at 250 °C and produces enough passageways to relieve the internal strain energy before it builds-up to a dangerously high level. In addition it was observed that after testing, extensive surface cracking had occurred. This was caused by the thermal strain incompatibilities between fibre and concrete matrix. These extensive micro cracks could have also released the vapour pressure from accumulating, thus preventing explosive spalling. Experiment work has recently been carried out in Switzerland [8.04] on sprayed concrete using micro, monofilament polypropylene fibre, macro fibre and steel fibre subjected to fuel fire. The micro, monofilament polypropylene fibre did not exhibit explosive

- 187 -

spalling but macro fibre did not prevented extensive explosive spalling. This may be due to the intensity of fibre in the concrete mixes. Concrete containing more fibres in the mix produces more passageways to relieve the internal strain energy before it builds-up. Thus micro, monofilament polypropylene fibre concrete performed better than macro polypropylene fibre concrete. Similarly due to the very high quantity of fibre in mixes, even with 1% volume replacement of aggregate, none of the fibre beams exploded.

8.1.3 Deterioration of beams after thermal cycling

All the beams deteriorated when subjected to these high temperatures as indicated in Tables 7.1, 7.2 and 7.3. The beams initially hogged before sagging on cooling. A number of concrete and fibre beams especially those that were preloaded before heating, failed by breaking during cooling due to constant load applied and loss in moisture. Two of the fibre beams failed during heating. The fibre beams that did not fail suffered minor to severe cracking and some exhibited large deflections. However most of the fibre concrete beams remained intact after failure, even though they exhibited extensive micro-cracking on the surface.

The reinforced concrete beams also remained intact after cooling with the preloaded beams sagging due to elastic and creep deflections. The unloaded

beams hogged due to the restraint produced by the steel end plates as the concrete expanded.

The highest expansion at 700 °C in Table 7.4 represents contributions from the thermal coefficient of expansion, shrinkage effects and cracks within the beams due to incompatibilities in movement of the aggregate and the prevailing conditions together with micro-cracking within the cement paste. *This is the reason that these expansion values were taken as criteria for assessing deterioration of the different types of concrete when the fractional factorial analyses were done.*

Comparing the deterioration for each type of concrete at the three rates of heating the following can be observed (see Table 7.4). For all the plain concrete beams the high rate of heating appears to create more damage than the lower rates. When the beam is subjected to the fast rate of heating, it is also subjected to rapid rates of change within the concrete matrix resulting in severe damage to the specimen. When the beam is subjected to the low rate of heating the temperature gradient is not so severe, thus causing less damage to the concrete matrix.

For the reinforced concrete it is difficult to distinguish between the damage due to the high rate and the low rate of heating because all the reinforced limestone concrete beams at the high rate of heating had failed violently.

There is no clear trend for the effect of heating rate on the damaging effect on the fibre concrete as they all had similar extensive surface damage.

8.2 Damage assessment by factorial analyses.

This section contains the assessment of explosive spalling and deterioration of concrete using the results from the fractional factorial analysis.

8.2.1 Explosive spalling

The criterion for assessing the factors influencing explosive spalling was based on the weight of intact concrete remaining after failure. Although only 6 of the 27 plain concrete beams and 7 of the 27 reinforced concrete beams exploded, it was possible to obtain meaningful averages for the analyses of the experiments using the factorial method of analysis.

The analyses of the variance for normal concrete beams and reinforced concrete beams showed interesting differences in the factors influencing explosive spalling as indicated in Table 8.1 and in Figure 8.1 below, which shows qualitatively the probability of explosive spalling relative to changes in factor levels.

The main effect data used to obtain the Figure 8.1 is from Table 7.8c & 7.11c

Table 8.1
ANOVA Significance of factor for explosive spalling
 for the plain and RC beams

	SIGNIFICANCE %	
FACTOR	Plain concrete	RC
A (Curing)	-	>90
B (Heating)	>95	>>99
C (Loading)	>90	-
D (W/c)	-	>95
E (Aggregate)	-	>>95
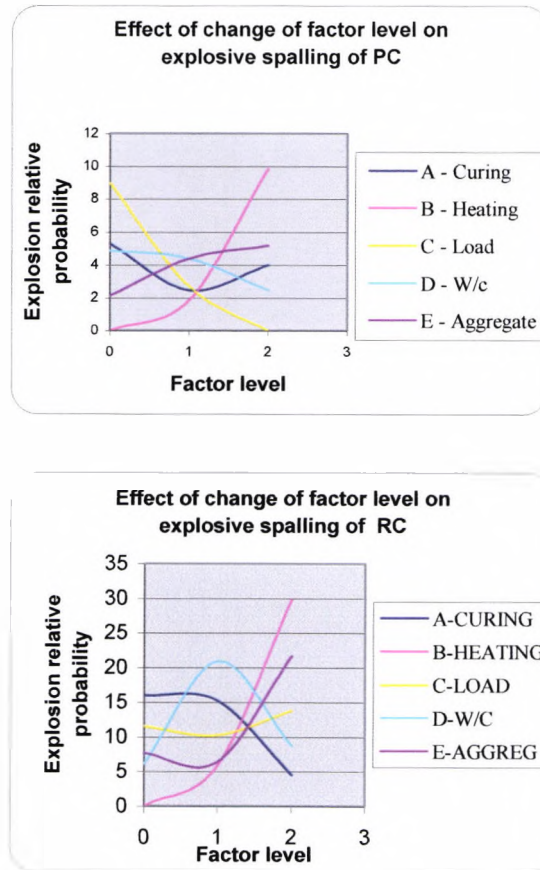
Figure 8.1 Effect of factor level on explosive spalling of PC and RC

8.2.1.1 Explosive spalling: Discussion of ANOVA results for plain concrete beams

Figure 8.1 indicates that the heating rate and loading influenced explosive spalling of the plain concrete beams in this experiment. A low heating rate produced the lowest number, increasing exponentially with heating rate.

Unloaded beams resulted in the highest number of explosive spallings this effect decreasing non-linearly with loading, no explosions occurring at the highest load.

As discussed earlier pre-loaded beams will prematurely (or initialy) crack thus relieving the strain energy before it build-up to cause explosive spalling.

Table 8.1 indicates that a change of factor level for heating for plain concrete is significant in excess of 95%. In general, furnace heating produced thermal gradients imposing lateral restraint, which could prevent cracks opening out during heating resulting in very high stresses within the concrete. This increases the strain energy and when this strain energy is suddenly released through a newly developed very small flaw in the concrete, explosive spalling occurs.

Table 8.1 indicates that loading for plain concrete is significant to excess of 90%. Although the other factors seem to vary with level, the analysis of variance indicates no significance i.e. below 90%. It will be recalled that a change in factor level which influences the overall average to a level of greater than 90%, has a probability lower than 10% of being due to the error of the experiment.

8.2.1.2 Explosive spalling: ANOVA discussion of results for reinforced concrete beams

Figure 8.1 shows all the significant factors for the reinforced concrete beams plotted against levels indicating that curing, heating rate, W/C and aggregates influenced explosive spalling.

Curing at 85% RH (level 2) gave the lowest probability of violent failure increasing non-linearly, levelling off at a point above 65% and decreasing non-linearly at a RH of 45%. The significance in the change of level in RH was in excess of 90%. Although plain and reinforced concrete beams had the same curing conditions, curing did have some influence on explosive spalling for reinforced concrete beams.

No explosions occurred at the low heating rate but explosions increased exponentially with rate, the significance for this factor was in excess of 99%.

The water cement ratio gave an interesting non-linear effect with 0.35 W/C ratio as a maximum. The significance in the change of level in W/C ratio was in excess of 95%. This means that the mixes with a W/C ratio of 0.35, which appeared to have a low permeability, were more susceptible to explosive spalling, as these latter mixes being more compact, have a higher resistance to vapour flow. This increases the thermal stresses arising within the concrete during heating; hence the increased internal strain energy leading to a greater propensity for explosion than in the more permeable mixes.

The limestone concrete was the most susceptible to explosive spalling with a minimum occurring between the lightweight aggregate and the modified normal concrete. The significance for this factor was in excess of 95%. It should be

observed that the limestone concrete was generally less permeable than LWA concrete thus increasing the thermal stresses arising within the concrete during heating. The internal strain energy in the limestone concrete leads to a greater propensity for explosion than the more permeable concrete, such as lightweight concrete.

8.2.2 Deterioration

The criterion for assessing the factors influencing deterioration in the experiment where explosive spalling did not take place, was based on the maximum dilation of all the beams in the fractional factorial experiment with fictitious extrapolated expansion values given to the beams that exploded for the plain concrete.

For the RC beams the actual expansion values were taken for the beams prior to explosion.

For the fibre concrete beams the criterion for assessing the factors influencing deterioration in the experiment where explosive spalling did not take place, was based on the maximum residual deflection values prior to failure.

Some of the factors influencing deterioration as they change from one level to another are shown in Figure 8.2 and the significance of their effect shown in Table 8.2. Figure 8.2 shows deterioration with increase in factor levels for the plain, reinforced and fibre concrete beams. Data for these Figures are obtained from Tables 7.9c, 7.10c and 7.12c.
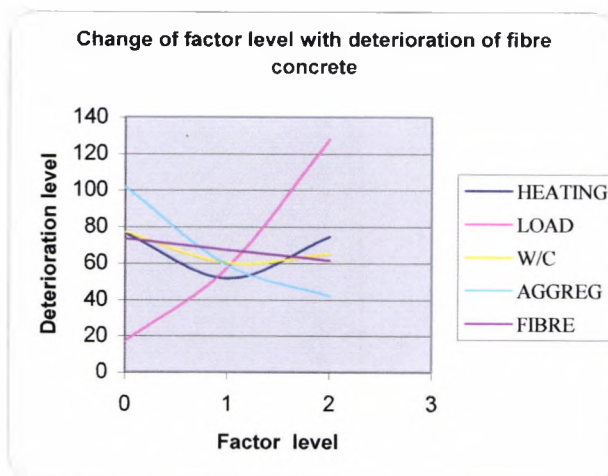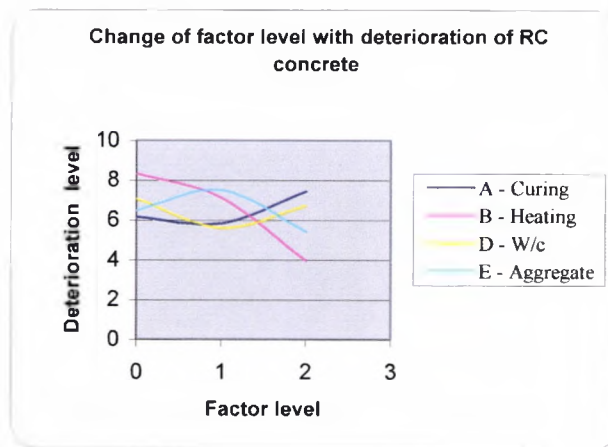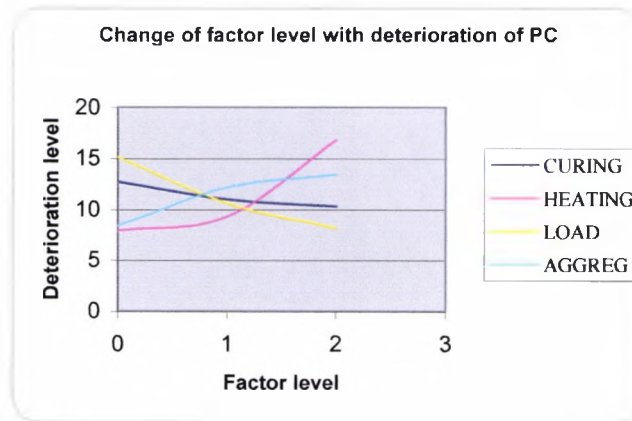
Figure 8.2 Change of factor level with deterioration of PC, RC, and FC

Table 8.2
ANOVA Significance of factor for deterioration for the plain,
reinforced and fibre concrete beams

	SIGNIFICANCE %		
FACTOR	Plain concrete	RC	Fibre concrete
A (Curing)	-	>90	Not applicable
B (Heating)	<95	>>99	-
C (Loading)	-	-	>>95
D (w/c)	-	>95	-
E (Aggregate)	>>95	>>95	>>90
F (Fibre)			-

8.2.2.1 Significance of factor on deterioration of plain concrete.

Only the significant factors have been plotted in Figure 8.2 and for the plain concrete beams heating rate and aggregate type influenced deterioration. A low rate heating produced the lowest deterioration, and increasing quasi-linearly with heating rate.

The LWA concrete (level 0) beams were the least deteriorated followed by the modified normal and the limestone concrete. The significance of the aggregate factor in normal concrete was in excess of 95%, again recalling that if the significance of a factor is high, then the less is the probability that the changes produced by the factor levels are due to the error factor.

The ANOVA Table for the plain concrete from Chapter 5 is partly reproduced in Table 8.3 and Figure 8.2a shows the significance of each factor with a change in level using overall strains as a criterion for deterioration. For the series of tests at the lower RH factor a previous research assistant carried out the experiments.
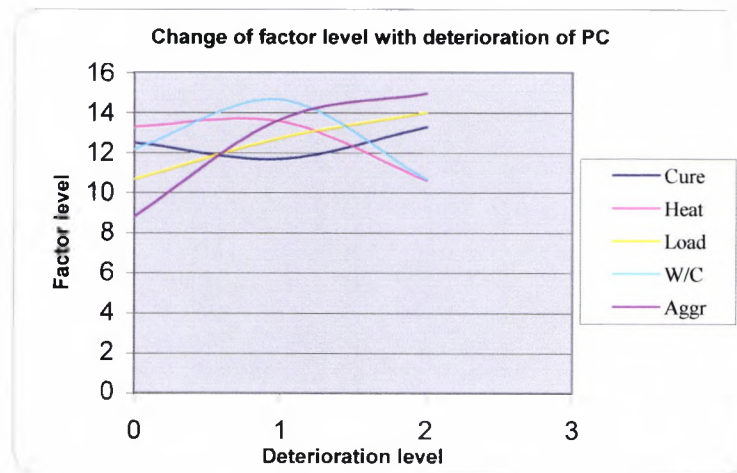
Figure 8.2a Change of factor level with deterioration of P.C

Table 8.3
ANOVA Significance for deterioration for the plain concrete cured at 65%, 45% & 0% RH

SIGNIFICANC %	
FACTOR	Plain concrete
A (Curing)	-
B (Heating)	>99
C (Loading)	>90
D (W/c)	>95
E (Aggregate)	>>99

Figure 8.2a shows that deterioration increased from LWA to limestone concrete due to increase in the thermal coefficient of expansion from LW concrete matrix

to limestone concrete matrix Table 8.3 shows the change in level being significant in excess of 99%.

Deterioration was highest at a W/C ratio of 0.35 decreasing towards the 0.25 and 0.5, W/C ratio being significant in excess of 95%. This was in agreement with the plain concrete series tested at the higher RH.

Deterioration also increased linearly with loading and loading factor being significant in excess of 90%.

Heating created higher damage at the low and medium rate of heating and lowest damage at the high heating rate, the effect being significant in excess of 99%. This is because the time taken for the furnace to reach 700 °C for the lower rate of heating was longer. Thus the average concrete temperature for the lower rate of heating was generally higher when the furnace first reached 700 °C and the beams were therefore subjected to a longer heating period. The effect on the reinforced concrete beams became more deteriorated at the lower rate of heating. But the plain concrete beams were marginally more damaged at the faster rate of heating. The effect of steeper temperature gradients due to the high rate of heating seems to have more deteriorating effect on the plain concrete then the reinforced concrete.

The intensity of damage for the plain concrete beams in the first series of tests (see Table 7.1) indicated that the cracks in the limestone concrete were more severe and deeper than for the modified and LWA concrete after the heat cycle.

This confirms the damage assessment above. This was also observed in the plain concrete beams cured at the higher RH shown in Table 7.2, although the LWA and modified concrete exhibited intensive surface cracking. Furthermore, Tables 7.1, 7.3 and 7.4 indicate that the lightweight aggregate concrete is the least damaged. The criterion of overall expansion values at 700 °C is lower than those of the modified and limestone concrete.

8.2.2.2 Discussion of deterioration of reinforced concrete.

Figure 8.2 shows some of the significant factors for the reinforced concrete beams plotted against levels indicating that curing, heating rate, W/C ratio and aggregates also influenced deterioration of reinforced concrete but in a different way to explosive spalling. Curing at above 85% RH (level 2) gave the highest probability of deterioration decreasing non-linearly from level 0 to level 1 of 65% RH and then increasing from level 1 to level 2 of 85 RH%. The significance in the change of level in RH was in excess of 90%. But for explosive spalling, curing at above 85% RH (level 2) gave the lowest probability of explosive spalling.

Deterioration was highest at the low heating rate decreasing non-linearly with increasing rate, the significance for this factor being in excess of 99%. This is because, as discussed earlier, the amount of time the beam is exposed to fire

decreases with increasing rate of heating. But for the explosive spalling it is reverse trend: a low heating rate gave the lowest probability of explosive spalling.

The water/cement ratio gave an interesting non-linear effect for deterioration with 0.35 W/C ratio as a minimum. The significance in the change of level in W/C was in excess of 95%. 0.35 W/C ratio gave maximum probability for explosive spalling.

The modified normal concrete (level 2) was the most susceptible to deterioration showing a maximum along a curve with a decreasing susceptibility towards the lightweight aggregate and the limestone concrete, the significance for this factor being in excess of 95%. But the modified normal concrete gave the least probability for explosive spalling.

8.2.2.3 Discussion on deterioration of fibre concrete.

Figure 8.2 also showing some of the significant factors for the fibre concrete beams plotted against levels indicating that loading and aggregates influenced the deterioration of fibre concrete.

The significance of loading on the deterioration of fibre concrete was in excess of 95%, with increase in loading deterioration increases and maximum deterioration at level 2.

Figure 8.2 indicate that the probability of deterioration for aggregate decreases non- linearly and minimum deterioration at level 2. This is also evident from concrete specimens after the experiment that lightweight concrete beams had more micro- cracks than others. The significance of aggregate on the deterioration of fibre concrete was in excess of 95%.

The significance of rate of heating and W/C on deterioration of fibre concrete was just below 90%, which statistically is not significant i.e. the effect of a change in factor level has more than 10% probability that it may be due to the error.

8.3 Thermal contours

The thermal distributions (Appendix A.5) of the limestone concrete beams show similar patterns for all the three rates of heating except that the peak temperatures are reached earlier for the high rate.

Local cold spots are evident, which are associated with cooling as moisture in the pores within the cement matrix starts to evaporate. These cold spots change in character during heating and if the beam does not explode these cold spots will disappear.

The thermal distributions (Appendix A.5) of the limestone concrete beams clearly showing that the furnace heating produced a higher temperature in the central part of the beam than at the ends. This is an effect of the design of the heating elements of the furnace, which tends to produce internal lateral restraint. These

restraints, together with the pressures within these local cold spots, increase stresses within the gel pore structure, which in their turn will increases the built-in strain energy.

If the concrete has a high strength with a stronger gel structure, it can behave as a rigid continuum, which can support higher strain energies before failure. If a part of the microstructure suddenly fails, the sudden releases of strain energy will cause a violent failure or explosive spalling.

On the other hand, if any cracks occur due to loading or other imposed stresses while the beam is being heated, the gel structure is no longer continuous and the cracks will release part of the strain energy. In this case cracking or local spalling may occur, but it is very unlikely that explosive spalling will.

8.4 Conclusions

8.4.1 Deterioration

Factors influencing the deterioration of different types of concrete are given in Table 8.4. The discussion below and the comments in the Table are given on those factors that have been assessed by an analysis of variance to be significant.

Table 8.4

Comment on deterioration for plain, reinforced and fibre concrete

COMMENT ON DETERIORATION				
FACTOR	Plain concrete	Plain concrete	RC	Fibre concrete
A (Curing)	Little effect	Little effect	60% to 85% RH	Not applicable
B (Heating)	Increases with Low to high rate	Increases with Low to high rate	Increases with High to low rate	Little effect
C (Loading)	Linear increase	Little effect	Little effect	Increases with factor level
D (W/C)	Maximum at 35%	Little effect	Minimum at 0.35	Little effect
E (Aggregate)	Increases with LWA to limestone	Increases with LWA to limestone	Maximum at Modified	Decreases from LWA to limestone
F (Fibre)	Not applicable	Not applicable	Not applicable	No effect

8.4.1.1 Conclusions relating to deterioration of plain concrete

- Deterioration increased slightly from level 0 to level 1 and increased dramatically from level 1 to level 2 with increasing rate of heating for the plain concrete. The significance of this factor is in excess of 95%.

- Curing is not statistically significance for plain concrete and it was observed from tested specimens that changes in curing did not have much effect on deterioration of normal concrete.

- From Figure 8.2, it can be observed that there was a tendency for deterioration to be a maximum for loading at level 0 but this was not statistically significant.

- There was a faster increase in deterioration from LWA concrete to modified normal concrete and modified normal concrete to limestone concrete. The significance of this factor is in excess of 95%.

- It should be observed from Table 8.2 that, in both series of plain concrete tests, aggregate and heating are the most significant factors in relating to deterioration.

8.4.1.2 Conclusions relating to deterioration of reinforced concrete

- Deterioration decreased non-linearly for the reinforced concrete with increasing rate of heating. The significance of the factor is in excess of 99%.

- Deterioration of the reinforced concrete decreases slightly from 45% to 65% RH and increases largely from 65% to 85% RH.

- For the reinforced concrete, a minimum deterioration at a W/C ratio of 0.35 with the 0.25 and 0.5 W/C increasing equally in deterioration. This is due to 0.35 W/C ratio mixes having a higher mortar fraction than the other mixes making the 0.35 W/C concrete more compact. The Significance of factor aggregate is in excess of 95%.

- For the reinforced concrete, where modified concrete showed a maximum deterioration, this deterioration decreased towards LWA and limestone reinforced concrete. The significance of factor aggregate is in excess of 95%.

8.4.1.3 Conclusions relating to deterioration of fibre reinforced concrete

- Rate of heating is not a significance factor for deterioration of fibre concrete.

- The deterioration of fibre concrete increases with increasing factor level. The significance of loading factor is in excess of 99%.

- Deterioration was at maximum for LWA fibre concrete and decreases non-linearly to a minimum for limestone aggregate concrete (level 2). The significance of aggregate factor for fibre concrete is in excess of 95%

- W/C ratio is not a significant factor for deterioration of fibre concrete.

- For more about fibre see page 235, 222.

8.4.2 Explosive spalling

In the experiments some plain and reinforced concrete beams with identical concrete mixes failed explosively at the high rate of heating. The design of the furnace creates a heating regime which imposes lateral restraint in addition to local cool spots especially at high heating rate. The stresses imposed by these effects and by pore pressures are locked in the pore gel structure and can produce quite high strain energies, particularly in the higher strength concrete, which can resist failure far longer. When a local defect releases this pent up strain energy a violent failure of the gel structure occurs. This is the mechanism by which the higher strength, more compact, moist concrete heated at the faster heating rate in conjunction with the various imposed restraints created explosive spalling in the tests.

Explosive spalling of the plain and reinforced concrete was also influenced by all the factors shown in Table 8.5, but again not in the same manner. Comments below and in the Table have only been made on the factors, which have been assessed by an analysis of variance to be significant.

Table 8.5
Increase in explosive spalling for plain and reinforced concrete

Increase in explosive spalling		
FACTOR	Plain concrete	RC
A (Curing)	Little effect	60% to 85% RH
B (Heating)	Medium to high	Medium to high
C (Loading)	High to low	Little effect

Table 8.5 continues

D (W/C)	High to low	Maximum at 0.35
E (Aggregate)	Little effect	Modified to limestone (slight increase to LWA)

The following comments apply to the plain, reinforced and fibre reinforced concrete beam.

8.4.2.1 Conclusions relating to explosive spalling of plain concrete

- The curing conditions did not affect explosive spalling of plain concrete beams.

- Increase in heating rate from medium to high rate increased the chances of explosive spalling for plain concrete due to the steep temperature gradient.

- At low heating rate there was no explosive spalling of plain concrete.

- Loading decreased the chance of explosive spalling to plain concrete because pre-loaded beams cracks pre-maturely and presence of cracks reduces the tendency to explosive spalling.

- In the plain concrete a W/C ratio of 0.35 and 0.25 resulted in a greater possibility of explosion than that with a W/C ratio of 0.5, but this was, however, not statistically significant.

- The aggregate type did not significantly affect plain concrete, although the modified mixes appear to be the least affected

- Only one explosion occurred in the first series of tests on plain concrete cured at the lower RH. This occurred on a limestone concrete beam with a W/C ratio of 0.35, cured at 65% heated at the high rate with no load applied.

8.4.2.2 Conclusions relating to explosive spalling of reinforced concrete

- Reinforced concrete beams were more susceptible to explosive spalling between 85% and 65% RH but this reduced considerably at 45% RH.

- A high heating rate increased the chances of explosive spalling from the medium to high rate of heating for reinforced concrete, due to steep temperature gradient.

- Loading did not prevent explosive spalling in reinforced concrete because the loading was not sufficient to produce enough cracks to release the strain energy.

- A W/C ratio of 0.35 appeared to give the greatest susceptibility for reinforced concrete to explode, with the susceptibility decreasing towards ratios of 0.25 and 0.5.

- Reinforced limestone concrete had a greater inclination to fail violently. This tendency was lower for modified and then slightly increased from modified to LWA reinforced concrete.

8.4.2.3 Conclusions relating to explosive spalling of fibre concrete

- No explosions took place for any of the fibre concrete beams; therefore factorial analysis on explosive spalling is not possible for these specimens.

- The fibre specimens had different fibre levels but were all cured at a nominal RH of 100% prior to testing. This clearly indicates that the presence of fibre at any level will have a significant effect on preventing explosive spalling on any type of concrete for the factors studied in this programme.

8.5 Recommendations

From the conclusions it is recommended that, if high strength concrete is liable to be exposed to transient high temperature, the following should minimise explosive spalling:

- 6 mm polypropylene fibres added to concrete will minimise explosive spalling in the event of fire. Polypropylene fibres, which have much higher thermal coefficient of expansions than concrete matrix, particularly in lightweight aggregate (LWA) concrete, produce a large number of micro-cracks, thus reducing the chances of explosive spalling.

- Factors which cause deterioration of the concrete at the initial stages of heating may reduce the chances of explosive spalling.

- Fibres that have similar melting and decomposing temperature as polypropylene fibre could also be used in concrete in order to prevent explosive spalling.

- A trade-off has to be established between a durable concrete and permeability, as impermeable concrete is more susceptible to explosive spalling.

- Limestone concrete, like gravel concrete should be avoided, for example, in nuclear reactors or offshore structure, as it increases the probability of explosive spalling in the event of fire.

- The highest rate of heating in the tests was lower than that under a cellulose fire and even lower than that of a fuel fire; the fractional factorial method of experimentation can predict the trend under these situations. The testing indicated that the probability of explosive spalling in reinforced concrete beams increased with rate of heating. The conditions which can occur in practice and the results of deterioration and probability of explosive spalling due to a change of level of the factors investigated, are valid. Therefore interpolation between levels to suit a given situation is possible.

- The factors influencing plain concrete and reinforced concrete affect deterioration in different ways. Care has to be exercised therefore when using data from plain concrete to predict behaviour of reinforced concrete.

- Shredded plastic aggregate produced from post-consumer car bumpers should be avoided in high strength concrete. [8.02]

8.5.1 Future research

- Other fibres such as ceramic fibre, which have thermal coefficient of expansions incompatible with the cement matrix, may also alleviate explosive spalling as explained earlier and this should be investigated in future research.

- Lightweight aggregate concrete has a great deal to recommend it, but tests by others [8.01] under a fuel fire have shown that continuous explosive spalling occurred during heating. Therefore more research is recommended to investigate the performance of lightweight aggregate.

- Deterioration always occurs during transient heating and limestone aggregates concrete deteriorated more than others. More research is recommended using basalt in conjunction with limestone to see any improvement on deterioration.

- Micro-cracks can relieve the built-in strain energies from the concrete thus alleviating the probability of explosive spalling. However, limestone concrete, which also exhibited higher deterioration than LWA concrete, was more prone to explosive spalling. Therefore more research recommended to study the micro cracks on limestone concrete.

- Harada's moisture model program can be developed to find the strain energy within the beam, before it explodes. This may lead to the development of user-friendly windows based programs that can predict the explosive spalling.

- Inclusion of plastic aggregate (10 mm) increases the probability of explosive spalling [8.02]. More research is recommended using powder plastic, to

establish whether it improve performance in a similar manner to polypropylene fibres.

- The beam which exploded from the first plain concrete series had very low expansion compare to the other 26 beams. Therefore more research recommended for beams with restraint at the ends.

- High temperature strain gauges were unable to measure the strain values beyond a concrete surface temperature of 300 °C. Therefore more research is recommended using high temperature strain gauges which can measure the strain values up to 700 °C.

8.6 Achievements of the research

- By the use of fractional factorial experimentation and the analysis of variance (ANOVA) the salient factors affecting the behaviour of different types of high strength concrete have been established together with the percentage significance of each factor change.

- Research carried out in the past was unable to distinguish the difference in flexural behaviour of plain and reinforced concrete in the manner revealed by this research.

- Research carried out in the past proposed the use of shredded plastic produced from post-consumer car bumpers in concrete, but the performance of such materials when exposed to high temperature was found to be ineffective and can give out toxic fumes. The present research also showed that these types of plastic aggregate would increase the probability of explosive spalling, the factor being significant in excess of 99%.

- The factors influencing the performance of plain and reinforced concrete were shown to be different as was the percentage significance of a change in factor level.

- Moisture cured polypropylene fibre concrete test proves that 6 mm fibre can be added to concrete with confidence in order to prevent spalling or explosive spalling.

- 1 kg polypropylene fibre per m^3 included in a high strength concrete mix is sufficient enough to prevent explosive spalling for the factors examined.

Appendix A.1

Fractional factorial analyses

Appendix A.1

Table A.1a to A.1.f shows a fractional factorial analysis for the plain concrete series of tests using total weight lost due to explosion and weight lost due to evaporisation to find significance factor of explosive spalling.

Table A.1.a
FRACTIONAL FACTORIAL ANALYSES for PLAIN CONCRETE (Including moisture lost)

FACTORS	CURING	HEATING	LOAD	W/C	AGGREG	Weight.loss
Test No.	A	B	C	D	E	kg
1	C1	L	0	O.25	LIGHT	0.83
2	C1	L	10	0.50	MOD	0.81
3	C1	L	20	0.35	NORMAL	0.91
4	C1	M	0	0.50	NORMAL	1.12
5	C1	M	10	0.35	LIGHT	0.61
6	C1	M	20	O.25	MOD	0.78
7	C1	H	0	0.35	MOD	7.64
8	C1	H	10	O.25	NORMAL	8.14
9	C1	H	20	0.50	LIGHT	0.64
10	C2	L	0	0.35	MOD	0.47
11	C2	L	10	O.25	NORMAL	9.63
12	C2	L	20	0.50	LIGHT	0.44
13	C2	M	0	O.25	LIGHT	0.64
14	C2	M	10	0.50	MOD	0.68
15	C2	M	20	0.35	NORMAL	0.61
16	C2	H	0	0.50	NORMAL	7.36
17	C2	H	10	0.35	LIGHT	0.43
18	C2	H	20	O.25	MOD	0.68
19	C3	L	0	0.50	NORMAL	1.08
20	C3	L	10	0.35	LIGHT	0.47
21	C3	L	20	O.25	MOD	0.96
22	C3	M	0	0.35	MOD	5.51

Table A.1.a continues

FACTORS	CURING	HEATING	LOAD	W/C	AGGREG	Weight.loss
23	C3	M	10	O.25	NORMAL	0.65
24	C3	M	20	0.50	LIGHT	0.46
25	C3	H	0	O.25	LIGHT	6.40
26	C3	H	10	0.50	MOD	0.55
27	C3	H	20	0.35	NORMAL	1.07

Table A.1.b
INTERACTION TABLE

COMBINAT	AB	AC	BC	DE	CD	CE
XiYi 00	2.56	9.59	2.38	7.87	7.87	7.87
XiYj 01	2.51	9.56	1.91	2.42	13.62	13.62
XiYk 02	16.42	2.33	2.31	9.42	9.56	9.56
10	1.54	8.47	7.27	1.51	9.42	1.51
11	1.93	1.74	1.94	13.62	1.51	2.04
12	8.47	1.73	1.85	2.59	2.04	9.42
20	2.51	12.99	21.40	1.54	2.42	1.54
21	6.62	1.67	9.12	2.04	2.59	2.42
22	8.02	2.49	2.39	9.56	1.54	2.59
TOT (SUMXiYk)	50.58	50.58	50.58	50.58	50.58	50.58

Table A.1.c
MAIN EFFECT

	CURING	HEATING	LOAD	W/C	AGGREG
	A	B	C	D	E
SUM1 (Xi)	21.49	6.61	31.05	19.71	10.92
SUM2 (Xj)	11.94	11.06	12.97	17.72	18.08
SUM3 (Xk)	17.15	32.91	6.55	13.14	21.57
Tot (Sxijk)	50.58	50.58	50.58	50.58	50.58

TableA.1.d
SUM OF SQUARES FROM MAIN EFFECT

SSXiXjX k/9	99.810	138.780	130.593	97.258	101.288
SSTot/27	94.734	94.734	94.734	94.734	94.734
SSXiXjXk/9-SSTot/27=Effect of factor X on O/A average					
Sa	5.07568	44.04528	35.85891	2.523677	6.553545

Table A.1.e
SUM OF SQUARES FROM INTERACTION EFFECT

	AB	AC	BC	DE	CD	CE
SSXiYi	474.73	444.32	621.56	448.99	448.99	448.99
SSXiYk/3 -SST/27	63.51	53.37	112.45	54.93	54.93	54.93
Sab	14.39	12.44	32.55	45.85		

Table A.1.f
ANALYSES OF VARIANCE

Source	df	Sa --- Sab	V	F(a)= V(a)/V(Er 1)	Significanc %	F(a)= V(a)/V(Er3)
A (Curing)	2	5.08	2.54	0.22		0.51
B (Heating)	2	44.05	22.02	1.92	>95	4.45
C (Loading)	2	35.86	17.93	1.56	>90	3.62
D (W/c)	2	2.52	1.26	0.11		0.26
E (Aggregate)	2	6.55	3.28	0.29		0.66
AB	4	14.39	3.60	0.31		
AC	4	12.44	3.11	0.27		
BC	4	32.55	8.14	0.71		
DE	4	45.85	11.46			2.32
Error	0	0				
(Error)1	4	45.85	11.46			
(Errror)3	12	59.37	4.95			

Heating is significance to > 95 and loading is significance to > 90 for explosive spalling of plain concrete.

Appendix A.2

Table A.2.a to A.2.f shows a fractional factorial analysis for the reinforced concrete series of tests using total weight lost due to explosion and weight lost due to evaporisation to find significance factor of explosive spalling.

Table A.2.a
FRAC TIONAL FACTORIAL ANALYSES for REINFORCED   CONCRETE
(Including moisture loss)

FACTORS	CURING	HEATING	LOAD	W/C	AGGREG	Weight.loss
Test No.	A	B	C	D	E	kg
1	C1	L	0	O.25	LIGHT	0.93
2	C1	L	10	0.50	MOD	1.16
3	C1	L	20	0.35	NORMAL	1.17
4	C1	M	0	0.50	NORMAL	1.00
5	C1	M	10	0.35	LIGHT	0.99
6	C1	M	20	O.25	MOD	1.03
7	C1	H	0	0.35	MOD	6.37
8	C1	H	10	O.25	NORMAL	6.12
9	C1	H	20	0.50	LIGHT	3.49
10	C2	L	0	0.35	MOD	1.15
11	C2	L	10	O.25	NORMAL	1.34
12	C2	L	20	0.50	LIGHT	1.10
13	C2	M	0	O.25	LIGHT	0.88
14	C2	M	10	0.50	MOD	1.19
15	C2	M	20	0.35	NORMAL	5.82
16	C2	H	0	0.50	NORMAL	5.20
17	C2	H	10	0.35	LIGHT	4.14
18	C2	H	20	O.25	MOD	0.98
19	C3	L	0	0.50	NORMAL	0.98
20	C3	L	10	0.35	LIGHT	0.75
21	C3	L	20	O.25	MOD	0.78
22	C3	M	0	0.35	MOD	0.88
23	C3	M	10	O.25	NORMAL	1.21
24	C3	M	20	0.50	LIGHT	0.88
25	C3	H	0	O.25	LIGHT	0.41
26	C3	H	10	0.50	MOD	1.09
27	C3	H	20	0.35	NORMAL	4.53

Table A.2.b
INTERACTION TABLE

COMBINAT	AB	AC	BC	DE	CD	CE
00	3.26	8.31	3.06	2.22	2.22	2.22
01	3.02	8.26	3.24	2.79	8.40	8.40
02	15.98	5.69	3.06	8.67	7.18	7.18
10	3.59	7.23	2.76	5.87	8.67	5.87
11	7.88	6.67	3.39	8.40	5.87	3.43
12	10.32	7.90	7.73	11.52	3.43	8.67
20	2.50	2.27	11.98	5.47	2.79	5.47
21	2.97	3.04	11.35	3.43	11.52	2.79
22	6.03	6.19	9.00	7.18	5.47	11.52
TOT (SUMXiYk)	55.55	55.55	55.55	55.55	55.55	55.55

Table A.2.c
MAIN EFFECT

	CURING	HEATING	LOAD	W/C	AGGREG
	A	B	C	D	E
SUM1 (Xi)	22.26	9.36	17.80	13.68	13.56
SUM2 (Xj)	21.79	13.87	17.97	25.79	14.61
SUM3 (Xk)	11.50	32.33	19.78	16.08	27.38
Tot (Sxijk)	55.55	55.55	55.55	55.55	55.55

TableA.2.d
SUM OF SQUARES FROM MAIN EFFECT

SSXiXjXk/9	122.509	147.202	114.557	123.424	127.450
SSTot/27	114.289	114.289	114.289	114.289	114.289
SSXiXjXk/9-SSTot/27=Effect of factor X on O/Average					
Sa	8.220057	32.91295	0.26768	9.135298	13.16097

Table A.2.e
SUM OF SQUARES FROM MAIN EFFECT

	AB	AC	BC	DE	CD	CE
SSXiYi	507.91	381.40	461.20	418.92	418.92	418.92
SSXiYk/3-SST/27	55.02	12.84	39.44	25.35	25.35	25.35
Sab	13.88	4.36	6.26	3.06		

Table A.2.f
ANALYSES OF VARIANCE

Source	df	Sa --- Sab	V	F(a)= V(a)/V(Er1)	Significance %	F(a)= V(a)/V(Er2)
A (Curing)	2	8.22	4.11	5.38	>90	2.39
B (Heating)	2	32.91	16.46	21.54	>>99	9.56
C (Loading)	2	0.27	0.13	0.18		0.08
D (W/c)	2	9.14	4.57	5.98	>95	2.65
E (Aggregate)	2	13.16	6.58	8.61	>95	3.82
AB	4	13.88	3.47	4.54	>90	
AC	4	4.36	1.09	1.42		ERRORS
BC	4	6.26	1.57	2.05		
DE	4	3.06	0.76			
Error	0	0				
(Error)1	4	3.06	0.76			
(Error)2	16	27.56	1.72			
(Errror)3	12	24.50	2.04			

Appendix A.3

Table A.3.a shows the strains of all the polypropylene fibre concrete beams tested with their overall high expansions selected. These high expansions occurring time various with different experiment. These strain values are processed in the last column by dividing the high expansion of each beam by the overall length and the average concrete temperature.

Table A.3.a to A.3.f shows fractional factorial analysis of polypropylene fibre concrete, using strain as a criterion to find significance factor of deterioration of fibre concrete.

Table A.3.a
FRACTIONAL FACTORIAL ANALYSES FOR POLYPROBINE CONCRETE

FACTORS	HEATING	LOAD	W/C	AGGREG	FIBRE	T.E.F*	CON. TEM	EXPAN SION	STRAIN
Test No.	A	B	C	D	E				
1	L	0	O.25	LIGHT	F1	187	690.56	9.44	16.09
2	L	0	0.35	NORMAL	F2	223	698.50	9.87	16.62
3	L	0	0.50	MOD	F3	201	694.19	7.37	12.50
4	L	10	0.25	NORMAL	F3	213	696.50	9.16	15.48
5	L	10	0.35	MOD	F1	201	694.19	9.46	16.03
6	L	10	0.50	LIGHT	F2	202	695.50	4.95	8.37
7	L	20	O.25	MOD	F2	184	687.25	7.44	12.73
8	L	20	0.35	LIGHT	F3	183	685.72	7.43	12.75
9	L	20	0.50	NORMAL	F1	212	695.50	8.63	14.60
10	M	0	O.25	MOD	F2	114	696.50	10.00	16.89
11	M	0	0.35	LIGHT	F3	126	698.50	8.45	14.23
12	M	0	0.5	NORMAL	F1	99	637.00	8.32	15.36
13	M	10	O.25	LIGHT	F1	94	686.38	9.66	16.56
14	M	10	0.35	NORMAL	F2	112	643.00	10.10	18.49
15	M	10	0.50	MOD	F3	110	692.84	7.81	13.26
16	M	20	O.25	NORMAL	F3	101	638.60	9.32	17.17
17	M	20	0.35	MOD	F1	104	690.66	10.22	17.41

Table A.3.a continues

FACTORS	HEATING	LOAD	W/C	AGGREG	FIBRE	T.E.F*	CON. TEM	EXPANSION	STRAIN
Test No.	A	B	C	D	E				
18	M	20	0.50	LIGHT	F2	90	683.50	6.68	11.50
19	H	0	O.25	NORMAL	F3	88	695.50	9.35	15.82
20	H	0	0.35	MOD	F1	71	664.50	9.98	17.67
21	H	0	0.50	LIGHT	F2	87	698.00	5.93	9.99
22	H	10	O.25	MOD	F2	65	651.00	11.12	20.10
23	H	10	0.35	LIGHT	F3	76	681.00	10.68	18.45
24	H	10	0.50	NORMAL	F1	76	668.72	8.68	15.27
25	H	20	O.25	LIGHT	F1	65	651.00	9.62	17.38
26	H	20	0.35	NORMAL	F2	65	617.90	9.76	18.58
27	H	20	0.50	MOD	F3	83	693.00	9.30	15.79

Table A.3.b
INTERACTION TABLE

COMBINAT	AB	AC	BC	DE	CD	CE
XiYi 00	45.203	44.296	48.795	50.028	50.028	50.028
XiYj 01	39.878	45.405	48.517	29.859	49.722	49.722
XiYk 02	40.085	35.465	37.849	45.436	48.469	48.469
10	46.48	50.628	52.138	51.110	45.437	51.11
11	48.311	50.128	52.971	49.721	51.11	53.685
12	46.084	40.12	36.906	41.553	53.685	45.437
20	43.477	53.295	47.287	45.232	29.859	45.233
21	53.826	54.698	48.744	53.684	41.554	29.859
22	51.752	41.061	41.891	48.469	45.233	41.554
TOT (SUMXiYk)	415.1	415.1	415.1	415.1	415.1	415.1

Table A.3.c
MAIN EFFECT

	A	B	C	D	E
SUM1 (Xi)	125.17	135.16	148.22	125.324	146.37
SUM2 (Xj)	140.88	142.01	150.23	142.385	133.27
SUM3 (Xk)	149.05	137.92	116.65	147.386	135.46
Tot (SXijk)	415.1	415.1	415.1	415.096	415.1

TableA.3.d
SUM OF SQUARES FROM MAIN EFFECT

SSXiXjXk/9	6414.4	6384.3	6460.5	6411.39	6392.6
SSTot/27	6381.66	6381.7	6381.6	6381.65	6381.7
SSXiXjXk/9-SSTot/27=Effect of factor X on O/A average					
Sa..Se	32.752	2.6427	78.85	29.7343	10.949

TableA.3.e
SUM OF SQUARES FROM INTERACTION EFFECT

	AB	AC	BC	DE	CD	CE
SSXiYi	19324	19485	19420	19547.3	19547	19547
SSXiYk/3 -SST/27	59.746	113.47	91.831	134.134	134.13	134.13
Saxb=Sab-Sa-Sb	24.351	1.8714	59.454	93.4515		

TableA.3.f
ANALYSES OF VARIANCE

Source	df	Sa --- Sab	V	F(a)= V(a)/V(Er1)		F(a)= V(a)/V(Er3)
A (Heat)	2	32.75	16.38	0.70		2.29
B (Load)	2	2.64	1.32	0.06		0.19
C (W/C)	2	78.85	39.43	1.69		5.52
D (Aggr)	2	29.73	14.87	0.64		2.08
E (Fibre)	2	10.95	5.47	0.23		0.77
AB	4	24.35	6.09	0.26		
AC	4	1.87	0.47	0.02		
BC	4	59.45	14.86	0.64		
DE	4	93.45	23.36			3.27
Error	0	0				
(Error)1	4	93.45	23.36			
(Error)2	16	179.13	11.20			
(Error)3	12	85.68	7.14			

Appendix A.4 figures
Total Pressure, Vapor pressure and Water content profile of normal concrete obtained from Harada's   program

A.4.1. When it is exposed to 30 minutes of high rate of heating
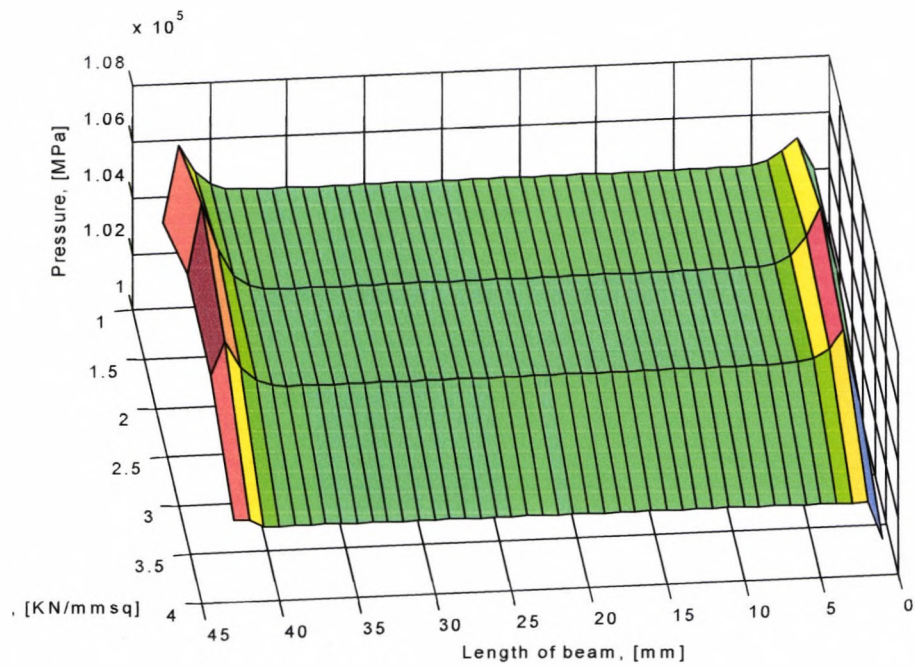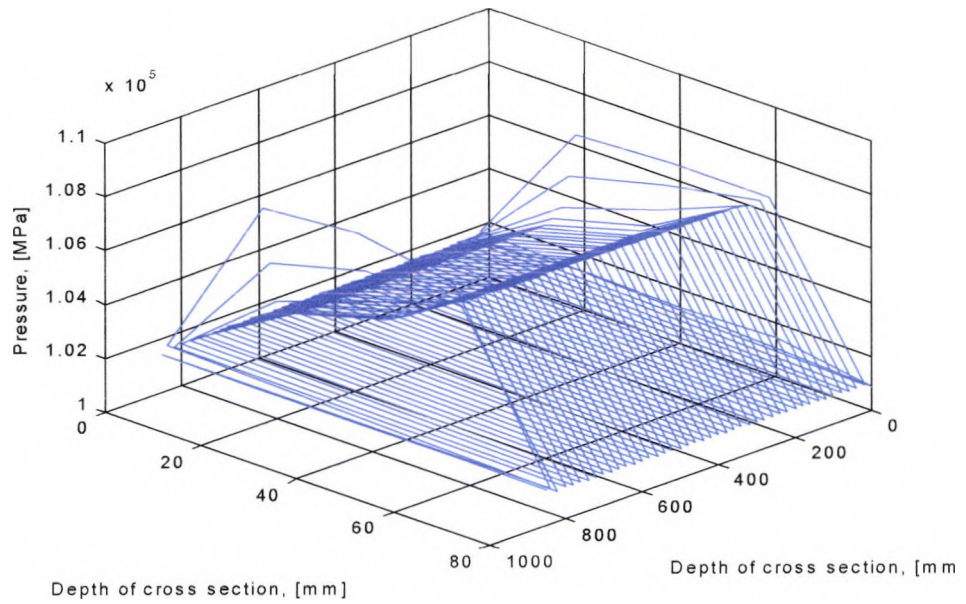
A.4.2. When it is exposed to 40 minutes of high rate of heating
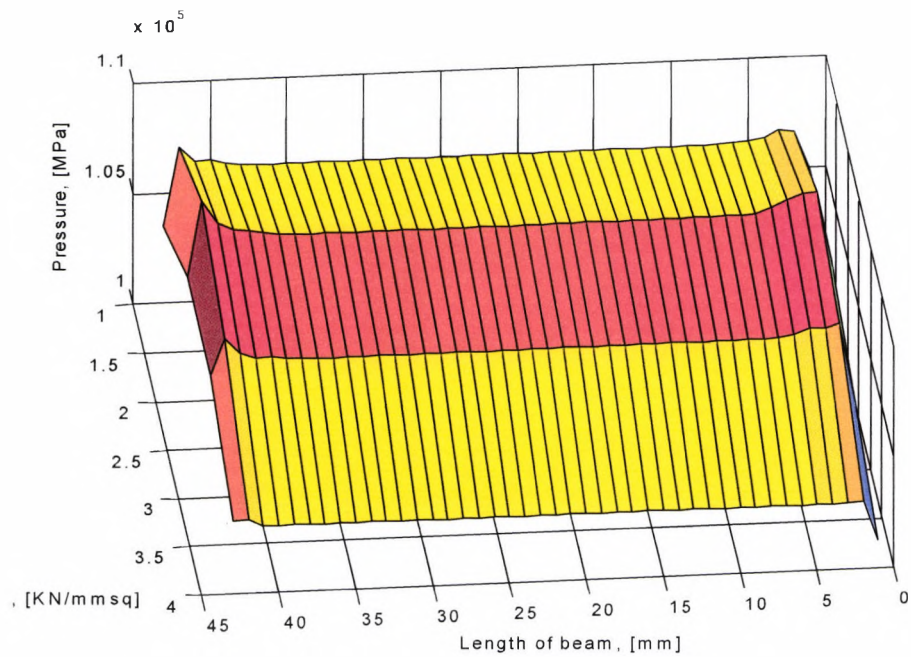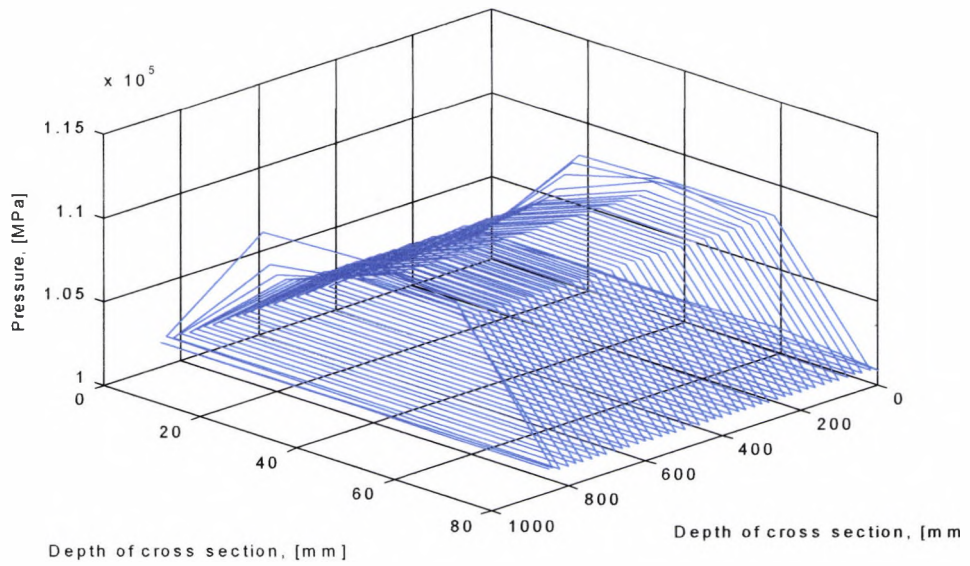
A.4.3.   When it is exposed to 50 minutes of high rate of heating
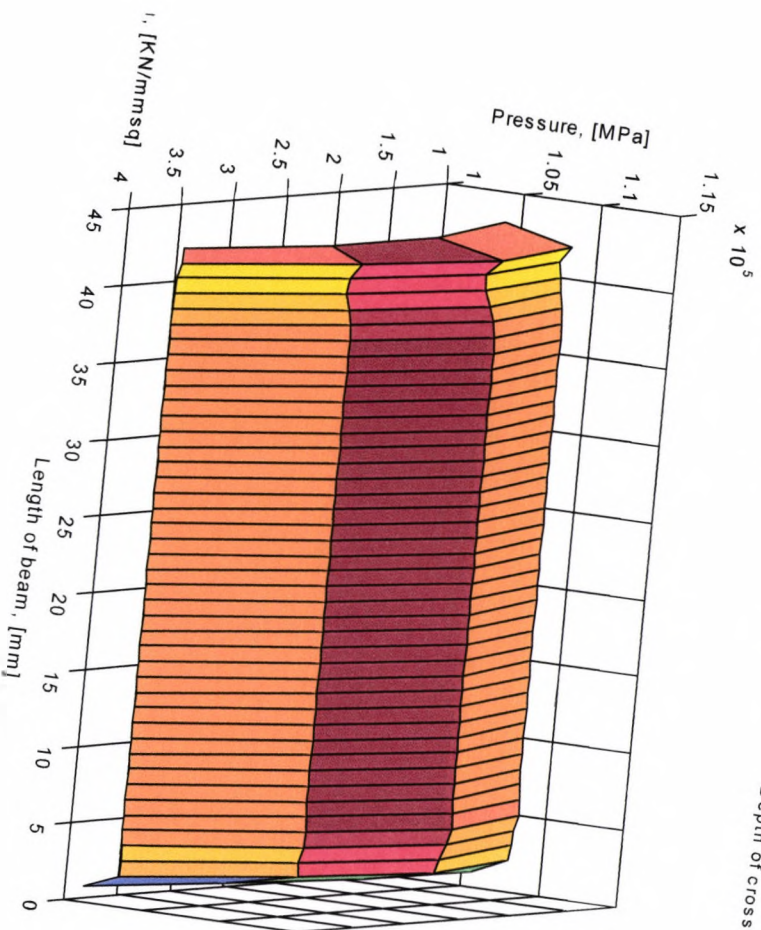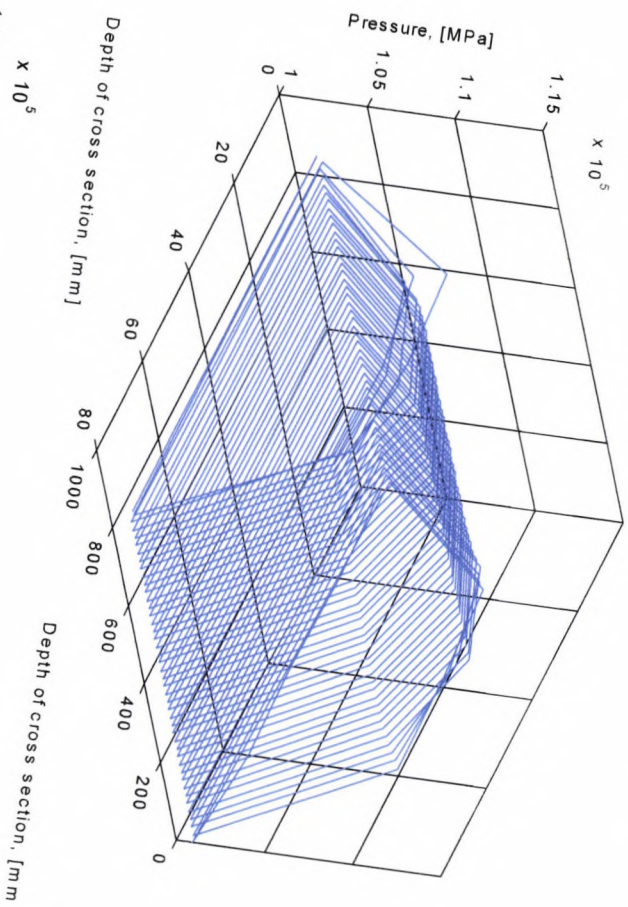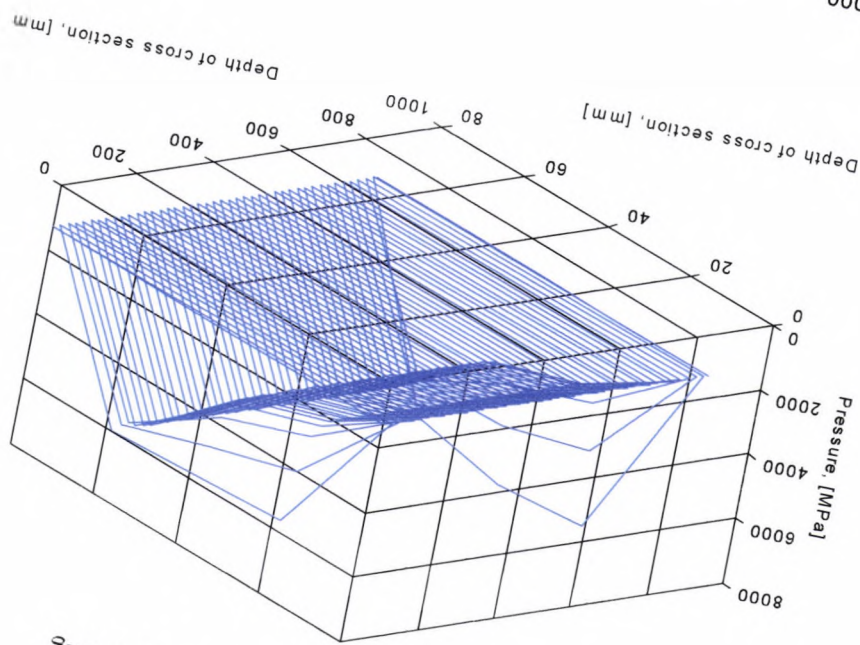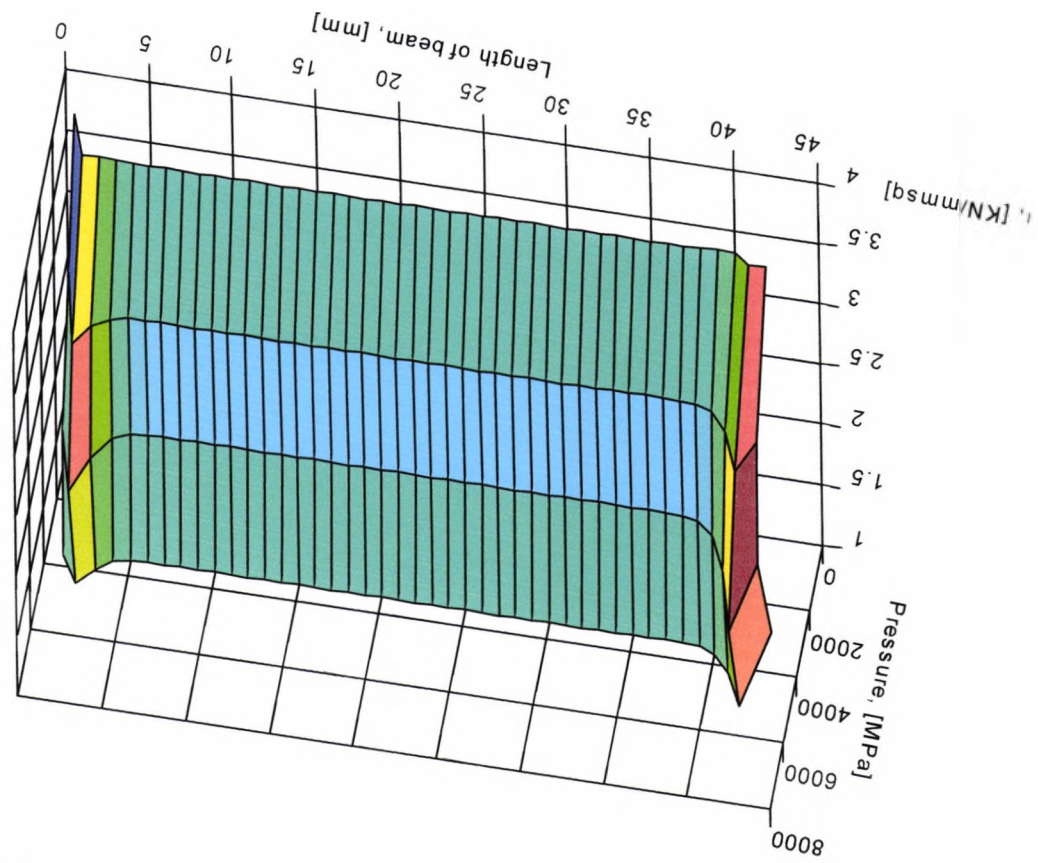
A.4.4. Vapor pressure after 30 minutes of high rate of heating

A.4 .5. Vapor pressure after 40 minutes of high rate of heating
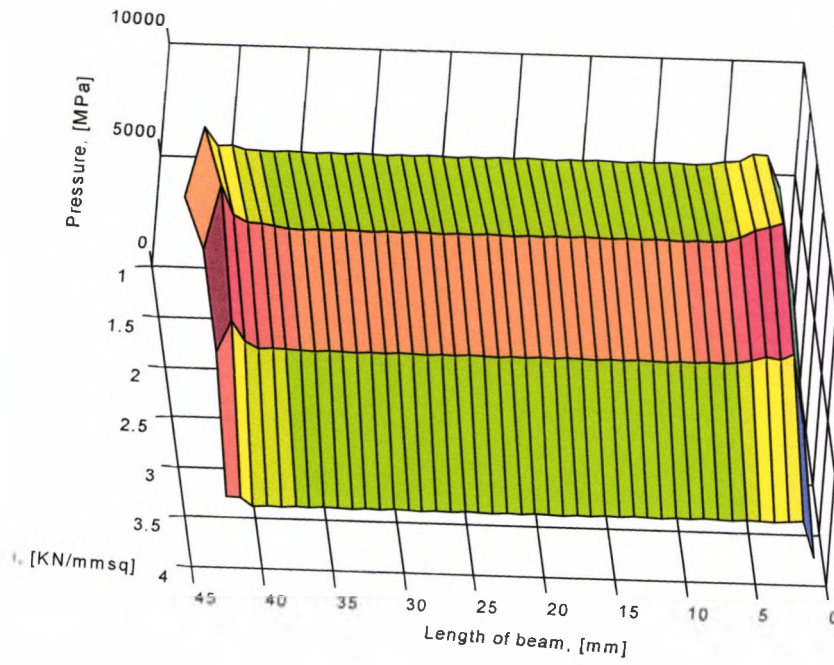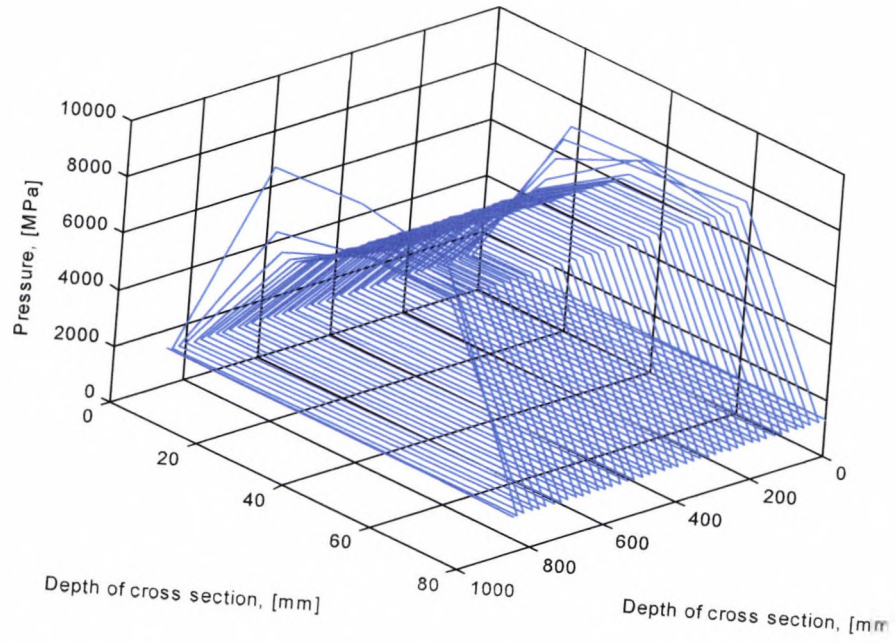
A.4.6. Vapor pressure after 50 minutes of high rate of heating
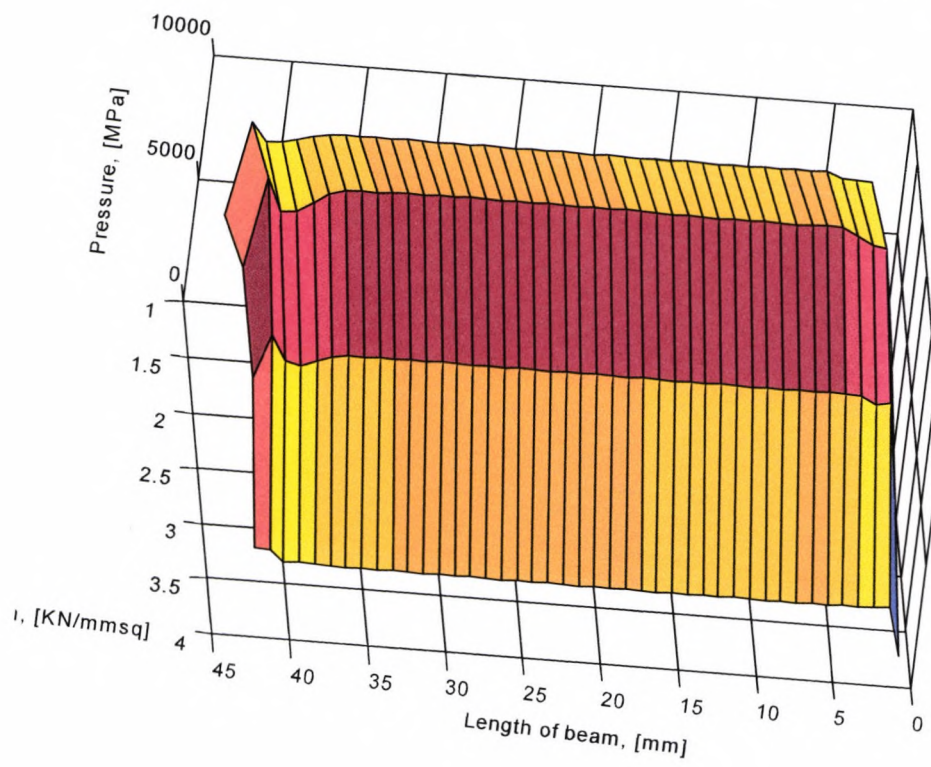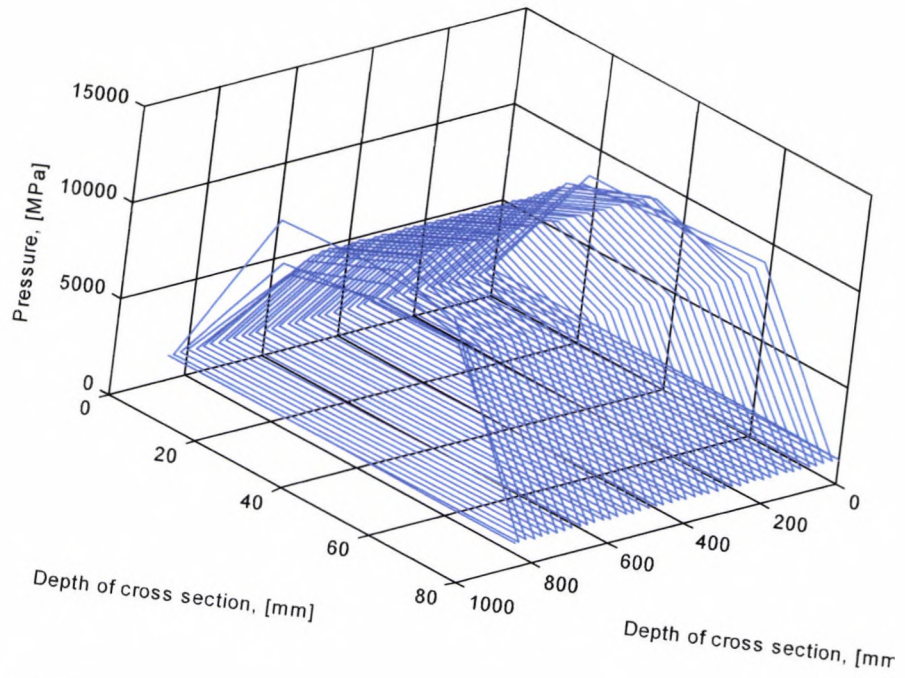
A.4.7. Water content after 10 minutes of high rate of heating
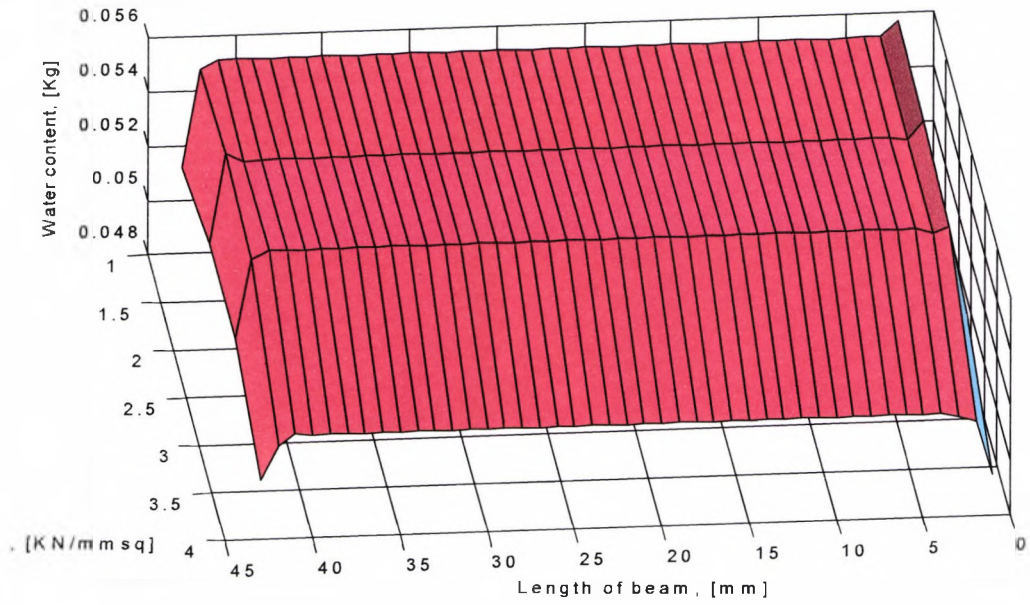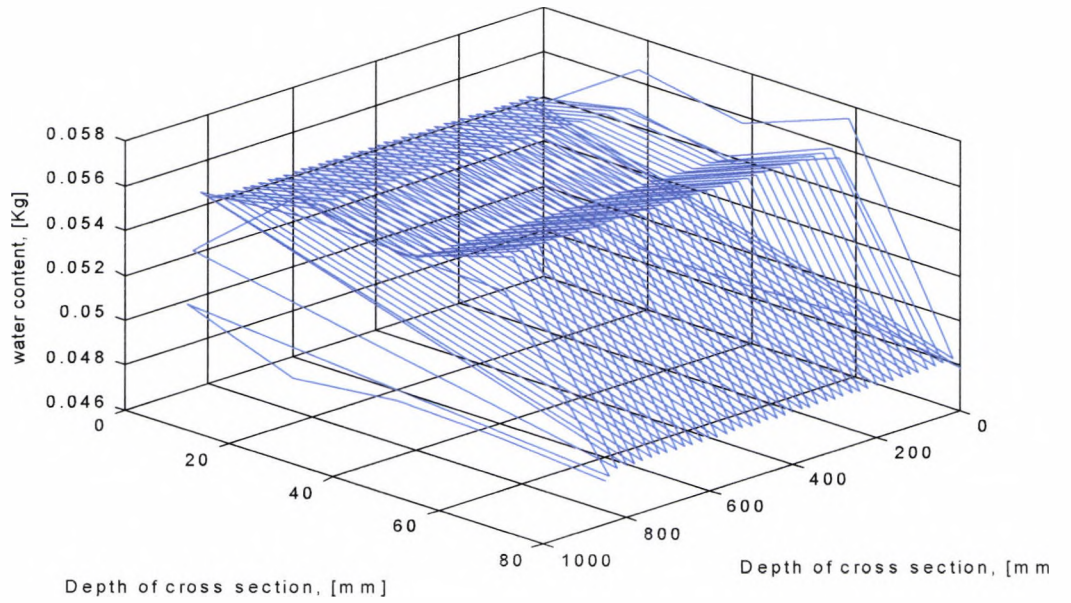
A.4.8. Water content after 30 minutes of high rate of heating
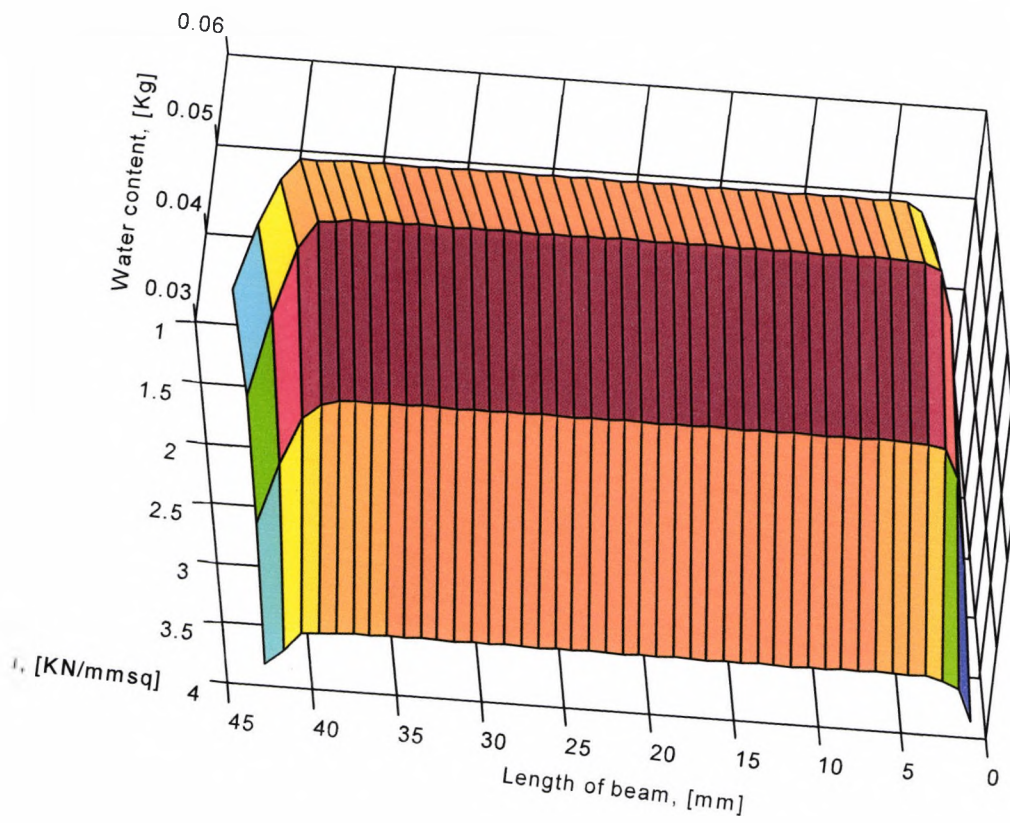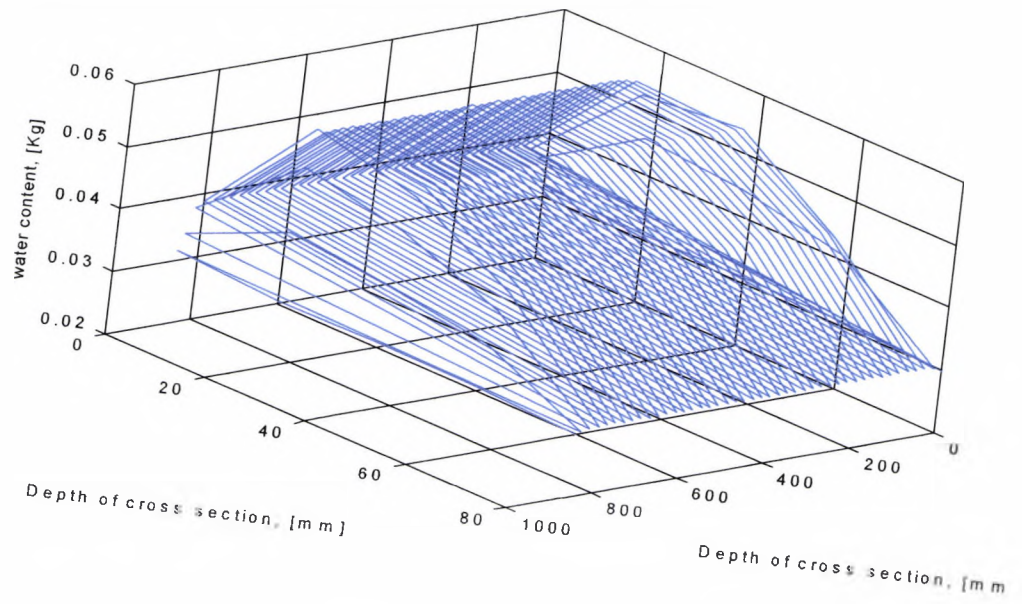
A.4.9. Water content after 50 minutes of high rate of heating

N/0.5/C2/HIGH RATE OF HEATING

10 minutes

20 minutes

30 minutes

40 minutes

50 minutes

60 minutes

'0 minutes

30 minutes

90 minutes

100 minutes

110 minutes
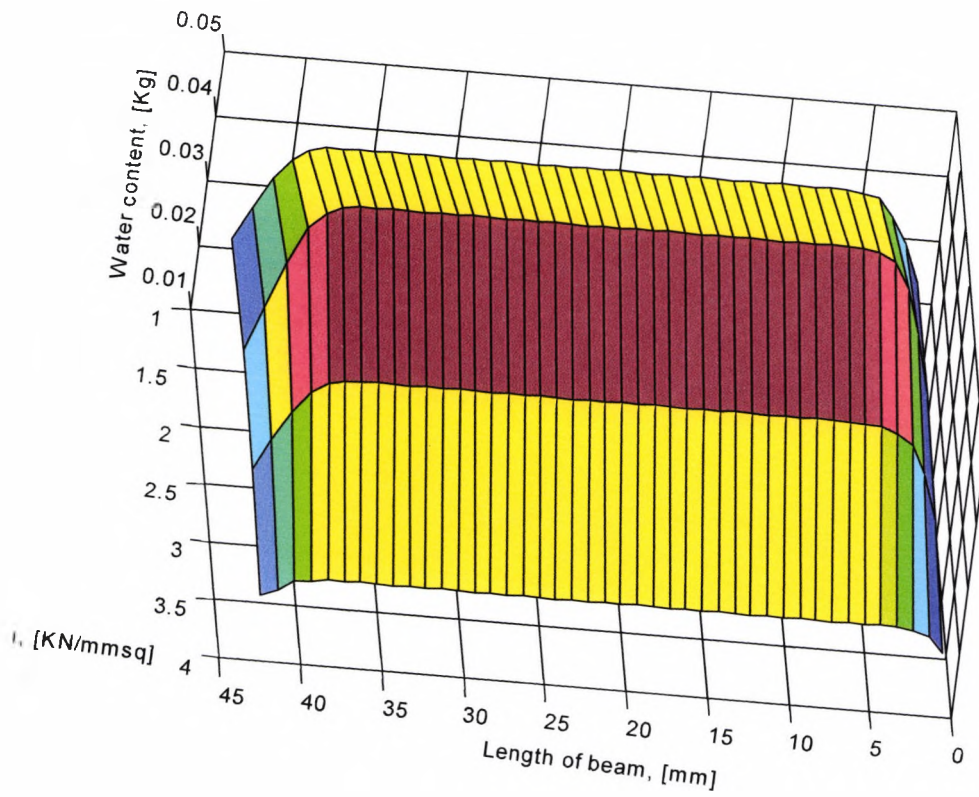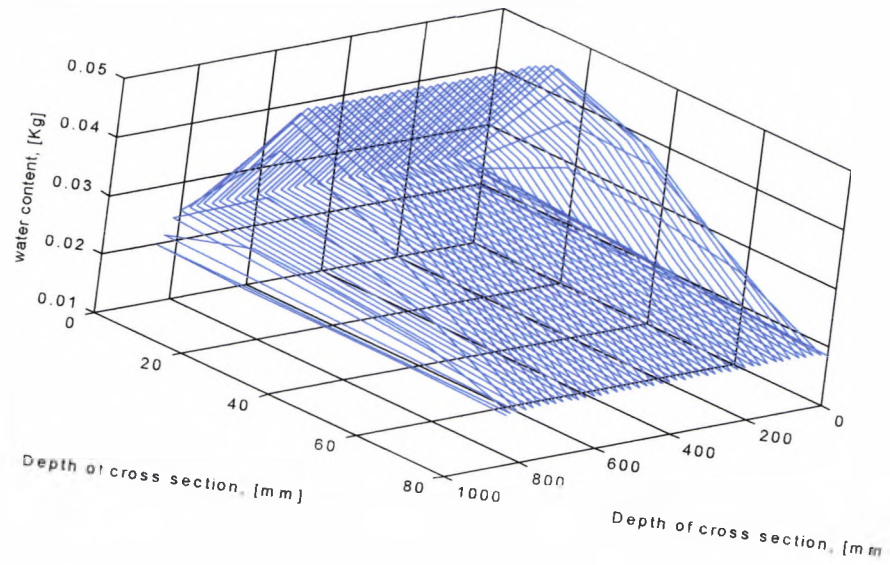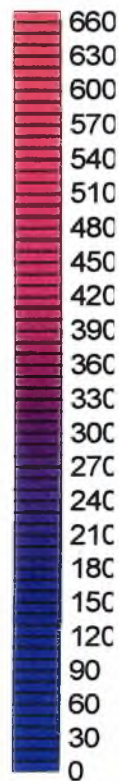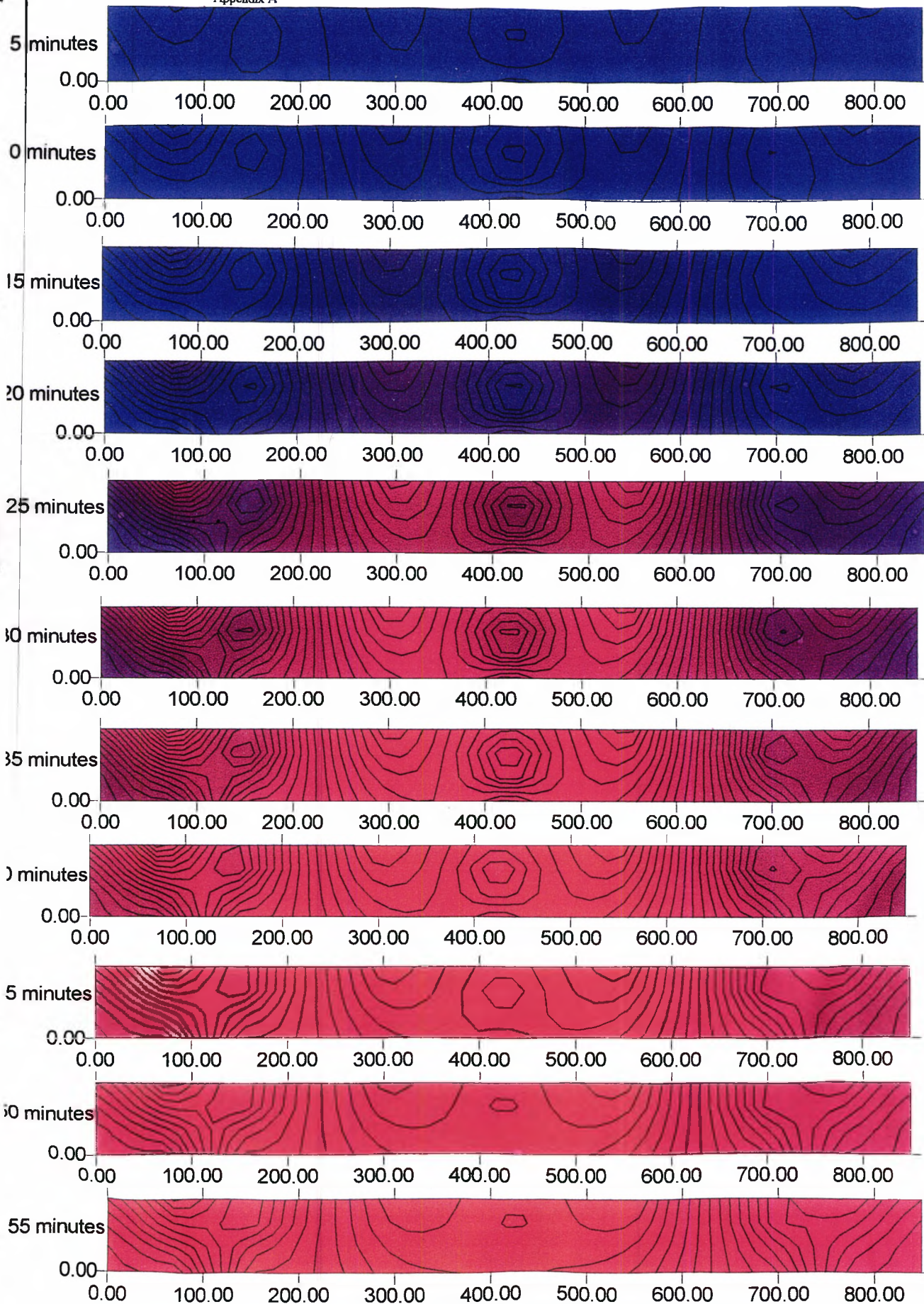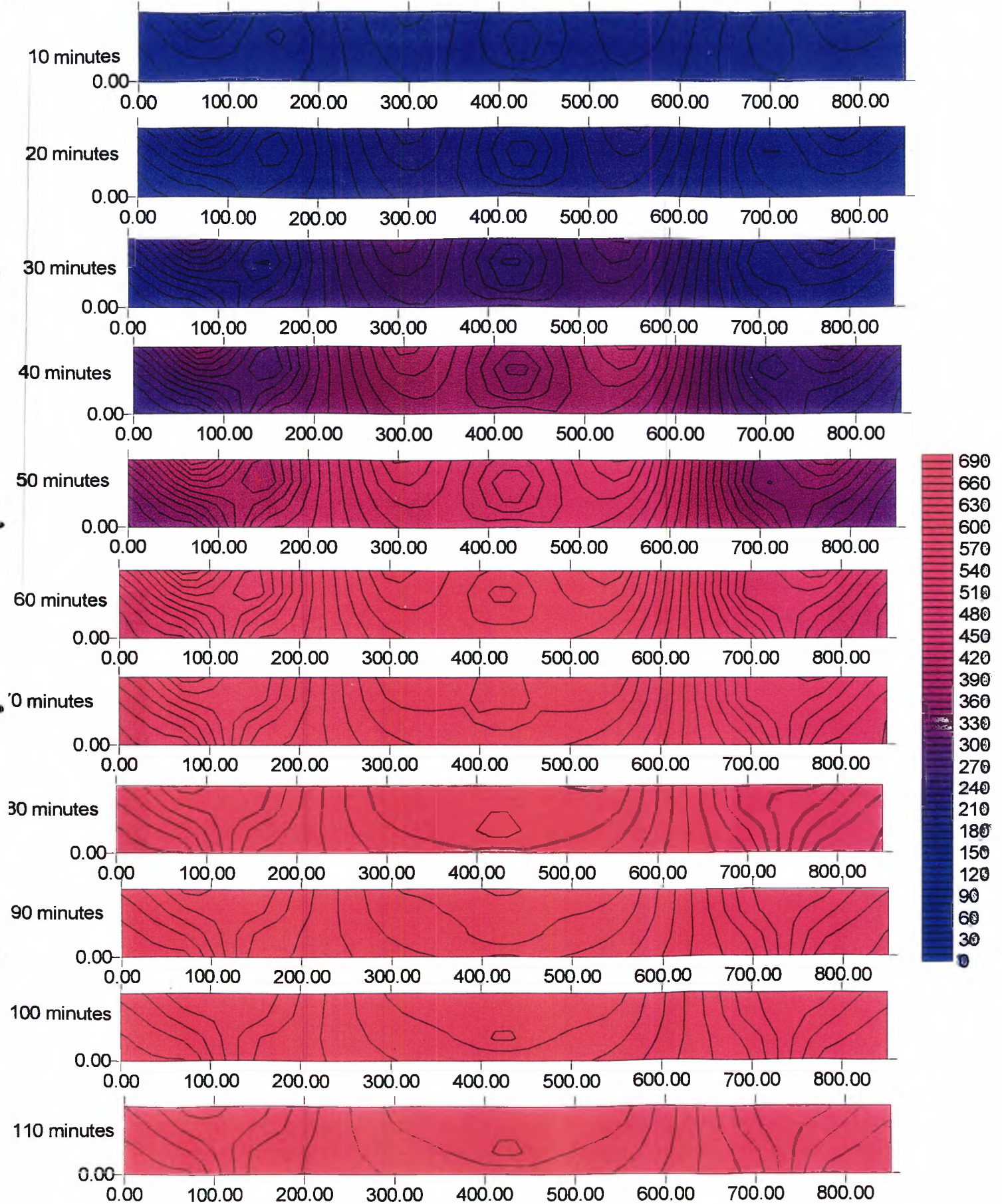
N/0.5/C2/MEDIUM RATE OF HEATING
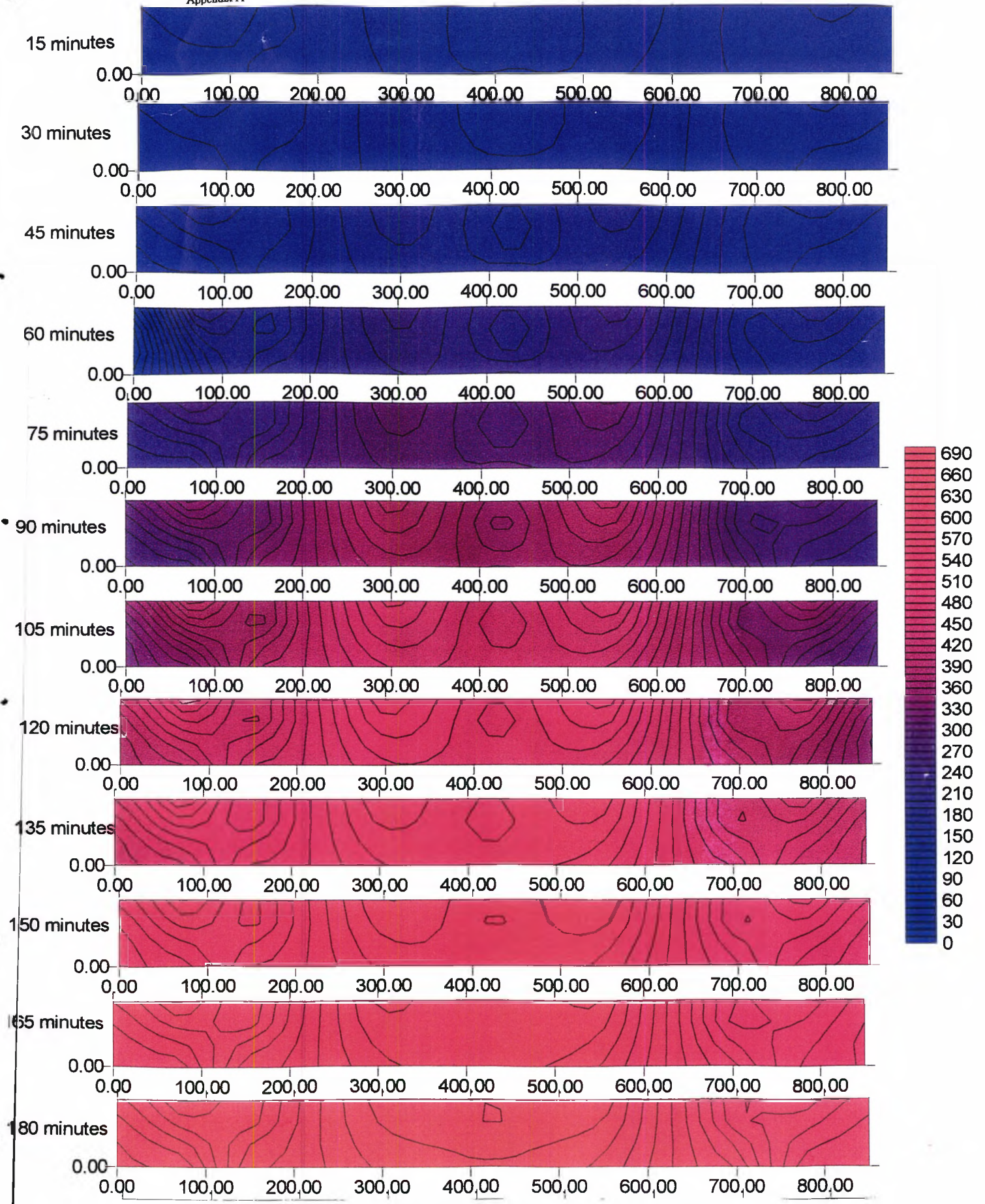
Appendix A

N/0.5/C2/LOW RATE OF HEATING

Appendix A .6

A.6.1 Typical processed results of heating and cooling cycles for light weight concrete

Table A.6.1
LIGHT WEIGHT/ 0.35/HEATING MEDIUM RATE/F3
(L0.35/00/HM/F3)

Time	Tem.Bot	Tem.Top	Axial	End 1	End 2	Centre	Quart-1	Quart-2
0	16	17	0.000	0.000	0.000	0.000	0.000	0.000
1	17	19	0.000	0.000	0.000	0.000	0.000	0.000
2	19	26	0.000	0.000	0.000	0.001	0.001	0.000
3	22	34	0.000	0.000	-0.001	0.002	0.003	0.000
4	25	39	0.001	0.000	-0.003	0.005	0.007	0.005
5	28	44	0.004	0.000	-0.003	0.014	0.013	0.008
6	32	48	0.009	0.000	-0.002	0.018	0.017	0.010
7	35	53	0.017	0.000	-0.002	0.024	0.022	0.011
8	39	58	0.025	0.001	-0.002	0.031	0.027	0.018
9	43	64	0.036	0.001	-0.001	0.037	0.034	0.025
10	47	68	0.051	0.001	-0.001	0.044	0.041	0.032
11	52	74	0.065	0.002	0.001	0.053	0.048	0.035
12	56	78	0.082	0.004	0.002	0.063	0.059	0.041
13	60	82	0.101	0.007	0.003	0.074	0.068	0.052
14	64	87	0.122	0.011	0.006	0.087	0.079	0.062
15	69	92	0.143	0.014	0.008	0.099	0.089	0.071
16	73	96	0.166	0.018	0.011	0.109	0.099	0.085
17	77	100	0.191	0.020	0.014	0.120	0.108	0.092
18	81	105	0.215	0.022	0.016	0.127	0.115	0.099
19	86	109	0.240	0.025	0.019	0.135	0.122	0.102
20	90	114	0.264	0.027	0.021	0.139	0.126	0.112
21	95	118	0.291	0.029	0.022	0.141	0.128	0.125
22	100	123	0.319	0.030	0.023	0.141	0.128	0.129
23	106	128	0.345	0.032	0.025	0.141	0.128	0.131
24	110	133	0.371	0.034	0.027	0.141	0.128	0.131
25	115	137	0.396	0.036	0.028	0.141	0.126	0.132
26	119	142	0.423	0.038	0.030	0.141	0.125	0.132
27	125	147	0.449	0.039	0.031	0.139	0.123	0.133
28	129	151	0.475	0.041	0.032	0.140	0.122	0.135
29	134	156	0.503	0.043	0.034	0.139	0.122	0.133
30	138	161	0.529	0.045	0.036	0.139	0.121	0.130
31	144	165	0.557	0.046	0.040	0.140	0.121	0.129
32	148	169	0.583	0.049	0.041	0.140	0.121	0.128
33	153	172	0.611	0.051	0.042	0.140	0.121	0.128
34	158	177	0.640	0.053	0.043	0.139	0.121	0.128

Table A.6.1 continues

Time	Tem.Bot	Tem.Top	Axial	End 1	End 2	Centre	Quart-1	Quart-2
35	162	182	0.668	0.056	0.045	0.138	0.120	0.125
36	167	189	0.698	0.059	0.048	0.136	0.118	0.123
37	171	198	0.727	0.060	0.048	0.131	0.114	0.119
38	176	203	0.760	0.062	0.048	0.124	0.109	0.115
39	181	213	0.789	0.063	0.048	0.118	0.103	0.113
40	185	209	0.826	0.058	0.043	0.091	0.083	0.109
41	190	216	0.854	0.059	0.043	0.085	0.074	0.099
42	195	225	0.887	0.071	0.054	0.092	0.076	0.096
43	200	227	0.917	0.071	0.054	0.082	0.067	0.080
44	204	238	0.946	0.071	0.054	0.075	0.061	0.079
45	208	237	0.975	0.071	0.054	0.069	0.056	0.075
46	213	241	1.005	0.071	0.055	0.064	0.051	0.065
47	217	241	1.036	0.072	0.056	0.059	0.047	0.063
48	221	244	1.065	0.072	0.057	0.057	0.044	0.061
49	226	249	1.094	0.074	0.059	0.055	0.043	0.055
50	229	255	1.121	0.076	0.060	0.054	0.043	0.051
51	233	259	1.151	0.077	0.061	0.053	0.042	0.049
52	238	262	1.180	0.079	0.062	0.052	0.042	0.045
53	243	269	1.206	0.081	0.064	0.052	0.043	0.042
54	248	275	1.232	0.082	0.065	0.054	0.044	0.041
55	253	284	1.257	0.084	0.067	0.054	0.044	0.042
56	259	288	1.283	0.086	0.068	0.054	0.044	0.043
57	264	287	1.308	0.088	0.069	0.055	0.045	0.045
58	269	293	1.331	0.090	0.070	0.057	0.046	0.046
59	277	301	1.362	0.092	0.071	0.057	0.049	0.048
60	286	313	1.405	0.096	0.072	0.057	0.057	0.056
61	298	323	1.469	0.252	0.222	0.173	0.260	0.244
62	308	334	1.509	0.254	0.222	0.189	0.273	0.255
63	316	344	1.548	0.262	0.230	0.210	0.292	0.261
64	329	355	1.584	0.273	0.243	0.241	0.311	0.289
65	337	364	1.619	0.280	0.250	0.255	0.323	0.299
66	349	375	1.655	0.289	0.261	0.268	0.335	0.310
67	355	386	1.694	0.299	0.269	0.279	0.346	0.319
68	367	399	1.728	0.307	0.276	0.288	0.354	0.345
69	376	410	1.764	0.317	0.281	0.298	0.364	0.362
70	386	422	1.800	0.327	0.288	0.307	0.371	0.370
71	395	433	1.840	0.339	0.297	0.317	0.381	0.378
72	405	443	1.889	0.349	0.302	0.320	0.385	0.380
73	413	453	1.943	0.365	0.308	0.322	0.388	0.385
74	422	464	1.999	0.376	0.315	0.323	0.389	0.386
75	435	475	2.083	0.385	0.323	0.321	0.387	0.389
76	445	486	2.145	0.395	0.335	0.315	0.380	0.385

Appendix A.

Table A.6.1 continues

Time	Tem.Bot	Tem.Top	Axial	End 1	End 2	Centre	Quart-1	Quart-2
77	455	496	2.225	0.402	0.348	0.305	0.372	0.360
78	464	506	2.312	0.407	0.362	0.295	0.365	0.355
79	474	517	2.406	0.417	0.375	0.287	0.355	0.345
80	484	527	2.508	0.428	0.384	0.287	0.347	0.344
81	495	537	2.620	0.441	0.389	0.298	0.344	0.352
82	505	548	2.744	0.450	0.395	0.300	0.335	0.346
83	515	557	2.881	0.471	0.413	0.246	0.339	0.344
84	524	567	3.011	0.477	0.414	0.247	0.337	0.335
85	534	577	3.157	0.488	0.415	0.263	0.338	0.330
86	544	586	3.312	0.496	0.412	0.229	0.328	0.310
87	552	595	3.473	0.507	0.412	0.242	0.331	0.305
88	561	604	3.640	0.527	0.431	0.223	0.346	0.320
89	570	614	3.821	0.539	0.439	0.252	0.349	0.335
90	579	623	4.012	0.556	0.458	0.264	0.350	0.345
91	587	632	4.216	0.586	0.492	0.239	0.354	0.350
92	596	640	4.436	0.631	0.512	0.231	0.356	0.353
93	604	648	4.665	0.641	0.505	0.103	0.284	0.305
94	613	656	4.906	0.652	0.538	0.078	0.276	0.289
95	621	664	5.151	0.660	0.540	0.003	0.229	0.279
96	629	671	5.394	0.662	0.542	-0.077	0.178	0.245
97	637	678	5.645	0.668	0.554	-0.171	0.117	0.195
98	646	685	5.888	0.671	0.573	-0.272	0.050	0.112
99	653	692	6.133	0.672	0.574	-0.399	-0.051	0.054
100	658	696	6.355	0.678	0.580	-0.483	-0.121	-0.110
101	661	698	6.557	0.677	0.576	-0.695	-0.365	-0.289
102	663	700	6.746	0.681	0.575	-0.738	-0.389	-0.301
103	664	701	6.926	0.685	0.576	-0.778	-0.399	-0.345
104	664	701	7.073	0.686	0.576	-0.820	-0.411	-0.399
105	664	701	7.212	0.685	0.565	-0.922	-0.510	-0.445
106	664	701	7.344	0.716	0.565	-0.947	-0.519	-0.449
107	664	701	7.450	0.736	0.565	-0.965	-0.523	-0.499
108	664	701	7.554	0.771	0.566	-0.986	-0.524	-0.511
109	664	700	7.647	0.807	0.567	-1.022	-0.528	-0.515
110	664	700	7.731	0.696	0.547	-1.153	-0.651	-0.589
111	663	700	7.794	0.708	0.548	-1.178	-0.661	-0.611
112	663	699	7.859	0.725	0.549	-1.192	-0.668	-0.624
113	663	699	7.923	0.731	0.550	-1.207	-0.682	-0.655
114	662	699	7.969	0.740	0.550	-1.216	-0.690	-0.665
115	662	698	8.016	0.758	0.550	-1.223	-0.689	-0.679
116	662	698	8.060	0.770	0.551	-1.228	-0.690	-0.685
117	661	698	8.103	0.783	0.552	-1.232	-0.689	-0.688
118	661	698	8.139	0.796	0.553	-1.232	-0.682	-0.679

Table A.6.1 continues

Time	Tem.Bot	Tem.Top	Axial	End 1	End 2	Centre	Quart-1	Quart-2
119	661	698	8.174	0.809	0.552	-1.233	-0.679	-0.675
120	661	698	8.206	0.818	0.552	-1.233	-0.676	-0.665
121	661	697	8.236	0.825	0.553	-1.234	-0.673	-0.659
122	661	697	8.265	0.831	0.552	-1.235	-0.671	-0.645
123	661	697	8.294	0.835	0.552	-1.236	-0.671	-0.635
124	661	697	8.323	0.840	0.552	-1.237	-0.669	-0.625
125	661	697	8.364	0.849	0.552	-1.238	-0.668	-0.611
126	626	664	8.448	0.815	0.584	-1.242	-0.698	-0.605
127	608	643	8.441	0.843	0.629	-1.227	-0.677	-0.602
128	591	625	8.359	0.867	0.673	-1.189	-0.648	-0.595
129	528	598	7.933	0.921	0.711	-0.982	-0.412	-0.489
130	497	576	7.402	0.935	0.788	-0.536	0.042	-0.112
131	476	556	6.765	0.963	0.857	-0.132	0.024	-0.044
132	455	537	6.154	0.964	0.791	-0.578	-0.033	-0.011
133	436	519	5.776	0.914	0.777	-0.705	-0.162	-0.099
134	419	501	5.481	0.877	0.769	-0.754	-0.219	-0.189
135	360	439	4.666	0.745	0.697	-0.898	-0.384	-0.365
136	346	425	4.525	0.720	0.681	-0.927	-0.416	-0.402
137	334	412	4.396	0.686	0.661	-0.959	-0.453	-0.432
138	323	400	4.281	0.659	0.641	-0.989	-0.482	-0.465
139	312	388	4.177	0.632	0.625	-1.018	-0.511	-0.502
140	303	377	4.087	0.607	0.609	-1.043	-0.541	-0.535
141	302	376	4.059	0.594	0.596	-1.045	-0.539	-0.544
142	302	376	4.059	0.594	0.596	-1.045	-0.539	-0.542
143	292	365	3.989	0.586	0.590	-1.046	-0.550	-0.535
144	283	354	3.909	0.567	0.581	-1.051	-0.557	-0.542
145	274	345	3.835	0.548	0.573	-1.055	-0.567	-0.555
146	266	335	3.777	0.531	0.565	-1.060	-0.577	-0.565
147	257	326	3.696	0.515	0.558	-1.065	-0.586	-0.579
148	251	317	3.645	0.499	0.550	-1.069	-0.596	-0.585
149	243	308	3.591	0.482	0.542	-1.076	-0.606	-0.601
150	237	300	3.540	0.464	0.531	-1.089	-0.620	-0.611
151	229	292	3.493	0.444	0.515	-1.111	-0.644	-0.632
152	223	285	3.449	0.423	0.501	-1.134	-0.666	-0.635
153	217	278	3.408	0.403	0.486	-1.156	-0.688	-0.655
154	212	271	3.369	0.390	0.474	-1.177	-0.709	-0.689
155	206	264	3.332	0.377	0.460	-1.199	-0.732	-0.702
156	202	257	3.296	0.358	0.447	-1.217	-0.751	-0.702
157	196	251	3.263	0.342	0.433	-1.235	-0.769	-0.735
158	191	245	3.230	0.327	0.421	-1.253	-0.788	-0.755
159	187	239	3.201	0.312	0.408	-1.275	-0.808	-0.796
160	182	233	3.175	0.298	0.397	-1.290	-0.825	-0.805

Table A.6.1 continues

Time	Tem.Bot	Tem.Top	Axial	End 1	End 2	Centre	Quart-1	Quart-2
161	178	228	3.147	0.285	0.386	-1.311	-0.845	-0.802
162	173	223	3.125	0.272	0.375	-1.330	-0.862	-0.835
163	169	218	3.102	0.258	0.364	-1.347	-0.880	-0.835
164	164	213	3.082	0.246	0.353	-1.365	-0.895	-0.855
165	162	208	3.062	0.236	0.343	-1.378	-0.910	-0.899
166	158	203	3.043	0.225	0.334	-1.390	-0.923	-0.911
167	153	199	3.024	0.214	0.322	-1.406	-0.939	-0.925
168	150	194	3.007	0.205	0.314	-1.420	-0.952	-0.926
169	148	190	2.990	0.195	0.306	-1.432	-0.965	-0.945
170	144	186	2.974	0.187	0.299	-1.445	-0.977	-0.965
171	141	182	2.958	0.179	0.293	-1.454	-0.987	-0.972
172	138	178	2.945	0.170	0.284	-1.468	-1.000	-0.989
173	135	174	2.931	0.163	0.279	-1.476	-1.008	-1.002
174	132	171	2.917	0.155	0.273	-1.490	-1.021	-1.011
175	130	167	2.905	0.148	0.266	-1.502	-1.030	-1.020
176	127	163	2.892	0.141	0.259	-1.514	-1.042	-1.035
177	124	160	2.882	0.134	0.252	-1.524	-1.051	-1.042
178	122	157	2.868	0.128	0.245	-1.533	-1.061	-1.045
179	120	153	2.859	0.122	0.239	-1.542	-1.071	-1.065
180	118	150	2.847	0.117	0.235	-1.549	-1.078	-1.055
181	115	147	2.837	0.111	0.229	-1.558	-1.087	-1.065
182	113	144	2.825	0.104	0.223	-1.567	-1.096	-1.079
183	111	141	2.817	0.098	0.218	-1.578	-1.105	-1.095
184	109	138	2.808	0.093	0.214	-1.585	-1.113	-1.105
185	107	135	2.800	0.088	0.209	-1.593	-1.120	-1.115
186	104	133	2.794	0.083	0.204	-1.601	-1.128	-1.121
187	103	130	2.785	0.076	0.199	-1.611	-1.137	-1.132
188	101	127	2.779	0.072	0.195	-1.617	-1.144	-1.114
189	99	125	2.770	0.067	0.192	-1.622	-1.150	-1.146
190	97	122	2.764	0.061	0.185	-1.634	-1.160	-1.155
191	95	120	2.758	0.057	0.181	-1.641	-1.165	-1.159
192	93	118	2.750	0.053	0.179	-1.646	-1.170	-1.162
193	92	115	2.745	0.049	0.176	-1.650	-1.174	-1.170
194	90	113	2.711	0.041	0.167	-1.661	-1.185	-1.172
195	89	111	2.710	0.040	0.166	-1.661	-1.187	-1.175
196	87	109	2.710	0.036	0.163	-1.668	-1.193	-1.189
197	86	107	2.710	0.031	0.158	-1.676	-1.199	-1.196
198	84	105	2.708	0.027	0.155	-1.682	-1.206	-1.199
199	83	103	2.708	0.024	0.153	-1.685	-1.209	-1.205
200	81	101	2.705	0.021	0.149	-1.691	-1.215	-1.210
201	80	99	2.701	0.018	0.146	-1.696	-1.219	-1.215
202	79	97	2.696	0.015	0.144	-1.701	-1.224	-1.219

Table A.6.1 continues

Time	Tem.Bot	Tem.Top	Axial	End 1	End 2	Centre	Quart-1	Quart-2
203	77	96	2.692	0.011	0.140	-1.707	-1.230	-1.225
204	76	94	2.689	0.009	0.139	-1.710	-1.233	-1.230
205	75	92	2.686	0.005	0.135	-1.716	-1.238	-1.235
206	74	91	2.681	0.002	0.132	-1.722	-1.243	-1.240
207	73	89	2.677	0.000	0.131	-1.724	-1.247	-1.252
208	72	88	2.674	-0.004	0.127	-1.730	-1.253	-1.255
209	70	86	2.672	-0.007	0.125	-1.734	-1.256	-1.262
210	69	85	2.666	-0.008	0.124	-1.734	-1.258	-1.263
211	68	83	2.664	-0.012	0.120	-1.742	-1.265	-1.265
212	67	82	2.661	-0.013	0.119	-1.743	-1.266	-1.272
213	66	81	2.656	-0.017	0.116	-1.748	-1.272	-1.285
214	65	79	2.653	-0.019	0.114	-1.754	-1.277	-1.289
215	64	78	2.651	-0.020	0.113	-1.755	-1.278	-1.301
216	64	77	2.633	-0.024	0.108	-1.760	-1.283	-1.305
217	63	76	2.634	-0.025	0.108	-1.760	-1.283	-1.311
218	62	74	2.634	-0.026	0.107	-1.761	-1.284	-1.325
219	61	73	2.632	-0.029	0.104	-1.765	-1.287	-1.329
220	60	72	2.630	-0.032	0.102	-1.770	-1.291	-1.330
221	60	71	2.629	-0.034	0.100	-1.773	-1.295	-1.336
222	59	70	2.626	-0.035	0.100	-1.774	-1.296	-1.345
223	58	69	2.620	-0.039	0.095	-1.782	-1.302	-1.342
224	57	68	2.620	-0.040	0.093	-1.786	-1.305	-1.355
225	57	67	2.616	-0.042	0.093	-1.787	-1.307	-1.366
226	56	66	2.612	-0.043	0.092	-1.789	-1.308	-1.367
227	55	65	2.610	-0.046	0.088	-1.794	-1.314	-1.369
228	55	65	2.608	-0.047	0.088	-1.794	-1.314	-1.370
229	54	64	2.607	-0.048	0.088	-1.795	-1.315	-1.372
230	54	63	2.604	-0.050	0.085	-1.800	-1.320	-1.375
231	53	62	2.602	-0.052	0.083	-1.804	-1.323	-1.376
232	52	61	2.601	-0.053	0.083	-1.805	-1.324	-1.378
233	52	61	2.600	-0.055	0.080	-1.809	-1.328	-1.382
234	51	60	2.597	-0.056	0.080	-1.809	-1.328	-1.385
235	51	59	2.595	-0.059	0.077	-1.815	-1.332	-1.389
236	50	58	2.592	-0.059	0.077	-1.815	-1.332	-1.390

A.6.2. Typical processed results of heating and cooling cycles for modified concrete

Table A.6.2
MODIFIED/ 0.25/HEATING MEDIUM RATE/F2
(M/0.25/HM/F2)

Time	Tem top	Tem.bot	Axial	End-1	End-2	Centre	Quart-1	Quart-2
0	48	50	0.00	0.00	0.00	0.00	0.00	0.00
1	69	57	0.00	0.00	0.00	0.00	0.00	0.00
2	98	69	0.00	0.00	-0.01	0.00	0.00	0.00
3	120	82	0.04	-0.02	-0.01	0.00	0.00	0.02
4	139	96	0.04	-0.03	-0.01	0.01	-0.01	0.02
5	157	109	0.06	-0.05	-0.01	0.01	-0.01	0.03
6	173	121	0.08	-0.07	-0.01	0.01	-0.01	0.03
7	189	132	0.11	-0.08	0.02	0.03	0.00	0.05
8	202	144	0.14	-0.11	0.02	0.03	-0.01	0.05
9	202	148	0.25	-0.16	0.02	0.02	-0.03	0.05
10	204	148	0.26	-0.18	0.02	0.02	-0.04	0.05
11	224	161	0.30	-0.21	0.02	0.02	-0.05	0.05
12	239	173	0.34	-0.22	0.02	0.02	-0.05	0.06
13	251	184	0.39	-0.22	0.02	0.02	-0.04	0.06
14	261	195	0.44	-0.22	0.02	0.03	-0.04	0.07
15	271	206	0.50	-0.22	0.02	0.04	-0.03	0.07
16	280	217	0.56	-0.22	0.02	0.04	-0.03	0.07
17	289	227	0.62	-0.22	0.02	0.05	-0.03	0.07
18	297	238	0.67	-0.22	0.02	0.05	-0.03	0.07
19	312	249	0.73	-0.22	0.02	0.06	-0.03	0.07
20	319	259	0.80	-0.22	0.03	0.06	-0.03	0.07
21	325	269	0.85	-0.23	0.03	0.06	-0.04	0.07
22	329	279	0.91	-0.24	0.03	0.06	-0.05	0.07
23	339	288	0.96	-0.25	0.04	0.06	-0.05	0.07
24	347	298	1.02	-0.26	0.04	0.06	-0.05	0.07
25	357	307	1.07	-0.27	0.04	0.06	-0.05	0.08
26	368	316	1.13	-0.29	0.05	0.06	-0.06	0.09
27	381	324	1.18	-0.31	0.05	0.07	-0.07	0.09
28	388	332	1.24	-0.33	0.06	0.08	-0.06	0.10
29	395	340	1.30	-0.34	0.07	0.09	-0.05	0.12
30	402	348	1.36	-0.36	0.07	0.11	-0.04	0.14
31	411	355	1.42	-0.38	0.08	0.14	-0.02	0.17
32	422	363	1.49	-0.40	0.09	0.17	0.00	0.20
33	428	370	1.56	-0.41	0.11	0.20	0.02	0.23
34	437	378	1.64	-0.42	0.12	0.22	0.04	0.27

Table A.6.2 continues

Time	Tem top	Tem.bot	Axial	End-1	End-2	Centre	Quart-1	Quart-2
35	448	386	1.72	-0.42	0.13	0.26	0.07	0.30
36	457	394	1.81	-0.42	0.15	0.31	0.11	0.35
37	467	403	1.90	-0.41	0.17	0.35	0.15	0.39
38	477	411	2.00	-0.40	0.18	0.39	0.18	0.43
39	486	419	2.11	-0.39	0.20	0.43	0.21	0.46
40	495	428	2.23	-0.41	0.22	0.45	0.22	0.48
41	504	436	2.36	-0.41	0.24	0.47	0.23	0.51
42	513	445	2.49	-0.40	0.26	0.49	0.24	0.53
43	521	454	2.64	-0.40	0.28	0.50	0.25	0.54
44	528	462	2.80	-0.40	0.29	0.52	0.25	0.55
45	536	471	2.96	-0.40	0.30	0.52	0.24	0.55
46	545	480	3.13	-0.40	0.31	0.52	0.23	0.55
47	553	489	3.31	-0.40	0.32	0.52	0.23	0.55
48	561	498	3.49	-0.40	0.34	0.53	0.23	0.57
49	569	507	3.68	-0.40	0.35	0.52	0.24	0.57
50	576	515	3.88	-0.40	0.36	0.52	0.24	0.57
51	585	524	4.08	-0.40	0.37	0.53	0.25	0.59
52	593	533	4.29	-0.38	0.39	0.55	0.28	0.62
53	601	542	4.51	-0.37	0.42	0.57	0.31	0.65
54	610	550	4.74	-0.36	0.44	0.61	0.35	0.69
55	618	559	4.98	-0.35	0.45	0.64	0.37	0.72
56	626	568	5.22	-0.33	0.47	0.67	0.40	0.77
57	633	576	5.47	-0.32	0.49	0.68	0.40	0.78
58	641	584	5.73	-0.30	0.52	0.68	0.40	0.78
59	648	592	5.98	-0.28	0.55	0.66	0.37	0.77
60	654	600	6.24	-0.25	0.55	0.60	0.32	0.72
61	660	607	6.50	-0.24	0.56	0.52	0.25	0.64
62	668	614	6.76	-0.22	0.58	0.44	0.18	0.56
63	674	622	7.02	-0.23	0.58	0.32	0.07	0.45
64	681	629	7.28	-0.23	0.57	0.19	-0.04	0.34
65	687	635	7.53	-0.23	0.57	0.06	-0.16	0.22
66	694	642	7.76	-0.23	0.56	-0.08	-0.27	0.10
67	700	649	8.00	-0.25	0.54	-0.21	-0.39	-0.02
68	706	656	8.22	-0.32	0.53	-0.37	-0.54	-0.16
69	709	660	8.41	-0.32	0.52	-0.49	-0.64	-0.26
70	710	662	8.59	-0.36	0.52	-0.59	-0.72	-0.35
71	710	664	8.77	-0.45	0.50	-0.72	-0.85	-0.46
72	710	665	8.90	-0.49	0.50	-0.79	-0.92	-0.53
73	709	665	9.03	-0.53	0.49	-0.86	-0.98	-0.59
74	708	666	9.12	-0.51	0.49	-0.88	-0.99	-0.60
75	706	666	9.21	-0.49	0.49	-0.89	-0.99	-0.61

Table A.6.2 continues

Time	Tem top	Tem.bot	Axial	End-1	End-2	Centre	Quart-1	Quart-2
76	706	666	9.30	-0.56	0.48	-0.95	-1.06	-0.65
77	705	667	9.37	-0.54	0.49	-0.95	-1.06	-0.65
78	704	667	9.45	-0.53	0.49	-0.95	-1.05	-0.65
79	703	667	9.50	-0.53	0.49	-0.96	-1.06	-0.65
80	702	668	9.55	-0.52	0.49	-0.96	-1.06	-0.65
81	702	668	9.59	-0.52	0.50	-0.96	-1.06	-0.65
82	701	668	9.64	-0.51	0.50	-0.96	-1.06	-0.65
83	700	668	9.68	-0.50	0.51	-0.96	-1.06	-0.65
84	700	668	9.71	-0.50	0.51	-0.96	-1.06	-0.65
85	699	669	9.75	-0.49	0.52	-0.96	-1.06	-0.65
86	699	669	9.77	-0.48	0.53	-0.96	-1.06	-0.65
87	699	670	9.80	-0.47	0.54	-0.96	-1.07	-0.65
88	698	670	9.83	-0.46	0.55	-0.96	-1.07	-0.65
89	698	670	9.85	-0.45	0.55	-0.96	-1.07	-0.65
90	698	671	9.87	-0.45	0.56	-0.96	-1.07	-0.65
91	698	671	9.89	-0.44	0.57	-0.96	-1.07	-0.65
92	697	671	9.90	-0.43	0.58	-0.96	-1.07	-0.65
93	697	671	9.91	-0.43	0.59	-0.96	-1.07	-0.65
94	697	671	9.92	-0.42	0.60	-0.96	-1.07	-0.65
95	697	671	9.93	-0.42	0.60	-0.96	-1.07	-0.65
96	697	672	9.94	-0.41	0.61	-0.96	-1.07	-0.65
97	697	672	9.95	-0.41	0.62	-0.96	-1.07	-0.65
98	697	672	9.96	-0.40	0.62	-0.96	-1.07	-0.65
99	697	673	9.96	-0.39	0.63	-0.96	-1.07	-0.65
100	697	673	9.96	-0.39	0.64	-0.96	-1.06	-0.65
101	697	673	9.97	-0.38	0.65	-0.96	-1.06	-0.65
102	697	673	9.97	-0.38	0.65	-0.96	-1.06	-0.65
103	696	674	9.98	-0.37	0.66	-0.96	-1.06	-0.65
104	697	674	9.98	-0.36	0.67	-0.95	-1.06	-0.64
105	697	674	9.98	-0.36	0.67	-0.95	-1.05	-0.64
106	696	674	9.99	-0.35	0.68	-0.95	-1.05	-0.64
107	696	675	9.99	-0.34	0.69	-0.95	-1.05	-0.64
108	696	675	9.99	-0.33	0.69	-0.95	-1.04	-0.64
109	696	675	9.99	-0.33	0.70	-0.94	-1.04	-0.64
110	696	673	9.99	-0.32	0.70	-0.94	-1.04	-0.63
111	696	674	9.99	-0.32	0.71	-0.94	-1.03	-0.63
112	696	674	9.99	-0.31	0.72	-0.93	-1.03	-0.63
113	696	674	9.99	-0.30	0.72	-0.93	-1.02	-0.62
114	696	674	10.00	-0.29	0.73	-0.94	-1.01	-0.61
115	696	674	10.00	-0.29	0.74	-0.93	-1.01	-0.61
116	696	675	10.00	-0.28	0.74	-0.93	-1.01	-0.61

Table A.6.2 continues

Time	Tem top	Tem.bot	Axial	End-1	End-2	Centre	Quart-1	Quart-2
117	696	675	10.00	-0.28	0.75	-0.93	-1.00	-0.60
118	696	675	10.00	-0.27	0.75	-0.93	-1.00	-0.60
119	696	675	10.00	-0.27	0.76	-0.92	-1.00	-0.60
120	696	676	10.00	-0.26	0.76	-0.92	-0.99	-0.59
121	665	645	10.00	-0.26	0.78	-0.90	-0.98	-0.56
122	639	620	9.94	-0.26	0.78	-0.87	-0.96	-0.54
123	622	574	9.60	-0.26	0.80	-0.77	-0.87	-0.42
124	590	540	9.28	-0.25	0.80	-0.63	-0.74	-0.30
125	563	512	8.90	-0.23	0.83	-0.38	-0.50	-0.05
126	539	483	8.37	-0.24	0.83	-0.30	-0.48	0.06
127	516	460	7.81	-0.33	0.75	-0.70	-0.80	-0.31
128	495	439	7.47	-0.39	0.70	-0.85	-0.92	-0.44
129	475	420	7.18	-0.43	0.65	-0.94	-1.00	-0.53
130	457	398	6.93	-0.48	0.61	-1.02	-1.07	-0.61
131	439	383	6.70	-0.52	0.58	-1.10	-1.14	-0.68
132	423	366	6.51	-0.56	0.54	-1.16	-1.20	-0.74
133	408	351	6.33	-0.60	0.50	-1.24	-1.27	-0.81
134	393	336	6.17	-0.64	0.46	-1.30	-1.33	-0.87
135	379	323	6.03	-0.67	0.42	-1.37	-1.38	-0.94
136	366	308	5.91	-0.71	0.39	-1.44	-1.43	-0.99
137	354	299	5.80	-0.75	0.35	-1.49	-1.49	-1.05
138	342	287	5.70	-0.78	0.32	-1.55	-1.56	-1.10
139	331	276	5.61	-0.81	0.29	-1.61	-1.61	-1.15
140	320	266	5.53	-0.84	0.26	-1.66	-1.66	-1.20
141	310	258	5.47	-0.87	0.23	-1.70	-1.71	-1.24
142	301	248	5.40	-0.90	0.21	-1.75	-1.75	-1.28
143	292	242	5.34	-0.93	0.18	-1.79	-1.79	-1.33
144	283	234	5.29	-0.95	0.15	-1.84	-1.83	-1.36
145	274	226	5.24	-0.97	0.13	-1.87	-1.86	-1.40
146	266	219	5.20	-1.00	0.11	-1.91	-1.90	-1.43
147	259	213	5.16	-1.02	0.09	-1.94	-1.93	-1.46
148	251	206	5.12	-1.04	0.07	-1.98	-1.96	-1.50
149	244	201	5.08	-1.05	0.05	-2.01	-1.99	-1.53
150	238	195	5.05	-1.07	0.03	-2.04	-2.02	-1.56
151	231	189	5.03	-1.09	0.02	-2.07	-2.05	-1.59
152	225	185	5.00	-1.11	0.00	-2.10	-2.08	-1.61
153	219	179	4.97	-1.12	-0.02	-2.12	-2.11	-1.64
154	213	174	4.95	-1.14	-0.03	-2.15	-2.13	-1.66
155	208	170	4.93	-1.15	-0.05	-2.17	-2.15	-1.68
156	202	166	4.91	-1.17	-0.06	-2.20	-2.17	-1.70
157	197	161	4.89	-1.18	-0.07	-2.22	-2.19	-1.72

Table A.6.2 continues

Time	Tem top	Tem.bot	Axial	End-1	End-2	Centre	Quart-1	Quart-2
158	192	157	4.88	-1.19	-0.09	-2.24	-2.21	-1.74
159	188	153	4.86	-1.21	-0.10	-2.26	-2.23	-1.76
160	183	149	4.85	-1.22	-0.11	-2.28	-2.25	-1.78
161	179	146	4.83	-1.23	-0.12	-2.30	-2.27	-1.80
162	175	142	4.82	-1.24	-0.13	-2.32	-2.28	-1.81
163	171	139	4.81	-1.25	-0.14	-2.34	-2.30	-1.83
164	166	135	4.80	-1.26	-0.15	-2.36	-2.32	-1.84
165	163	132	4.79	-1.27	-0.16	-2.37	-2.33	-1.86
166	159	129	4.78	-1.28	-0.16	-2.39	-2.34	-1.87
167	156	126	4.77	-1.29	-0.17	-2.40	-2.36	-1.88
168	152	124	4.76	-1.30	-0.18	-2.41	-2.37	-1.90
169	149	120	4.75	-1.31	-0.19	-2.43	-2.38	-1.91
170	145	118	4.75	-1.32	-0.20	-2.44	-2.40	-1.92
171	142	116	4.74	-1.33	-0.20	-2.46	-2.41	-1.94
172	139	113	4.73	-1.33	-0.21	-2.47	-2.42	-1.95
173	136	111	4.73	-1.34	-0.22	-2.48	-2.43	-1.96
174	133	108	4.72	-1.35	-0.22	-2.49	-2.44	-1.97
175	130	107	4.72	-1.35	-0.23	-2.50	-2.45	-1.98
176	127	104	4.72	-1.36	-0.23	-2.51	-2.46	-1.99
177	125	102	4.71	-1.37	-0.24	-2.52	-2.47	-2.00
178	122	100	4.71	-1.37	-0.24	-2.53	-2.48	-2.01
179	119	98	4.70	-1.38	-0.25	-2.54	-2.49	-2.01
180	117	96	4.70	-1.38	-0.25	-2.55	-2.50	-2.02
181	115	94	4.69	-1.39	-0.26	-2.55	-2.51	-2.03
182	112	92	4.69	-1.39	-0.26	-2.56	-2.52	-2.04
183	110	91	4.68	-1.40	-0.27	-2.57	-2.53	-2.04
184	108	89	4.68	-1.40	-0.27	-2.58	-2.53	-2.05
185	106	88	4.68	-1.41	-0.28	-2.59	-2.54	-2.06
186	103	86	4.67	-1.41	-0.28	-2.60	-2.55	-2.06
187	101	84	4.67	-1.42	-0.28	-2.60	-2.55	-2.07
188	100	83	4.67	-1.42	-0.29	-2.61	-2.56	-2.08
189	98	81	4.66	-1.43	-0.29	-2.62	-2.57	-2.08
190	96	80	4.66	-1.43	-0.30	-2.62	-2.57	-2.09
191	94	78	4.66	-1.43	-0.30	-2.63	-2.58	-2.09
192	92	77	4.66	-1.44	-0.30	-2.63	-2.59	-2.10
193	91	76	4.65	-1.44	-0.31	-2.64	-2.59	-2.11
194	89	75	4.65	-1.44	-0.31	-2.65	-2.60	-2.11
195	88	73	4.65	-1.45	-0.31	-2.65	-2.60	-2.12
196	86	72	4.65	-1.45	-0.32	-2.66	-2.61	-2.12
197	84	71	4.65	-1.45	-0.32	-2.66	-2.61	-2.12
198	83	70	4.65	-1.46	-0.32	-2.66	-2.62	-2.13

Table A.6.2 continues

Time	Tem top	Tem.bot	Axial	End-1	End-2	Centre	Quart-1	Quart-2
199	82	69	4.64	-1.46	-0.32	-2.67	-2.62	-2.13
200	80	67	4.64	-1.46	-0.32	-2.67	-2.63	-2.14
201	79	66	4.64	-1.46	-0.33	-2.68	-2.63	-2.14
202	77	65	4.64	-1.47	-0.33	-2.68	-2.63	-2.15
203	76	65	4.64	-1.47	-0.33	-2.69	-2.64	-2.15
204	75	63	4.63	-1.47	-0.34	-2.69	-2.64	-2.16
205	74	63	4.63	-1.47	-0.34	-2.70	-2.64	-2.16
206	71	61	4.63	-1.48	-0.34	-2.70	-2.65	-2.16
207	69	61	4.63	-1.48	-0.34	-2.70	-2.65	-2.17
208	70	60	4.63	-1.48	-0.34	-2.71	-2.66	-2.17
209	69	59	4.63	-1.48	-0.34	-2.71	-2.66	-2.17
210	68	58	4.63	-1.49	-0.35	-2.71	-2.66	-2.18
211	67	57	4.62	-1.49	-0.35	-2.72	-2.67	-2.18
212	66	57	4.62	-1.49	-0.35	-2.72	-2.67	-2.18
213	64	56	4.61	-1.49	-0.35	-2.73	-2.67	-2.19
214	64	55	4.61	-1.49	-0.35	-2.73	-2.68	-2.19
215	63	55	4.61	-1.50	-0.36	-2.73	-2.68	-2.19
216	62	54	4.61	-1.50	-0.36	-2.73	-2.68	-2.20
217	61	53	4.61	-1.50	-0.36	-2.74	-2.69	-2.20
218	60	53	4.61	-1.50	-0.36	-2.74	-2.69	-2.20
219	59	52	4.61	-1.50	-0.36	-2.74	-2.69	-2.20
220	59	51	4.61	-1.50	-0.36	-2.75	-2.69	-2.21
221	58	51	4.61	-1.51	-0.36	-2.75	-2.70	-2.21
222	57	50	4.61	-1.51	-0.37	-2.75	-2.70	-2.21
223	56	50	4.61	-1.51	-0.37	-2.75	-2.70	-2.21
224	55	49	4.60	-1.51	-0.37	-2.76	-2.70	-2.22
225	54	49	4.60	-1.51	-0.37	-2.76	-2.71	-2.22
226	54	48	4.60	-1.51	-0.37	-2.76	-2.71	-2.22
227	24	38	4.57	-1.54	-0.46	-2.80	-2.76	-2.25
228	23	36	4.57	-1.55	-0.46	-2.81	-2.77	-2.25
229	23	34	4.57	-1.55	-0.46	-2.81	-2.77	-2.25

A.6.3 Typical processed results of heating and cooling cycles for normal concrete.

Table A.6.3
NORMAL /0.5/ C1/ HEATING MEDIUM RATE
(N/0.5/C1/HM)

Time	TemTop	Tem.Bot	Axial	End1	End2	Centre	Quart1	Quart2
0	21	19	0.00	0.00	0.00	0.00	0.00	0.00
1	43	24	0.00	0.00	0.00	0.00	0.01	0.00
2	60	28	0.00	0.00	0.00	0.01	0.02	0.01
3	76	32	0.01	0.00	0.00	0.02	0.02	0.01
4	91	34	0.03	0.00	0.00	0.03	0.03	0.02
5	104	40	0.04	0.00	0.00	0.04	0.04	0.03
6	117	45	0.06	0.01	0.00	0.05	0.05	0.04
7	129	53	0.09	0.01	0.01	0.07	0.07	0.06
8	140	56	0.11	0.01	0.01	0.08	0.08	0.07
9	151	60	0.14	0.02	0.01	0.10	0.09	0.08
10	161	71	0.17	0.02	0.02	0.12	0.10	0.09
11	171	75	0.20	0.02	0.02	0.14	0.12	0.11
12	182	84	0.24	0.03	0.03	0.16	0.13	0.12
13	192	89	0.28	0.03	0.03	0.18	0.14	0.13
14	200	91	0.33	0.03	0.04	0.20	0.15	0.14
15	209	99	0.37	0.04	0.04	0.20	0.16	0.15
16	218	107	0.42	0.04	0.05	0.21	0.16	0.15
17	227	112	0.46	0.04	0.05	0.20	0.16	0.15
18	235	118	0.51	0.04	0.05	0.20	0.16	0.15
19	242	122	0.55	0.04	0.06	0.19	0.15	0.14
20	249	129	0.58	0.04	0.06	0.17	0.14	0.13
21	256	135	0.63	0.04	0.06	0.16	0.13	0.12
22	264	140	0.66	0.04	0.06	0.14	0.12	0.11
23	271	146	0.70	0.04	0.06	0.13	0.11	0.10
24	277	152	0.73	0.03	0.06	0.12	0.10	0.09
25	283	158	0.76	0.03	0.07	0.11	0.10	0.09
26	291	164	0.80	0.03	0.07	0.10	0.09	0.08
27	298	169	0.82	0.03	0.07	0.09	0.08	0.07
28	305	175	0.85	0.03	0.07	0.09	0.08	0.07
29	310	180	0.89	0.03	0.07	0.08	0.08	0.07
30	318	186	0.91	0.03	0.08	0.08	0.07	0.06
31	322	192	0.94	0.03	0.08	0.08	0.07	0.06
32	329	198	0.97	0.04	0.08	0.07	0.07	0.06
33	334	203	1.00	0.04	0.09	0.07	0.07	0.06
34	342	209	1.02	0.04	0.09	0.07	0.07	0.06

Table A.6.3 continues

Time	TemTop	Tem.Bot	Axial	End1	End2	Centre	Quart1	Quart2
35	345	214	1.05	0.04	0.09	0.08	0.08	0.07
36	352	220	1.08	0.04	0.10	0.08	0.08	0.07
37	359	225	1.11	0.04	0.10	0.08	0.08	0.07
38	366	231	1.14	0.05	0.11	0.10	0.09	0.08
39	373	237	1.17	0.05	0.12	0.11	0.10	0.09
40	379	242	1.20	0.06	0.12	0.12	0.11	0.10
41	385	247	1.23	0.06	0.13	0.14	0.12	0.11
42	391	253	1.26	0.07	0.14	0.15	0.13	0.12
43	398	260	1.30	0.08	0.14	0.16	0.14	0.13
44	405	266	1.33	0.08	0.15	0.18	0.15	0.14
45	410	271	1.36	0.09	0.16	0.19	0.17	0.16
46	416	276	1.39	0.10	0.17	0.21	0.18	0.17
47	422	282	1.43	0.11	0.18	0.22	0.19	0.18
48	428	287	1.46	0.11	0.19	0.23	0.20	0.19
49	435	292	1.49	0.12	0.20	0.25	0.21	0.20
50	442	298	1.53	0.13	0.20	0.26	0.22	0.21
51	448	305	1.56	0.13	0.21	0.28	0.23	0.22
52	455	310	1.59	0.14	0.22	0.29	0.25	0.24
53	461	316	1.63	0.15	0.23	0.31	0.26	0.25
54	467	320	1.66	0.16	0.24	0.32	0.27	0.26
55	473	325	1.69	0.16	0.25	0.34	0.29	0.28
56	479	331	1.72	0.17	0.26	0.36	0.30	0.29
57	485	335	1.75	0.18	0.27	0.37	0.32	0.31
58	491	341	1.79	0.19	0.28	0.39	0.33	0.32
59	497	346	1.82	0.20	0.29	0.41	0.35	0.34
60	503	351	1.85	0.21	0.31	0.43	0.37	0.36
61	509	355	1.89	0.22	0.32	0.45	0.39	0.38
62	515	360	1.92	0.23	0.33	0.47	0.40	0.39
63	521	364	1.96	0.24	0.33	0.49	0.42	0.41
64	527	370	1.99	0.25	0.34	0.51	0.44	0.43
65	532	375	2.02	0.26	0.35	0.53	0.45	0.44
66	538	380	2.06	0.27	0.36	0.56	0.47	0.46
67	544	385	2.09	0.28	0.38	0.58	0.49	0.48
68	550	390	2.13	0.29	0.39	0.61	0.51	0.50
69	556	392	2.17	0.30	0.40	0.63	0.54	0.53
70	562	398	2.21	0.32	0.42	0.80	0.56	0.55
71	567	402	2.25	0.33	0.43	0.83	0.59	0.58
72	573	407	2.29	0.34	0.45	0.86	0.61	0.60
73	579	410	2.34	0.36	0.46	0.88	0.63	0.62
74	585	415	2.40	0.37	0.47	0.91	0.67	0.66
75	591	420	2.46	0.38	0.49	0.93	0.69	0.68
76	596	424	2.52	0.39	0.50	0.95	0.71	0.70

Table A.6.3 continues

Time	TemTop	Tem.Bot	Axial	End1	End2	Centre	Quart1	Quart2
77	602	429	2.59	0.40	0.52	0.98	0.73	0.72
78	607	434	2.66	0.41	0.53	1.00	0.75	0.74
79	612	439	2.73	0.42	0.55	1.03	0.78	0.77
80	617	442	2.81	0.43	0.57	1.06	0.80	0.79
81	622	448	2.88	0.45	0.58	1.10	0.83	0.82
82	627	453	2.96	0.46	0.60	1.13	0.86	0.85
83	632	457	3.05	0.48	0.62	1.16	0.88	0.87
84	637	462	3.13	0.49	0.64	1.19	0.91	0.90
85	641	467	3.22	0.50	0.66	1.21	0.92	0.91
86	646	471	3.32	0.51	0.67	1.22	0.93	0.92
87	651	477	3.42	0.51	0.69	1.22	0.94	0.93
88	656	482	3.53	0.52	0.71	1.21	0.95	0.94
89	660	486	3.64	0.52	0.73	1.20	0.95	0.94
90	665	492	3.76	0.53	0.75	1.16	0.93	0.92
91	670	497	3.88	0.53	0.76	1.11	0.90	0.89
92	674	502	4.01	0.53	0.78	1.04	0.86	0.85
93	679	506	4.13	0.53	0.79	0.95	0.81	0.80
94	683	510	4.26	0.53	0.80	0.85	0.74	0.73
95	688	515	4.42	0.52	0.81	0.71	0.65	0.64
96	692	519	4.56	0.50	0.81	0.57	0.55	0.54
97	697	524	4.73	0.47	0.81	0.42	0.45	0.44
98	701	529	4.86	0.45	0.82	0.27	0.35	0.34
99	706	532	5.00	0.44	0.85	0.13	0.24	0.23
100	710	535	5.16	0.43	0.86	0.00	0.14	0.13
101	714	541	5.29	0.42	0.86	-0.15	0.03	0.02
102	718	545	5.42	0.41	0.86	-0.29	-0.08	-0.09
103	720	546	5.53	0.41	0.86	-0.42	-0.17	-0.18
104	720	545	5.66	0.40	0.86	-0.56	-0.27	-0.28
105	719	546	5.77	0.39	0.86	-0.68	-0.37	-0.38
106	718	545	5.86	0.39	0.86	-0.79	-0.45	-0.46
107	717	543	5.94	0.39	0.85	-0.89	-0.53	-0.54
108	716	543	6.02	0.39	0.85	-0.98	-0.59	-0.60
109	714	542	6.10	0.39	0.84	-1.07	-0.67	-0.68
110	713	542	6.17	0.38	0.84	-1.15	-0.73	-0.74
111	712	541	6.23	0.37	0.84	-1.22	-0.79	-0.80
112	711	541	6.29	0.37	0.84	-1.29	-0.84	-0.85
113	710	541	6.34	0.36	0.84	-1.36	-0.89	-0.90
114	708	540	6.39	0.36	0.84	-1.43	-0.95	-0.96
115	708	539	6.44	0.36	0.84	-1.51	-1.01	-1.02
116	707	540	6.49	0.35	0.83	-1.54	-1.08	-1.09
117	706	540	6.55	0.34	0.83	-1.61	-1.14	-1.15
118	706	540	6.59	0.34	0.83	-1.69	-1.20	-1.21

Table A.6.3 continues

Time	TemTop	Tem.Bot	Axial	End1	End2	Centre	Quart1	Quart2
119	705	540	6.63	0.34	0.83	-1.76	-1.26	-1.27
120	704	542	6.67	0.34	0.83	-1.82	-1.31	-1.32
121	704	543	6.71	0.34	0.83	-1.87	-1.35	-1.36
122	704	543	6.74	0.34	0.83	-1.91	-1.39	-1.40
123	704	544	6.77	0.34	0.82	-1.94	-1.42	-1.43
124	701	540	6.80	0.34	0.82	-1.97	-1.45	-1.46
125	662	512	6.80	0.34	0.82	-2.01	-1.49	-1.50
126	635	494	6.68	0.32	0.83	-1.95	-1.47	-1.48
127	613	478	6.52	0.29	0.83	-1.86	-1.42	-1.43
128	593	461	6.38	0.29	0.84	-1.71	-1.29	-1.30
129	575	447	6.07	0.30	0.83	-1.49	-1.12	-1.13
130	558	433	5.71	0.32	0.81	-1.33	-1.03	-1.04
131	543	420	5.37	0.32	0.77	-1.43	-1.14	-1.15
132	529	408	5.12	0.31	0.74	-1.46	-1.18	-1.19
133	515	395	4.92	0.30	0.71	-1.46	-1.19	-1.20
134	502	384	4.74	0.28	0.68	-1.45	-1.19	-1.20
135	490	372	4.59	0.27	0.66	-1.44	-1.19	-1.20
136	478	361	4.45	0.26	0.62	-1.44	-1.20	-1.21
137	467	352	4.33	0.24	0.60	-1.43	-1.20	-1.21
138	456	340	4.21	0.23	0.58	-1.43	-1.20	-1.21
139	445	330	4.09	0.22	0.56	-1.42	-1.20	-1.21
140	435	321	3.99	0.20	0.54	-1.42	-1.20	-1.21
141	425	313	3.90	0.19	0.52	-1.42	-1.21	-1.22
142	415	302	3.80	0.17	0.50	-1.42	-1.21	-1.22
143	406	293	3.72	0.16	0.48	-1.42	-1.22	-1.23
144	397	284	3.64	0.14	0.46	-1.42	-1.23	-1.24
145	388	278	3.56	0.13	0.44	-1.43	-1.24	-1.25
146	379	271	3.49	0.11	0.42	-1.43	-1.25	-1.26
147	371	263	3.42	0.10	0.40	-1.44	-1.26	-1.27
148	363	256	3.36	0.08	0.38	-1.45	-1.27	-1.28
149	355	247	3.31	0.07	0.36	-1.46	-1.28	-1.29
150	347	242	3.24	0.06	0.35	-1.46	-1.29	-1.30
151	340	235	3.19	0.04	0.33	-1.47	-1.30	-1.31
152	333	230	3.14	0.03	0.32	-1.48	-1.31	-1.32
153	326	224	3.10	0.02	0.30	-1.49	-1.32	-1.33
154	319	219	3.05	0.00	0.29	-1.49	-1.33	-1.34
155	313	213	3.01	-0.01	0.28	-1.50	-1.34	-1.35
156	306	208	2.97	-0.02	0.26	-1.51	-1.35	-1.36
157	300	202	2.93	-0.03	0.25	-1.52	-1.36	-1.37
158	294	197	2.89	-0.05	0.24	-1.53	-1.37	-1.38
159	288	193	2.85	-0.06	0.22	-1.55	-1.38	-1.39
160	282	188	2.82	-0.07	0.21	-1.56	-1.39	-1.40

Table A.6.3 continues

Time	TemTop	Tem.Bot	Axial	End1	End2	Centre	Quart1	Quart2
161	277	185	2.79	-0.08	0.20	-1.57	-1.40	-1.41
162	271	180	2.76	-0.10	0.19	-1.58	-1.41	-1.42
163	266	176	2.72	-0.11	0.18	-1.59	-1.43	-1.44
164	261	171	2.70	-0.12	0.17	-1.60	-1.44	-1.45
165	256	168	2.67	-0.13	0.16	-1.61	-1.45	-1.46
166	251	164	2.64	-0.14	0.15	-1.62	-1.46	-1.47
167	246	160	2.61	-0.15	0.14	-1.63	-1.47	-1.48
168	241	158	2.59	-0.16	0.13	-1.64	-1.48	-1.49
169	236	154	2.57	-0.17	0.12	-1.65	-1.49	-1.50
170	232	151	2.54	-0.18	0.11	-1.66	-1.50	-1.51
171	228	148	2.52	-0.19	0.10	-1.67	-1.51	-1.52
172	223	145	2.50	-0.20	0.09	-1.68	-1.52	-1.53
173	219	143	2.48	-0.20	0.09	-1.69	-1.53	-1.54
174	215	140	2.46	-0.21	0.08	-1.70	-1.54	-1.55
175	211	138	2.44	-0.22	0.07	-1.70	-1.55	-1.56
176	207	135	2.42	-0.23	0.07	-1.71	-1.55	-1.56
177	204	132	2.41	-0.24	0.06	-1.72	-1.56	-1.57
178	200	130	2.39	-0.24	0.05	-1.73	-1.57	-1.58
179	196	128	2.37	-0.25	0.05	-1.74	-1.58	-1.59
180	193	125	2.36	-0.26	0.04	-1.74	-1.58	-1.59
181	189	123	2.32	-0.26	0.04	-1.75	-1.59	-1.60
182	186	121	2.30	-0.27	0.03	-1.76	-1.60	-1.61
183	183	118	2.29	-0.28	0.02	-1.77	-1.61	-1.62
184	180	116	2.28	-0.28	0.02	-1.77	-1.61	-1.62
185	176	113	2.26	-0.29	0.01	-1.78	-1.62	-1.63
186	173	112	2.25	-0.29	0.01	-1.79	-1.63	-1.64
187	170	110	2.24	-0.30	0.00	-1.79	-1.63	-1.64
188	167	107	2.23	-0.30	0.00	-1.80	-1.64	-1.65
189	164	107	2.22	-0.31	-0.01	-1.81	-1.65	-1.66
190	162	104	2.21	-0.31	-0.01	-1.81	-1.65	-1.66
191	159	101	2.20	-0.32	-0.02	-1.82	-1.66	-1.67
192	156	101	2.18	-0.32	-0.02	-1.83	-1.66	-1.67
193	153	100	2.17	-0.33	-0.03	-1.83	-1.67	-1.68
194	151	98	2.16	-0.33	-0.03	-1.84	-1.67	-1.68
195	148	96	2.15	-0.34	-0.03	-1.84	-1.68	-1.69
196	146	95	2.15	-0.34	-0.04	-1.85	-1.68	-1.69
197	143	93	2.14	-0.35	-0.04	-1.85	-1.69	-1.70
198	141	92	2.13	-0.35	-0.04	-1.86	-1.69	-1.70
199	139	90	2.12	-0.35	-0.05	-1.87	-1.70	-1.71
200	136	89	2.11	-0.36	-0.05	-1.87	-1.70	-1.71
201	134	86	2.11	-0.36	-0.05	-1.88	-1.71	-1.72
202	132	86	2.10	-0.36	-0.06	-1.88	-1.71	-1.72

Table A.6.3 continues

Time	TemTop	Tem.Bot	Axial	End1	End2	Centre	Quart1	Quart2
203	130	84	2.09	-0.37	-0.06	-1.89	-1.72	-1.73
204	128	85	2.08	-0.37	-0.06	-1.89	-1.72	-1.73
205	126	82	2.08	-0.37	-0.06	-1.89	-1.73	-1.74
206	124	80	2.07	-0.38	-0.07	-1.90	-1.73	-1.74
207	122	80	2.07	-0.38	-0.07	-1.90	-1.73	-1.74
208	120	76	2.06	-0.39	-0.07	-1.91	-1.74	-1.75
209	118	77	2.05	-0.39	-0.08	-1.91	-1.74	-1.75
210	116	76	2.05	-0.39	-0.08	-1.91	-1.75	-1.76
211	114	75	2.04	-0.40	-0.08	-1.92	-1.75	-1.76
212	112	73	2.04	-0.40	-0.08	-1.92	-1.76	-1.77
213	110	73	2.03	-0.40	-0.09	-1.93	-1.76	-1.77
214	109	72	2.03	-0.40	-0.09	-1.93	-1.76	-1.77
215	107	68	2.02	-0.41	-0.09	-1.94	-1.76	-1.77
216	105	71	2.02	-0.41	-0.09	-1.94	-1.77	-1.78
217	104	68	2.01	-0.41	-0.09	-1.94	-1.77	-1.78
218	102	66	2.01	-0.41	-0.10	-1.94	-1.77	-1.78
219	101	65	2.01	-0.42	-0.10	-1.95	-1.78	-1.79
220	99	66	2.00	-0.42	-0.10	-1.95	-1.78	-1.79
221	98	61	2.00	-0.42	-0.10	-1.96	-1.78	-1.79
222	96	66	1.99	-0.42	-0.10	-1.96	-1.79	-1.80
223	95	63	1.99	-0.42	-0.11	-1.96	-1.79	-1.80
224	94	62	1.98	-0.43	-0.11	-1.97	-1.79	-1.80
225	92	62	1.98	-0.43	-0.11	-1.97	-1.79	-1.80
226	91	63	1.98	-0.43	-0.11	-1.97	-1.80	-1.81
227	90	61	1.97	-0.44	-0.12	-1.98	-1.80	-1.81
228	88	59	1.97	-0.44	-0.12	-1.98	-1.80	-1.81
229	87	59	1.97	-0.44	-0.12	-1.98	-1.80	-1.81
230	86	58	1.96	-0.44	-0.12	-1.98	-1.81	-1.82
231	85	57	1.96	-0.44	-0.12	-1.99	-1.81	-1.82
232	84	56	1.96	-0.44	-0.12	-1.99	-1.81	-1.82
233	82	57	1.96	-0.45	-0.12	-1.99	-1.81	-1.82
234	81	56	1.95	-0.45	-0.12	-1.99	-1.82	-1.83
235	80	56	1.95	-0.45	-0.12	-2.00	-1.82	-1.83
236	79	52	1.94	-0.45	-0.13	-2.00	-1.82	-1.83
237	78	55	1.94	-0.45	-0.13	-2.00	-1.82	-1.83
238	77	54	1.94	-0.45	-0.13	-2.01	-1.83	-1.84
239	76	53	1.94	-0.46	-0.13	-2.01	-1.83	-1.84
240	75	53	1.93	-0.46	-0.13	-2.01	-1.83	-1.84
241	74	50	1.93	-0.46	-0.13	-2.01	-1.83	-1.84
242	73	53	1.92	-0.46	-0.14	-2.02	-1.83	-1.84
243	73	51	1.92	-0.46	-0.14	-2.02	-1.84	-1.85
244	72	51	1.92	-0.46	-0.14	-2.02	-1.84	-1.85

Table A.6.3 continues

Time	TemTop	Tem.Bot	Axial	End1	End2	Centre	Quart1	Quart2
245	71	51	1.92	-0.46	-0.14	-2.02	-1.84	-1.85
246	70	49	1.92	-0.47	-0.14	-2.03	-1.84	-1.85
247	69	49	1.91	-0.47	-0.14	-2.03	-1.84	-1.85
248	68	50	1.91	-0.47	-0.14	-2.03	-1.84	-1.85
249	68	48	1.91	-0.47	-0.14	-2.03	-1.85	-1.86
250	67	47	1.90	-0.47	-0.15	-2.04	-1.85	-1.86
251	66	46	1.90	-0.47	-0.15	-2.04	-1.85	-1.86
252	65	46	1.90	-0.48	-0.15	-2.04	-1.85	-1.86
253	65	45	1.90	-0.48	-0.15	-2.04	-1.85	-1.86
254	64	45	1.90	-0.48	-0.15	-2.04	-1.85	-1.86
255	63	45	1.89	-0.48	-0.15	-2.04	-1.86	-1.87
256	62	41	1.89	-0.48	-0.15	-2.05	-1.86	-1.87
257	62	42	1.89	-0.48	-0.15	-2.05	-1.86	-1.87
258	61	43	1.89	-0.48	-0.15	-2.05	-1.86	-1.87
259	60	42	1.89	-0.48	-0.15	-2.05	-1.86	-1.87
260	60	41	1.89	-0.48	-0.15	-2.05	-1.86	-1.87
261	59	42	1.88	-0.48	-0.15	-2.05	-1.86	-1.87
262	58	42	1.88	-0.49	-0.16	-2.06	-1.87	-1.88
263	58	41	1.88	-0.49	-0.16	-2.06	-1.87	-1.88
264	57	41	1.88	-0.49	-0.16	-2.06	-1.87	-1.88
265	57	40	1.88	-0.49	-0.16	-2.06	-1.87	-1.88
266	56	42	1.88	-0.49	-0.16	-2.06	-1.87	-1.88

Appendix B.1

Format of the Orion data file from PC data logger.

```
02.12.98.M5L       S T 1 00:48:33.6

:                  C 001-04.9583  Vdc    :        C 002-03.7756  Vdc
:                  C 003-02.3521  Vdc    :        C 004-03.9973  Vdc
:                  C 005-02.5211  Vdc    :        C 006-07.4278  Vdc
:                  C 007-03.8236  Vdc    :        C 008 0.0247804Vdc
:                  C 009 0016.11  dgC    :        C 010 0016.50  dgC
                      D T 1

02.12.98.M5L       S T 1 00:49:33.6

:                  C 001-04.9583  Vdc    :        C 002-03.7756  Vdc
:                  C 003-02.3521  Vdc    :        C 004-03.9972  Vdc
:                  C 005-02.5210  Vdc    :        C 006-07.4277  Vdc
:                  C 007-03.8235  Vdc    :        C 008 0.0247805Vdc
:                  C 009 0016.74  dgC    :        C 010 0026.22  dgC
                      D T 1

02.12.98.M5L       S T 1 00:50:33.6

:                  C 001-04.9582  Vdc    :        C 002-03.7756  Vdc
:                  C 003-02.3518  Vdc    :        C 004-03.9971  Vdc
:                  C 005-02.5210  Vdc    :        C 006-07.4276  Vdc
:                  C 007-03.8235  Vdc    :        C 008 0.0247808Vdc
:                  C 009 0019.99  dgC    :        C 010 0037.54  dgC
                      D T 1

02.12.98.M5L       S T 1 00:51:33.6

:                  C 001-04.9582  Vdc    :        C 002-03.7756  Vdc
:                  C 003-02.3512  Vdc    :        C 004-03.9968  Vdc
:                  C 005-02.5209  Vdc    :        C 006-07.4275  Vdc
:                  C 007-03.8242  Vdc    :        C 008 0.0247797Vdc
:                  C 009 0024.08  dgC    :        C 010 0045.08  dgC
                      D T 1

02.12.98.M5L       S T 1 00:52:33.6

:                  C 001-04.9581  Vdc    :        C 002-03.7757  Vdc
:                  C 003-02.3504  Vdc    :        C 004-03.9961  Vdc
:                  C 005-02.5146  Vdc    :        C 006-07.4275  Vdc
:                  C 007-03.8259  Vdc    :        C 008 0.0247784Vdc
:                  C 009 0027.89  dgC    :        C 010 0051.14  dgC
                      D T 1
```

```
02.12.98.M5L        S T 1 00:53:33.6

:                   C 001-04.9582  Vdc  :        C 002-03.7757  Vdc
:                   C 003-02.3495  Vdc  :        C 004-03.9948  Vdc
:                   C 005-02.5136  Vdc  :        C 006-07.4273  Vdc
:                   C 007-03.8289  Vdc  :        C 008 0.0247790Vdc
:                   C 009 0032.34  dgC  :        C 010 0059.18  dgC
                      D T 1

02.12.98.M5L        S T 1 00:54:33.6

:                   C 001-04.9582  Vdc  :        C 002-03.7757  Vdc
:                   C 003-02.3485  Vdc  :        C 004-03.9935  Vdc
:                   C 005-02.5127  Vdc  :        C 006-07.4273  Vdc
:                   C 007-03.8318  Vdc  :        C 008 0.0247786Vdc
:                   C 009 0036.93  dgC  :        C 010 0067.06  dgC
                      D T 1

02.12.98.M5L        S T 1 00:55:33.6

:                   C 001-04.9584  Vdc  :        C 002-03.7756  Vdc
:                   C 003-02.3475  Vdc  :        C 004-03.9924  Vdc
:                   C 005-02.5116  Vdc  :        C 006-07.4272  Vdc
:                   C 007-03.8357  Vdc  :        C 008 0.0247786Vdc
:                   C 009 0040.99  dgC  :        C 010 0074.34  dgC
                      D T 1

02.12.98.M5L        S T 1 00:56:33.6

:                   C 001-04.9593  Vdc  :        C 002-03.7756  Vdc
:                   C 003-02.3466  Vdc  :        C 004-03.9913  Vdc
:                   C 005-02.5106  Vdc  :        C 006-07.4272  Vdc
:                   C 007-03.8403  Vdc  :        C 008 0.0247788Vdc
:                   C 009 0045.05  dgC  :        C 010 0081.13  dgC
                      D T 1

02.12.98.M5L        S T 1 00:57:33.6

:                   C 001-04.9606  Vdc  :        C 002-03.7758  Vdc
:                   C 003-02.3458  Vdc  :        C 004-03.9906  Vdc
:                   C 005-02.5098  Vdc  :        C 006-07.4274  Vdc
:                   C 007-03.8453  Vdc  :        C 008 0.0247791Vdc
:                   C 009 0049.31  dgC  :        C 010 0086.30  dgC
                      D T 1

  02.12.98.M5L        S T 1 00:58:33.6

:                   C 001-04.9615  Vdc  :        C 002-03.7755  Vdc
:                   C 003-02.3446  Vdc  :        C 004-03.9893  Vdc
:                   C 005-02.5086  Vdc  :        C 006-07.4270  Vdc
:                   C 007-03.8506  Vdc  :        C 008 0.0247782Vdc
:                   C 009 0052.91  dgC  :        C 010 0091.88  dgC
                      D T 1
```

Appendix B.2

Program to read Orion Data files and write in ascii form

```
c       Program to read Orion Data files and write in ascii form
c

character*80 tmp

dimension it(50)

dimension t(50)
c       read no of data sets avaialble

read (*,*) n

write (*,*) n

do 10 i=1,n

read(*,*) tmp

read(*,*)

read(*,l)(tmp,it(j),t(j),tmpj=1,4)

read(*,l)(tmp,itO),t(J),tmpJ=5,8)

read(*,l)(tmp,it(j),tCJ),tmp,j=9,12)

read(*,l)(tmp,it(j),t(j),tmp,j=13,16)

read(*,l)(tmp,it(j),t(J),tmp,j=17,20)

read(*,l)(tmp.itCJ),t(j),tmp,j=21,24)

read(*,l)(tmp.it(j),t0),tmp,j=25,28)

read(*,l)(tmp,it(j),t(J),tmp,j=29,32)

read(*,2)(tmp,it(J),t(J),tmp,j=33,34)

read(*,*)

read(*.*)tmp
```

```
readC*,*)

k=i

write(*,3)k,(t(J)J=1,34)
10      continue

write(*,*)

1       format(8(a2,i3,f8.2,a7))

2       format(2(a2,i3,f8.2,a7))

3       format(i4,34(f5.0))
stop
end
```

Appendix B.3

Program to read ascii file created by dread and convert them the data to displacements and temperatures

```
c      Program to read ascii file created by dread and convert them
c      the data to displacements and temperatures
c
c
c      character*80 ttl
       dimension di (10),d(10),cf(10)
c      Conversion Factors
       cf(1)=1.0/0.3998
       cf(2)=1.0/0.3998
       cf(3)=1.0/0.20327
       cf(4)=1.0/0.2029
       cf(5)=1.0/0.2031
       cf(6)=1.0/0.4108
       cf(7)=1.0/0.4108
c      Write Headers
       ttl='Time   Axial   Quart-1   Center   Quart-2   Tem1   Tem2'
       write (*,2) ttl
c      read no of data sets available
       read (*,*)  n
c      read initial data
       read (*,*)k,(di(j),J=1,10)
c      Write Initial Data
       kk=k-1
       axd=0.0
       qpd1=0.0
       qpd2=0.0
       cntd=0.0
       tmp1=di(9)
       tmp2=di(10)
       write (*,1)kk, axd, qpd1,cntd,qpd2,tmp1,tmp2
       do 10 I=2,n
c      read data
       read(*,*)k,(d(j),j=1,10)
c      Convert data
       do 20 j=1,7
       d(j)=(d(j)-di(j))*cf(j)
   20  continue
       kk=k-1
       axd=-(d(1)=d(7))
       qpd1=d(3)
```

```
        qpd2=d(5)
        cntd=d(4)
        tmp1=d(9)
        tmp2=d(10)
        write(*,1)kk,axd,qpd1,cntd,qpd2,tmp1,tmp2

   10  continue
   1    format (i4,1x,4(f8.3,2x),f5.0,2x,f5.0)
   2    format (a80)
        write (*,*)
        write (*,*)
        write (*,*) 'SIGN CONVENTION'
        write (*,*)
        write (*,*) 'Axial Deflection =      +Expansion'
        write (*,*) 'Lateral Deflection =       +Upwards
c12345678901234567890123456789012345678901234567890123456789012345 67
        stop
        end
```

Appendix B.4

Moisture model program to calculate the pressure.

```
C
***************************************************************
************
C      FEM2 -----   TWO DIMENSIONAL HEAT AND WATER CONDUCTION ANALYZER
C                   BY FINITE ELEMENT METHOD.
C
C         ORIGINALLY CODED BY K.HARADA              1985/10/15
C                      REVISED                      1989/10/01
C                      REVISED BY F.ARITA & K.HARADA   2001/ 1/31
***************************************************************
************
        IMPLICIT REAL*4 (A-H,O-Z)
        PARAMETER (NNDE= 1000 , NNEL=  1000)
        DIMENSION X(NNDE) , Y(NNDE) , TEMP(NNDE)
        DIMENSION PRES(NNDE) , PRESV(NNDE) ,PRESA(NNDE)
        DIMENSION TOLD(NNDE) , GENM(NNDE) , RLH(NNDE) , DTDT(NNDE)
        DIMENSION WCONT(NNDE), PVSAT(NNDE)
        DIMENSION NBC(NNEL) , IBC(NNEL) , MCODE(NNEL) , LM(NNEL,3)
        DIMENSION WMAT(NNDE,NNDE) , FVEC(NNDE)
        DIMENSION WEQ(NNDE), WEQDPV(NNDE), EVV(NNDE)
        PARAMETER (PATM = 101325.)
        PARAMETER (NR   = 11)
        PARAMETER (NFT = 26, NFP  = 27, NFPV = 28, NFWC = 29)
        PARAMETER (IBUG = 0, IPAUSE = 0)
C
C       (ASSIGN FILE UNIT)
        open(unit=nr,  file='input.prn')
        open(unit=nft, file='value-t.txt')
        open(unit=nfp, file='value-p.txt')
        open(unit=nfpv,file='value-pv.txt')
        open(unit=nfwc,file='value-wc.txt')
C
C       (SIGN ON MESSAGE)
        CALL SIGNON
C
C       (READ INITIAL VALUE)
        CALL RDDATA(NR,X,Y,TEMP,WCONT
       +            ,MCODE,LM,NBC,IBC,DELT,NSTP,NOUT
       +            ,NUMNP,NNDE,NUMEL,NNEL)
C
C       (SET INITIAL VALUE)
        CALL VERPAS(TEMP,NUMNP   ,  Pvsat)
C
        PRES  = PATM
        PRESV = PVSAT
        PRESA = PATM - PRESV
        TOLD = TEMP
        ISTP = 0
        IOUT = 0
```

```
C
      CALL WRFILE ( TEMP,NFT, NUMNP,NNDE,DELT,ISTP)
      CALL WRFILE ( PRES,NFP, NUMNP,NNDE,DELT,ISTP)
      CALL WRFILE (PRESV,NFPV,NUMNP,NNDE,DELT,ISTP)
      CALL WRFILE (WCONT,NFWC,NUMNP,NNDE,DELT,ISTP)
C
C     ..... START OF CALCULATION .....
 7777 ISTP = ISTP + 1
      IOUT = IOUT + 1
C
C     (CALCULATE NODAL PARAMETERS)
      CALL DELTT(TOLD,TEMP,DELT,NUMNP , DTDT)
      CALL VERPAS(TEMP,NUMNP , PVSAT)
      CALL EQUILW(TEMP,PRESV,PVSAT,NUMNP , WEQ,WEQDPV)
      CALL EVAP(WCONT,WEQ,WEQDPV,DELT,NUMNP , GENM,EVV)
      CALL LATENT(TEMP,NUMNP  , RLH)
      WRITE(*,*) '...... step =',istp,' .....'
C
C     (MAKE SIMULTANEOUS EQUATIONS FOR
TEMPERATURE).....................
      CALL MKEQST(X,Y,TEMP,GENM,RLH
     *            ,NBC,IBC,MCODE,LM
     *            ,NUMNP,NNDE,NUMEL,NNEL,DELT,ISTP
     *            ,WMAT,FVEC)
C
      IF (IBUG .EQ. 1) THEN
        WRITE(*,9201)  ISTP
      END IF
 9201 FORMAT(//,'  ISTP =',I9)
 9202 FORMAT(' ',6(1PE10.3,1X),1X,1PE10.3)
C
C     (UPDATE TEMPERATURE)
      CALL SWEEP(WMAT,FVEC,NUMNP,NNDE,ICON)
      CALL CHKERR(ICON,ISTP,'TEMPERATURE   ')
      TOLD = TEMP
      TEMP = FVEC
C
C     (MAKE SIMULTANEOUS EQUATIONS FOR VAPOR
PRESSURE)..................
      CALL DELTT(TOLD,TEMP,DELT,NUMNP , DTDT)
      CALL VERPAS(TEMP,NUMNP , PVSAT)
      CALL EQUILW(TEMP,PRESV,PVSAT,NUMNP , WEQ,WEQDPV)
      CALL EVAP(WCONT,WEQ,WEQDPV,DELT,NUMNP , GENM,EVV)

C
      CALL MKEQSV(X,Y,TEMP,DTDT,PRES,PRESV,WCONT,GENM,EVV
     *            ,NBC,IBC,MCODE,LM,NUMNP,NNDE
     *            ,NUMEL,NNEL,DELT,ISTP
     *            ,WMAT,FVEC)
C
C     (SOLVE SIMULTANEOUS EQUATIONS(PRESV))
      CALL SWEEP(WMAT,FVEC,NUMNP,NNDE,ICON)
      CALL CHKERR(ICON,ISTP,'VAPOR PRESSURE')
      PRESV = FVEC
      DO I = 1,NUMNP
```

```
          IF (PRESV(I).LE.0.0) PRESV =0.0
          ENDDO
C
C     (MAKE SIMULTANEOUS EQUATIONS FOR AIR
PRESSURE).....................
          CALL MKEQSA(X,Y,TEMP,DTDT,PRES,PRESA,WCONT
     *            ,NBC,IBC,MCODE,LM
     *            ,NUMNP,NNDE,NUMEL,NNEL,DELT,ISTP
     *            ,WMAT,FVEC)
C
C     (SOLVE SIMULTANEOUS EQUATIONS(PRESA))
          CALL SWEEP(WMAT,FVEC,NUMNP,NNDE,ICON)
          CALL CHKERR(ICON,ISTP,'AIR PRESSURE  ')
          PRESA = FVEC
          DO I = 1,NUMNP
          IF (PRESA(I).LE.0.0) PRESA =0.0
          ENDDO
          PRES = PRESV + PRESA
C
C     (UPDATE WATER CONTENT)
          CALL EQUILW(TEMP,PRESV,PVSAT,NUMNP , WEQ,WEQDPV)
          CALL EVAP(WCONT,WEQ,WEQDPV,DELT,NUMNP , GENM,EVV)
          CALL WATER(GENM,NUMNP,DELT , WCONT)
C
C     (OUTPUT)
          IF (IOUT .GE. NOUT) THEN
            IOUT=0
C
            CALL WRFILE( TEMP,NFT, NUMNP,NNDE,DELT,ISTP)
            CALL WRFILE( PRES,NFP, NUMNP,NNDE,DELT,ISTP)
            CALL WRFILE(PRESV,NFPV,NUMNP,NNDE,DELT,ISTP)
            CALL WRFILE(WCONT,NFWC,NUMNP,NNDE,DELT,ISTP)
            CALL WRFILE(genm,61,NUMNP,NNDE,DELT,ISTP)
            CALL WRFILE(dtdt,62,NUMNP,NNDE,DELT,ISTP)
          END IF
C
      IF (IPAUSE .EQ. 1) pause
      IF (ISTP .LT. NSTP) GO TO 7777
C
      STOP
      END
C
C
*****************************************************************
**
      SUBROUTINE CONDUC(T,MC   ,  RAMDA)
C
*****************************************************************
**
      IMPLICIT REAL*4 (A-H,O-Z)
C
      DUMMY = T
      IF (MC .EQ. 1) THEN
*                                  (CONCRETE)
          if(T.le.500) then
```

```fortran
      RAMDA = 1.5-(0.5/500)*T
      else
      RAMDA = 1.25-(0.15/300)*T
      end if
      if (RAMDA.le.0.85) RAMDA = 0.85

      call dens(rho)
      frac = ((1.7/1000)*rho - 2.5)/1.5
      ramda = ramda * frac
*
      else if (MC .eq. 2) then
*                               (CONCRETE/upper bound)
      RAMDA = 1.5-(0.5/800)*T
      if (ramda .lt. 1.0) ramda=1.0
      ramda = ramda*1.3
      else if (MC .eq. 3) then
*                               (CONCRETE/lower bound)
      RAMDA = 1.5-(0.5/800)*T
      if (ramda .lt. 1.0) ramda=1.0
      ramda = ramda*0.7
      else if (MC .eq. 4) then
*                               (LW.CONCRETE/lower bound)
      RAMDA = 1.0-(0.6/800)*T
      if (ramda .lt. 0.6) ramda=0.6
      ELSE IF (MC .EQ. 9) THEN
C     (AIR GAP : H=8W/M2.K , D=0.05)
      RAMDA = 8.0*0.05
      ELSE
      WRITE(*,9001) MC
      WRITE(*,*) '+++ INPUT DATA ERROR +++'
      STOP
      END IF
      RETURN
C
 9001 FORMAT(//
     *        ,' ** ERROR IN CONDUC ROUTINE **',/
     *        ,' UNDEFINED MATERIAL CODE ',I8,' IS DETECTED.',/
     *        ,' STOP -- PROGRAM ABORT.')
      END
C
********************************************************************
**
      SUBROUTINE VCAPA(T,MC  ,  ROUC)
C
C     DEFINE VOLUMETRIC HEAT CAPARITY (ROU*C) OF MATERIALS
C
C     [INPUT]    T         TEMPERATURE          (C)
C     [INPUT]    MC        MATERIAL CODE
C                              1 ...... PMMA
C                              2 ...... PLOY VINYL CLORIDE
C                              3 ...... PLOY STYLEN
C                              4 ...... PLOY ETHILEN
C                              5 ...... PLASTER BOARD
C     [OUTPUT]   ROUC      VOLUMETRIC HEAT CAPACITY      (J/M3.K)
```

```
C
* * * * * * * * * * * * * * * * * * * * * * * * * * * * * * * * * * * * * * * * * * * * * * * * * * * * * * * * * * * * * * * * * * * * *
* *
      IMPLICIT REAL*4 (A-H,O-Z)
C
      DUMMY = T
      CALL DENS(RHO)
C
      IF (MC .LE. 4) THEN
C       (concete/normal/average)
         ROUC = rho*930
      ELSE IF (MC .EQ. 9) THEN
C       (AIR GAP)
         ROUC =  0.0
      ELSE
         WRITE(*,9001) MC
         WRITE(*,*) '+++ INPUT DATA ERROR +++'
         STOP
      END IF
      RETURN
 9001 FORMAT(' (VCAPA) UNDEFINED MATERIAL CODE ',I8,'.')
      END
*.........................(end of configuration
section)..............
C
C
* * * * * * * * * * * * * * * * * * * * * * * * * * * * * * * * * * * * * * * * * * * * * * * * * * * * * * * * * * * * * * * * * * * * * * * * * * * * * * *
* * * * * * * * * * * * *
      SUBROUTINE MKEQST(X,Y,TEMP,GENM,RLH
     *                 ,NBC,IBC,MCODE,LM
     *                 ,NUMNP,NNDE,NUMEL,NNEL,DELT,ISTP
     *                 ,WMAT,FVEC)
C
C      MAKE SIMULTANEOUS EQUATIONS
C
C     [INPUT]     X(*)           X COORDINATE OF THE NODAL POINTS
C     [INPUT]     Y(*)           Y COORDINATE OF THE NODAL POINTS
C     [INPUT]     TEMP(*)        TEMPERATURE OF THE NODAL POINTS [C]
C     [INPUT]     PRES(*)        VOID PRESSURE OF THE NODAL POINTS
[ATM]
C     [INPUT]     GENM(*)        GENETARION OF VAPORIZING WATER
[KG/M3*S]
C     [INPUT]     RLH(*)         LATENT HEAT [J/KG]
C     [INPUT]     NBC(*)         LOCATION OF EXTERNAL BOUNDARY
C     [INPUT]     IBC(*)         BOUNDARY CONDITION CODE
C     [INPUT]     MCODE(*)       MATERIAL CODE
C     [INPUT]     LM(*,*)        NODE ELEMENT ALLOCATION TABLE
C     [INPUT]     NUMNP          NUMBER OF NODES
C     [INPUT]     NNDE           SIZE OF THE ARRAYS X(*),Y(*),TEMP(*)
ETC.
C     [INPUT]     NUMEL          NUMBER OF ELEMENTS
C     [INPUT]     NNEL           SIZE OF THE ARRAY LM(*)
C     [INPUT]     DELT           TIME INCREMENT
C     [INPUT]     ISTP           TIME INCREMENT
```

```
C      [OUTPUT]    WMAT(*,*)     COEFFICIENT MATRIX OF THE WHOLE
EQUATIONS
C      [OUTPUT]    FVEC(*)       R.H.S. VECTOR OF THE WHOLE EQUATIONS
C
*****************************************************************
*************
       DIMENSION X(NUMNP) ,Y(NUMNP) ,TEMP(NUMNP)
       DIMENSION GENM(NUMNP), RLH(NUMNP)
       DIMENSION NBC(NNEL), IBC(NNEL) , MCODE(NNEL) , LM(NNEL,3)
       DIMENSION WMAT(NNDE,NNDE), FVEC(NUMNP)
C      (LOCAL VARIABLES)
       DIMENSION XE(3), YE(3), TE(3), GENME(3), RLHE(3)
       DIMENSION BMT(3,3) , CMT(3,3) , GMTM(3,3)
       DIMENSION WM(3,3) , FV(3)
C
C      (CLEAR ARRAYS)
       FVEC = 0.0
       CALL CLEAR2D(WMAT,NNDE,NUMNP)
C
       DO NEL = 1 , NUMEL
C        (CLEAR LOCAL ARRAYS)
         FV = 0.0
         CALL CLEAR2D(WM,3,3)
C
C        (MAKE ELEMENT EQUATIONS)
         DO I = 1 , 3
           IX = LM(NEL,I)
           XE(   I) = X(   IX)
           YE(   I) = Y(   IX)
           TE(   I) = TEMP(IX)
           GENME(I) = GENM(IX)
             RLHE( I) = RLH( IX)
         ENDDO
         MC = MCODE(NEL)
         NB = NBC(NEL)
         IB = IBC(NEL)
         CALL ELCALT(NEL,XE,YE,TE,GENME,RLHE,MC,NB,IB,DELT,ISTP
     *              ,WM,FV)
C
C        (PUT ELEMENT EQUATIOS INTO WHOLE EQUATIONS)
         CALL BUILD(NEL,LM,WM,FV,NNDE,NNEL   ,  WMAT,FVEC)
       ENDDO
C
       RETURN
       END
C
C
*****************************************************************
*******
       SUBROUTINE ELCALT(NEL,XE,YE,TE,GENME,RLHE
     *                  ,MC,NB,IB,DELT,ISTP
     *                  ,WM,FV)
C
C      MAKE ELEMENT EQUATIONS
C      [INPUT]         NEL              ELEMENT NUMBER
```

```
C       [INPUT]           XE(*)         X-COORDINATES OF NODES IN THE
ELEMENT
C       [INPUT]           YE(*)         Y-COORDINATES OF NODES IN THE
ELEMENT
C       [INPUT]           TE(*)         TEMPERATURE AT THE NODES IN THE
ELEMENT
C       [INPUT]           DTDTE(*)      TIME DERIVERTIVE
C       [INPUT]           GENME(*)      GENETARION OF VAPORIZING WATER
(KG/M3*S)
C       [INPUT]           RLH(*)           LATENT HEAT (J/KG)
C       [INPUT]           NB               EXTERNAL BOUNDARY POSITION
C       [INPUT]           IB               BOUNDARY CONDITION CODE
C       [INPUT]           MC               MATERIAL CODE OF THE
ELEMENT
C       [INPUT]           DELT          TIME INCREMENT (s)
C       [INPUT]           ISTP          TIME INDEX
C       [OUTPUT]   WM(*,*)              COEFFICIENT MATRIX OF THE
ELEMENT EQ.
C       [OUTPUT]   FV(*)         R.H.S. VECTOR OF THE ELEMENT EQ.
C
******************************************************************
*******
        DIMENSION XE(3), YE(3), TE(3), GENME(3), RLHE(3)
        DIMENSION WM(3,3), FV(3)
C     (LOCAL VARIABLES)
        DIMENSION BMT(3,3) , CMT(3,3) , GMTM(3,3)
C
C     (CONDUCTIVITY/CAPACITY MATRIX)
        CALL ELMATT(NEL,XE,YE,TE,MC   ,   CMT,BMT,GMTM)
C
C     (ADD SOURCE TERM TO R.H.S VECTOR)
        CALL ADDGENT(GENME,RLHE,GMTM   ,   FV)
C
C     (ADD BOUNDARY CONDITION TO BM)
        CALL FINDBC(NB,NB1,NB2,NB3)
        CALL FINDBC(IB,IB1,IB2,IB3)
C
        TIME = DELT*ISTP
        IF (NB1 .EQ. 1) THEN
          CALL ADDBCT(1,2,XE,YE,TIME,IB1   ,   BMT,FV)
        END IF
        IF (NB2 .EQ. 1) THEN
          CALL ADDBCT(2,3,XE,YE,TIME,IB2   ,   BMT,FV)
        END IF
        IF (NB3 .EQ. 1) THEN
          CALL ADDBCT(3,1,XE,YE,TIME,IB3   ,   BMT,FV)
        END IF
C
C     (IMPLICIT TIME SCHEME)
        CALL IMPLCT(BMT,CMT,FV,TE,DELT   ,   WM)
C
        RETURN
        END
C
```

```
C
* * * * * * * * * * * * * * * * * * * * * * * * * * * * * * * * * * * * * * * * * * * * * * * * * * * * * * * * * * * * * * * * * * * * * * * * * * * * *
* * * * * * *
        SUBROUTINE ELMATT(NEL,XE,YE,TE,MC   ,   CMT,BMT,GMTM)
C
C      CONDUCTIVITY AND CAPACITY MATRIX
C      [INPUT]            NEL                 ELEMENT NUMBER
C      [INPUT]            XE(*)        X-COORDINATES  OF  NODES  IN  THE
ELEMENT
C      [INPUT]            YE(*)        Y-COORDINATES  OF  NODES  IN  THE
ELEMENT
C      [INPUT]            TE(*)         TEMPERATURE  AT  THE  NODES  IN  THE
ELEMENT
C      [INPUT]            MC                  MATERIAL CODE
C      [OUTPUT]    CMT(*,*)    CAPACITY MATRIX
C      [OUTPUT]    BMT(*,*)    CONDACTANCE MATRIX
C      [OUTPUT]    GMTM(*,*)   SOURCE MATRIX OF DELTT OF THE ELEMENT
C
* * * * * * * * * * * * * * * * * * * * * * * * * * * * * * * * * * * * * * * * * * * * * * * * * * * * * * * * * * * * * * * * * * * * * * * * * * * * *
* * * * * * *
        DIMENSION XE(3) , YE(3) , TE(3)
        DIMENSION BMT(3,3) , CMT(3,3) , GMTM(3,3)
C
C      (GET MATERIAL CONSTANTS)
        CALL ELMAVE(TE,TM)
        CALL CONDUC(TM,MC  ,  RAMDA)
        CALL VCAPA (TM,MC   ,   ROUC)
C
C      (CALCULATE COEFFICIENTS)
        B1 = YE(2) - YE(3)
        B2 = YE(3) - YE(1)
        B3 = YE(1) - YE(2)
C
        C1 = XE(3) - XE(2)
        C2 = XE(1) - XE(3)
        C3 = XE(2) - XE(1)
        CALL CLAREA(NEL,XE,YE  ,  AREA)
C
        FCTRB = RAMDA*(XE(1)+XE(2)+XE(3))/(12.*AREA)
        BMT(1,1) = (B1*B1 + C1*C1)*FCTRB
        BMT(1,2) = (B1*B2 + C1*C2)*FCTRB
        BMT(1,3) = (B1*B3 + C1*C3)*FCTRB
        BMT(2,1) = (B2*B1 + C2*C1)*FCTRB
        BMT(2,2) = (B2*B2 + C2*C2)*FCTRB
        BMT(2,3) = (B2*B3 + C2*C3)*FCTRB
        BMT(3,1) = (B3*B1 + C3*C1)*FCTRB
        BMT(3,2) = (B3*B2 + C3*C2)*FCTRB
        BMT(3,3) = (B3*B3 + C3*C3)*FCTRB
C
        FCTRC = ROUC*AREA/60.
        CMT(1,1)= (6*XE(1)+2*XE(2)+2*XE(3))*FCTRC
        CMT(1,2)= (2*XE(1)+2*XE(2)+XE(3))*FCTRC
        CMT(1,3)= (2*XE(1)+XE(2)+2*XE(3))*FCTRC
        CMT(2,1)= (XE(1)+2*XE(2)+2*XE(3))*FCTRC
        CMT(2,2)= (2*XE(1)+6*XE(2)+2*XE(3))*FCTRC
```

```
      CMT(2,3)= (XE(1)+2*XE(2)+2*XE(3))*FCTRC
      CMT(3,1)= (2*XE(1)+XE(2)+2*XE(3))*FCTRC
      CMT(3,2)= (2*XE(1)+2*XE(2)+XE(3))*FCTRC
      CMT(3,3)= (6*XE(1)+2*XE(2)+2*XE(3))*FCTRC
C
      FCTRGM = AREA/60.
      GMTM(1,1)= (6*XE(1)+2*XE(2)+2*XE(3))*FCTRGM
      GMTM(1,2)= (2*XE(1)+2*XE(2)+XE(3))*FCTRGM
      GMTM(1,3)= (2*XE(1)+XE(2)+2*XE(3))*FCTRGM
      GMTM(2,1)= (XE(1)+2*XE(2)+2*XE(3))*FCTRGM
      GMTM(2,2)= (2*XE(1)+6*XE(2)+2*XE(3))*FCTRGM
      GMTM(2,3)= (XE(1)+2*XE(2)+2*XE(3))*FCTRGM
      GMTM(3,1)= (2*XE(1)+XE(2)+2*XE(3))*FCTRGM
      GMTM(3,2)= (2*XE(1)+2*XE(2)+XE(3))*FCTRGM
      GMTM(3,3)= (6*XE(1)+2*XE(2)+2*XE(3))*FCTRGM
C
      RETURN
      END
C
C
********************************************************************
****************
      SUBROUTINE ADDGENT(GENME,RLHE,GMTM  ,  FV)
C
C     [INPUT]      GMTM(*,*)   SOURCE MATRIX
C     [INPUT]         GENME(*)    GENETARION OF VAPORIZING WATER
(KG/M3*S)
C     [INPUT]      RLHE(*)     LATENT HEAT IN THE ELEMENT(J/KG)
C     [OUTPUT]     FV(*)       R.H.S. VECTOR OF THE ELEMENT EQ.
C
********************************************************************
****************
      DIMENSION GENME(3), RLHE(3), GMTM(3,3), FV(3)
C
      DO I = 1 , 3
        DO J = 1 , 3
          FV(I) = FV(I) - GMTM(I,J)*RLHE(J)*GENME(J)
        ENDDO
      ENDDO
C
      RETURN
      END
C
C
********************************************************************
****************
      SUBROUTINE LATENT(TEMP,NUMNP  ,  RLH)
C
C     [INPUT]            TEMP(*)           NODAL TEMPERATURE [C]
C     [INPUT]            NUMNP        NUMBER OF NODES
C     [OUTPUT]   RLH(*)            LATENT HEAT OF EVAPORATION
[J/KG]
C
********************************************************************
      DIMENSION TEMP(NUMNP) , RLH(NUMNP)
      PARAMETER (RLHZ = 2.469E+06 , DCP = -2.344E+03)
```

```
C
      RLH = RLHZ + DCP*TEMP
C
      RETURN
      END
C
C
***********************************************************************
**
      SUBROUTINE ADDBCT(N1,N2,XE,YE,TIME,IB  ,  BMT,FV)
C
C     ADD BOUNDARY CONDITION TERM TO THE CONDUCTIVITY MATRX AND
C     R.H.S. VECTOR.
C
C     [INPUT]     N1,N2     LOCAL NODE NO. OON THE EXTERNAL BOUNDARY
C     [INPUT]     XE(*)     X-COORDINATE OF NODES IN THE ELEMENT
C     [INPUT]     YE(*)     Y-COORDINATE OF NODES IN THE ELEMENT
C     [INPUT]     TIME      TIME FROM EXPOSURE                    [S]
C     [INPUT]     IB        BOUNDARY CONDITION CODE
C     [OUTPUT]    BMT(*,*)  CONDUCTIVITY MATRIX OF THE ELEMENT
C     [OUTPUT]    FV(*)     R.H.S. VECTOR OF THE ELEMENT
C
***********************************************************************
**
      DIMENSION XE(3) , YE(3) , BMT(3,3) , FV(3)
C
      CALL BOUNDT(TIME,IB  ,  QR,H,TINF,ID)
C
      DX   = XE(N1) - XE(N2)
      DY   = YE(N1) - YE(N2)
      RLEN = SQRT(DX**2+DY**2)
C
      FCTR = H*RLEN/6.
      BMT(N1,N1) = BMT(N1,N1) + (3*XE(N1)+XE(N2))*FCTR
      BMT(N1,N2) = BMT(N1,N2) + (XE(N1)+XE(N2))*FCTR
      BMT(N2,N1) = BMT(N2,N1) + (XE(N1)+XE(N2))*FCTR
      BMT(N2,N2) = BMT(N2,N2) + (3*XE(N1)+XE(N2))*FCTR
C
      FCTR   = (H*TINF+QR)*RLEN/6.
      FV(N1) = FV(N1) + (2*XE(N1)+XE(N2))*FCTR
      FV(N2) = FV(N2) + (XE(N1)+2*XE(N2))*FCTR
C
      RETURN
      END
C
C
***********************************************************************
**
      SUBROUTINE BOUNDT(TIME,IBC  ,  QR,H,TINF,ID)
C
C     DEFINE BOUNDARY CONDITION PARAMETERS OF THE HEATED SURFACE
C
C     [INPUT]   TIME    TIME FROM EXPOSURE                      [S]
C     [INPUT]   IBC     BOUNDARY CONDITION CODE
C     [OUTPUT]  QR      INCIDENT RADIATIVE HEAT FLUX         [W/M2]
```

```
C       [OUTPUT]   H        HEAT TRANSFER COEFFICIENT            [W/M2*K]
C       [OUTPUT]   TINF     SURROUNDING TEMPERATURE             [C]
C       [OUTPUT]   ID       ID CODE OF BOUNDARY CONDITION
C                           0 ..... QR,H,TINF ARE GIVEN
C                           1 ..... TS(=TINF) IS GIVEN
C
********************************************************************
**
        IMPLICIT REAL*4 (A-H,O-Z)
C
        DUMMY = TIME
        IF (IBC .EQ. 1) THEN
          QR   =     0.    ! INCOMING RADIATION FROM EXTERMAL
ENVIRONMENT
          H    =    23.0   ! HEAT TRANSFER COEFFICIENT (W/M2.K)
          TINF =    20. + 20.*(TIME/60.)
          ID   =     0     ! ID=0 FOR GAS HEATED CONDITION
C
        ELSE IF (IBC .EQ. 2) THEN
          QR   =     0.    ! INCOMING RADIATION FROM EXTERMAL
ENVIRONMENT
          H    =    23.0   ! HEAT TRANSFER COEFFICIENT (W/M2.K)
          TINF =    20. + 19.*(TIME/60.)
          ID   =     0     ! ID=0 FOR GAS HEATED CONDITION
C
        ELSE IF (IBC .EQ. 3) THEN
          QR   =     0.    ! INCOMING RADIATION FROM EXTERMAL
ENVIRONMENT
          H    =    23.0   ! HEAT TRANSFER COEFFICIENT (W/M2.K)
          TINF =    20. + 5.*(TIME/60.)
          ID   =     0     ! ID=0 FOR GAS HEATED CONDITION
C
        ELSE IF (IBC .EQ. 4) THEN
          QR   =    20.0*1000
          H    =    23.0
          TINF =    20.0
          ID   =     0
C
        ELSE IF (IBC .EQ. 5) THEN
          QR   =     0.0
          H    =    23.0
          call iso834(time,tinf)
          ID   =     0
        ELSE
          WRITE(*,9001) IBC
          WRITE(*,*) '+++ INPUT DATA ERROR +++'
          STOP
        END IF
C
        RETURN
 9001 FORMAT(//
      *       ,' ** ERROR IN BOUND ROUTINE **',/
      *       ,' UNDEFINED BOUNDARY CONDITION CODE ',I8,' IS
DETECTED.',/
      *       ,' STOP -- PROGRAM ABORT.')
```

```
        END
* *********************************************************************
        subroutine iso834(time,Tf)
* *********************************************************************
        tmin=time/60.
        Tf = 345 * Log10(8 * tmin + 1.)+20
C
        return
        end
C
C
**********************************************************************
****
        SUBROUTINE MKEQSV(X,Y,TEMP,DTDT,PRES,PRESV,WCONT,GENM,EVV
     *                  ,NBC,IBC,MCODE,LM,NUMNP,NNDE
     *                  ,NUMEL,NNEL,DELT,ISTP
     *                  ,WMAT,FVEC)
C
C       MAKE SIMULTANEOUS EQUATIONS
C       [INPUT]      X(*)            X COORDINATE OF THE NODAL POINTS
C       [INPUT]      Y(*)            Y COORDINATE OF THE NODAL POINTS
C       [INPUT]      TEMP(*)            TEMPERATURE OF THE NODAL
POINTS
C       [INPUT]      TOLD(*)         PREVIOUS TEMPERATURE OF THE NODAL
POINTS
C       [INPUT]      GENM(*)         GENETARION OF VAPORIZING WATER
[KG/M3*S]
C       [INPUT]      PRES(*)         PRESSURE OF THE NODAL POINTS
C       [INPUT]      PRESV(*)        VOID PRESSURE OF THE NODAL POINTS
C       [INPUT]      PRESA(*)        AIR PRESSURE OF THE NODAL POINTS
C       [INPUT]      NBC(*)          LOCATION OF EXTERNAL BOUNDARY
C       [INPUT]      IBC(*)          BOUNDARY CONDITION CODE
C       [INPUT]      MCODE(*)        MATERIAL CODE
C       [INPUT]      LM(*,*)         NODE ELEMENT ALLOCATION TABLE
C       [INPUT]      NUMNP           NUMBER OF NODES
C       [INPUT]      NNDE            SIZE OF THE ARRAYS X(*),Y(*),TEMP(*)
ETC.
C       [INPUT]      NUMEL           NUMBER OF ELEMENTS
C       [INPUT]      NNEL            SIZE OF THE ARRAY LM(*)
C       [INPUT]      DELT            TIME INCREMENT
C       [INPUT]      ISTP            TIME INCREMENT
C       [OUTPUT]     WMAT(*,*)       COEFFICIENT MATRIX OF THE WHOLE
EQUATIONS
C       [OUTPUT]     FVEC(*)         R.H.S. VECTOR OF THE WHOLE EQUATIONS
C
**********************************************************************
*******
        DIMENSION X(NNDE) , Y(NNDE) , TEMP(NNDE) , DTDT(NNDE)
        DIMENSION PRES(NNDE) , PRESV(NNDE), WCONT(NNDE) , GENM(NNDE)
        DIMENSION NBC(NNEL) , IBC(NNEL) , MCODE(NNEL) , LM(NNEL,3)
        DIMENSION WMAT(NNDE,NNDE) , FVEC(NNDE) , EVV(NNDE)
C       (LOCAL VARIABLE)
        DIMENSION XE(3) , YE(3) , TE(3)
        DIMENSION PE(3) , PVE(3) , WE(3)
        DIMENSION GENME(3) , DTDTE(3)
```

```
        DIMENSION WM(3,3) , FV(3) , EVVE(3)
C
C     (CLEAR ARRAYS)
        FVEC = 0.0
        CALL CLEAR2D(WMAT,NNDE,NUMNP)
C
        DO 2000 NEL = 1 , NUMEL
C
C       (MAKE ELEMENT EQUATIONS)
          FV = 0.0
          CALL CLEAR2D(WM,3,3)
C
          DO I = 1 , 3
            IX = LM(NEL,I)
            XE(I)    = X(IX)
            YE(I)    = Y(IX)
            TE(I)    = TEMP(IX)
            PE(I)    = PRES(IX)
            PVE(I)   = PRESV(IX)
            GENME(I) = GENM(IX)
            DTDTE(I) = DTDT(IX)
            WE(I)    = WCONT(IX)
            EVVE(I)  = EVV(IX)
          ENDDO
          MC = MCODE(NEL)
          NB = NBC(NEL)
          IB = IBC(NEL)
          CALL ELCALV(NEL,XE,YE,TE,PE,PVE,WE,GENME,EVVE,DTDTE
       *              ,NB,IB,MC,DELT,ISTP  ,  WM,FV)
C
C       (PUT ELEMENT EQUATIOS INTO WHOLE EQUATIONS)
          CALL BUILD(NEL,LM,WM,FV,NNDE,NNEL   ,  WMAT,FVEC)
 2000 CONTINUE
C
      RETURN
      END
C
C
* * * * * * * * * * * * * * * * * * * * * * * * * * * * * * * * * * * * * * * * * * * * * * * * * * * * * * * * * * * * * * * * * * * * * * * *
* * * * *
      SUBROUTINE ELCALV(NEL,XE,YE,TE,PE,PVE,WE,GENME,EVVE,DTDTE
     *                  ,NB,IB,MC,DELT,ISTP  ,  WM,FV)
C
C     MAKE ELEMENT EQUATIONS
C
C    [INPUT]      NEL          ELEMENT NUMBER TO BE CALCULATED.
C    [INPUT]      XE(*)        X-COORDINATES OF NODES IN THE
ELEMENT(NEL)
C    [INPUT]      YE(*)        Y-COORDINATES OF NODES IN THE
ELEMENT(NEL)
C    [INPUT]      TE(*)        TEMPERATURE   OF NODES IN THE
ELEMENT(NEL)
C    [INPUT]      BMV(*,*)     CONDUCTIVITY MATRIX
C    [INPUT]      CMV(*,*)     CAPACITY MATRX
```

```
C     [INPUT]     GMVM(*,*)     SOURCE MATRIX OF WATER VAPOR OF THE
ELEMENT
C     [INPUT]     GMVT(*,*)     SOURCE MATRIX OF DELTT OF THE ELEMENT
C     [INPUT]     NB            EXTERNAL BOUNDARY POSITION
C     [INPUT]     IB            BOUNDARY CONDITION CODE
C     [INPUT]     MC            MATERIAL CODE OF THE ELEMENT(NEL)
C     [INPUT]     DELT          TIME INCREMENT
C     [INPUT]     ISTP          TIME INDEX
C     [OUTPUT]    WM(*,*)       COEFFICIENT MATRIX OF THE ELEMENT
C     [OUTPUT]    FV(*)         R.H.S. VECTOR OF THE ELEMENT
C
*****************************************************************
*****
      DIMENSION XE(3) , YE(3) , TE(3)
      DIMENSION PE(3) , PVE(3) , WE(3)
      DIMENSION GENME(3) , DTDTE(3)
      DIMENSION WM(3,3) , FV(3) , EVVE(3)
C     (LOCAL VARIABLES)
      DIMENSION BMV(3,3) , CMV(3,3) , GMVM(3,3) , GMVT(3,3)
C
C     (CONDUCTIVITY/CAPACITY MATRIX)
      CALL ELMATV(NEL,XE,YE,TE,PE,PVE,EVVE,MC
     *              , CMV,BMV,GMVM,GMVT)

C
C     (ADD SOURCE TERM TO FV)
      CALL ADDGENV(GMVM,GMVT,GENME,DTDTE   , FV)
C
C     (ADD BOUNDARY CONDITION TO BMV)
      CALL FINDBC(NB,NB1,NB2,NB3)
      CALL FINDBC(IB,IB1,IB2,IB3)
C
      IF (NB1 .EQ. 1) THEN
        CALL ADDBCV(1,2,XE,YE,TE,WE,IB1 , BMV,FV)
      END IF
      IF (NB2 .EQ. 1) THEN
        CALL ADDBCV(2,3,XE,YE,TE,WE,IB2 , BMV,FV)
      END IF
      IF (NB3 .EQ. 1) THEN
        CALL ADDBCV(3,1,XE,YE,TE,WE,IB3 , BMV,FV)
      END IF
C
C     (IMPLICIT TIME SCHEME)
      CALL IMPLCT(BMV,CMV,FV,PVE,DELT   ,  WM)
C
      RETURN
      END
C
C
*****************************************************************
********
      SUBROUTINE ELMATV(NEL,XE,YE,TE,PE,PVE,EVVE,MC
     *              , CMV,BMV,GMVM,GMVT)
C
C       CONDUCTIVITY,CAPACITY AND GENERATION MATRIX OF WATER VAPOR
```

```
C
C      [INPUT]       NEL          ELEMENT NUMBER TO BE CALCULATED
C      [INPUT]       XE(*)        X-COORDINATES OF NODES IN THE
ELEMENT(NEL)
C      [INPUT]       YE(*)        Y-COORDINATES OF NODES IN THE
ELEMENT(NEL)
C      [INPUT]       TE(*)        TEMPERATURE OF NODES IN THE ELEMENT(NEL)
C      [INPUT]       PE(*)        PRESSURE OF NODS IN THE ELEMENT(NEL)
C      [INPUT]       ATE(*)       ABSOLUTE TEMPERATURE OF NODES IN THE
ELEMENT(NEL)
C      [INPUT]       PVE(*)       VAPOR RESSURE OF NODES IN THE
ELEMENT(NEL)
C      [INPUT]       MC           MATERIAL CODE OF THE ELEMENT
C      [INPUT]       EPSR         VOID RATIO
C      [INPUT]       KAPPA
C      [INPUT]       EV           CONDUCTIVITY OF WATER VAPOR
C      [INPUT]       KV           CAPACITY OF WATER VAPOR
C      [INPUT]       RV
C      [OUTPUT]      CMV(*,*)     CAPACITY MATRIX OF WATER VAPOR OF THE
ELEMENT
C      [OUTPUT]      BMV(*,*)     COEFFICIENT MATRIX OF WATER VAPOR OF THE
ELEMENT
C      [OUTPUT]      GMVM(*,*)    SOURCE MATRIX OF WATER VAPOR OF THE
ELEMENT
C      [OUTPUT]      GMVT(*,*)    SOURCE MATRIX OF DELTT OF THE ELEMENT
C
**********************************************************************
*******
       DIMENSION XE(3) , YE(3) , TE(3) , PE(3) , PVE(3) , EVVE(3)
       DIMENSION BMV(3,3) , CMV(3,3) , GMVM(3,3) , GMVT(3,3)
       REAL KAPP,KV
       PARAMETER (RV = 0.002165)
C
       CALL VOID(EPSR)
       CALL ELMAVE(TE,TEM)
       ATM = TEM + 273.2
       CALL ELMAVE(EVVE,EVVEM)
       EV = (EPSR*RV/ATM) + EVVEM
*
       CALL ELMAVE(PE ,PM)
       CALL ELMAVE(PVE,PVM)
       FAI = PVM / PM
       CALL TRIM(FAI,0.00000001,0.9999999999)
*
       CALL PERMEA(EPSR,KAPP)
       KV = KAPP*RV*PVM/(FAI*ATM)
C
C      (CALCULATE COEFFICIENTS)
       B1 = YE(2) - YE(3)
       B2 = YE(3) - YE(1)
       B3 = YE(1) - YE(2)
C
       C1 = XE(3) - XE(2)
       C2 = XE(1) - XE(3)
       C3 = XE(2) - XE(1)
```

```
C
      CALL CLAREA(NEL,XE,YE   ,  AREA)
C
      FCTRB = KV*(XE(1)+XE(2)+XE(3))/(12.*AREA)
      BMV(1,1) = (B1*B1 + C1*C1)*FCTRB
      BMV(1,2) = (B1*B2 + C1*C2)*FCTRB
      BMV(1,3) = (B1*B3 + C1*C3)*FCTRB
      BMV(2,1) = (B2*B1 + C2*C1)*FCTRB
      BMV(2,2) = (B2*B2 + C2*C2)*FCTRB
      BMV(2,3) = (B2*B3 + C2*C3)*FCTRB
      BMV(3,1) = (B3*B1 + C3*C1)*FCTRB
      BMV(3,2) = (B3*B2 + C3*C2)*FCTRB
      BMV(3,3) = (B3*B3 + C3*C3)*FCTRB
C
      FCTRC = EV*AREA/60.
      CMV(1,1)= (6*XE(1)+2*XE(2)+2*XE(3))*FCTRC
      CMV(1,2)= (2*XE(1)+2*XE(2)+XE(3))*FCTRC
      CMV(1,3)= (2*XE(1)+XE(2)+2*XE(3))*FCTRC
      CMV(2,1)= (XE(1)+2*XE(2)+2*XE(3))*FCTRC
      CMV(2,2)= (2*XE(1)+6*XE(2)+2*XE(3))*FCTRC
      CMV(2,3)= (XE(1)+2*XE(2)+2*XE(3))*FCTRC
      CMV(3,1)= (2*XE(1)+XE(2)+2*XE(3))*FCTRC
      CMV(3,2)= (2*XE(1)+2*XE(2)+XE(3))*FCTRC
      CMV(3,3)= (6*XE(1)+2*XE(2)+2*XE(3))*FCTRC
C
      FCTRGM = AREA/60.
      GMVM(1,1)= (6*XE(1)+2*XE(2)+2*XE(3))*FCTRGM
      GMVM(1,2)= (2*XE(1)+2*XE(2)+XE(3))*FCTRGM
      GMVM(1,3)= (2*XE(1)+XE(2)+2*XE(3))*FCTRGM
      GMVM(2,1)= (XE(1)+2*XE(2)+2*XE(3))*FCTRGM
      GMVM(2,2)= (2*XE(1)+6*XE(2)+2*XE(3))*FCTRGM
      GMVM(2,3)= (XE(1)+2*XE(2)+2*XE(3))*FCTRGM
      GMVM(3,1)= (2*XE(1)+XE(2)+2*XE(3))*FCTRGM
      GMVM(3,2)= (2*XE(1)+2*XE(2)+XE(3))*FCTRGM
      GMVM(3,3)= (6*XE(1)+2*XE(2)+2*XE(3))*FCTRGM
C
      FCTRGT = (EV*PVM/ATM)*(AREA/60.)
      GMVT(1,1)= (6*XE(1)+2*XE(2)+2*XE(3))*FCTRGT
      GMVT(1,2)= (2*XE(1)+2*XE(2)+XE(3))*FCTRGT
      GMVT(1,3)= (2*XE(1)+XE(2)+2*XE(3))*FCTRGT
      GMVT(2,1)= (XE(1)+2*XE(2)+2*XE(3))*FCTRGT
      GMVT(2,2)= (2*XE(1)+6*XE(2)+2*XE(3))*FCTRGT
      GMVT(2,3)= (XE(1)+2*XE(2)+2*XE(3))*FCTRGT
      GMVT(3,1)= (2*XE(1)+XE(2)+2*XE(3))*FCTRGT
      GMVT(3,2)= (2*XE(1)+2*XE(2)+XE(3))*FCTRGT
      GMVT(3,3)= (6*XE(1)+2*XE(2)+2*XE(3))*FCTRGT
C
      RETURN
      END
C
**************************************************************
**
      SUBROUTINE ELMAVE(VAR,AVE)
```

```
C
*************************************************************************
**
      DIMENSION VAR(3)

      AVE= (VAR(1) + VAR(2) + VAR(3))/3.

      RETURN
      END
C
*************************************************************************
*********
      SUBROUTINE ADDGENV(GMVM,GMVT,GENME,DTDTE   , FV)
C
C    [INPUT]       GEVM(*,*)    GENARATATION MATRIX OF WATER VAPOR OF
THE ELEMENT
C    [INPUT]       GMVT(*.*)    GENARATATION MATRIX OF DELTT OF THE
ELEMENT
C    [INPUT]       GENME(*)     ENTGENETARION OF VAPORIZING WATER
(KG/M3*S)
C    [INPUT]       DTDTE(*)     TIME DERIVERTIVE
C    [OUTPUT]      FV(*)        R.H.S. VECTOR OF THE ELEMENT
C
*************************************************************************
*********
      DIMENSION GMVM(3,3) , GMVT(3,3) , GENME(3) , DTDTE(3), FV(3)
C
      DO I = 1 , 3
        DO J = 1 , 3
          FV(I) = FV(I) + GMVM(I,J)*GENME(J) +GMVT(I,J)*DTDTE(J)
        ENDDO
      ENDDO
C
      RETURN
      END
C
C
*************************************************************************
**
      SUBROUTINE DELTT(TOLD,TEMP,DELT,N , DTDT)
C
C    [INPUT]       TOLD(*)       PREVIOUS TEMPERATURE OF THE NODAL
POINTS
C    [INPUT]       TEMP(*)       TEMPERATURE OF THE NODAL POINTS
C    [INPUT]       DELT          TIME INCREMENT
C    [OUTPUT]      DTDT(*)       TIME DERIVERTIVE
C
*************************************************************************
**
      DIMENSION TEMP(N),TOLD(N),DTDT(N)
C
      DTDT = (TEMP-TOLD)/DELT
C
      RETURN
      END
```

```
C
C
************************************************************************
*********
      SUBROUTINE ADDBCV(N1,N2,XE,YE,TE,WE,IB   ,  BMV,FV)
C
C     ADD BOUNDARY CONDITION TERM TO THE CONDUCTIVITY MATRX AND
C     R.H.S. VECTOR.
C
C     [INPUT]      N1,N2        LOCAL NODE NO. OON THE EXTERNAL
BOUNDARY
C     [INPUT]      XE(*)        X-COORDINATE OF NODES IN THE ELEMENT
C     [INPUT]      YE(*)        Y-COORDINATE OF NODES IN THE ELEMENT
C     [INPUT]      TIME         TIME FROM EXPOSURE               (S)
C     [INPUT]      IB           BOUNDARY CONDITION CODE
C     [OUTPUT]     BMV(*,*)     COEFFICIENT MATRIX OF WATER VAPOR OF
THE ELEMENT
C     [OUTPUT]     FV(*)        R.H.S. VECTOR OF THE ELEMENT
C
************************************************************************
*********
      DIMENSION XE(3) , YE(3) , TE(3), WE(3) , BMV(3,3) , FV(3)
      PARAMETER (PATM = 101325.)
C
      TAVE = (TE(N1)+TE(N2))/2.
      WAVE = (WE(N1)+WE(N2))/2.
      CALL BOUNDV(TAVE,WAVE , PVZ)
      DX   = XE(N1) - XE(N2)
      DY   = YE(N1) - YE(N2)
      RLEN = SQRT(DX**2+DY**2)
C
      CALL TRANSFV(HV)
      FCTR = HV*RLEN/12.
      BMV(N1,N1) = BMV(N1,N1) + (3*XE(N1)+XE(N2))*FCTR
      BMV(N1,N2) = BMV(N1,N2) + (  XE(N1)+XE(N2))*FCTR
      BMV(N2,N1) = BMV(N2,N1) + (  XE(N1)+XE(N2))*FCTR
      BMV(N2,N2) = BMV(N2,N2) + (3*XE(N1)+XE(N2))*FCTR
C
      FCTR   = (HV*PVZ)*RLEN/6.
      FV(N1) = FV(N1) + (2*XE(N1)+  XE(N2))*FCTR
      FV(N2) = FV(N2) + (  XE(N1)+2*XE(N2))*FCTR
C
      RETURN
      END
C
*
************************************************************************
**
      SUBROUTINE BOUNDV(TAVE,WAVE , PVZ)
*
*     calculate boundary value for vapor pressure
*
*     [INPUT]           Tave  average temperature of the boundary
(c)
```

```
*       [INPUT]             Wave   average water content of the boundary
(kg/kg)
*       [OUTPUT]    Pvz          boundary value for vapor pressure (Pa)
*
****************************************************************************
**
      PVZ = 1257.1721
C
      RETURN
      END
C
C
****************************************************************************
*******
      subroutine equilp(temp,wcont,numnp   ,   presveq)
C
C     calculation of equilibrium vapor pressure (inverse function of
C     equilw, use Newton's iteration method)
C
C     [INPUT]             temp(*)             nodal temperature array
(C)
C     [OUTPUT]    wcont(*)    nodal water content array [kg/kg]
C     [INPUT]             numnp          number of nodal points
C     [INPUT]             prevseq(*)  initial guess (if unknown
negative)
C     [OUTPUT]    presveq(*)  nodal vapor pressure at equilibrium
state (Pa)
*
****************************************************************************
*******
      IMPLICIT REAL*4 (A-H,O-Z)
      dimension temp(numnp), wcont(numnp)
      dimension presveq(numnp)
*     local variables
      dimension temp1(1), presv1(1), pvsat1(1), weq1(1), weqdpv1(1)
      dimension dp(1)
      parameter (zero = 1.)
*
      do i = 1 , numnp
        temp1(1) = temp(i)
        call VERPAS(TEMP1,1   ,   PVSAT1)
        if (presveq(1) .ge. 0.0) then
          presv1(1) = presveq(i)
        else
          presv1(1) = pvsat1(1)*0.8
          presv1(1) = 0.0
        end if
1000    continue
        call EQUILW(TEMP1,PRESV1,PVSAT1,1 , WEQ1,WEQDPV1)
        dp = (weq1-wcont(i))/weqdpv1
        if (abs(dp(1)) .lt. zero) then
          presveq(i) = presv1(1)
          goto 5000
        else
          presv1(1) = presv1(1) - dp(1)
```

```
            if (presv1(1) .lt.         0.0) presv1(1) = 0.0
            if (presv1(1) .gt. pvsat1(1)) presv1(1) = pvsat1(1)
            presveq(i) = presv1(1)
            goto 1000
          end if
 5000    continue
       enddo
       return
       end
C
C
********************************************************************
**
       SUBROUTINE MKEQSA(X,Y,TEMP,DTDT,PRES,PRESA,WCONT
      *                 ,NBC,IBC,MCODE,LM
      *                 ,NUMNP,NNDE,NUMEL,NNEL,DELT,ISTP
      *                 ,WMAT,FVEC)
C
C     MAKE SIMULTANEOUS EQUATIONS
C
C    [INPUT]     X(*)          X COORDINATE OF THE NODAL POINTS
C    [INPUT]     Y(*)          Y COORDINATE OF THE NODAL POINTS
C    [INPUT]     TEMP(*)       TEMPERATURE OF THE NODAL POINTSC
C    [INPUT]     PRES(*)       PRESSURE OF THE NODAL POINTS
C    [INPUT]     PRESV(*)      VOID PRESSURE OF THE NODAL POINTS
C    [INPUT]     PRESA(*)      AIR PRESSURE OF THE NODAL POINTS
C    [INPUT]     DTDT(*)       TIME DERIVERTIVE
C    [INPUT]     NBC(*)        LOCATION OF EXTERNAL BOUNDARY
C    [INPUT]     IBC(*)        BOUNDARY CONDITION CODE
C    [INPUT]     MCODE(*)      MATERIAL CODE
C    [INPUT]     LM(*,*)       NODE ELEMENT ALLOCATION TABLE
C    [INPUT]     NUMNP         NUMBER OF NODES
C    [INPUT]     NNDE          SIZE OF THE ARRAYS X(*),Y(*),TEMP(*)
ETC.
C    [INPUT]     NUMEL         NUMBER OF ELEMENTS
C    [INPUT]     NNEL          SIZE OF THE ARRAY LM(*)
C    [INPUT]     DELT          TIME INCREMENT
C    [INPUT]     ISTP          TIME INCREMENT
C    [OUTPUT]    WMAT(*,*)     COEFFICIENT MATRIX OF THE WHOLE
EQUATIONS
C    [OUTPUT]    FVEC(*)       R.H.S. VECTOR OF THE WHOLE EQUATIONS
C
********************************************************************
*****
       DIMENSION X(NNDE) ,Y(NNDE) ,TEMP(NNDE) , DTDT(NNDE)
       DIMENSION PRES(NNDE) ,   PRESA(NNDE), WCONT(NNDE)
       DIMENSION NBC(NNEL) , IBC(NNEL) , MCODE(NNEL) , LM(NNEL,3)
       DIMENSION WMAT(NNDE,NNDE) , FVEC(NNDE)
C     (LOCAL VARIABLES)
       DIMENSION XE(3), YE(3), TE(3) , DTDTE(3)
       DIMENSION PE(3) , PVE(3) , PAE(3) , WE(3)
       DIMENSION WM(3,3) , FV(3)
C
C     (CLEAR ARRAYS)
       FVEC = 0.0
```

```
        DO I = 1 , NUMNP
          DO J = 1 , NUMNP
            WMAT(I,J) = 0.0
          ENDDO
        ENDDO
C
        DO 2000 NEL = 1 , NUMEL
C
C       (MAKE ELEMENT EQUATIONS)
          FV = 0.0
          DO 2050 I = 1 , 3
            DO 2050 J = 1 , 3
              WM(  I,J) = 0.0
 2050     CONTINUE
          DO I = 1 , 3
            IX = LM(NEL,I)
            XE(   I) = X(IX)
            YE(   I) = Y(IX)
            TE(   I) = TEMP(IX)
            DTDTE(I) = DTDT(IX)
            PE(   I) = PRES(IX)
            PAE(  I) = PRESA(IX)
            WE(   I) = WCONT(IX)
          ENDDO
          MC = MCODE(NEL)
          NB = NBC(NEL)
          IB = IBC(NEL)
          CALL ELCALA(NEL,XE,YE,TE,DTDTE,PE,PAE,WE
     *                ,NB,IB,MC,DELT,ISTP
     *                ,WM,FV)
C
C       (PUT ELEMENT EQUATIOS INTO WHOLE EQUATIONS)
          CALL BUILD(NEL,LM,WM,FV,NNDE,NNEL   ,   WMAT,FVEC)
 2000 CONTINUE
C
      RETURN
      END
C
C
* * * * * * * * * * * * * * * * * * * * * * * * * * * * * * * * * * * * * * * * * * * * * * * * * * * * * * * * * * * * * * * * * * * * * * * * * * *
* *
      SUBROUTINE ELCALA(NEL,XE,YE,TE,DTDTE,PE,PAE,WE
     *                  ,NB,IB,MC,DELT,ISTP
     *                  ,WM,FV)
C
C     MAKE ELEMENT EQUATIONS
C
C   [INPUT]      NEL           ELEMENT NUMBER TO BE CALCULATED.
C   [INPUT]      XE(*)         X-COORDINATES OF NODES IN THE
ELEMENT(NEL)
C   [INPUT]      YE(*)         Y-COORDINATES OF NODES IN THE
ELEMENT(NEL)
C   [INPUT]      TE(*)         TEMPERATURE   OF NODES IN THE
ELEMENT(NEL)
C   [INPUT]      PE(*)         PRESSURE OF NODES IN THE ELEMENT(NEL)
```

```
C     [INPUT]      PVE(*)        VOID PRESSURE OF NODES IN THE
ELEMENT(NEL)
C     [INPUT]      PAE(*)        AIR PRESSURE OF NODES IN THE
ELEMENT(NEL)
C     [INPUT]      BMA(*,*)      CONDUCTIVITY MATRIX
C     [INPUT]      CMA(*,*)      CAPACITY MATRX
C     [INPUT]      GMAT(*,*)     SOURCE MATRIX OF DELTT OF THE ELEMENT
C     [INPUT]      NB            EXTERNAL BOUNDARY POSITION
C     [INPUT]      IB            BOUNDARY CONDITION CODE
C     [INPUT]      MC            MATERIAL CODE OF THE ELEMENT(NEL)
C     [INPUT]      DELT          TIME INCREMENT
C     [INPUT]      ISTP          TIME INDEX
C     [OUTPUT]     WM(*,*)       COEFFICIENT MATRIX OF THE ELEMENT
C     [OUTPUT]     FV(*)         R.H.S. VECTOR OF THE ELEMENT
C
* * * * * * * * * * * * * * * * * * * * * * * * * * * * * * * * * * * * * * * * * * * * * * * * * * * * * * * * * * * * * * * *
* *
      DIMENSION XE(3) , YE(3) , TE(3) , DTDTE(3)
      DIMENSION PE(3) , PAE(3), WE(3) , WM(3,3) , FV(3)
C     (LOCAL VARIABLES)
      DIMENSION BMA(3,3) , CMA(3,3) , GMAT(3,3)
C
C     (CONDUCTIVITY/CAPACITY MATRIX)
      CALL ELMATA(NEL,XE,YE,TE,PE,PAE,MC   ,   CMA,BMA,GMAT)
C
C     (ADD SOURCE TERM TO FV)
      CALL ADDGENA(GMAT,DTDTE   ,   FV)
C
C     (ADD BOUNDARY CONDITION TO BM)
      CALL FINDBC(NB,NB1,NB2,NB3)
      CALL FINDBC(IB,IB1,IB2,IB3)
C
      TIME = DELT*ISTP
      IF (NB1 .EQ. 1) THEN
        CALL ADDBCA(1,2,XE,YE,TE,WE,IB1   ,   BMA,FV)
      END IF
      IF (NB2 .EQ. 1) THEN
        CALL ADDBCA(2,3,XE,YE,TE,WE,IB2   ,   BMA,FV)
      END IF
      IF (NB3 .EQ. 1) THEN
        CALL ADDBCA(3,1,XE,YE,TE,WE,IB3   ,   BMA,FV)
      END IF
C
C     (IMPLICIT TIME SCHEME)
      CALL IMPLCT(BMA,CMA,FV,PAE,DELT   ,   WM)
C
      RETURN
      END
C
C
* * * * * * * * * * * * * * * * * * * * * * * * * * * * * * * * * * * * * * * * * * * * * * * * * * * * * * * * * * * * * * * *
* *
      SUBROUTINE ELMATA(NEL,XE,YE,TE,PE,PAE,MC   ,   CMA,BMA,GMAT)
C
C     CONDUCTIVITY,CAPACITY AND GENERATION MATRIX OF WATER VAPOR
```

```
C
C      [INPUT]         NEL                    ELEMENT NUMBER
C      [INPUT]         XE(*)         X-COORDINATES OF NODES IN THE
ELEMENT
C      [INPUT]         YE(*)         Y-COORDINATES OF NODES IN THE
ELEMENT
C      [INPUT]         MC                     MATERIAL CODE OF THE
ELEMENT
C      [OUTPUT]   CMT(*,*)    CAPACITY MATRIX
C      [OUTPUT]   BMT(*,*)    CONDACTANCE MATRIX
C      [OUTPUT]   GMTM(*,*)   SOURCE MATRIX OF DELTT OF THE ELEMENT
C
**************************************************************************
**
       DIMENSION XE(3) , YE(3), TE(3), PE(3), PAE(3)
       DIMENSION BMA(3,3) , CMA(3,3) , GMAT(3,3)
       REAL KAPP,KA
       PARAMETER (RA = 0.003464)
C
C    (GET MATERIAL CONSTANTS)
       CALL ELMAVE(TE,TM)
       ATM = TM + 273.2
       CALL VOID(EPSR)
       EA = EPSR*RA/ATM
*
       CALL PERMEA(EPSR,KAPP)
       CALL ELMAVE(PAE,PAM)
       CALL ELMAVE(PE, PM)
       FAI = PAM/PM
       CALL TRIM(FAI,0.00000001,0.9999999999)
       KA = KAPP*RA*PAM/(FAI*ATM)
C
C    (CALCULATE COEFFICIENTS)
       B1 = YE(2) - YE(3)
       B2 = YE(3) - YE(1)
       B3 = YE(1) - YE(2)
C
       C1 = XE(3) - XE(2)
       C2 = XE(1) - XE(3)
       C3 = XE(2) - XE(1)
C
       CALL CLAREA(NEL,XE,YE  ,  AREA)
C
       FCTRB = KA*(XE(1)+XE(2)+XE(3))/(12.*AREA)
       BMA(1,1) = (B1*B1 + C1*C1)*FCTRB
       BMA(1,2) = (B1*B2 + C1*C2)*FCTRB
       BMA(1,3) = (B1*B3 + C1*C3)*FCTRB
       BMA(2,1) = (B2*B1 + C2*C1)*FCTRB
       BMA(2,2) = (B2*B2 + C2*C2)*FCTRB
       BMA(2,3) = (B2*B3 + C2*C3)*FCTRB
       BMA(3,1) = (B3*B1 + C3*C1)*FCTRB
       BMA(3,2) = (B3*B2 + C3*C2)*FCTRB
       BMA(3,3) = (B3*B3 + C3*C3)*FCTRB
C
       FCTRC = EA*AREA/60.
```

```
      CMA(1,1)= (6*XE(1)+2*XE(2)+2*XE(3))*FCTRC
      CMA(1,2)= (2*XE(1)+2*XE(2)+  XE(3))*FCTRC
      CMA(1,3)= (2*XE(1)+  XE(2)+2*XE(3))*FCTRC
      CMA(2,1)= (  XE(1)+2*XE(2)+2*XE(3))*FCTRC
      CMA(2,2)= (2*XE(1)+6*XE(2)+2*XE(3))*FCTRC
      CMA(2,3)= (  XE(1)+2*XE(2)+2*XE(3))*FCTRC
      CMA(3,1)= (2*XE(1)+  XE(2)+2*XE(3))*FCTRC
      CMA(3,2)= (2*XE(1)+2*XE(2)+  XE(3))*FCTRC
      CMA(3,3)= (6*XE(1)+2*XE(2)+2*XE(3))*FCTRC
C
      FCTRGT = (EA*PAM/ATM)*(AREA/60.)
      GMAT(1,1)= (6*XE(1)+2*XE(2)+2*XE(3))*FCTRGT
      GMAT(1,2)= (2*XE(1)+2*XE(2)+  XE(3))*FCTRGT
      GMAT(1,3)= (2*XE(1)+  XE(2)+2*XE(3))*FCTRGT
      GMAT(2,1)= (  XE(1)+2*XE(2)+2*XE(3))*FCTRGT
      GMAT(2,2)= (2*XE(1)+6*XE(2)+2*XE(3))*FCTRGT
      GMAT(2,3)= (  XE(1)+2*XE(2)+2*XE(3))*FCTRGT
      GMAT(3,1)= (2*XE(1)+XE(2)+  2*XE(3))*FCTRGT
      GMAT(3,2)= (2*XE(1)+2*XE(2)+  XE(3))*FCTRGT
      GMAT(3,3)= (6*XE(1)+2*XE(2)+2*XE(3))*FCTRGT
C
      RETURN
      END
C
C
************************************************************
*****
      SUBROUTINE ADDGENA(GMAT,DTDTE , FV)
C
C    [INPUT]      GMAT(*,*)   SOURCE MATRIX OF DELTT OF THE ELEMENT
C    [INPUT]      DTDTE(*)    TIME DERIVERTIVE OF NODES IN THE
ELEMENT(NEL)
C    [OUTPUT]     FV(*)       R.H.S. VECTOR OF THE ELEMENT
C
************************************************************
*****
      DIMENSION DTDTE(3)
      DIMENSION GMAT(3,3) , FV(3)
C
      DO I = 1 , 3
        DO  J = 1 , 3
          FV(I) = FV(I) + GMAT(I,J)*DTDTE(J)
        ENDDO
      ENDDO
C
      RETURN
      END
C
C
************************************************************
*****
      SUBROUTINE ADDBCA(N1,N2,XE,YE,TE,WE,IB  , BMA,FV)
C
C    ADD BOUNDARY CONDITION TERM TO THE CONDUCTIVITY MATRX AND
C    R.H.S. VECTOR.
```

```
C
C      [INPUT]     N1,N2        LOCAL NODE NO. OON THE EXTERNAL
BOUNDARY
C      [INPUT]     XE(*)        X-COORDINATE OF NODES IN THE ELEMENT
C      [INPUT]     YE(*)        Y-COORDINATE OF NODES IN THE ELEMENT
C      [INPUT]     TE(*)        TEMPERATURE   OF NODES IN THE
ELEMENT(NEL)
C      [INPUT]     WE(*)        EQUILIBRIUM WATER CONTENT[KG/KG]
C      [INPUT]     IB           BOUNDARY CONDITION CODE
C      [OUTPUT]    BMA(*,*)     CONDUCTIVITY MATRIX
C      [OUTPUT]    FV(*)        R.H.S. VECTOR OF THE ELEMENT
C
********************************************************************
*****
       DIMENSION XE(3) , YE(3) , TE(3), WE(3), BMA(3,3) , FV(3)
C
       TAVE = (TE(N1)+TE(N2))/2.
       WAVE = (WE(N1)+WE(N2))/2.
       CALL BOUNDV(TAVE,WAVE , PVZ)
       CALL BOUNDA(PVZ , PAZ)
C
       DX   = XE(N1) - XE(N2)
       DY   = YE(N1) - YE(N2)
       RLEN = SQRT(DX**2+DY**2)
C
       CALL TRANSFA(HA)
       FCTR = HA*RLEN/12.
       BMA(N1,N1) = BMA(N1,N1) + (3*XE(N1)+XE(N2))*FCTR
       BMA(N1,N2) = BMA(N1,N2) + (XE(N1)+XE(N2))*FCTR
       BMA(N2,N1) = BMA(N2,N1) + (XE(N1)+XE(N2))*FCTR
       BMA(N2,N2) = BMA(N2,N2) + (3*XE(N1)+XE(N2))*FCTR
C
       FCTR   = (HA*PAZ)*RLEN/6.
       FV(N1) = FV(N1) + (2*XE(N1)+XE(N2))*FCTR
       FV(N2) = FV(N2) + (XE(N1)+2*XE(N2))*FCTR
C
       RETURN
       END
C
C
********************************************************************
**
       SUBROUTINE BOUNDA(PVZ , PAZ)
*
*      calculate boundary value for vapor pressure
*
*      [INPUT]          Pvz          boundary value for vapor
pressure (Pa)
*      [OUTPUT]   Paz          boundary value for air pressure (Pa)
*
********************************************************************
**
       PARAMETER (PATM = 101325.)
C
       PAZ = PATM  - pvz
```

```
        if (paz.le.0.0) paz = 0.0
C
        RETURN
        END
C
C
*****************************************************************
*****
        SUBROUTINE IMPLCT(BM,CM,FV,TE,DELT   ,  WM)
C
C     IMPLICIT TIME INTEGRATING SCHEME
C
C     [INPUT]     BM(*,*)          CONDUCTIVITY MATRIX
C     [INPUT]     CM(*,*)          CAPACITY MATRIX
C     [INPUT]     FV(*)            LOAD VECTOR
C     [INPUT]     TE(*)            TEMPERATURE OF THE NODES IN THE
ELEMENT
C     [INPUT]     DELT             TIME INCREMENT
C     [OUTPUT]    WM(*,*)          COEFFICIENT MATRIX OF THE ELEMENT
C     [OUTPUT]    FV(*)            LOAD VECTOR
C
*****************************************************************
*****
        DIMENSION BM(3,3) , CM(3,3) , WM(3,3) , FV(3) , TE(3)
C
        DO 1000 I = 1 , 3
          DO 1000 J = 1 , 3
            FV(I) = FV(I) + CM(I,J)/DELT*TE(J)
 1000 CONTINUE
C
        DO 1100 I=1,3
          DO 1100 J=1,3
            WM(I,J) = CM(I,J)/DELT + BM(I,J)
 1100 CONTINUE
C
        RETURN
        END
C
C
*****************************************************************
        SUBROUTINE RDDATA(NR,X,Y,TEMP,WCONT
     *                   ,MCODE,LM,NBC,IBC,DELT,NSTP,NOUT
     *                   ,NUMNP,NNDE,NUMEL,NNEL)
C
C     READ DATA FROM FILE
C
C     [INPUT]     X(*)             X-POSITION OF NODAL POINTS
C     [INPUT]     Y(*)             Y-POSITION OF NODAL POINTS
C     [INPUT]     TEMP(*)          TEMPERATURE OF NODAL POINTS
C     [INPUT]     PRESV(*)         VOID PRESSURE OF NODAL POINTS
C     [INPUT]     PRESA(*)         AIR PRESSURE OF NODAL POINTS
C     [INPUT]     MCODE(*)         MATERIAL CODE
C     [INPUT]     LM(*,*)          NODE-ELEMENT ALLOCATION TABLE
C     [INPUT]     NBC(*)           POSITION OF EXTERNAL BOUNDARY
C     [INPUT]     IBC(*)           BOUNDARY CONDITION CODE
```

```
C        [INPUT]       DELT         TIME INCREMENT
C        [INPUT]       NSTP         NUMBER OF TIME STEPS
C        [INPUT]       NOUT         LIST INTERVAL
C        [INPUT]       NUMNP        NUMBER OF NODAL POINTS
C        [INPUT]       NNDE         MAXIMUM VALUE OF 'NUMNP'
C        [INPUT]       NUMEL        NUMBER OF ELEMENTS
C        [INPUT]       NNEL         MAXIMUM NUMBER OF NUMEL
C
****************************************************************
      DIMENSION X(NNDE) , Y(NNDE) , TEMP(NNDE)
      DIMENSION WCONT(NNDE)
      DIMENSION MCODE(NNEL) , LM(NNEL,3) , NBC(NNEL) , IBC(NNEL)
C
C    (READ CONTROL DATA)
      READ (NR,   *)    DELT , NSTP , NOUT
      WRITE(*, 9010)    DELT , NSTP , NOUT
C
C    (READ NODAL DATA)
      READ (NR,     *)  NUMNP
      WRITE(*,  9020)   NUMNP
      IF (NUMNP .GT. NNDE) THEN
        WRITE(*,9012) NUMNP , NNDE
        WRITE(*,9535)
        WRITE(*,   *)  '+++ INPUT DATA ERROR +++'
        STOP
      END IF
      DO 1000 I=1,NUMNP
        READ (NR,   *) N , X(I) , Y(I) , TEMP(I) , WCONT(I)
        WRITE(* ,9025)  N , X(I) , Y(I) , TEMP(I) , WCONT(I)

        IF (N .NE. I) THEN
          WRITE(*  ,9531) I
          WRITE(NWT,9535)
          WRITE(*,     *) '+++ INPUT DATA ERROR +++'
          STOP
        END IF
 1000 CONTINUE
C
C    (READ ELEMENTAL DATA)
      READ (NR,      *)  NUMEL
      WRITE(*,  9030)    NUMEL
      IF (NUMNP .GT. NNDE) THEN
        WRITE(*,9031) NUMEL , NNEL
        WRITE(*,9535)
        WRITE(*,*) '+++ INPUT DATA ERROR +++'
        STOP
      END IF
      DO 2000 I=1,NUMEL
        READ (NR,    *) N,NBC(I),IBC(I),MCODE(I),(LM(I,J),J=1,3)
        TM = 0.0
        DO 2100 J = 1 , 3
          TM = TM + TEMP(LM(I,J))
 2100   CONTINUE
        TM = TM / 3.
        MC = MCODE(I)
```

- 286 -

```
          CALL CONDUC(TM,MC   ,   RAMDA)
          CALL VCAPA (TM,MC   ,   ROUC)
          WRITE(NWT,9040)   N , NBC(I) , IBC(I) , MCODE(I)
     *                    , RAMDA , ROUC , (LM(I,J),J=1,3)
          IF (N .NE. I) THEN
            WRITE(*,9532) I
            WRITE(*,9535)
            WRITE(*,*) '+++ INPUT DATA ERROR +++'
            STOP
          END IF
 2000 CONTINUE
      RETURN
C
 9010 FORMAT(//
     *          ,' *** CONTROL DATA ***',/
     *          ,'   TIME INCREMENT          (DELT) : ',1PE11.4,/
     *          ,'   NUMBER OF TIME STEPS (NUMNP) : ',I11,/
     *          ,'   LIST INTERVAL          (NOUT) : ',I11)
 9012 FORMAT(' NUMBER OF NODES (NUMNP=',I6,') IS GREATER ',/
     *          ,' THAN THE LIMIT ',I6,'.',/
     *          ,' PLEASE CHANGE THE VALUE (NNDE) OF THE MAIN ROUTINE.')
 9020 FORMAT(/
     *          ,' *** NODAL DATA ***',/
     *          ,' NUMBER OF NODAL POINTS (NUMNP) : ',I8,/
     *          ,'  NO.  X-POSITION  Y-POSITION TEMPEARTURE WATER
CONT.')
 9025 FORMAT(' ',I4,1X,F8.2,1X,F10.2,1X,F10.2,1X,F7.4)
 9030 FORMAT(/
     *          ,' *** ELEMENTAL DATA ***',/
     *          ,' NUMBER OF ELEMENTS (NUMEL) : ',I8,/
     *          ,' NO.  NBC  IBC MC  THRM.COND. VLM.H.CAP.'
     *          ,'  ALLOCATION TABLE')
 9031 FORMAT(' NUMBER OF ELEMENTS (NUMEL=',I6,') IS GREATER ',/
     *          ,' THAN THE LIMIT ',I6,'.',/
     *          ,' PLEASE CHANGE THE VALUE (NNEL) OF THE MAIN ROUTINE.')
 9040 FORMAT(' ',I3,1X,2(I4,1X),I2,1X,2(1PE10.3,1X),1X,8(I3,1X))
 9531 FORMAT(' DATA ERROR (NODAL    DATA, LINE=',I4,')')
 9532 FORMAT(' DATA ERROR (ELEMENTAL DATA, LINE=',I4,')')
 9535 FORMAT(' STOP --- PROGRAM ABORT',//)
      END
C
C
*****************************************************************
**
      SUBROUTINE SIGNON
C
*****************************************************************
**
C
      WRITE(*,9001)
      RETURN
 9001 FORMAT('
',10X,'*******************************************',/
     *          ,/
     *          ,' ',10X,'          HEAT CONDUCTION ANALYZER.',/
```

```
     *          ,' ',10X,'                            FEM2',/
     *          ,' ',10X,'     2-DIMENSIONAL FINITE ELEMENT METHOD',/
     *          ,' ',10X,'            (TRIANGULAR LINER ELEMENT)',/
     *          ,/
     *          ,'
',10X,'*********************************************',/
     *          ,/)
       END
C
C
*********************************************************************
* * * * * * * * * * * *
       SUBROUTINE SWEEP(A,B,N,ND,ICON)
C
C      SOLVE SIMULTANEOUS EQUATIONS BY THE GAUSS-JORDIN ELIMINATION
C
C      [INPUT]     A(*,*)             COEFFICIENT MATRIX
C      [INPUT]     B(*)               R.H.S. VECTOR
C      [INPUT]     N                  NUMBER OF EQUATIONS
C      [INPUT]     ND                 SIZE OF THE ARRAYS A(*,*) AND B(*)
C      [OUTPUT]    B(*)               SOLUTION VECTOR
C      [OUTPUT]    ICON               CONDITION CODE
C                                         =     0    NORMAL END
C                                         = 20000    THE EQUATIONS SEEMS
TO BE SINGULAR
C                                         = 30000    THE INPUT PARAMETERS
ARE INCORRECT
C
*********************************************************************
* * * * * * * * * * * * *
       DIMENSION A(ND,ND),B(ND)
C
C      (CHECK PARAMETERS)
       IF ((N .GT. ND) .OR. (N .LT. 2)) THEN
         ICON = 30000
         RETURN
       END IF
C
C      (GET PIVOT VALUE)
       ABM = -1.0E10
       DO 1000 I=1,N
         DO 1000 J=1,N
           IF (ABS(A(I,J)) .GT. ABM) ABM=ABS(A(I,J))
 1000 CONTINUE
C
C      (CHECK IF THE EQUATIONS ARE SINGULAR)
       DO 2000 K = 1 , N
         C = ABS(A(K,K))/ABM
         IF (C.LT.1.0E-12) THEN
           ICON = 20000
           RETURN
         END IF
 2000 CONTINUE
C
       DO 3000 K = 1 , N-1
```

```
        DO 3000 J = K+1 , N
          SW = A(J,K)/A(K,K)
          B(J) = B(J) - B(K)*SW
          DO 3000 I = K+1 , N
            A(J,I) = A(J,I) - SW*A(K,I)
 3000 CONTINUE
      B(N) = B(N)/A(N,N)
C
      DO 4000 K = N-1 , 1 , -1
        DO 4500 J = K+1 , N
          B(K) = B(K) - B(J)*A(K,J)
 4500   CONTINUE
        B(K) = B(K)/A(K,K)
 4000 CONTINUE
C
      ICON = 0
      RETURN
      END
C
C
********************************************************************
*
      SUBROUTINE WRDATA(VALUE,NW,ISW,NUMNP,NNDE,DELT,ISTP)
C
********************************************************************
*
      IMPLICIT   REAL*4 (A-H,O-Z)
      DIMENSION  VALUE(NUMNP)
C
      TIME = DELT*FLOAT(ISTP)
      IHR  =  INT(TIME/3600.)
      IMIN =  INT((TIME-IHR*3600)/60)
      SEC  =  TIME-IHR*3600-IMIN*60
C
      WRITE(NW,9001) ISTP,IHR,IMIN,SEC
      IF (ISW .EQ. 1) THEN
        WRITE(NW,9012) (VALUE(I),I=1,NUMNP)
      ELSE IF (ISW .EQ. 2) THEN
        WRITE(NW,9013) (VALUE(I),I=1,NUMNP)
      ELSE
        WRITE(NW,9014) (VALUE(I)*100,I=1,NUMNP)
      END IF
C
      RETURN
C
 9001 FORMAT(' ** STEP ',I6,'  TIME ',I2,':',I2,':',F6.2' **')
 9012 FORMAT(100(' ',5(0PF11.2,1X),/))
 9013 FORMAT(100(' ',5(0PF11.0,1X),/))
 9014 FORMAT(100(' ',5(0PF11.2,1X),/))

C
      END
C
********************************************************************
*
```

```fortran
      SUBROUTINE WRFILE(VALUE,NF,NUMNP,NNDE,DELT,ISTP)
C
**********************************************************************
*
      IMPLICIT    REAL*4 (A-H,O-Z)
      DIMENSION   VALUE(NUMNP)
C
      TIME = DELT*FLOAT(ISTP)
      WRITE(NF,9001)  ISTP,TIME,(VALUE(I),I=1,NUMNP)
      RETURN
C
 9001 FORMAT(' ',i6,1x,f8.2,5000(1PE11.4,1X))
C
      END
C
**********************************************************************
**
      SUBROUTINE CLAREA(NEL,XE,YE  ,  AREA)
C
**********************************************************************
**
C
C     CALCULATE THE AREA OF THE ELEMENT
C
C    [INPUT]      NEL          ELEMENT NUMBER TO BE CALCULATED.
C    [INPUT]      XE(*)        X-COORDINATES OF NODES IN THE
ELEMENT(NEL)
C    [INPUT]      YE(*)        Y-COORDINATES OF NODES IN THE
ELEMENT(NEL)
C    [OUTPUT]     AREA         AREA OF THE ELEMENT
C
**********************************************************************
**
      DIMENSION XE(3) , YE(3)
C
      AREA =(   XE(2)*YE(3) + XE(1)*YE(2) + XE(3)*YE(1)
     *        - XE(1)*YE(3) - XE(2)*YE(1) - XE(3)*YE(2) )*0.5
      IF (AREA .LE. 0.0) THEN
        WRITE(*,9001) AREA , NEL
        WRITE(*,*) '+++ INPUT DATA ERROR +++'
        STOP
      END IF
      RETURN
C
 9001 FORMAT(' (CLAREA) ZERO OR NEGATIVE AREA (',1PE11.4,') IN ',I6)
      END
C
**********************************************************************
*****
      SUBROUTINE EVAP(WCONT,WEQ,WEQDPV,DELT,NUMNP , GENM,EVV)
C
C    [INPUT]      TE(*)        TEMPERATURE   OF NODES IN THE
ELEMENT(NEL)
C    [INPUT]      PVE(*)       VOID PRESSURE OF NODES IN THE
ELEMENT(NEL)
```

```
C      [OUTPUT]    GENM(*)       GENETARION OF VAPORIZING WATER
(KG/M3*S)
C
*********************************************************************
*****
       DIMENSION WCONT(NUMNP) , WEQ(NUMNP) , GENM(NUMNP)
       DIMENSION WEQDPV(NUMNP) , EVV(NUMNP)
       CALL EVAPGANM(GANM)
C
       DO I = 1,NUMNP
         GENM(I) =  GANM*(Wcont(I)-Weq(I))
         EVV(I)  =  GANM*WEQDPV(I)*DELT
       enddo
C
       RETURN
       END
C
*
*********************************************************************
**
       subroutine EQUILW(TEMP,PRESV,PVSAT,NUMNP , WEQ,WEQDPV)
C
C      CONDUCTIVITY,CAPACITY AND GENERATION MATRIX OF WATER VAPOR
C
C      [INPUT]         temp(*)             nodal temperature array
(C)
C      [INPUT]         presv(*)    nodal vapor pressure array (Pa)
C      [INPUT]         pvsat(*)    nodal saturated vapor pressure
array [Pa]
C      [INPUT]         numnp       number of nodal points
C      [OUTPUT]   weq(*)           equilibrium water content
[kg/kg]
C      [OUTPUT]   weqdpv(*)   gradiant of weq with respect to
C                                   vapor pressure
[(kg/kg)/Pa]
*
*********************************************************************
**
       IMPLICIT REAL*4 (A-H,O-Z)
       dimension temp(numnp), presv(numnp), pvsat(numnp)
       dimension weq(numnp), weqdpv(numnp)
*      (local array)
       dimension tabs(numnp), rh(numnp), cx(numnp), wcut(numnp)
       dimension rlogrh(numnp)
*
       parameter (r = 8314.3, rhcut = 0.9999  , wmax = 0.12)
*      (adsorption parameters)
       parameter (rh0   = 0.0001)
*      (freundlich parameters)
       parameter (rh1   = 0.625, cf = 5.24006844 , rnf = 1.27403355)
*      (halsey parameters)
       parameter (ch =15.4065733, rnh = 2.71069145)
*
       do i = 1 , numnp
         tabs(i) = temp(i) + 273.2
```

```
         rh(i) = presv(i)/pvsat(i)
*
         if (rh(i) .le. 0) then
           weq(i) = 0.0
             weqdpv(i) = 0.0
         else if (rh(i) .le. rh0) then
           cx(i) = (1./(r*tabs(i)))**(1./rnh)
           rnfi  = 1./rnf
           rh0n  = rh0**rnfi
           rh0nm1= rh0**(rnfi-1.)
           weq(i) = (cx(i)*cf)*(rh0n + rnfi*rh0nm1*(rh(i)-rh0))
             weqdpv(i) = ((cf*cx(i))*(1./rnf)*(rh0**(1./rnf-
1.)))/pvsat(i)
         else if (rh(i) .lt. rh1) then
*        ((( frundlich equation )))
           cx(i)      = (1./(r*tabs(i)))**(1./rnh)
           weq(i)     = (cf*cx(i))*(rh(i)**(1./rnf))
             weqdpv(i) = (cf*cx(i))*(1./rnf)*(rh(i)**(1./rnf-1.))
         else if (rh(i) .lt. rhcut) then
*        ((( halsey equation )))
           rlogrh(i) =   log(rh(i))
           weq(i)     = (-ch/(r*tabs(i)*rlogrh(i)))**(1./rnh)
           weqdpv(i) = - weq(i)/(rnh*presv(i)*rlogrh(i))
         else
*        ((( almost saturated )))
           rlogrh(i) =   log(rhcut)
           weq(i)     = (-ch/(r*tabs(i)*rlogrh(i)))**(1./rnh)
           weqdpv(i) = - weq(i)/(rnh*presv(i)*rlogrh(i))
         end if
*
      enddo
*
      return
      end
C
C
*****************************************************************
******************
      SUBROUTINE VERPAS(TEMP,NUMNP   , PVSAT)
C
C    [INPUT]     TEMP(*)        TEMPERATURE OF NODS IN THE
ELEMENT(NEL)
C    [INPUT]     ATEMP(*)       ABSOLUTE TEMPERATURE OF NODES IN THE
ELEMENT(NEL)
C    [OUTPUT]    PVSAT(*)       SATURATED VAPOR OF WATER OF NODS IN
THE ELEMENT(NEL)
C
*****************************************************************
**************
      DIMENSION TEMP(NUMNP) , PVSAT(NUMNP)
C
      DO I=1, NUMNP
        T = TEMP(I)
        CALL VERPAS1(T   , PVS)
        PVSAT(I) = PVS
```

```
      ENDDO
C
      RETURN
      END
C
**********************************************************************
**
      SUBROUTINE VERPAS1(T   ,   PVS)
C
**********************************************************************
**
      PARAMETER (R    = 8314.3)
      PARAMETER (AV   = 9.7262E+11 , EV = 4.98858E+07)
      PARAMETER (EVSR = EV/R)
C
      ATEMP = T+273.16
      PVS = AV*EXP(-EVSR/ATEMP)
C
      RETURN
      END
C
C
**********************************************************************
*******
      SUBROUTINE WATER(GENM,NUMNP,DELT , WCONT)
C
C   [INPUT]       GENM       GENETARION OF VAPORIZING WATER [KG/M3*S]
C   [INPUT]       WCONT      WATER CONTENT [KG/KG]
C   [INPUT]       RHO        DENSITY IF CONCRETE [KG/KG]
C   [INPUT]       DELT       TIME INCREMENT
C   [OUTPUT]      WCONT      WATER CONTENT [KG/KG]
C
**********************************************************************
*******
      DIMENSION GENM(NUMNP) , WCONT(NUMNP)
C
      CALL DENS(RHO)
      WCONT=WCONT-GENM*DELT/rho
      DO 1000 I = 1 , NUMNP
      IF (WCONT(I).LE.0.0) THEN
      WCONT(I) = 0.0
      END IF
 1000 CONTINUE
C
      RETURN
      END
C
C
**********************************************************************
******
      SUBROUTINE BUILD(NEL,LM,WM,FV,NNDE,NNEL   ,  WMAT,FVEC)
C
C     PUT ELEMENTAL EQUATIONS INTO WHOLE EQUATIONS.
C
C   [INPUT]       NEL            ELEMENT NUMBER
```

```
C     [INPUT]     LM(*,*)        NODE-ELEMENT ALLOCATION TABLE
C     [INPUT]     WM(*,*)        COEFFICIENT MATRIX OF THE ELEMENTAL
EQUATIONS
C     [INPUT]     FV(*)          R.H.S VECTOR OF THE ELEMENTAL
EQUATIONS
C     [INPUT]     NNDE           SIZE OF THE ARRAYS WMAT(*,*) , FVEC(*)
C     [INPUT]     NNEL           SIZE OF THE ARRAY LM(*,*)
C     [OUTPUT]    WMAT(*,*)      COEFFICIENT MATRIX OF THE
WHOLEEQUATIONS
C     [OUTPUT]    FVEC(*)        R.H.S VECTOR OF THE WHOLE EQUATIONS
C
*******************************************************************
*******
      DIMENSION WM(3,3) , FV(3)
      DIMENSION WMAT(NNDE,NNDE) , FVEC(NNDE) , LM(NNEL,3)
C
      DO 1000 I = 1 , 3
        IX = LM(NEL,I)
        FVEC(IX) = FVEC(IX) + FV(I)
        DO 1000 J = 1 , 3
          IY = LM(NEL,J)
          WMAT(IX,IY) = WMAT(IX,IY) + WM(I,J)
 1000 CONTINUE
C
      RETURN
      END
C
*******************************************************************
      SUBROUTINE TRIM(X,XMIN,XMAX)
C
*******************************************************************
C
      IF (X .LT. XMIN) X = XMIN
      IF (XMAX .LT. X) X = XMAX
C
      RETURN
      END
C
C
C
C
*******************************************************************
C
*******************************************************************
C     SLAVE ROUTINES
C
*******************************************************************
C
*******************************************************************
C
C
*******************************************************************
      SUBROUTINE CLEAR2D(ARRAY,ND,N)
C
*******************************************************************
```

```
      DIMENSION ARRAY(ND,ND)
C
      DO I = 1 , N
        DO J = 1 , N
          ARRAY(I,J) = 0.0
        ENDDO
      ENDDO
C
      RETURN
      END
C
*****************************************************************
      SUBROUTINE FINDBC(NB,NB1,NB2,NB3)
C
*****************************************************************
C
      NB1 =   NB                   / 100
      NB2 = (NB-NB1*100)           /  10
      NB3 = (NB-NB1*100-NB2*10)
C
      RETURN
      END
C
*****************************************************************
      SUBROUTINE CHKERR(ICON,ISTP,VAR)
C
*****************************************************************
      CHARACTER*14 VAR
C
      IF (ICON .NE. 0) THEN
        WRITE(*,9000)
        WRITE(*,9010) ISTP
        WRITE(*,9020) VAR
        STOP
      END IF
C
      RETURN
 9000 FORMAT(' +++ SOLUTION ERROR +++ ')
 9010 FORMAT('    STEP = ',I8)
 9020 FORMAT('    VAR  = ',A14)
      END
C
C
C
*****************************************************************
C     CONFIGURATION SECTION
C
*****************************************************************
C
C
C
*****************************************************************
      SUBROUTINE TRANSFV(HV)
C
*****************************************************************
```

```fortran
C
      HV = 0.001
C
      RETURN
      END
C
**********************************************************************
      SUBROUTINE TRANSFA(HA)
C
**********************************************************************
C
      HA = 0.001
C
      RETURN
      END
C
**********************************************************************
      SUBROUTINE PERMEA(EPSR,KAPP)
C
**********************************************************************
      REAL KAPP
C
      KAPP = 0.00000000447*(EPSR**3/(1.-EPSR)**2)
C
      RETURN
      END
C
**********************************************************************
      SUBROUTINE DENS(RHO)
C
**********************************************************************
C
      RHO = 2500.
C
      RETURN
      END
C
C
**********************************************************************
**
      SUBROUTINE VOID(EPSR)
C
**********************************************************************
**
C
      EPSR = 0.11858
C
      RETURN
      END
C
**********************************************************************
**
      SUBROUTINE EVAPGANM(GANM)
```

```
C
***********************************************************************
**
C
      GANM=1.
C
      RETURN
      END
```

Appendix B.5

MATLAB Program to draw 3D graphs of moisture model program results

```
%Display of the data like a topography and smoothing
clear all
hold off


load chelvam.txt;

Pressure1= chelvam (:,3);
Pressure2= chelvam (:,4);
Pressure3= chelvam (:,5);
Pressure4= chelvam (:,6);
Pressure5= chelvam (:,7);
Pressure6= chelvam (:,8);
Pressure7= chelvam (:,9);
x= chelvam (:,1);
y= chelvam (:,2);

nr=size(chelvam);
NumberOfReadings=nr(1);



%surf(result(p,q));


%plot(y,x);



plot3(chelvam (:,1), chelvam (:,2), chelvam (:,5))
grid on;
view([1 1 1]);
ylabel('Thickness of beam, [mm]')
xlabel('Length of beam, [mm]')
zlabel('Pressure, [MPa]')
```

Appendix B.6

MATLAB Program to draw 3D graphs of moisture model program results

```
clear all
hold off


load chelvam.txt;


x= chelvam (:,1);
y= chelvam (:,2);

    ii=1:7;

Pressure(:,ii)= chelvam (:,2+ii);


nr=size(chelvam (:,2+ii));
NumberOfReadings=nr(1);

counter2=1;
    j=1:NumberOfReadings-1;
        (abs(abs(x(j+1))-abs(x(j)))>5);
        counter2=counter2+1;
        end;
    end;

counter=1;
    i=1:10-1;
    (floor(x(i+1))==floor(x(i))& floor(x(1))==floor(x(i+1)));
        counter=counter+1 ;
        else
        end;
    end;


    l=1:2:counter2;
        m=1:counter;
            matrix(m,l,ii)=Pressure(m+counter*(l-1),ii);
        end;
    end;

    s=2:2:counter2;
        t=1:counter;
            matrix(t,s,ii)=Pressure(s*counter-t,ii);
        end;
    end;

    q=1:counter2-1;
        p=1:counter-1;
```

```
result(p,q,ii)=(matrix(p,q,ii)+matrix(p,q+1,ii)+matrix(p+1,q,ii)+mat
rix(p+1,q+1,ii))./4;
        %result(p,q,ii)=matrix(p,q,ii);
    end;
end;


figure(ii)
surf(result(:,:,ii));
view([.3 3 4]);


ylabel('Thickness of beam, [mm]')
xlabel('Length of beam, [mm]')
zlabel('Pressure, [MPa]')
grid on;

   end
```

References

1.01. Hertz K.D. heat induced explosion of dense concrete. Report No.166, Institute of Building Design Technology, University of Denmark, 1984

1.02. Castillo C. and A.J. Durrani. Effect of Transient High Temperature on High Strength Concrete. *ACI Materials Journal*, **V.87**, No.1, Jan-Feb 1990

1.03 Sanjayan G. and Stocks L.J. Spalling of high-Strength Silica Fume Concrete in fire. *ACI Materials Journal* **V.90**, No.2, Mar-Apr 1993

1.04. Diederichs U, Jumpannen U., Morita T., Nause P. and Schneider U. Concerning Spalling Behaviour of High Strength Concrete Columns. *ACI Materials Journal*. 1995

1.05. Tachibana D., Kumagai H. and Suzuki T. High Strength Concrete for Building Construction. *ACI Materials Journal*, **V.9, No.4**, 1994.

1.06. Copier W.J. The spalling of normal weight and light weight concrete exposed to fire. *Journal of the American Concrete Institute*. **Vol.12, No.4**, 1983

1.07. Hanneman. M and Thomas. H. Resistance of reinforced concrete elements and floors on fires. In Deutscher Ausschub fur Stahlbeten 132, W. Ernest and Son Berlin 1959

1.08. Malhotra II.L. Spalling of concrete in fires. Technical report 118. Construction Industry Research and Information Association, London,1984

1.09. Meyer - Ottens C. The question of spalling of concrete structural elements of standard concrete under fire loading. PhD Thesis, Technical University of Braunschweig, Germany, 1972

1.10. Nekrasov K.D., Fire resistance concrete Moscow, Strousdat, 1974

1.11. Connolly. R., P.J.E. Sullivan., Spalling of high strength concrete at elevated temperatures Applied fire science Vol 6(1)3-4, 1996-97

1.12. Zhukov V.V. Explosive failure of concrete during a fire. Proceedings - Fire resistant Concrete. Stroezdat, Moscow. 1970

1.13. Christiaanse A, Langhorst A. and Gerriste A. Discussion of fire resistance of lightweight concrete and spalling. Dutch Society of Engineers (STUVO), report 12, Holland .1971 .

1.14. Hertz K.D. Danish Investigations on Silica Fume Concrete at Elevated Temperatures. *ACI Materials Journal*, **V.89, No.4**, 1992

1.15. Williamson R.B. and Rashed I. High strength concrete and mortars in high temperature environments. Proceedings of Materials Research Society Symposium, V.42, 1985, California

1.16. Shirley T., Burg R.G. and Fiorato A.E. Fire endurance of High-Strength Concrete Slabs. *ACI Materials Journal* **V.85, No.2**, March-April 1988,

1.17. Ashton L.A. and Davey N. Investigations of building fires - part 5. National Building Studies Research Paper 12, HMSO, London 1953

1.18. Bogoslovski V. and Roitman V.M. Explosive failure of concrete in fire. Beton I Zhelzobeton, V.24, No.6, 1978, pp 39 - 41

1.19. Furumura F., Ave T., Shinohara Y., Tomaturi K. Mechanical properties of high strength concrete at high temperatures. Report of the Research

Laboratory of Engineering Materials, Tokyo, Institute of technology No. 187, Japan, 1993

1.20. Connolly R.J. Spalling of concrete in Fire. PhD Thesis, University of Aston, Birmingham, April, 1995, pp288

1.21. Akhtaruzzaman A.A. and Sullivan P.J.E. Explosive spalling of concrete exposed to high temperature. Imperial College, Research report CSTR 70 / 2. London, The College, December, 1970, 24pp

1.22 Castillo C. and A.J. Durrani. Effect of Transient High Temperature on High Strength Concrete. *ACI Materials Journal*, **V.87, No.1**, Jan-Feb 1990

1.23 C.I.B. Fire design of concrete structures in accordance with CEB/FIP Model code 90. Information bulletin No. 28, C.E.B. Switzerland,1991

1.24 Harmathy, T.Z, and Shorter, G.W......Proc. Institution of Civil Engineers, vol 20, 1965, pp 313.

1.25 Tachibana D., Kumagai H. and Suzuki T., High Strength Concrete for Building Construction. *ACI Materials Journal*,V.9, No.4,1994.

1.26 Dougill J.W. The effect of high temperature on concrete with referance to thermal spalling. PhD thesis. King's College, London, 1972

1.27 Hertz K.D. Heat induced explosion of dense concrete. Report No.166, Institute of Building Design Technology, University of Denmark, 1984

2.01 Woolson, I.H.. Investigation of the Effect of Heat on the Crushing Strength and the Elastic Properties of Concrete. Proc. ASTM vol 5, p335. 1905.

2.02 Norton, C.L. Some Thermal Properties of Concrete.Journal of the ASME vol 35, part I, pp 1011 - 1021. 1913.Also in Engineering Neus, p711, 1910.

2.03 Lea, F.C. The Effect of Temperature on Some of the Properties of Materials. Engineering vol 110, No 2852, pp 293 - 298, 1920.

2.04 Grun, R. and Beckman.H. The Behaviour of Cement, Aggregates and Concrete at High Temperatures. Cement and Cement Manufacture, vol 3. No 3. pp 430 - 442. 1930.

2.05   Willis.T.F. and DeReus.M.E. Thermal Volume Change and Elasticity of Aggregates and their Effects on Concrete. Proc. ASTM vol -39, pp 919. 1939.

2.06   Giles R.T. What Heat will Concrete withstand without Deterioration. Proc. ACI vol 35, pp 417. 1939.

2.07   Walker.S, Bloem. D.L. and Mullen, W.G. Effect of Temperature Changes on Concrete as Influenced by Aggregates. Proc. ACI, vol 48, pp 661 - 679. 1952

2.08   Mitchell.L.J Thermal Expansion Tests on Aggregates, Neat Cements and Concretes. Proc. ASTM vol 53, pp 963.1953.

2.09   Harada. T., Thermal expansion of concrete at high temperature. Trans. AIJ, No 46, pp 1-10. 1953.

2.10   Murashev. V.I. Some Characteristics of the Theory of Design of Heat Resistant Plain and Reinforced Concrete. State press for literature on building and Architecture.Moscow 1954.

2.11   Malhotra. H.L. The Effect of Temperature on the Compressive Strength of Cement. Proc vol 8 No 23, pp 85-94 1956

2.12   Seaman .J.C. and Washa.G.W. Variation of mortar and concrete properties with high temperature Proc. ACI Vol 54 pp 385 .1957.

2.13   Philleo.R.E. Some Physical Properties of Concrete at High Temperature. Proc.ACI. Vol 54, pp 857-864. 1958.

2.14   Dougill .J.W. An investigation into the residual compressive strength of concrete after exposure to high temperatures Msc. Thesis University of London. 1960.

2.15   Zoldners. N.G. Malhotra. V.M. and Wilson H.S. High Temperature Behavior of Aluminous Cement Concrete Containing Differect Aggregates. Proc. ASTM vol 63.1960.

2.16   Hannant D.J. and Pell, P.S. Thermal Stresses in Reinforced Concrete Slabs. MCR vol 41, pp 91 - 98. 1962.

2.17   Hatano.T. Temperature Effect on the Deformation and Failure of Concrete under Statical Compressive Load. Trans. JSCE, No 111, pp 11 - 15. November 1964.

2.18   Campbell-Allen. D., Low. E.W.E. and Roper.H. An Investigation on the Effect of Elevated Temperatures on Concrete for Reactor Vessels. Nuclear Structural Engineering vol 2, pp 382 - 388. 1965.

2.19   Cruz.C.R. Elastic Properties of Concrete at High Temperature. PCA Journal vol 8, No 1, pp 37 - 45. 1966.

2.20   Harmathy.T.Z. and Berndt.J.E. Hydrated Portland Cement and Lightweight Concrete at Elevated Temperatures. Proc.ACI vol 63, pp 93 - 112. 1966.

2.21   Furumura. F. The Stress-Strain Curve of Concrete at High Temperature. No 1. Report for Meeting of the Architectural Institute of Japan. 1966.

2.22   Campbell-Allen.D. and Desai. P.M. The Influence of Aggregate on the Behavior of Concrete at Elevated Temperatures. Nuclear Engineering and Design,vol 6, pp 65 - 77.1967.

2.23   Harada.T., Takeda. J, Yamane.S. and Furumura. F, Strength, Elasticity and Thermal Properties of Concrete Subjected to Elevated Temperatures. ACI seminar on Concrete for Nuclear Reactors. West Berlin. 1970.

2.24   Takeda. J. Harada.T., Effect of Curing Temperature on Strength and Elasticity of Concrete Subjected to Elevated Temperatures. ACI seminar on Concrete for Nuclear Reactors. West Berlin. 1970.

2.25   Nasser,K.W., Marzouk,H.M., Properties of Mass Concrete Containing Fly ash at High Temperatures, ACI J 76 (4) 1974.

2.26   Grainger, B.N., Concrete at high temperature, Central Electricity Research Laboratories, U.K. 1979.

2.27   Diederichs,U., Jumppanen, U.M.,Penttala,V., Behaviour of high strength concrete at high temperatures, Report No. 92 Helsinki University of Technology, Department of structural Engineering, 1989.

2.28   Sullivan, P.J.E., and Sharshar,R., The performance of concrete at elevated temperatures. Fire Technology ,. pp 240. August 1992.

2.29   Sarshar,R., Khoury,G.A., Material and environmental factors influencing the compressive strength of unsealed cement paste and concrete at high temperatures, Magazine of Concrete Research 45 (162). 1993.

2.30   Hammer,T.A., High strength concrete phase 3, compressive strength and E - modulus at elevated temperature, SP 6 Fire Resistance Report 6.1 SINTEF Structures and concrete STF 70 A95023, 1995.

2.31   Ghosh,S., Nasser,K.W., Effect of high temperature and pressure on strength elasticity of lignite fly ash and silica fume concrete, *ACI Material Journal*. 1998.

2.32   Khoury, G., Felicetti, R., Mechanical behaviour of HPC and UHPC Concretes at High Temperature in Compression and Tension. ACI International Conference. 1999.

2.33   Wong,Y.L., Poon,C.S., Anson,M., Yigang,X., Residual properties of PFA concrete subjected to high temperatures. International Symposium on high Performance Concrete, Hong Kong, December 2000.

2.34 Wu, B., Li,H., Su,X., Effect of high temperature on residual mechanics properties of confined and unconfined high strength concrete. *ACI Material Journal.* August 2002

2.35 Davis H.S., Effects of High Temperature Exposure on Concrete. Materials Research and Standards, vol 7, No 10,pp 452 - 459. 1967

2.36 Crook.D.N. and Murray, M.J. Regain of Strength after Firing of Concrete.MCR vol 22, No 72, pp 149 - 154.1970

2.37 Sullivan. P.J.E, The Structural Behavior of Concrete at Elevated Temperature.Ph D Thesis. University of London. 1970.

2.38 Nishizawa.N. and Okamura, H. Strength and Inelastic Properties of Concrete at Elevated Temperature. Paper presented at the ACI seminar on Concrete for Nuclear Reactors. West Berlin. 1972

2.39 Khoury,A..,. Sullivan. P.J.E., Grainger,B.N., Transient thermal strain of concrete during first heating cycle to 600 °C , Magazine of Concrete Research. 1986.

2.40 Xuli, Fu., Chung, L., Effect of Admixtures on Thermal and Thermomechanical Behaviour of cement paste. *ACI Material. Journal* 1999.

2.41 Baker.G. The Performance of Reinforced and pre-stressed Concrete Beams after exposure to High Temperatures. 2000. (Personal Contract).

2.42 Binsheng,Z., Neand, B., Residual fracture toughness of normal and high strength gravel concrete after heating to 600 ° C. *ACI Material. Journal* June 2002.

3.01 Hull.W.A., The Behavior of Reinforced Concrete Columns under Fire Test. Concrete and Constructional Engineering. vol 15, pp 187 and 262. 1920. Also published in the Proc. ACI vol 16, p 20. 1920.

3.02 Menzel.C.A., Tests of the Fire Resistance and Strength of Walls of Concrete Masonary Units. Proc. ASTM vol 31,part II, p 607. 1931.

3.03 Menzel.C.A., Tests of the Fire Resistance and Thermal Properties of Solid Concrete Slabs and Their Significance. Proc. ASTM vol 43, pp 1099 - 1147. 1943.

3.04 Ashton.L.A. The Fire Resistance of Prestressed Concrete Floors. Civil Engineering and Public Works Review, vol 46. pp 843 - 845, and 940 - 943. 1951.

3.05 Robertson.A.F. and Ryan.J.V., Proposed Criteria for Defining Load Failure of Beams, Floors and Roof Construction during Fire Tests. Journal of Research, National Bureau of Standards, vol 63C, p 121. 1959.

3.06 Ashton.L.A. and Bate.S.C.C., The Fire Resistance of Prestressed Concrete Beams. *ACI Journal*, vol 32, 1961.

3.07 Harmathy.T.Z., A Treatise on the Theoretical Fire Endurance Rating. ASTM Special Technical Publication No 301, pp 10 - 40. 1961.

3.08 Selvaggio.S.L. and Carlson.C.C., Effect of Restraint on Fire Resistance of Prestressed Concrete. ASTM Special Technical Publication No 344. pp 91 - 115. 1962.

3.09 Selvaggio.S.L. and Carlson.C.C., Fire Resistance of Prestressed Concrete Beams. *Journal of the PCA*, vol 60,No 1,2. January - May, 1964.

3.10 Ashton.L.A., Effects of Restraint on Longitudinal Deformation or Rotation. Symposium on Firs Resistance of Prestressed Concrete Beams held in Braunschweig, West Germany,1965.

3.11 Pearse.N.S. and Stanzak.W.W., Load and Fire Test Data on Steel Supported Floor Assemblies. Fire Test Methods, Restraint and Smoke. ASTM Special Technical Publication No 422. 1966.

3.12 Selvaggio. S.L. and Carlson.C.C., Restraint in Fire Tests of Concrete Floors and Roofs. Fire Test Methods, Restraint and Smoke. ASTM Special Technical Publication No 422. 1966.

3.13 Harmathy.T.Z., Deflection and Failure of Steel Supported Floors and Beams in Fire. Fire Test Methods, Restraint and Smoke. ASTM Special Technical Publication No 422. 1966.

3.14 Bletzacker.R.W., Fire Resistance of Protected Steel Beam Floor and Restraint. Fire Test Methods, Restraint and Smoke. ASTM Special Technical Publication No 422. 1966. pp 63 – 92.

3.15   Dougill.J.W., The Relevance of the Established Method of Structural Fire Testing to Reinforced Concrete. Applied Materials Research vol 5, No 4, pp 235 - 240. 1966.

3.16   Issen.L, Scaled Models in Fire Research on Concrete Structures. Journal of the PCA Research and Development. September 1966. pp 10 - 26.

3.17   Gustaferro.A.H. and Selvaggio., S.L. Fire Endurance of Simply Supported Prestressed Concrete Slabs. Journal of the Prestressed Concrete Institute, vol 12, No 1, pp 37 - 53. 1967.

3.18   Abrams.M.S. and Gustaferro., A.H Fire Endurance of Concrete Slabs as Influenced by Thickness, Aggregate type and Moisture. *Journal of the PCA* Research and Development, vol 10, No 2, 1968.

3.19   Saito. H., Behaviour of End Restraint Concrete Member in Fire. Building Research Institute. Research Paper No 32 Building Research Institute, Ministry of Construction. Govt. of Japan. Japan. 1968.

3.20   Issen. L.A., Gusfcaferro. A.H., and Carlson. C.C., Fire Tests of Concrete Members : An Improved Method for Estimating Thermal Restraint Forces. ASTM Special Technical Publication No 464. pp 153 - 185. 1970.

3.21   Abrams. M.S., Gustaferro. A.H. and Salse., Fire Tests of Concrete joist-Floors and Roofs. PCA Research and Development Bulletin No 006.01. 1973.

3.22   Gustaferro. A.H., Abrams. M.S. and Salse., Fire Resistance of Prestressed Concrete Beams : Study C - Structural Behaviour during Fire Tests.PCA Rasearch and Development Bulletin No 009.01B. 1974.

3.23   Malhotra. H.L., Fire Resistance of Structural Concrete Beams. Fire Research Note No 741. Fire Research Station. May 1969.

3.24   Meyer-Ottens. C., Abplatzungversuche. Braunschweig Symposium. Pp 60 - 66. 1965.

3.25   Dougill J.W. Contribution to the Discussion of a paper by H.L. Malhotra and R.F. Stevens. Proceedings of Institution of Civil Engineers, vol 29 pp 451-452.1964.

3.26   Dougill J.W . Some Aspects of Spalling of Concrete Caused by Explosure to High Temperatures. Report Submitted to the Fire Research Station. 1969

3.27   Dougill J.W The Effect of High Temperature on the Strength of Concrete with Reference to Thermal Spaling. PhD Thesis, University of London1971.

3.28   Shorter.G.W and Harmathy.T.Z., Contribution to the Discussion of paper by L.A Ashton and S.C.C Bate, Proceedings, Institute of Civil Engineers, vol 20, pp 313-315.1 961

3.29   Harmathy.T.Z., Effect of Moisture on the Fire Endurance of Building Elements. ASTM Special Technical Publication no385 pp74-94. 1965

3.30   Newman.K. The Structure and Engineering Properties of Concrete. In J.R Rydzewski Theory of Arch Dams. Pergamon, 1965 pp683-712.

3.31   Timoshenko.S Theory of Plates and Shells. 1stEdition. Mcgraw- Hill 1940.

3.32   Odeen.K., Fire Resistance of Reinforced Concrete Beams Braunschweig Symposium. pp 75 - 79. 1965.

3.33   Saito. H., Explosive Spalling of Prestressed Concrete in Fire. Japanese Government. Ministry of Construction, Building Research Institute Occasional Report No 22, pp 18 1965.

3.34   Harmathy.T.Z., Effect of Moisture on the Fire Endurance of Building Elements. ASTM Special Technical Publication No 385, pp 74 - 94. 1965.

3.35   Dougill. J.W., The Effects of High Temperature on the Strength of Concrete With Reference to Thermal Spalling. Ph D Thesis. University of London. 1976.

3.36   Hertz, K.D., Heat Induced Explosion of Dense Concrete, Report No 166, Institute of Building Technology, University of Denmark, 1984

3.37   Williamson.R.B ,. Rashed I., High Strength Concrete and Mortars in High Temperature Environments. Proceeding of Materials Research Society Symposium, *42,* California, 1985.

3.38   Shirley.T, Burg R.G.,. Fiorato,A.E, Fire Endurance of High Strength Concrete Slabs, *ACI Materials Journal.* 85:2, March-April 1988.

3.39   Castillo,C. Durrani,A.J., Effect of Transient High Temperature on High Strength Concrete, *ACI Materials Journal*, 87:1, January-February 1990.

3.40   Hertz, K. Danish, Investigations on Silica Fume Concretes at Elevated Temperatures, *ACI Materials Journals* 89 (4) 1992

3.41   Sanjayan,G.,. Stocks,L.J, Spalling of High-Strength Silica Fume Concrete in Fire, *ACI Materials Journal*, 90:2, March-April 1993.

3.42   Furumura,F., Ave,T., Shinohara,Y., Tomaturi,K., Kuroha,K, Kokubo,I., Mechanical Properties of High Strength Concrete at High Temperatures, Report of the Research Laboratory of Engineering Materials Tokyo, Institute of technology No. 187, Japan, 1993

3.43   Tachibana,D., Kumagai.H., Yamazaki,N., Suzuki,T.,   High Strength Concrete for Building Construction, *ACI Materials Journal*,9:4,pp.390-400, 1994.

3.44   Khoury. G., High performance Concrete at High Temperature ACI Spring Convention March 1999.

3.45   Felicetti.R., Gambarova, P.G., Effects of high temperature on the residual compressive strength of high strength siliceous concretes, *ACI Materials Journal* 95 (4) 1998.

3.46   Chi-sun Poon , Azhar,S., Comparison of the Strenth and Durability Performance of Normal and High Strength Pozzolanic Concretes at Elevated Temperatures (Personal contract)

3.47   Dorn .J.E Journal of Mechanical Physics and solids. 1955

3.48   BSS 476 Part 3 Fire Tests on Building Materials and Structures. British Standard Specification for Standard Furnace Tests.

4.01   Powers, T.C.and Brownyard T.L. studies of the physical   properties of hardened Portland cement Paste. Proc. ACI vol 43, 1947, also Bulletin no, 22 of Research and Development Laboratories of the Portland Cement Association, Chicago, 1948.

4.02   Luikov, A.V. Heat and mass transfer in Capillary Porous Bodies. Pergamon Press, London, pp 191 – 195.

4.03   Nielsen, K.E.C. Measurement of Water Vapour Pressure in Hardened Concrete.Bulletin no. 35 of Swedish Cement and Concrete Research Institute. Stockholm, 1967. pp9 -15,

4.04   Ishai, O. Drying Shrinkage Mechanism in Hardened Cement Paste and mortar. Applied materials Research vol 5, No, 3 July 1966. pp 154 - 161.

4.05   Vos, B, H. and Tammes, E Moisture and Moisture Transfer in Porous Materials. Report No, BI-69-96, Institute TNO for Building Materials and Building Structures. Netherlands, 1969.

4.06   Gilkey, H.G Engineeriny News Record, vol 119, 1937. PP 630.

4.07   Lea, F.M. and Desch, C.H Chemistry of cement and concrete Revised Edition, Edward Arnold Limited, London, 1956, pp 537.

4.08   Mills, R.H Strength - Maturity Relationships for Concrete
Which is allowed to dry, Proceedings, Symposium on Concrete and Reinforced Concrete in hot Countries, RILEM. Paris, 1960, Part I, pp1-28

4.09   Neville, A.M. Properties of concrete. Sir Isaac Pitman and sons Ltd. London, Reprinted.1968.

4.10   Hannant, D.C Effect of Heat on Concrete Strength. Engineering
        (London), vol 197, no, 21, February 1964, pp 302.

4.11   Lankard D.R., Birkimer, Q.L. and Fondriest, F.F., and Snyder. Effects of
        Moisture. Content on the Structural Properties of Portland Cement
        Concrete Exposed to Temperature up to 500F. ACI Special Publication
        No, SP-25, Temperature and Concrete, 1971, pp 59-102

4.12   Harmathy, T.Z Experimental Study on Moisture and Fire Endurance, Fire
        Technology, 1968, pp 52-59

4.13   Harmathy, T.Z A Treaties on Theoretical Fire Endurance Rating,
        Symposium on Fire Test Methods, ASTM Special Technical Publication
        No, 301, 1961. pp 10-40

4.14   Harmathy, T.Z Effect of Moisture on the Fire Endurance of Building
        Elements, Moistures of Materials in Relation to Fire Tests, ASTM
        Special Technical Publication No, 385,1965, pp 74 – 95.

4.15   Brams,L. M.S, and Gustaferro, A.H Fire Endurance of Concrete Slabs as Influenced by Thickness, Type and Moisture, *Journal of the Portland Cement Association.* Research and Development laboratories, May 1968.

4.16   Brams. M.S, end Orals, D.L Concrete Drying Methods and their Effect on Fire Resistance, Moisture of Materials in Relation to Fire Tests, ASTM Special Technical Publications No, 385. 1965, pp 52-73.

4.17   Jesser,L Zement, Sweden. vol 16, 1927. p 741.

4.18   Seito.L. Explosive Spalling of Concrete in Fire, Occasional Report No. 22, ministry of Construction. Building Research institute. Govt. of Japan, pp 18. Also reprinted in the Braunschweig Sympasium on Fire Resistance of Prestressed Concrete, June 1965. pp 80-91

4.19   Philleo, R.E. Introductory remarks to a discussion on thermal and Freezing-Thawing Behaviour, Conference on the Matrix of Concrete, *ACI Material* Report No, 313, 1968.

4.20   Harmathy, T.Z, and Shorter, G.W. Proc, Institution of Civil Engineers, vol 20, 1965. pp 313.

4.21 Dougill, J.W Some Aspects of Spalling of Concrete caused by exposure to High Temperature. Report to Fire Research Station. July, 1969.

4.22 Meyer, Ottens, C. Symposium on Fire Resistance of Prestressed Concrete, pp 59-66. 1965.

4.23 Harmathy.T.Z. Simultaneous moisture and heat transfer in porous systems ICE fundamentals 8-1,92-103,1969.

4.24 Matsumoto, M. Doctoral Dissertation (in Japanese), Faculty of Engineering, Kyoto University, Japan 1978.

4.25 Harada, K. Heat and mass transfer in an intensely heated wall. Faculty of Engineering, Kyoto University, Japan 1995.

4.26 Harada.K. Terai. T. Numerical simulation of fire resistance test of a concrelte slab Fire safety science. Proc. 2 [nd] International Symposium on fire safety science 707-717 .1989.

4.27 J.A. Purkiss, L.Y.Li, R.T.Tenchev. Finite element analysis of coupled heat and moisture transfer in concrete subjected to fire. Numerical heat transfer. Part A , 39: 685- 710 2001.

4.28   J.A.Purkiss,   L.Y.Li, R.T.Tenchev. The prediction of spalling in high
        strength concrete under fire. Cement and concrete as such, expected to be
        published.

4.29   G.A. Khoury, C.E. Majorana, F. Pesavento , B.A. Schreflert., Modelling
        of heated concrete. Magazine of concrete research 2002, 54, No. 2, April
        77- 101.

5.01   Kelley, Truman L., "Comment on Wilson and Worcester's 'Note on Factor
        Analysis'", Psychometrika, 1940, p.120

5.02   Fisher, R.A., "Design of Experiments", 11th Edition, Oliver and Boyd,
        1957

5.03   Cochran, W.G. and Cox, G.M., "Experimental Designs", 2nd Edition,
        Wiley, New York, 1957

5.04   Winer, B.J., "Statistical Principles in Experimental Design", 2nd Edition,
        McGraw-Hill, 1971

6.01   Sullivan.P.J.E.   The Structural Behaviour of concrete at elevated Temperature PhD Thesis, University of London 1970.

8.01   Copier WJ. The spalling of normal weight and lightweight concrete exposed to fire. *Journal of The American Concrete Institute*. Vol. 80, No. 4, 1983. pp. 352-353.

8.02   Sullivan P.J.E. and Thiruchelvam. C.., *Journal of Applied fire science* , High strength plastic concrete at elevated temperature., Nov 2000.

8.03   Al- Manaseer.A. and.Dalal T.R, Concrete Containing Platic Aggregates, Concrete International, pp 47-52, August 1997.

8.04   Tatnall .P. Modern use of wet mix sprayed concrete for underground support. Proceeding of the fourth international symposium on sprayed concrete, Davos Switzerland September 2002 p 320- 328.